THE ESSENTIAL ROLE OF P73 IN MULTICILIATED CELL DEVELOPMENT

By

Clayton Benjamin Marshall

Dissertation

Submitted to the Faculty of the

Graduate School of Vanderbilt University

in partial fulfillment of the requirements

for the degree of

DOCTOR OF PHILOSOPHY

in

Biochemistry

May, 2016

Nashville, Tennessee

Approved:

Jennifer A. Pietenpol, Ph.D.
David K. Cortez, Ph.D.
Scott W. Hiebert, Ph.D.
Lawrence J. Marnett, Ph.D.
Christine M. Eischen, Ph.D.

To my parents

and

to my wife, Erin

ACKNOWLEDGEMENTS

So many people have played a role in my success in life as well as the time I have spent in graduate school. I plan to use this section to put into words to the insurmountable debt of gratitude I feel toward so many who in many ways made this dissertation even possible.

I have the deepest respect and gratitude for the support that I have been given by Dr. Jennifer Pietenpol. My time at Vanderbilt and work on my dissertation would never have been possible without the foresight and efforts of Jennifer. Jennifer's excitement and drive is second to none, she instills in her students the importance of the work we conduct and expects the best we can possibly give. She reminds us constantly that we can accomplish much more than we think we can, if we put in the hours and work harder than we ever imagined. I am so thankful that I will have the imprint of such a great leader and mentor on the way that I will lead and mentor others in whatever career direction I take. I will take so much from being able to work in a position so close to such an admirable person as Dr. Jennifer Pietenpol.

I would also like to thank the members of my thesis committee Drs. Christine Eischen, Dave Cortez, Larry Marnett, and Scott Hiebert. Each of these scientists are experts in their respective fields, and have provided great support through my progression into science. I am thankful for the constructive support and feedback on the direction of my project over the last several years. My project was much better because of the direction and support each of you provided.

I have to thank the current and former members of the Pietenpol lab portion of the “p73 team”: Jennifer Rosenbluth, Deb Mays, Scott Beeler, Tim Shaver, and Gabriela Santos. This team provided me so much support and helpful discussion of directions and priorities. I have great appreciation for the hard work and mental obsession of this team toward the goal of figuring out p73. I will forever be grateful to these members of my team for making this work span a much bigger picture than the project I started with and envisioned writing this dissertation about. My dissertation is much more deep and broad in the p73 field than I ever expected because of this stellar team. Jennifer Rosenbluth did a lot of the pioneering work with p73 in the Pietenpol Laboratory. Without her drive and commitment to p73 the dissertation to follow would not have been possible. Deb Mays provided much expertise and experienced hands to this project. She was constantly making sure I was thinking through everything, asking all questions, and at the end of the day moving the project forward. Thank you for sharing in my desire to figure out p73. Scott Beeler and Tim Shaver provided critical insight into the bioinformatic analysis of sequencing data generated through ChIPseq. They not only provided their skills for bioinformatics analysis, but also were constantly excited to uncover and postulate about mechanisms. Their excitement to dig deeper in data to better understand p73 was instrumental into the final product of this dissertation. Gabriela started as my rotation student and then continued on to join our lab. Her excitement and drive for science helped me get through days where frustrating results needed a different perspective. I am very thankful for the excitement she added to the

p73 project. I can never sufficiently express in words the gratitude I feel toward this team for their hard work leading into this dissertation.

I would like to thank the rest of the Pietenpol laboratory for their friendship and suggestions over the last several years. I first must thank Dr. Katy Eby and Dr. Josh Bauer for allowing young hands to rotate on their projects and share authorship with this young scientist. I have to thank Lucy Tang for her diligence, hard work, and technical assistance. The work ethic that Lucy has shown in her life is inspiring. Kim Johnson, lab mother, has her "kids" best interest at heart whether that is expediting our science by handling ordering or listening to us vent about science not working. As mayor of PRB Kim wears a lot of hats, and wears them well. I must thank Bojana Jovonovic, Chris Pendleton, Christopher Barton, Brian Lehmann, and Brad Creamer for their continual support and friendship throughout my time at Vanderbilt. I could have not asked for a better group of people to laugh harder, focus more, and commiserate with than you five. I would also like to thank the newest trainees in our lab; Johanna Shafer, and Taylor Sundby for their excitement and commitment to research. The excitement each of you have for science is inspiring to say the least. Also , I thank Vasiliy Polosukhin, for technical assistance with ALI, Violeta Sanchez for help with tissue processing and staining, and Harold Moses for assistance in pathology analysis.

I must thank the Vanderbilt University "p73 team" members. Of Yu Shyr, Qi Liu, Mark Magnuson, Bryan Venters, and Kelli Boyd. Yu Shyr and Qi Liu validated and confirmed the bioinformatic analysis conducted by members of the Pietenpol lab. Mark Magnuson was instrumental in the initial design and experimentation that led to the

engineering of the p73 -/- mouse used throughout my dissertation research. Bryan Venters provided necessary guidance for the development and successful *in situ* tracheal ChIP-seq experiments. Kelli Boyd was instrumental in the analysis of phenotypes within p73 deficient animals. I greatly appreciate her willingness to take the time to educate and lead us through samples from select tissues ensuring that we were thorough with our analysis of all tissues within the p73-/- mice.

I am very thankful for the Interdisciplinary Graduate Program, Biochemistry Department, Vanderbilt Ingram Cancer Center, (training grant department) for the support in funding and training throughout my dissertation work. I must specifically thank Marlene Jayne, Peggy Fisher, Robert Dortch, Jan Lotterer, and Lynnette Stanton-Williams for their administrative support. My dissertation research was supported by NIH grants CA105436, CA070856 and CA68485 (J.A.P.) and T90DA022873 (C.B.M.).

I must also thank the scientists, creative, thinkers, and encouragers who helped prepare me for this venture into graduate school. A select few of the many important educators that directly influenced my scientific direction are to thank for preparing me to write this dissertation. Sharon McElroy was a phenomenal high school educator that first taught me how to conduct research and express my ideas scientifically. With her help I was able to compete on national and international levels, and without this exposure to science early I would not have known it was a perusable option for someone from very rural southern Indiana. I must also thank Dr. Becky Cargile for chasing me down and convincing me a minor in English would be useful to a scientist. I also am thankful to Dr. Lewis Pannell at the University of Southern Alabama and the

National Science Foundation-Research Experience for Undergrads. His mentoring during the summer research experience opened my eyes to what a graduate school experience would be like.

My parents have been and continue to be such great examples to me, their support throughout my education has not been unappreciated. From never ending a conversation without telling me you love me and are proud of me to constantly reminding me of how much I have to be thankful for; you both have been such lights to me throughout my life. My older brother has been such an example and a great support to me throughout my education. I have to pause and thank the strongest support system that anyone could ask for in my immediate family, as well as my extended family. I get to be the first of many generations to ever obtain a post graduate level degree-- for that, everyone in my family tree take pride in the impact each of them have had on delivering me to this point.

My wife, Erin, has been one of the greatest blessings that I have ever been given. She has been so very understanding of my frustrations, even when things that I complained about made little sense. I am so thankful for her supporting me when science kept me away from home longer than expected and understood when timepoints went long. I am so thankful for your desire to further your own education and I look forward to being able to support you and hope to do it half as well as you have for me. I am so very lucky to get many years to thank you for the debt of gratitude I have for your help over the last several years of graduate school.

TABLE OF CONTENTS

Page

DEDICATION ii

ACKNOWLEDGEMENTS iii

LIST OF TABLES xi

LIST OF FIGURES xii

LIST OF ABBREVIATIONS xv

Chapter

I. Introduction 1

Discovery of the p53 family 1
p53 1
p73 2
p63 2
Similarity of the p53 family structure and function 3
p73/p63 co-association and co-regulation 6
Complex splicing of the p73 gene confers complex function 7
p73 function determined by knockout murine models 9
The role of p73 and p63 in tumors 12
p73 in lung cancer 13
Expression of p73 within lung cancer 14
Promoter methylation shift 15
G4C14-to-A4T14 15
Pulmonary development 16
Initiation of lung development 17
Pulmonary epithelial cell milieu 19
Neuroendocrine cells 20
Brush cells 21
Multiciliated cells 22
Club cells 23
Basal cells 24
Goblet/Mucin cells 26
Ciliary development within the multiciliated cells 27
Discovery and description of cilia 27
Differentiation and development of multiciliated cells 28

Cilia and disease 29
Transcriptional control of ciliary development 31
Rfx transcription factor family 31
Forkhead box gene family 32
Mcidas and Myb 34
The role of p73 in development: goals of this dissertation 35

II. Materials and Methods 37

Cultured cells 37
Cellular growth conditions 37
Lentiviral generation of shRNA and overexpression vectors 39
Protein harvest 41
Immunoblot analysis 42
Immunoprecipitation 42
mRNA isolation and expression analysis by qRT-PCR 44

Murine model 46
Generation of p73 knockout mice 46
Murine tissue harvest 48
Histological staining of murine tissue 48
Immunoflourescence 49
Tissue protein harvest 50
Tissue mRNA isolation and quantification 51
Murine Tracheal Epithelial Cell (MTEC) isolation 51
Air Liquid Interface (ALI) differentiation 52
Immediate ex-vivo murine tracheal crosslinking and ChIP-seq 53
ChIP-seq data analysis 58
Scraped murine tracheal RNA harvest, qRT-PCR and Sanger sequencing 59
MTEC exogenous overexpression and RNA harvest 59
shRNA-mediated gene knockdown in MTECs 60
RNA-seq and analysis 60

III. p73 Is Required for Multiciliogenesis and Regulates The Foxj1- Associated Gene Network 62

Introduction 62
Results 64
p73-/- mice lack MCCs, have areas of focal epithelial hyperplasia but overall loss of airway epithelium 64
The airways of p73-/- mice have reduced numbers of basal cells in addition to MCC-deficient phenotype 74

The airways of p63-/- mice have reduced numbers of club and basal cells 74
p73 is expressed in basal cells of the airway epithelium and co-expressed with Foxj1in MCCs 77
In situ p73 and p63 ChIP-seq in murine tracheal epithelial cells 79
p73 binds and regulates genes required for the development and function of MCCs 83
Discussion 92
Conclusion 99

IV. Mechanisms of p73 Regulation 101

Introduction 101
Results 103
Known Regulator of p73, MDM2, inhibition by Nutlin 3 103
Yeast two-hybrid screen to identify p73 co-associated proteins 112
EPN1 114
RAP80 118
TAB2 122
Conclusion 126

V. Future Directions and Conclusions 128

Introduction 128
p73 and MCC differentiation 128
Interplay of p73 and p63 within a subset of basal cells 130
p73 and p63 regulation of pulmonary epithelial repair after damage and stress 132
The role of p73 in inflammatory response 135
Notch pathway 136
Lung branching phenotype 139
Regulation of p73 through protein-protein interactions 141
p73 status in diseases and cancer 145
Conclusions 147

REFERENCES 149

LIST OF TABLES

Table Page

1. List of Antibodies Utilized 43

2. List of Primers Utilized 45

LIST OF FIGURES

Figure Page

1. p53 Family Sequence Identity and Complex Splicing....4

2. Stages of Pulmonary Development....18

3. Generation of the *p73*$^{floxE7\text{-}9}$ Mice....47

4. Novel p73 Knockout Mouse Recapitulates Earlier Published Phenotypes....65

5. *p73-/-* Mice Have Increased Mortality and are Sterile....66

6. Global Ablation of p73 Eliminates MCCs....68

7. Generation of the *p73*$^{floxE7\text{-}9}$ Mice....70

8. *p73-/-* Mice Exhibit Severe Airway Phenotypes Including Hyperplasia and Epithelial Loss....72

9. *p73-/-* Mice Show Evidence of Infection and Inflammation of the Lung, Sinus and Ears....73

10. Loss of p73 and p63 in the Respiratory Epithelium Leads to Significant Changes in Cellular Composition....75

11. Representative Images from the Trachea and Bronchioles Used for the Quantification of Respiratory Epithelium, Cell Types Shown in Figure 10....76

12. p73 is Expressed in a Subset of Basal Cells in the Murine Trachea as well as in the MCCs....78

13. p73 is Expressed in a Subset of Basal Cells within the Murine Airway....80

14. p73 is Expressed in Ciliated and Basal Cells within the Human Airway....81

15. Analysis of DNA-Binding Profiles After *in situ* Protein-DNA Crosslinking and ChIP-seq (p73, p63 and Pol II) of Murine Tracheal Cells 84

16. p73 binds and Regulates Target Genes Found in Cilia-Associated Gene Set 87

17. Additional p73 Binding to Novel Target Genes in Cilia-Associated Gene Set 89

18. p73 Regulates the Expression of Foxj1 91

19. *p73-/-* Mice Exhibit Increased Proliferation of the bronchiole epithelium 96

20. p63 Positive Cells Observed Within the Bronchioles of p73-/- Animals 98

21. Graphical Representation of the Role of p73 Within the Pulmonary Epithelium 100

22. Newly synthesized (-)- Nutlin 3 exhibits comparable activity to Nutlin-3 105

23. IC_{50} Values for TNBC cell lines treated with (-)- Nutlin 3 107

24. Immunoblot Analysis of TNBC Cell Lines after Treatment with Doxorubicin and (-)- Nutlin 3 108

25. (-)- Nutlin 3 Activity affects p73 protein levels and p73 dependent activity 110

26. Yeast two-Hybrid Identified Putative Binding Partners of ΔNp73β 113

27. Exogenous Validation of p73-EPN1 Interaction and Regulation of p73 Activity 116

28. Endogenous Validation of p73-EPN1 Interaction 117

29. Exogenous p73-RAP80 Interaction and Co-localization 121

30. Exogenous Validation of p73-TAB2 Interaction and Localization 123

31. Endogenous Validation of p73-TAB2 Interaction.....125

32. Quantification of Bronchioles.....140

33. Tracheal ChIP-seq binding of p73/p63 in proximity to *Cuedc1* and *Ubc*.....144

LIST OF ABBREVIATIONS

ALI	Air Liquid Interface
ARF	Alternate Reading Frame
ATCC	American Type Culture Collection
BEGM	Bronchiole Epithelial Growth Medium
B-ALI	Bronchiole Air Liquid Interface
BPE	Bovine Pituitary Extract
ChIP	Chromatin Immunoprecipitation
Cdkn1a/p21	Cyclin-Dependent Kinase Inhibitor 1 (p21)
cDNA	Complementary DNA
Cy3	Cyanine 3
Co-IP	Co-Immunoprecipitation
CPI	Complete Protease Inhibitor
C-terminal	carboxy-terminal
Cuedc1	CUE domain containing 1
DBD	DNA Binding Domain
DLL	Delta-Like (1-4)

DNA	Deoxyribonucleic Acid
DMEM	Dulbecco's Modified Eagle's Medium
DTT	Dithiothreitol
EDTA	Ethylenediaminetetraacetic acid
EGF	Epidermal Growth Factor
EPN1	Epsin 1
EPN2	Epsin 2
FITC	Fluorescein Isothiocyanate
FBS	Fetal Bovine Serum
FOXJ1	Forkhead Box Protein J1
GEMs	Genetic Modified Mouse Model
GFP	Green Fluorescent Protein
H&E	Hemotoxylin and Eosin
hEGF	human Epidermal Growth Factor
HMEC	Human Mammary Epithelial cells
IACUC	Institutional Animal Care and Use Committee
IFT	Intraflagellar Transport

JAG1	Jagged 1
JAG2	Jagged 2
KRT14	Keratin 14
KRT5	Keratin 5
KS	Kartagener's Syndrome
LOH	Loss of heterozygosity
LPS	Lipopolysaccharide
NOXA	Phorbol-12-myristate-13-acetate-induced protein 1
MCC	Multicilliated Cell
MCIDAS	Multicillin
MDM2	Mouse Double Minute 2
mTEC	Mouse Tracheal Epithelial Cell
Myb	V-Myb avian Myeloblastosis Viral Oncogene Homolog
NBF	Neutral Buffered Formalyin
NES	Nuclear export signal
NGS	Next Generation Sequencing
NICD	Notch intracellular domain

NLS	Nuclear localization signal
NSCLC	Non-small cell lung cancer
N-terminal	Amino-terminal
OD	Oligomerization domain
p53	Tumor protein p53
p63	Tumor protein p73-like
p73	Tumor protein p73
PAGE	Polyacrylamide Gel Electrophoresis
PBS	Phosphate Buffered Saline
PCD	Primary Ciliary Dyskinesia
PCR	Polymerase Chain Reaction
PFA	Paraformaldehyde
PUMA	p53 Up-Regulated Modulator of Apoptosis
qRT-PCR	quantitative Real-Time Polymerase Chain Reaction
RAP80	Retinoid X Receptor Interacting Protein
RFX	Regulatory factor x
RIPA	Radio Immunoprecipitation Assay

RNA	Ribonucleic Acid
RPMI	Roswell Park Memorial Institute
RUNX	Runt-Related Transcription Factor 2
SAM	sterile alpha motif
SCC	small-cell carcinoma
SDS	Sodium Dodecyl Sulfate
shRNA	Small Hairpin RNA
siRNA	small interfering RNA
shRNA	short hairpin RNA
STAT3	Signal transducer and activator of transcription 3
TA	Transactivation domain
TAB2	TAK1-binding protein 2
Tgf-β	Transforming growth factor beta
TNBC	Triple Negative Breast Cancer
TRAF3IP1	TNF receptor-associated factor 3 interacting protein 1
TPSR	Vanderbilt Translational Pathology Shared Resource
TTBS	Tris-Tween Buffered Saline

UBC	Polyubiquitin-C
VANTAGE	Vanderbilt Technologies for Advanced Genomics

CHAPTER I

INTRODUCTION

Complex signaling pathways regulate the cellular processes that are required for proper development and function of life. Transcription factors are vital to the expression of genes at specific time points within biological processes and are required for regulation of differentiation, morphogenesis, homeostasis, and further response to the environment. In this chapter, the p53 family of transcription factors will be introduced with a particular focus on p73, and the process of multiciliated cell (MCC) development will be further discussed. This dissertation focuses primarily on the discovery that p73 is necessary for the development of MCCs in mice, with an emphasis on the trachea and bronchiole epithelium. This work identifies p73 as a regulator of MCC development, which may have implications for many pulmonary diseases and cancers that have not previously been linked to the activity of this transcription factor[1].

Discovery of the p53 Family

p53

p53 was initially discovered as a protein in complex with the large T antigen in SV40-transformed cells[2,3] and expressed in tumors[4]. The tumor suppressive roles of p53 were demonstrated when inactivating mutations in p53 were found in more than 50% of human tumors[5,6] and germline mutations of p53 were identified as being causative of Li-Fraumeni syndrome. These findings

were strengthened when p53 was ablated in murine models, which developed normally but exhibited increased mortality due to spontaneous tumor formation[7].

The tumor suppressive role of p53 is due to its ability to transcriptionally activate many genes involved in tumor suppression including Cdkn1a[8] and Puma[9] and many other genes that directly regulate the cell cycle, DNA damage repair, as well as apoptosis[10-13]. These protective roles of p53 have lead many to commonly refer to the functional role of p53 as the "guardian of the genome"[14].

p73

A p53 homologous protein, p73, was discovered in 1997[15] and due to its high level of sequence identity with p53 it was initially thought to be redundant to p53 and primarily function as a tumor suppressor. The generation of p73-deficient mice discovered phenotypes that were unique from p53, including pheromonal, inflammatory, growth, and neurological defects[16]. Further discovery and targeted ablation of multiple isoforms of p73 suggested that it can act as a p53 like tumor suppressor in certain biological contexts, but is much more complexly regulated[17]. All of which will be further discussed below.

p63

After the discovery of p73, through sequencing technologies the presence of a third p53-related protein was discovered[18-20], and in 1998 p63 was discovered and functionally described[21]. Its similarity to p53 suggested that p63 may also be redundant to p53; however, the generation of the p63 deficient mouse revealed a unique biological role from the other two known family

members. The ablation of p63 in mice leads to perinatal mortality due to severe developmental defects including a lack of stratified epithelia, absence of limbs, as well as craniofacial defects[22]. The mice also lacked all glandular epithelial tissues including mammary, lachrymal, salivary, prostate, and bladder tissues[22,23]. This initial discovery of p63 as a master regulator of epithelial development led many subsequent studies of its biological role in development.

Similarity of p53 Family: Structure and Function

The p53 family of transcription factors all descended from a single ancestral gene and to share a common domain structure and have a high degree of sequence identity[24]. p53, p63 and p73 all share conserved domains including (N)-terminal transactivation (TA), DNA binding (DBD) and oligomerization domains[25,26]. When comparing the whole amino acid sequence of the p53 family, p53 and p73 share 30% sequence identity, p63 shares 25% sequence identity with p53, and p73 shares 52% sequence identity with p63. The identical amino acids are concentrated in functional domains of the p53 family for example, 60% of the amino acids are identical between the p53 family of proteins in the DBD with 100% conservation of the essential residues that contact DNA for all three family members[27,28]. The most significant homology within the family is in the DBD of p73 and p63, with 87% amino acid identity (Figure 1A)[29]. The shared DBD identity between the three proteins results in them all binding to the canonical p53 consensus response element made up of two half sites (RRRCWWGYYY - R=purine, C=cytosine, W=adenine or thymidine, G=guanine,

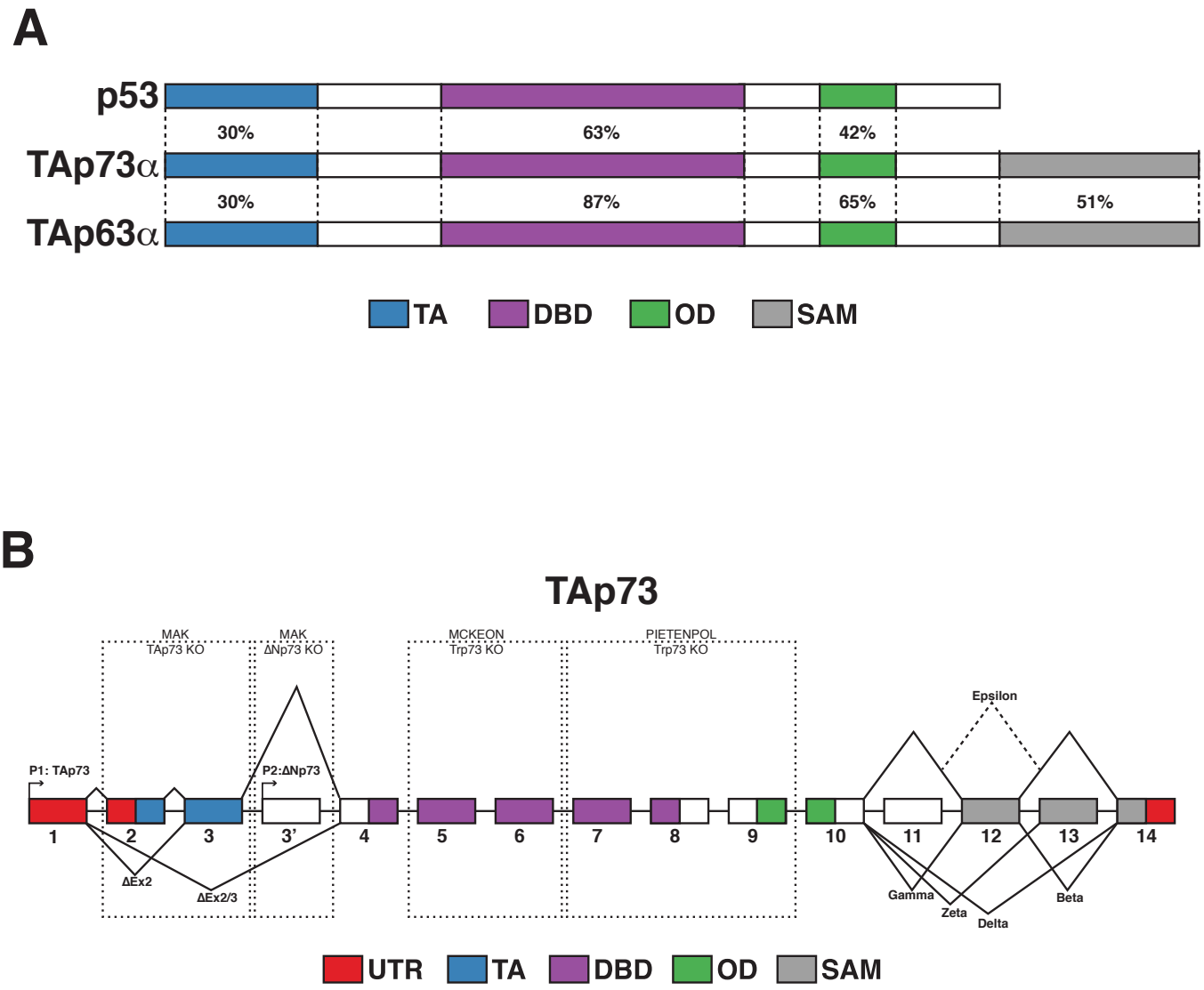

Figure 1. p53 Family Sequence Identity and Complex Splicing. (A) Representation of the p53 family members with the known domains shaded in blue [Transactivating (TA)], purple [DNA binding domain (DBD)], green [Oligimerization domain (OD)], and gray [sterile alpha motif (SAM)]. Percentages between the known domains represent the sequence identity that is shared between each of the family members domains. (B) Cartoon representation of the 14 exon structure of the p73 gene. Splicing is annotated utilizing lines with product of that splicing labeled. The known domains of p73 are shaded in to annotate on which exon those domains are found. Dashed line boxes indicate knockout mice that were utilized to study the biological function of the p73 gene.

and Y=pyrimidine) separated by a spacer of up to thirteen base pairs[30-35]. p63[36,37] and p73[35,37,38] are capable of binding to slightly different response elements, conferring responsiveness to independently regulated genes as well.

The earliest p53 ancestor gene that has been identified to date exists in choanoflagellates, which are the closest extant relative of metazoans[39]. These unicellular protists contain two distinct ancestor genes, one is more p53-like and the other is more p63/p73- like. To date no p53 family member has been identified within fungi except for the Opisthokonts[40]. p53-like genes exist in a broad number of taxa including sea squirts[41], cnidarians[42,43], and platyhelminthes extending throughout vertebrates. The primitive metazoan sea anemone contains a p63/p73 hybrid called nvp63 that responds to UV light by inducing a DNA damage response resulting in apoptosis within the gametes[43]. The p53 response to DNA damage in the germline of this primitive organism is functionally similar to what is observed in many other organisms including *Drosophila*[44,45] and mice[46].

Further biological complexity is conferred through the expression of alternate splicing and promoter use within the genes that code the p53 family. There are nine known isoforms of p53, six of p63, and 35 of p73 that arise from complex promoter usage and alternative splicing[47,48]. p63 and p73 genes can be transcribed from different promoters and alternatively spliced to yield multiple protein products[21,49]. p63 and p73 each have two upstream promoters (P1 and P2). Isoforms transcribed from P1 contain the transactivation (TA) domain

(TAp63 and TAp73), and isoforms transcribed from P2 lack the TA domain (ΔNp63 and ΔNp73)[15,21]. The N-terminus of TAp73 and TAp63 contains a single activation domain that is approximately 25% homologous with the first activation domain of p53[50]. ΔNp73 contains 13 unique residues, which generate a much weaker activation domain allowing for abated transcriptional activation at target genes[38]. Both ΔNp63[51,52] and ΔNp73[38] have been shown to directly activate target genes as well albeit at a significantly reduced rate from their TA containing counterparts TAp63 and TAp73 respectively. Predominately the prescribed function of ΔN isoforms of p63 and p73 is attributed to be dominant-negative effectors of transcriptional activity of the p53 family of transcription factors[38,50].

p73/p63 Co-Association and Co-Regulation

There are functional and physical interactions amongst the three family members, and co-regulation of many of the same target genes. Three potential mechanisms for physical and functional interactions exist depending on cell context and relative levels of expression of the various isoforms. First, the regulation of transcription occurs through cooperation and competition at conserved p53/p63/p73 binding sites of shared target genes[53-56]. Second, direct physical interaction of the p63 and p73 isoforms occurs[23,57,58], because cells that co-express both p63 and p73 they associate[59-61]. Third, mutant p53 protein that has lost tumor suppressive activity, which is expressed in numerous tumors, is capable of binding and inactivating p73 by either sequestering from the nucleus or inhibiting DNA binding[62,63-72].

Shared consensus binding-sites between p53 family members indicate that they compete for binding at shared genomic binding sites when they are co-expressed. It is likely that this competition of binding is only exacerbated through protein-protein interactions that may be unique among family members. All of the p53 family binds to DNA as tetramers in which the members interact through dimerization of dimers mediated by the oligomerization domain[28,50,73]. p73 and p63 are capable of regulating the function of each other[73], and through this interaction in which ΔN isoforms bind with transcriptionally active TA isoforms and exhibit titration of their transactivation capabilities. Also of interest, there is a p53 response element upstream of the ΔN isoforms of p73 and p63 promoters and p53 and TAp73 regulate their expression providing a negative feedback loop[74-77]. In several cell types ΔNp63 isoforms are the predominate isoforms expressed[16,78] it has been shown that in these systems the ratio of expression of ΔN to TA regulates downstream transcriptional activity[21].

Complex Splicing of the p73 Gene Confers Complex Function

The differential splicing of the C-terminus of p73 results in several isoforms that have different transcriptional activity[79]. p73 is expressed highly as the TAp73α transcript in a majority of adult mouse tissues[80]. For example, p73 isoforms α and β are instrumental in normal myeloid differentiation, and γ,δ,ε, and θ have been linked to leukemic blasts[81,82]. The isoforms TAp73γ and TAp73δ are involved in terminal differentiation of human skin keratinocytes[83].

However in some tissues, such as the lung, RNA and protein of all isoforms can be detected upon treatment with DNA damaging agents[80].

The differential function of p73 isoforms can be partially attributed to the alternate splicing of the C-terminal domains of p73. One domain in particular the sterile alpha motif (SAM), is not conserved in all isoforms of p73 and p63 due to C-terminal splicing differences[6]. This domain is conserved in many other transcription factors as far back as yeast and mediates protein-protein interactions. It was coined as sterile, because of its presence in four proteins required for yeast sexual differentiation, and alpha because of secondary structure predictions of α-helices[84]. Mutations in the p63 SAM domain are causative for AEC syndrome a developmental disease that causes ectodermal dysplasia and facial clefting[85], while the p73 SAM domain binds to anionic and zwitterionic lipids[86]. The SAM also acts in an inhibitory manner toward the transactivation domain of both p63 and p73 by possibly inhibiting the association of co-activators of transcription and the activation domains within the N-terminus[27]. Functionally, TAp73β is the most transcriptionally active isoform of p73 and it lacks the core of the SAM domain[87,88].

The C-terminal portion of p73 is not the only area in which p73 is spliced differentially to generate multiple isoforms. Complexity also is conferred through alternative splicing within the N-terminus generating Δex2p73 and Δex2/3p73 in which exon 2 or exons 2 and 3 are alternatively spliced from the full length p73 henceforth collectively called ΔTAp73 (Figure 1B)[89,90]. These isoforms lack all or

the majority of the transactivation domain and they differ from ΔNp73 in that their transcription is driven from P1 promoter upstream of exon 1. The study of these isoforms has been predominately limited to their role in tumorigenesis and has been shown to be biologically similar to ΔNp73 and to be preferentially expressed in tumors[89-93]. Much like ΔNp73, the ΔTAp73 isoforms retain their DNA-binding and tetramerization abilities and act as dominant-negative inhibitors of the rest of the p53 family[75,93-95]. ΔTAp73 isoforms are biologically relevant oncogenes in many culture systems[75,93-95]. ΔTAp73 overexpression in NIH3T3 cells drives malignant transformation to produce tumors in nude mice[93] as well as interferes with the Rb tumor suppressor pathway[96]. The ΔTAp73 isoforms are upregulated in many cancer types and further correlates with poor survival [90,97,98]. As high throughput deep sequencing of human samples becomes more readily available it will be of great interest to determine the expression of N-terminal and C-terminal isoforms to determine their role in normal tissues and disease states.

p73 Function Determined by Knockout Murine Models

There have been multiple murine p73 genetic models developed that target multiple domains within p73[16,99-105]. These engineered models are annotated in Figure 1B (dashed boxes). The global ablation of p73 by targeting exons within the DBD[16], which resulted in hippocampal dysgenesis, hydrocephalus, sterility, chronic infections and inflammation of the lung and sinus, abnormalities in the pheromone sensing pathways, runting, as well as increased rates of postnatal death[16].

After the generation of this model, subsequent studies were focused on the neurological defects observed in p73-deficient animals. In *p73* null mice the brain lacked expression of Reelin leading to the hippocampal dysgenesis observed[16]. The expression of ΔNp73 in murine brain provides an anti-apoptotic pro-survival signal that leads to the maintenance of the neural stem progenitor cells[102,106]. More recently, p73 activity has been implicated in the development and maintenance of ependymal cells[107,108]. It was observed that the ependymal cells in p73-deficient animals were increasingly apoptotic and exhibited dysfunctional cilia architecture[107]. A second study did not observe apoptosis within the ependymal cells of *p73*-null animals, but noted a denuding of ependymal cells due to lack of differentiation from radial glia cells into ependymal cells causing the loss of the motile cilia in the process resulting in hydrocephalus and hippocampal dysgenesis[108].

The use of global pan-isoform targeting murine models failed to parse the individual functions of the multiple p73 isoforms, which confounded the complex biology of this transcription factor. For example, two murine models that ablate ΔNp73 expression as well as TAp73 expression independently[17,99] revealed a role of p73 in neurodegeneration, but those mice did not exhibit the sterility phenotypes observed in the *p73-/-*. *ΔNp73* knockouts also exhibited increased levels of apoptosis and expression of p53 family target genes confirming the anti-apoptotic function of p73 *in vivo*. Injection of E1A and Ras transformed *ΔNp73*-deficient MEFs into athymic nude mice resulted in smaller, slower growing

tumors when compared to those transformed from wild-type animals suggesting that ΔNp73 expression is important for transformed cells to initiate tumors[99].

Isoform specific deletion of *TAp73* in mice caused infertility, hippocampal dysgenesis, expedited aging, genomic instability, and increased frequency of carcinogen-induced tumors[17]. The oocytes of *TAp73*-/- mice exhibited spindle abnormalities leading to genomic instability within the female mouse follicle development[17]. *TAp73*-/- male mice also exhibit severely impaired spermatogenesis resulting in increased DNA damage and apoptosis of spermatogonia[101] leading to a nearly empty seminiferous tubule[103]. TAp73 also regulates the adhesion and migration factors that uphold the germ-sertoli connection that is required for proper spermatogenesis[103]. Other studies indicated that the transactivation activity of TAp73 at target genes required for mitochondrial function, such as Cox4i1, was required for processing reactive oxygen species. The knockout mice revealed increases in senescence and oxidative damage from reactive oxygen species leading to premature aging[100].

Like the *ΔNp73*-null mice, the *TAp73* ablated mice exhibit hippocampal dysgenesis and hydrocephalus indicating that all isoforms of p73 are necessary for proper neural development[17]. The peripheral nervous system of the TAp73 mice is also affected due to the absence of p73 transactivation of the p75 neurotrophin receptor, which resulted in a loss of sensory but not motor neurons[105]. These isoform knockouts indicate that the p73 isoforms, studied to date, exhibit independent and co-dependent roles within development. Further

studies of c-terminal variants will further enable greater understanding of biological roles of all of the other isoforms commonly expressed.

The Role of p73 and p63 in Tumors

Unlike p53, p63 and p73 are rarely mutated during tumorigenesis[6,109-111]. Although p63 and p73 can activate apoptosis *in vitro*[21,53,112-114], it is clear that they are not classic Knudson-like tumor suppressors. The human p63 gene maps to 3q27-28, a region frequently amplified in squamous cell carcinomas[115-117], with overexpression also reported independently of gene amplification[118]. ΔNp63α is overexpressed in ~80% of head and neck squamous cell carcinoma (HNSCC) and in other epithelial cancers including lung[23,58,117,119-122]. p63 is amplified in 88% of squamous carcinomas, 42% of large cell carcinomas, and 11% of adenocarcinomas of the lung[110]. ΔNp63a was the predominant isoform expressed at the protein level within these tumors[110], which suggests that p63 genomic amplification has an early role in lung tumorigenesis[110]. Although reported levels of p63 expression in breast carcinomas have varied[123-128], elevated p63 levels have been noted in a subset classified by a 'basal' phenotype[129].

For select tumor types, overexpression of ΔNp63α has been associated with favorable outcome[117,130], and for others, loss is associated with invasion, metastasis and poor outcome[90,122,131,132]. One hypothesis to reconcile these findings is that in early tumorigenesis, ΔNp63α contributes to maintaining a self-renewing epithelial state and allowing growth in a local tumor-host environment;

however, as cells accumulate additional genetic events, loss of p63 facilitates an epithelial to mesenchymal transition enabling migration [130].

p73 is overexpressed, rather than mutated or deleted, in a large number of tumor types[6]. ΔNp73 or ΔNp63 overexpression or loss of TAp73 may be required to inactivate presumptive tumor-suppressive properties of TAp73[23,58,91,133-136]. In head and neck squamous cell carcinoma (HNSCC) and 'basal-like' breast cancer cell lines, ΔNp63:TAp73 complexes suppress p73-dependent apoptosis through direct protein interaction and competition for binding at key target genes. The latter is supported by *in vivo* evidence in these tumor types[23,58,136]. The ability of either ΔNp63 or ΔNp73 to inhibit TAp73 may obviate the need for mutation of p73 during tumorigenesis. There is evidence that p73 is important in the pathogenesis of lung cancer[137-139]. Loss of heterozygosity (LOH) at the p73 locus is reported in 62% of squamous cell carcinomas found in the lung[140], and the p73 G4C14-to-A4T14 polymorphism is associated with increased risk of lung cancer[141] (discussed in detail in the following section).

p73 in Lung Cancer

Thirty percent of *TAp73*+/- mice and 73% of *TAp73*-/- mice developed malignancies with lung adenocarcinoma being the most frequently observed cancer representing 44% of all tumors observed in *TAp73*-/- mice[17]. The lung adenocarcinomas observed in knockout mouse models as the primary tumor produced in a p73 ablated state led many to research the role of p73 in lung

tumorigenesis. Unlike its family member p53, the coding sequence of p73 is rarely mutated even within lung tumors[6].

Expression of p73 Within Lung Cancers

In initial studies after the discovery of p73, most looked at pan p73 expression, with no knowledge of splicing variants, across cancers. In one such study, 87% of patients' p73 is overexpressed while only 5% of patients have reduced expression of p73 as compared to normal controls[142]. In later studies, ΔNp73 was shown to be significantly overexpressed in higher staged lung tumors from patients, and its expression indicated poorer prognosis and outcome in patients with high expression[143], by an increase in the risk of death by a factor of 3.38[143,144]. Others noted in non-small cell lung cancer (NSCLC) that the mRNAs for Δex2p73 and Δex2/3p73 were higher expressed while other isoforms were down modulated[145]. Interestingly in many of the studies of p73 expression in NSCLC localization of TAp73 appears to shift from the nucleus to the cytoplasm[143-146].

Further investigation of the p53 family indicated that ΔNp63 is highly overexpressed, while TAp63 is expressed at lower levels in squamous cell carcinoma (SCC) while overexpression in adenocarcinoma is not observed[144,145]. A study investigating the role of alterations within ARF, p53 and p73 in NSCLC noted LOH of p73 in cases where either and/or p53 were abnormal[147].

Promoter Methylation Shift

There are two CpG islands localized at the P1 and P2 promoters. The larger of the two is found at the P1 promoter and was hypermethylated in hematopoetic cancers but rarely within other tumors[148-153]. The smaller CpG island correlating with P2 is almost always fully methylated under normal conditions within tissues[151,152]. In a few studies of NSCLC both TAp73 and ΔNp73 were observed to be overexpressed in a majority of cases[146,154-156]. P1 promoter was very rarely hypermethylated at 6.8%[155] but generally observed to be unmethylated. These studies showed that the P2 promoter was hypomethylated within the tumors but hypermethylated in the normal tissues used as controls[146,155]. P2 hypomethylation was observed to be most frequent in SCC[155], indicating that unrestrained expression of ΔNp73 may shift the balance from the transcriptionally active TAp73 isoforms that suppresses tumorigenesis.

G4C14-to-A4T14 Polymorphism and Lung Cancer

A G4C14-to-A4T14 dinucleotide polymorphisms is present in neuroblastoma, and it forms a stem loop structure that affects the expression of TAp73[15]. This polymorphism is observed three base pairs from the splice site for exon one and exon two of TAp73. It is also twenty base pairs from the initial methionine of TAp73. Many publications indicate that this polymorphism occurs in approximately 20% of lung cancer patients[141,157-160]. Two studies indicated that G4C14-to-A4T14 increased the risk of tumors in a dose dependent manner depending on the allelic frequency of the polymorphism[141,157]. However, the

polymorphism was protective against the development of lung tumors[161]. All of these were combined as individual case controlled experiments into one large cohort, and it was observed that the polymorphism was not associated with the development of lung cancer in the Asian populations as initially described. However, the polymorphism was correlated with cancer risk in the studies that pooled the data from Caucasian populations with lung cancer[162].

The G4C14-to-A4T14 polymorphism appears to correlate with lung tumorigenesis within some races or sampling sets published, but it does not confer risk across all populations and is likely linked to other factors of tumorigenesis. A study of Korean lung cancer patients observed a correlation of p73 polymorphisms and lung cancer risk, which was observed to be significantly higher in the patients that also exhibited the MDM2 309T-309G polymorphism[163]. A more recent study, p73 G4C14-to-A4T14 and MDM2 309T-309G conferred decreased survival of patients with NSCLC when measured in combination with p53 R72P[164]. More studies of the correlation of this p73 polymorphism in reference to other mutations or polymorphisms in the p53 signaling network are needed to better understand the conflicting results observed across the published literature in reference to the G4C14-to-A4T14 polymorphism.

Pulmonary Development

The pulmonary system is a complex arrangement of branches stemming from the tracheal tube leading to alveolar structures where the capillaries are closely proximal to the epithelium to allow for the exchange of oxygen and carbon

dioxide required for life. Each minute the human lungs bidirectionally process approximately six liters of air[165] over approximately 70 m^2 of surface area[166]. The air that is processed in the lungs carries with it many contaminants and pollutants that must be processed and controlled to protect the underlying cells. The lungs have developed methods for transport of those toxins, how much space they cover, air exchange, how much mucous is moved out daily.

Initiation of Lung Development

Early growth of the lung has been organized into five periods of development that occur during precise times in mouse/human: Embryonic (M: E9-11.5 / H: 3-7 wk gestation), Pseudoglandular (M: E11.5-16.5 / H: 5-17 wk gestation), Canalicular (M: 16.5-17.5 / H: 16-26 wk gestation), Saccular (M: E17.5-PN5 / H: 24-38 wk gestation), and Alveolar (murine PN5-28 / H: 38 wk gestation to maturity) (Figure 2). Initiation of lung buds occur in the embryonic period of development when cells marked with the expression of TTF1 and Foxa2 transcription factors[167-169] proliferate and differentiate from the primitive oesopagus[170,171]. In order for proper branching of the lung, cells must migrate from the foregut endoderm-derived epithelium into the splanchnic mesoderm forming the respiratory bronchioles and alveolar spaces integrating vascularization and surfaces for air exchange[170].

The respiratory branching tree continues into the pseudoglandular stage of development, during which the bronchiole branches are lined with undifferentiated epithelial cells[172]. During this phase of development

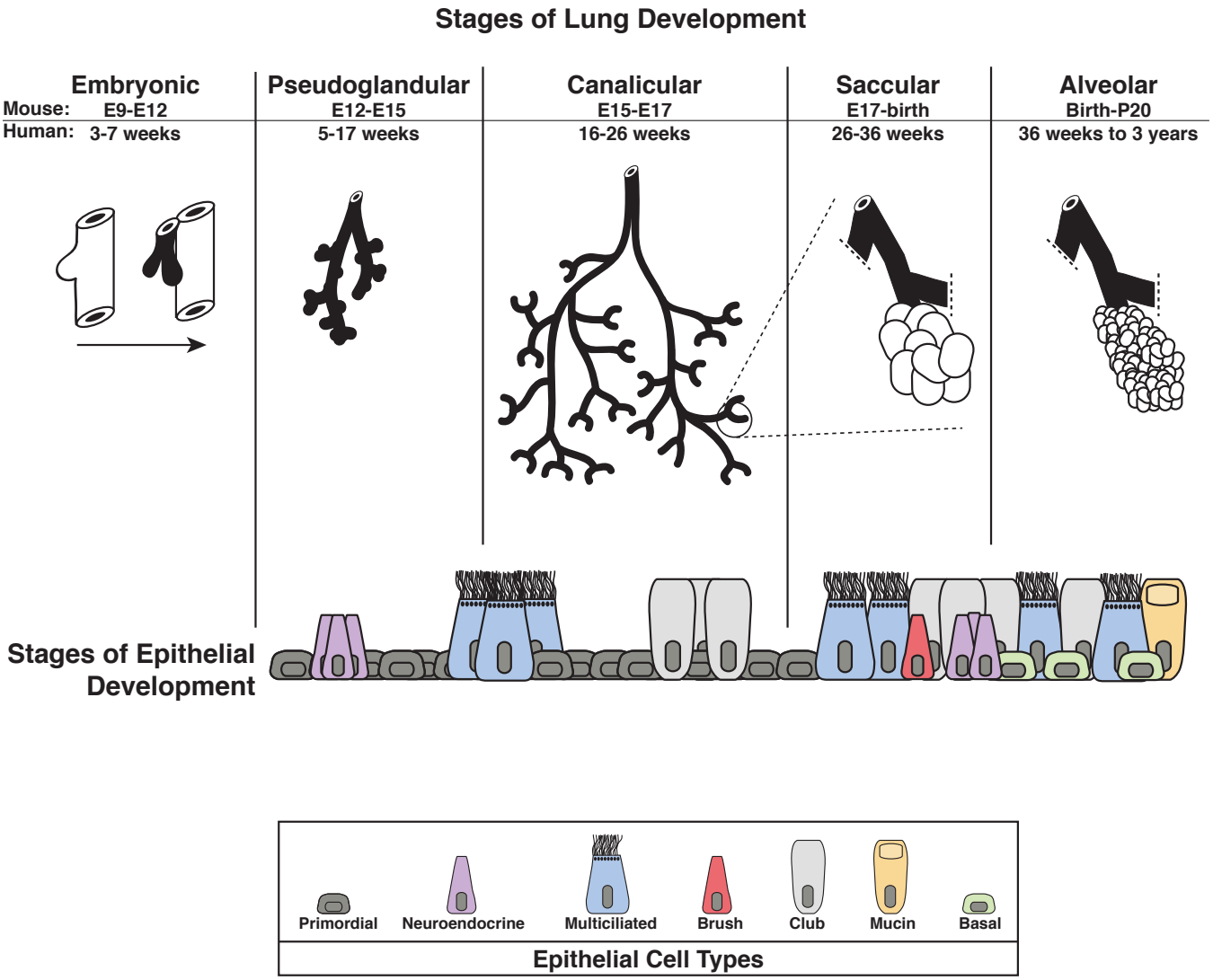

Figure 2. Stages of Pulmonary Development. Overlapping stages of lung maturation take place through a series of branching and developmental changes. The top labels annotate the gestation time at which the lung develops within both mouse and human. Cartoon depictions of the stages of development are shown below. The epithelial cell types observed throughout the murine epithelium are shown at the bottom corresponding to the time at which they can first be observed to develop in the lungs.

vasculogenesis and angiogenesis establish pulmonary veins and lymphatic[173] smooth muscles cells differentiate along the bronchial tubes[174], and cartilage develops along the trachea and bronchi[175] establishing the structure on which the various pulmonary epithelial cells can differentiate late in the pseudoglandular stage and through the canalicular stage. In rodents, lungs continue to grow throughout the life of the animal keeping pace with the size of the body, but that pace of growth slows with age[176]. The consensus for the epithelial cell turnover in adult mice is greater than 100 days[177,178] with multiciliated cell turnover rate is much slower with a significant number of cells still present at 18 months of age[179]. Thus the pulmonary epithelial cells that develop prior to birth are present when the animals reach maturity, and some are still present at the animal's death.

Pulmonary Epithelial Cell Milieu

Before the end of the pseudoglandular to canalicular stage transition of development the cells lining the trachea and bronchioles remain undifferentiated, but in later development these cells must differentiate into several cell types including; neuroendocrine, brush, multiciliated, club, basal, and goblet/mucin cells (Figure 2). It is the balance of these epithelial cells, described in more detail to follow, that permit proper breathing and pulmonary health.

Neuroendocrine Cells

Neuroendocrine cells first appear in proximal conducing airways during the end of the Pseudoglandular stage of development (Figure 2) then later at the sites of airway branches and distal airways, creating a proximal to distal wave of development in developing pulmonary epithelium[180-183]. Precursor neuroendocrine cells become innervated by ganglion cells and can then proliferate to become neuroepithelial bodies[181], which regulate the further proliferation and development of adjacent epithelial cells[180,184-186]. The neuroepithelial bodies also act as focal sites for secretory cell differentiation[180,184-186].

Neuroendocrine cells are sensors of damage in the lung, and their frequency increases in conditions of prolonged hypoxia[187] and in many lung injury models[188]. For example they act as the primary O_2 sensing chemoreceptors within the lung[189]. These cells express both neural and endocrine phenotypes[189]. They secrete dopamine, serotonin, gastrin-releasing peptide and somastostatin [189-191]. These factors assist in the transition of the lungs to postnatal life by regulating the ion and fluid transport; for example, dopamine is highly expressed at birth and assists in increasing Na+ channel and Na+/K+ ATPase activity[192,193] and serotonin a similar function[194]. In the pulmonary system, neuroendocrine cells are early-differentiated cells that lay the signaling groundwork for the further development of the epithelial cells to follow and regulate the transition from *in utero* to postnatal life[182,183,190,195].

Brush Cells

There is a highly viscous mucous layer of protection within the airways and under that layer there is a lower viscous layer of liquid lining the airway surface that is made up of antimicrobial substances, amino acids, and lipids[196,197]. The balance of these layers must be maintained for healthy respiration. The brush cells provide a chemosensory role for the pulmonary epithelium to maintain the correct protective balances of cells and secreted factors within the airways.

The first description of a brush cell in rat trachea was identified as an isolated cell with the presence of a "brush" of microvilli with long rootlets that can reach as far as the pairnuclar region[198]. These cells make up approximately 0.5 percent of all epithelial cells within the murine tracheal epithelium[199-202]. They were later identified in human00 lungs[203] and digestive tract[204,205] and are concentrated in the gallbladder[204-206]. Several bitter taste-related molecules link the brush cell to the taste bud and indicates it may be operating in a chemosensory role[207]. For many years brush cells were identified in the airway epithelium by ultrastructural imaging to observe the tuft of microvilli and rootlets and now can be immunostained with villin and fimbrin[208].

Brush cells in the trachea are directly contacted by nerve fibers[205] that stem from the sensory vagal ganglia[201,209]. Brush cells detect bitter-tasting molecules released by bacteria in the nose[209] and trachea[210] and likely other signals of change within the pulmonary epithelium. Brush cells respond to stimuli

by coordinated release of local responses for the surrounding tissue but also through activation of the connected sensory nerve fibers initiating avoidance as well as defense[211,212]. In the trachea and lungs this generally results in a cough reflex or decreases in the frequency of breathing as well as altered cellular secretions[201,213,214]

Multiciliated Cells

Airway MCCs are terminally differentiated cells that are not capable of self-renewal[180] and are first observed at the end of the pseudoglandular stage of pulmonary development (Figure 2)[165]. In a tissue-specific manner, epithelial cells generate 200-300 individual cilia (multicilia) to aid in motility or movement of fluids in those tissues[215]. Maturation of a ciliated cell only is considered completed when the ciliated border of the cell is full of the proper number of motile cilia and the actions of the organelles is fully coordinated[180]. Motile cilia are generally comprised of 9 microtubule doublets surrounding a central pair of microtubules (9+2). Motility in cilia is derived from the coordinated activation and inactivation of dynein proteins that line the inner and outer dynein arms along the entire axoneme[216,217]. The motility of these cilia is required for mucocilliary clearance in the respiratory tissues[218,219] and also for ependymal flow within the brain[220]. Comparisons have been made between respiratory MCCs and those of the sinus, oviducts, epididymis, and ependymal compartment. The ependymal cilia beat approximately twice as frequently as the cilia found in the respiratory system and are significantly longer at 8 μm as compared to 5 μm in the airway[221].

There are also far fewer cilia per cell in the ependymus with an average of 16 cilia per cell[222].

Within the pulmonary system of healthy humans the coordinated beating of cilia propel mucus 4 to 20 mm/min[223]. The cilia only touch the mucous layer on the forward stroke and pass underneath it on the backward stroke[224,225] to propel it through the vocal cords and pharynx[223]. Healthy cilia are a requirement for proper pulmonary function, and the complex process of multiciliary biogenesis and homeostasis is described in more detail in further sections.

Club Cells

Club cells are non-mucous, non-serous cuboidal secretory cells[226-228] that are club shaped with a luminal surface that extends above the surrounding epithelial cells. Their differentiation initiates at the beginning of the canalicular stage of pulmonary development (Figure 2)[165]. They were initially identified due to the granules that contain surfactants that were observed to be secreted from these cells[229-231]. Club cells also produce P450 enzymes that are required for the metabolism of inhaled pollutants[232,233]. The balance of club/ciliated cells is of extreme importance within the pulmonary epithelium, because together they regulate the balance of mucosecretory ciliary clearance of the lung. Within the tracheal epithelium, the balance is shifted to require more frequent ciliated cells and a few club cells, while the bronchiole epithelium contains an abundance of club cells in comparison to ciliated cells[234-236]. It has been previously reported

that the Notch pathway is a necessary factor in the development of the club cells by regulation of the club/ciliated cell fate decision[237-240].

Club cells retain stem like capabilities throughout the life of an organism. After administration of external damaging agents club cells were capable of generating basal cells, albeit at very low efficiency[241]. They were previously shown to be capable of self-renewal and differentiation into MCCs[242-244]. Other studies in the prostate[245] and other organ systems show that daughters of stem cells can revert to regain stem characteristics after injury[246]. Lineage tracing experiments indicated that the pulmonary epithelial cells that result from de-differentiated club cells are replaced over time by basal cell proliferation, and thus, club cells do not de-differentiate into functional long term stem cells of the lung[241].

Basal Cells

Thirty percent of the pseudostratified epithelium of the murine trachea is made up of basal cells[234,235] that express p63[235], cytokeratin 5 (Krt5)[247], and cytokeratin 14 (Krt14)[234,248,249]. Basal cells in the uppermost tracheal epithelium form a monolayer but are distributed in clusters in the more distal trachea and upper bronchioles of mice[249], and can be observed just before birth at the termination of the saccular development stage (Figure 2)[165]. The differentiation of basal cells that takes place late in utero and completes postnatally is dependent upon the expression of p63[250]. It is hypothesized that there are multiple basal cell types within the pulmonary epithelium that exhibit varying stem

cell capacity for re-population of epithelial cell types[171,235,236,251]. Most basal cells express Krt5 and only a smaller subset express Krt14 until the epithelium undergoes toxic damage (e.g. naphthalene injury), upon which Krt14 cells greatly expand and recapitulate the many epithelial cells[234,248].

Through lineage tracing experiments, basal cells proliferate into daughter basal cells as well as differentiate into ciliated and club cells[234,235,248]. Tracheal epithelial cells can be individually sorted and in clonal tracheosphere experiments determined that p63+/Ngfr+/Krt5+ cells were the cells that self-renewed and repopulated epithelial cell types[235,251].

In unchallenged lungs, we hypothesize that it is the balance of p63 isoforms that allow a subset of cells to maintain proliferative potential while maturing into stratified epithelium. At E15.5 stem cells of the esophagus and trachea express p63 and within the tracheal epithelium those cells first differentiate into MCCs and later into the p63 expressing Basal cells[250]. Unlike the skin where p63 loss leads to loss of the epithelium, ablation of p63 in mice did not result in absence of the tracheal and esophageal epithelium but results in hyperciliation of the trachea and bronchioles of developing embryonic animals[250]. In human bronchiole epithelial cells (VA10 cell line) that can differentiate into a stratified pulmonary epithelium in culture[252] ΔNp63 expression mimics what is observed in murine knockout models[253].

p63 has been shown to provide the molecular switch that initiates and regulates epithelial stratification in the tissues where it is expressed[254]. Ectopic

expression of TAp63 in alveolar cells led to the expression of Krt5 and Krt14 and further stratification of alveolar cells[254]. Also, when airways are damaged due to infection a wide-ranging regeneration must take place to repopulate both the alveolar spaces as well as the epithelial cells. Club cells act as progenitors in the repair process of bronchiole epithelium[241]; however, after damage by H1N1 infection or bleomycin treatment, p63-positive cells proliferate and migrate[255] to areas of damage and begin the process of reconstruction of the both the alveolar cell types[255,256]. Further ablation of these p63-positive cells inhibits the lung repair and leads to pre-fibrotic lesions and reduced oxygen exchange[257].

Goblet/Mucin Cells

The lung is coated with a bilayer of differentially viscous liquids that provides protection from external toxin damage to the underlying epithelial cells. The upper mucus layer comes in contact with inhaled air while there is a sterile periciliary layer that contacts the underlying epithelial cells[258,259]. The topmost of the highly viscous mucus contains large heavily glycosylated proteins also known as mucins, for which there have been over 20 mucin genes identified to date[260]. The most abundantly expressed mucin genes in the goblet cells are MUC5AC and MUC5B[223,258,260,261]. The function of the mucus layer in the lungs is to trap inhaled particles and other toxins including bacteria and viruses[262-264]. In humans the mucins are secreted by the submucosal gland and goblet cells of the respiratory epithelium; however this layer is generated in mice solely from the mucous cells also known as goblet cells that are stimulated by inflammatory

responses predominately after birth (Figure 2)[264]. During normal physiological states murine lungs are nearly devoid of goblet cells; however, in human lungs there are goblet cells present without damaging events[258]. Goblet cells can arise from both the differentiation of basal cells[235,265-267], as well as from the club cells in response to damaging allergens, inflammation or other toxins[259,265].

The differentiation of Goblet cells must be tightly regulated for proper function of the pulmonary epithelium and air exchange. If goblet cells produce excessive mucins it can change the viscosity of the mucus throughout the pulmonary system and not allow for proper mucociliary clearance, which leads to many diseases[258-260,268]. The Notch pathway has been determined to be active in the proliferation of the goblet cells, through its activation in the basal cells[267] or in the differentiated club cells of the pulmonary epithelium[237]. Loss of Notch lead to loss of the club and goblet cells with increases in the frequency of ciliated cells[238,240]. On the other hand, FoxA2 inhibits the differentiation of goblet cells in the airways. The expression of Foxa2 is inhibitory of the goblet cell gene expression[269]. Foxa3 and Spdef regulate each other as well as promote the expression of genes observed within goblet cells[270,271].

Ciliary Development Within Multiciliated Cells

Discovery and Description of Cilia

Cilia were first observed by Antonie van Leeuwenhoek in 1676, making them the first organelle to be discovered[272,273]. Cilia are membrane bound microtubule cores that extend from a basal body. The innermost cytoskeletal

structure that makes up the cilia is referred to as the axoneme[274]. The axoneme structure is made up of 9 radial doublets of microtubules that may or may not surround an inner/central pair of microtubules, 9+0 and 9+2 configurations respectively, depending upon the function of the cilia.

Many cells within vertebrates generate a monocilium (primary cilia). Unlike the other cellular organelles, cilia are only generated after a cell has exited the cell cycle into a quiescent and/or differentiated state[275]. The primary cilia arise from a single basal body, formed by 9 doublet microtubules (9+0) but lack a central pair of microtubules. The basal body that this cilia is fixed to is the centriole that the cell used to split during mitosis. During interphase the centriole attaches to the membrane and microtubule assembly takes place directly onto the centriole[216,276]. These primary sensory cilia act as an antenna for receiving and sending both intracellular as well as extracellular signaling events[277-280].

Differentiation and development of multiciliated cells

For MCC differentiation, cells will initially develop a primary cilia some days before developing the fully ciliated border[281]. The development of cilia is a highly synchronized process that follows a consistent and tightly regulated process. Cilia are generated beginning with cell cycle arrest followed by basal body amplification/duplication, which then dock to the apical cellular membrane and further develop motile cilia[282]. Basal bodies in ciliated cells can arise directly from pre-existing centrioles as well as independently from centrioles within deuterosomes in close proximity to the centrioles that already exist[281,282]. The

deuterosome acts as an organizational center for the basal bodies of ciliated cells[281]. Basal bodies are generated in a highly organized and wave like manner, and the construction of cilia begins as soon as each wave of basal bodies are completed[281]. The forming basal bodies associate with membrane vesicles that later fuse with the membrane, which establishes the cilia/membrane compartment. At the base of the cilia, in many organisms and tissues, the basal body and plasma membrane forms a transition zone that includes a ciliary pocket, which is an invagination of the membrane and regulates the movement of factors between the cytoplasm of the cell and the cytoplasm within the cilia[283]. Microtubules are assembled exclusively at the distal end of the cilia[284], and since proteins are synthesized in the cytoplasm the elongation of the cilia requires intraflagellar transport (IFT) through kinesin and dynein motor-based transport[282,285].

Cilia and Disease

Patients with heart and abdominal viscera positioned in a mirror image to normal placement (also called *situs inversus*) also exhibited respiratory problems[286]. This disease was initially called Kartagener's Syndrome (KS) but was later grouped with other ciliated diseases into a larger grouping term of primary ciliary dyskinesia (PCD). More recent data incorporated right left randomization and respiratory illnesses both due to loss of motile cilia. A motile monocilia is observed at the node of developing mammals during embryogenesis that rotate in a clockwise direction creating a "nodal flow" of fluids[287]. When the

nodal cilia are either immotile or absent the nodal flow is deregulated and this leads to randomization of *situs*[288-290], as well as heart looping or randomized organ turning[288,291].

Some of the first patients that were diagnosed with a motile cilia disease were initially characterized in Denmark and Sweden, when the spermatozoa in sterile men were determined to be lacking the dynein arms within their individual flagella[292,293]. The patients also exhibited chronic rhinitis, sinusitis, bronchitis, and otitis. When both the tracheal[294] and bronchiolar[295] ciliated epithelium were investigated they also lacked dynein arms in these patients. Patients exhibiting these symptoms began to be grouped under the broad PCD diagnosis.

PCD is a heterogeneous diagnosis that is in reality a group of mostly autosomally recessive inherited genetic disorders that affects one in twenty thousand individuals at birth[296]. In patients with PCD, the airway cilia can be immotile, dysmotile, or absent causing the symptoms above. Many patients with PCD also exhibit asthma as well, and all of these respiratory characteristics combined can lead to the dilation of the bronchial airway, bronchiectasis, which is highly destructive to respiration[286]. Male infertility is very common in PCD due to immotility of sperm[297,298]. However, female sterility is infrequent in PCD. It has been shown that female patient infertility can be due to dysfunction among the motile cilia lining the fallopian tubes and uterine lining[298].

Hydrocephalus is a condition characterized by accumulation of cerebrospinal fluid in the ventricles of the brain. There are a few causes of this

condition including impaired cerebrospinal fluid flow, excess production, or lack of reabsorption[299-301]. Hydrocephalus caused by impaired fluidic flow of cerebrospinal fluid has been linked to abnormal or dysfunctional cilia within the ependymal cells lining the cerebral aqueduct[220,299,302] .

Transcriptional Control of Ciliary Development

Regulatory Factor X Transcription Factor Family

The regulatory factor X (Rfx) family of transcription factors regulates the expression of the components of the different types of cilia utilized in multiple tissue types[303]. All members within this family contain a winged-helix DNA binding domain that binds either as monomers or dimers within the minor grove of DNA[303] to X-box regions found in promoters of many genes. There have been eight individual mammalian Rfx family members identified[304-307] that are named Rfx1- Rfx8 respectively, and all of these eight are found within all vertebrates analyzed except within fishes where there are 9 Rfx factors[308].

Rfx5, Rfx7, and Rfx9 regulate biological functions outside of ciliary biogenesis, while Rfx1-Rfx4, Rfx6, and Rfx8 are evolutionarily conserved in the process of ciliary biogenesis[308]. Inactivation of any one of these factors results in mild defects of ciliogensis, indicating that there is functional redundancy and cooperatively among the different factors due to overlapping expression within MCCs[309-311]. The Rfx gene family is capable of homo- and hetero-dimerization at DNA binding sites indicating coordinated and interdependent transactivation of target genes[304,311,312]. Many of the genes regulated by the Rfx family encode

components of core ciliary biogenesis processes including structural components of the basal body and axoneme as well as components of the intraflagellar transport machinery[313-316], which leads to the specification of precursor cells into ciliated cell types[313,315,316].

Forkhead Box Gene Family, Foxj1, Role in Ciliogenesis

The Fox genes regulate transcription and were named after the *Drosophila melanogaster* gene fork head (fkh). This gene, when mutated, resulted in involution of the drosophila head during embryogenesis resulting in a head spike in adult flies[317]. Fox genes are present in saccharomyces cerevisiae (four genes) to humans (50 genes) and are subclassified into 19 subfamilies (e.g. Foxj1). The canonical forkhead domain directly binds to DNA is homologous between all species in which the Fox genes are expressed[318]. The canonical forkhead domain, also referred to as a winged-helix structure, is made up of three β-sheets, three α-helices and two 'wing' regions flanking the final β-sheets, and through structural studies binds to DNA as monomers, contacting DNA by the third α-helix and two wing structures[319-323]. The wing structures of the fork head domain dictate specificity and affinity of the proteins for their respective target sequences[323].

Several proteins from the subgroups of the Fox family contain two nuclear localization sequences (NLS)[324-326]. Of the two NLS, the one in the C-terminal portion of the forkhead domain is more highly conserved [324]. Thus, it is hypothesized that it acts as a common nuclear transport signal that is shared for

all Fox family members. Although the Forkhead domain is highly conserved between all members of the Fox family, the regions that flank this DBD contain poorly conserved highly specific effector domains that regulate the fox family functions. For example, some forkhead factors can act in tandem with other families of proteins through direct binding domains including the SMAD3 effector of Tgf-β, STAT3, or HoxA5[327,328].

A wide overview of Fox family member expression in human tissues indicates that the vast majority of the family proteins are expressed in a very selective/tissue-specific manner[329]. A small portion of the family members are expressed nearly ubiquitously across all tissues[330]. The tissue specific expression of the individual members of this family is thought to give rise to a wide array of activity within this family of genes. One would hypothesize that the tissue specific expression of each of these proteins leads to a very diverse role of Fox family genes in development and homeostasis of the tissues in which they are expressed.

FoxJ1 was first cloned from a rat lung cDNA library by PCR of the forkhead domain[331]. *In situ* hybridization showed that the expression of FoxJ1 was restricted to the mammalian tissues that require motile cilia[204,331-333]. FoxJ1 nuclear expression accumulated prior to ciliogenesis in the lung, trachea, oviducts, spermatids, and ependymal cells[334-336]. FoxJ1-deficient animals exhibited a complete loss of axonemes and motile cilia of the airways, oviducts, ependymal cells and also exhibit left-right asymmetry defects[337,338]. In the

deficient animals cells, the basal body docking to the cell membrane was impaired, but the amplification of basal bodies was not impaired[337,339,340]. Thus, FoxJ1 stimulates the later stages of multiciliogenesis in addition to ciliary commitment[341]. A transgenic mouse missexpressing Foxj1 off of the surfactant protein C promoter (commonly expressed in club and alveolar cells) triggered ectopic cilia formation in cells, which caused links between the alveoli that do not naturally produce cilia[334,335].

The role of Foxj1 in ciliary biogenesis is conserved across many species including xenopus and zebrafish[342,343]. Forkhead-like 13/hepatocyte nuclear factor 3 forkhead homolog 4 (Foxj1) is thought to be the oldest family member, and is found in the opisthokont, the last common ancestor of Fungi and Metazoans[344]. Of note, p73 is also expressed in this evolutionary ancestor[40].

Mcidas and Myb

Recently, multicilin [MCI (*Xenopus*) or Mcidas (mouse)] was identified; it is a coiled-coil protein that is negatively regulated by Notch and highly expressed in developing epithelia where MCCs form[345]. Inhibiting MCI specifically blocks MCC formation in *Xenopus*, whereas ectopic expression induces the differentiation of MCCs in ectopic locations. Multicilin activates gene expression required for MCC formation, including FoxJ1, and genes mediating centriole assembly. Although Mcidas has a coiled-coil domain and can activate transcription if tethered to the DNA through fusion with a DBD, it has not been shown to directly bind DNA[345] and likely functions as a co-activator of

transcription. It is thought to be necessary and sufficient to promote MCC differentiation in MTEC cultures[345].

Myb is a transcription factor encoded by the myeloblastosis proto-oncogene and is a member of the Myb family of TFs involved in cell cycle regulation and progenitor cell proliferation[341]. Myb is expressed in post-mitotic epithelial cells of the mouse airways destined to become MCCs and is thought to promote centriole amplification and the later steps of the multiciliogenesis program[346]. Conditional inactivation of Myb in the developing airway delays centriole amplification, expression of FoxJ1 and multicilogenesis[341]. There is not a total loss, rather a reduction of MCCs in Myb-deficient animals[346]. A working model is that Myb has an early role in multiciliogenesis, including a novel S-like phase in which centriole amplification can occur uncoupled from DNA synthesis, and that induction of later stages of ciliary biogenesis

Taken together, Myb and Mcidas are thought to act in one pathway, with Mcidas acting downstream of Notch signaling, but upstream of Myb, to activate genes that drive multiple basal body formation and to switch on FoxJ1 to activate genes required for basal body docking, ciliary outgrowth and motility[346,345,347].

The Role of p73 in Development: Goals of this Dissertation

Transcription factors regulate a wide array of cellular processes. To date, the mechanistic understanding of the p73 protein has primarily been focused on its role in tumorigenesis. Like p53, the role of p73 in cell cycle regulation and apoptosis has been widely studied to determine if there is a possible treatment

angle for patients with intact p73 signalling to treat cancers. Unlike p63, the role of p73 in development has been very minimally understood, with most focus on the development of the brain (due the phenotypic changes in mouse models in which p73 was ablated). Our study further unifies the diverse phenotypic changes observed in the *p73-/-* mouse models under a single biological function of p73 in the regulation of MCC development[1].

CHAPTER II

MATERIALS AND METHODS

CULTURED CELLS

Cellular Growth Conditions

The majority of the following cell lines were purchased from American Type Culture Collection (ATCC). BT549, DU4475, HCC1143, HCC1187, HCC1395, HCC1599, HCC1806, HCC1937, HCC38, and HCC70 were maintained in Roswell Park Memorial Institute (RPMI) 293FT, CAL120, CAL51, HCT116, H1299, HDQP1, HS578T, MDAMB157, MDAMB231 MDAMB436, MDAMB453, MDAMB468, RKO, SW527 maintained in Dulbecco's Modified Eagle's Medium (DMEM) (Life Technologies, Carlsbad, CA). BT20 and CAL851 were maintained in DMEM supplemented 10% fetal bovine serum (FBS) (Gemini Biologicals, West Sacramento, CA) and sodium pyruvate (Life Technologies, Carlsbad, CA). MCF10A were maintained in DMEM/F12 (Life Technologies, Carlsbad, CA) supplemented with horse serum (Gibco, Life Technologies, Carlsbad, CA), hEGF (Gibco, Life Technologies, Carlsbad, CA), 1.0 μg/ml hydrocortisone (Sigma-Aldrich, St. Louis, MO), 1 ng/ml cholera enterotoxin (ICN Biomedicals, Inc., Aurora, OH) and 1.0 μg/ml insulin (Novo Nordisk, Princeton, NJ). CAL148 were maintained in DMEM supplemented with 20% FBS and 1 μg/ml hEGF. MFM223 were maintained in MEM (Earle's Salts) (Life Technologies, Carlsbad, CA) supplemented with 15% FBS, insulin, apo-transferrin (Sigma-Aldrich, St. Louis, MO), and 15 nM sodium selenite (Sigma-

Aldrich, St. Louis, MO). SUM149, SUM159, and SUM185 were maintained in F12 Ham's (Life Technologies, Carlsbad, CA) supplemented with 5% FBS, insulin, and hydrocortisone.

Human Mammary Epithelial Cells (HMECs) were isolated by Kimberly Johnson from normal breast tissue that was acquired in coordination with the Vanderbilt-Ingram Human Tissue Acquisition and Pathology Shared Research (TPSR). The cells were cultured in DMEM/F12 medium 1:1 supplemented with 1.0 μg/ml insulin, 1.0 μg/ml hydrocortisone, 10 μg/ml, 0.1 mM phosphoethanolamine (Sigma-Aldrich, St. Louis, MO), 2.0 beta-estradiol (Sigma-Aldrich, St. Louis, MO), 10 nM 3,3',5-triiodo-L-thyronine sodium salt (Sigma-Aldrich, St. Louis, MO), 15 nM sodium selenite, 2.0 mM L-glutamine (Gibco, Life Technologies, Carlsbad, CA), 1% penicillin-streptomycin (Gibco, Life Technologies, Carlsbad, CA), 1 ng/ml cholera enterotoxin (ICN Biomedicals, Inc., Aurora, OH), 1% FBS and 35 μg/ml BPE (Gibco, Life Technologies, Carlsbad, CA).

Murine Tracheal Epithelial Cells (MTEC), whose harvest is described in a later section in full detail, were grown DMEM/F12 supplemented with [1M HEPES (Sigma-Aldrich, St. Louis, MO), 200 mM L-glutamine (Sigma-Aldrich, St. Louis, MO), 7.5% $NaHCO_3$ (Sigma-Aldrich, St. Louis, MO), 1% penicillin-streptomycin (Gibco, Life Technologies, Carlsbad, CA), Fungizone (Life Technologies, Carlsbad, CA), 10 μg/ml Insulin (Novo Nordisk, Princeton, NJ), 5 μg/ml apo-transferrin, 0.1 μg/ml cholera toxin (Sigma-Aldrich, St. Louis, MO), 25 ng/ml

hEGF, 0.03 mg/ml bovine pituitary extract (Gibco, Life Technologies, Carlsbad, CA), 5% and retinoic acid (Sigma-Aldrich, St. Louis, MO)]

VA10, human bronchiole epithelial cells, were generously shared with us by the Thórarinn Guõjónsson group at the University of Iceland[253]. Cells were cultured in Bronchiole Epithelial Growth Media (BEGM) (Lonza Walkersville, Inc., Walkersville, MD) supplemented with single-quots of bovine pituitary extract (BPE), hydrocortisone, human epidermal growth factor (hEGF), epinephrine, apo-transferrin, insulin, retinoic acid, triiodothyronine, and 1% penicillin-streptomycin all provided from Lonza Walkersville, Inc., Walkersville, MD. VA10 cell line was passaged by trypsinizing cells for approximately 5 minutes at 37˚C, neutralizing trypsin with 0.5 mg/ml soybean trypsin inhibitor (Gibco, Life Technologies, Carlsbad, CA), centrifuging cells at 1500 RPM for eight minutes, and re-plating in their normal growth media.

All medias were supplemented with 10% FBS (Life Technologies, Carlsbad, CA) and 1% penicillin-streptomycin (Gibco, Life Technologies, Carlsbad, CA) and trypsinized using 0.25% Trypsin at 37˚C unless otherwise noted.

Lentiviral Generation of shRNA and Overexpression Vectors

Lentiviral methods of RNAi-mediated knockdown or cDNA overexpression were utilized for the following dissertation work. Lentiviral vectors were transfected with Lipofectamine 2000 (Invitrogen, Life Technologies, Carlsbad, CA) into 293FT cells along with 10 μg PAX2 and 10 μg pMD2 viral packaging

vectors. Media containing lentiviral particles was harvested 48 hours after transfection filtered through 0.45 μM filters, and concentrated using Lenti-X concentrator (Clontech, Mountain View, CA). Prior to infection of target cells polybrene (Sigma-Aldrich, St. Louis, MO) was added to the media at a final concentration of 6 μg/ml and incubated at room temperature for 15 minutes. Viral media was immediately added to target cells and not frozen because it resulted in maximal shRNA knockdown.

shRNA gene targeting: The human pSicoR lentiviral system was utilized for knockdown of p73[31,60,348,349]. The combination of TAp73-1 and TAp73-2 shRNAs yielded the best knockdown of p73. We also utilized Sigma-Aldrich Mission pLKO.5-puro shRNA system (Sigma-Aldrich, St. Louis, MO) for knock down of p73 in human and mouse cells. TRCN0000272526, TRCN0000272527, and TRCN0000272587 yielded the greatest knockdown in human cells and TRCN0000430727 and TRCN0000012757 yielded the best results in MTECs. 24 hours after infection, target cells transduced with Mission lentivirus were selected for by addition of puromycin at the concentration determined to have optimal effects at 48 h for each individual cell line.

Exogenous Overexpression vectors: p73 isoform specific exogenous overexpression experiments were conducted using pcDNA3 backbone constructs that were kindly provided by Backendorf and Melino[79,350]. Yeast two-hybrid candidate interacting proteins were cloned into 3xFLAG cDNA vector (Sigma-Aldrich, St. Louis, MO). Transfection was performed using Lipofectamine in

H1299 and 293 cells (Invitrogen, Life Technologies, Carlsbad, CA). FoxJ1 lentiviral overexpression cDNA vector (Thermo Scientific, Waltham, MA) was used to express full length FoxJ1 by viral production in 293FT and further infection of target cells. Cells were lysed for immunoprecipitation, RNA analysis, and immunoblot 24-48 hours after transfection.

Protein Harvest

Cells were trypsinized, pelleted, and washed with ice-cold phosphate-buffer saline. Depending upon the downstream uses for the protein lysate cells were lysed with radio immunoprecipitation assay (RIPA) buffer [150 mM NaCl, 1% Nonidet P-40, 0.5% deoxycholate, 0.1% SDS, 50 mM Tris [pH 8.0], 5 mM 39 EDTA] or EBC lysis buffer [50mM Tris pH 7.5, 100mM NaCl, 0.5% NP40]. Lysis buffers were supplemented with phosphatase inhibitors [50 mM NaF, 0.2 mM NaVanadate, 10 mM p-nitrophenyl phosphate] and protease inhibitors [antipain (10 mg/ml), leupeptin (10 mg/ml), pepstatin A (10 mg/ml), chymostatin (10 mg/ml) (Sigma-Aldrich, St. Louis, MO), 4-(2-aminoethyl)-benzenesulfonylfluoride (200 mg/ml) (Merck, EMD Millipore, Darmstadt)]. Cells were incubated in lysis buffer for 30 minutes total and vortexed for 10 seconds every ten minutes for a total of 3 vortex cycles. The lysate was centrifuged at 13,500 RPM for 15 minutes at 4°C and the supernatant was collected. Protein levels were determined using the Bio-Rad Protein Assay (Bio-Rad Laboratories, Inc., Hercules, CA) kit and the lysates were stored at -80.

Immunoblot Analysis

Protein lysate was boiled in 1x Laemmli sample buffer for five minutes and then separated using SDS polyacrylamide gel electrophoresis (SDS-PAGE). Proteins were transferred to Immobilon-P membranes (Millipore, Billerica, MA) using the Transblot Turbo (Bio-Rad Laboratories, Inc., Hercules, CA) system. Membranes were blocked in 5% nonfat dry milk dissolved in TTBS (100mM Tris-HCL pH 7.5, 150mM NaCl, 0.1% Tween-20) for one hour at room temperature and incubated in primary antibody overnight at 4˚C. All antibodies used in immunoblot analysis and the concentrations at which they were used can be found in Table 1. All immunoblots were washed in TTBS (50 mM Tris, 150 mM NaCl, and 0.05% Tween 20 pH 7.6) washes and incubated for an hour in HRP-conjugated secondary antibodies. After this incubation the immunoblots were rocked in three successive ten minute TTBS washes. Finally, enhanced chemiluminescence (ECL) reagent for film exposure was used for visualization of protein expression levels.

Immunoprecipitation

Co-immunoprecipitation (co-IP) of p73 with possible binding partners was performed following cellular protein lysis using EBC Buffer [120 mM NaCl, 0.5 (v/v) Nonidet P-40, 5 μg/ml leupeptin, 10 μg/ml aprotinin, 50 mM Tris-Cl (pH8.0] supplemented with phosphatase inhibitors and protease inhibitors as above. Protein G Dynabeads (ThermoFisher Scientific, Waltham, MA) were incubated with 0.5-1 mg of protein from cellular lysates for one to two hours. After this pre-

Antibodies Utlized For the Study of p73							
Epitope	**Alt. Name/ Catalog no.**	**Company**	**Species**	**Western**	**Immunoflourescence**	**IP/ChIP validated**	
p73	EP436Y	Epitomics/Abcam	Rabbit	1 to 500	1 to 1,200**	Y	**p53 Family Antibodies**
p73	A300-126A-2	Bethyl	Rabbit	1 to 1,000		Y	
p73	IMG-246	Imgenex	Rabbit	1 to 200			
p73	IMG-259	Imgenex	Rabbit	1 to 200			
p63	4A4	Santa Cruz	Rabbit	1 to 1,000			
p63	H129	Santa Cruz	Rabbit	1 to 500	1 to 40 and/or 1 to 1,000 **	Y	
p53	DO1	Santa Cruz	Mouse	1 to 1,000			
Uteroglobin	Ab40873	Abcam	Rabbit		1 to 140,000**		**Lung Markers and Proteins**
PGP9.5	Ab8189	Abcam	Rabbit		1 to 750		
FoxJ1	14-9965	eBiosciences	Mouse		1 to 200**		
FoxJ1	Sc-517	Santa Cruz	Mouse	1 to 200			
C-MYB	C-19	Santa Cruz	Rabbit		1 to 1,000**		
acetelated Alpha tubulin	6-11B-1	Sigma Aldrich	Mouse		1 to 50,000		
Traf3ip1			Rabbit		1:3000**		
Gamma tubulin	H-183	Santa Cruz	Rabbit		1 to 2,000**		
Cytokeratin 5	20R-CP003	Fitzgerald	Guenia Pig		1 to 200		
Keratin 14	30R-2140	Fitzgerald	Guenia Pig		1 to 200		
p21	F5 (sc-6246)	Santa Cruz	Mouse	1 to 300			**Downstream Targets of p53 Family**
p21	556430	BD	Mouse	1 to 300			
MDM2	Ab1	Calbiochem	Mouse	1 to 250			
MDM2	Smp14	Santa Cruz	Mouse	1 to 200			
puma	4976	Cell Signalling	Rabbit	1 to 500			
Noxa	114C307	Calbiochem	Mouse	1 to 250			
PARP	9542	Cell Signalling	Rabbit	1 to 500			**Biological Readout**
Actin	A5316	Sigma Aldrich	Mouse	1 to 10,000			
Ki-67	550609	BD Pharmagen	Mouse		1 to 1,000**		
FLAG	F3165	Sigma Aldrich	Mouse	1 to 500		Y	**Co-associated Proteins (Yeast two-Hybrid)**
Tab2	C88H10	Cell Signalling	Rabbit	1 to 500			
TAB2	A302-759A	Bethyl	Rabbit	1 to 500			
TAK	3456-1	Epitomics	Rabbit	1 to 500			
EPN1	h-130 (sc-25521)	Santa Cruz	Rabbit	1 to 300			
EPN2	c-16 (sc-5414)	Santa Cruz	mouse	1 to 500			
NEDD4-2	46521	Abcam	Rabbit	1 to 1,000			
RSL1D1	SAB1400486	Sigma Aldrich	Mouse	1 to 500			
ITCH	H-110	Santa Cruz	Rabbit	1 to 200			
iASPP	A4605	Sigma Aldrich	Rabbit	1 to 1,000			
iASPP	ab34898	Abcam	Rabbit	1 to 500			
WWP2	N-15 (sc-11896)	Santa Cruz	Goat	1 to 500			
WWP1	K-20 (sc-11894)	santacruz	Goat	1 to 500			

Table 1. Antibodies Used in the Study of p73 and its Biological Roles. Antibody epitope target is listed along with the catalog number and company purchased from. Western blot analysis and/or immunoflourescence experiments were conducted using the antibody at the dilution indicated in the table in either 2% milk (Western blot) or 5% goat serum (immunofloursecence). Antibodies utilized for immunoprecipitation have been annotated in the above table. Each of the antibodies are further categorized by the biological function.

clearing of the lysate, a slurry of beads complexed with optimized antibody of interest (in general 1-3 μg antibody was added to 1 mg IP) was added to the lysate and incubated for 2-4 hours with end-over-end rotation at 4˚C. The beads were washed (via magnetic separation) a total of four times 10 minutes each in respective cell lysis buffer utilized for each cell type. Lamilli sample loading buffer was added to the bead, antibody, co-IP mixture. These samples were then incubated at 95˚C for six minutes and analyzed by Western analysis.

mRNA Isolation and Expression Analysis by qRT-PCR:

RNA was harvested from cells using the Aurum Total RNA Mini kit (Bio-Rad Laboratories, Inc., Hercules, CA). Cells were needle passaged 25 times through a 23-gauge needle in the enclosed lysis buffer to ensure complete lysis of cells for mRNA harvest. Samples were incubated with DNase for 30 minutes at room temperature directly on the column during RNA purification

cDNA was generated from total RNA using the TaqMan Reverse Transcription kit (Applied Biosystems, Roche, Basel, Switzerland). A total of 750 ng of RNA was added to each reaction and resultant cDNA was diluted 1:5 before conducting qRT-PCR. qRT-PCR was conducted using an iCycler (Bio-Rad Laboratories, Inc., Hercules, CA) instrument and the iQ SYBR Green Supermix (Bio-Rad Laboratories, Inc., Hercules, CA). Primers for genes of interest were designed using Primer-3 software[351] or manually. All primers that were utilized for this dissertation work can be found in Table 2. A standard curve and melting curve analysis was conducted for each qRT-PCR to assess PCR

Primer Sequences Utlized for the Study of p73			
Primer Name	**Sequence**	**Human**	**Mouse**
p73-Exon 5 For	GACATGCCCCATCCAGATCA	✓	✓
p73- Exon 5 Rev	AGCTCGTGGTTGGGGCAGCG	✓	✓
p73-Exon 6-7 For	GTGGATGACCCTGTCACCGG	✓	✓
p73-Exon 6-7 Rev	GAAGTTGTACAGGATGGTGG	✓	✓
p73-Exon 10 For	GGAGCTTGTGCCCCAGCCTTTG	✓	✓
p73-Exon 10 Rev	GGTGACTCGGCCTCTGTAGG	✓	✓
FoxJ1 For 1.2	TGACAGCCTGACCAGCCTGC	✓	✓
Foxj1 Rev 1	TGGTGGTAGCCGTGGGGGTC	✓	✓
Cdc20b For 2	CTGGTCTTCGAAATGACTAC	✓	✓
Cdc20b Rev 2	ACTTCTCCCTCGCTGGTGCC	✓	✓
Mcin For 3	CTGGATAAGCTGATGATCAC	✓	✓
Mcin Rev 3	GGATGGCGTCCACTTCCGCG	✓	✓
Dll1 For 3	TTCCCCTGGGTGGCCGTGTG	✓	✓
Dll1 Rev 3	CGGACGCGACCACCACAGC	✓	✓
E2f5 For 1	CTGGATCTCAAAGCGGCTGC	✓	✓
E2f5 Rev 1	CAATTCCCTCTAAGACATTG	✓	✓
Notch1 For 5	GGCTTCACGGGCAGCTACTG	✓	✓
Notch1 Rev 5	GCACAAGGTTCTGGCAGTTG	✓	✓
Notch3 For 3	GGCGTGGGCTCCTTTTCCTG	✓	✓
Notch3 Rev 3	CGGTGAAGGAGGCCACGTG	✓	✓
Mdm2 For 3	TTTCCTTAGCTGACTATTGG	✓	✓
Mdm2 Rev 3	TGAGTTTTCCAGTTTGGCTT	✓	✓
Rrad For 1	TTCATTGAGACATCAGCGGC	✓	✓
Rrad Rev 1	GTGGCAGGACTTGGATTTGG	✓	✓
Dnaili For1	CGGGCGGTCACCATCAACTG	✓	✓
Dnail1 Rev 1	TGCAGTGCCTTCCTCATGCC	✓	✓
Ppp1cc For 2	GACCAACTGATGTACCAGATC	✓	✓
Ppp1cc Rev 2	CCAAATGTGAAGGACACTCC	✓	✓
Ccp110 For 2	GTTAGCTTTTGAAGAAATGCG	✓	✓
Ccp110 Rev 2	CTCCTGCTCTTCTATTTCCTT	✓	✓
Gmnn For2	AAGAAATTGAACAAAAGGAC	✓	✓
Gmnn Rev 1.2.3	CTTCAGAATCAAATTCCTGA	✓	✓
Mdm2 For	CCCCTTCCATCACATTGC	---	✓
Mdm2 Rev	TTACAATCAGGAACATCAAAGC	---	✓
Cdkn1a For	CCTTGGCCTGCCCAAGC	---	✓
Cdkn1a Rev	CTTGGAGAAGATCAGCCG	---	✓
Gapdh For	CATGTTCCAATATGATTCC	---	✓
Gapdh Rev	CCTGGAAGATGGTGATG	---	✓
p73-For 2	ACTTTCCAGCAGTCCAGCAC	---	✓
p73-Rev 2	GGACACCTTGATCTGGATGG	---	✓
p73-For 3	GTCAGCCACCTGGACGTACT	---	✓
p73-Rev 3	GGAGCAGACTGTCCTTCGTT	---	✓

Primer Sequences Utlized for the Study of p73			
Primer Name	**Sequence**	**Human**	**Mouse**
Puma For 2	CCACCACCATCTCAGGAAAG	---	✓
Puma Rev 2	ACGTTTGGCTCATTTGCTCT	---	✓
Puma For 3	TGAGCCAAACGTGACCACTA	---	✓
Puma Rev 3	GCAGAGCACAGGATTCACAG	---	✓
Noxa For	CCGTGTGTAGTTGGCATCTC	---	✓
Noxa Rev	CCCACTCAGCGACAGAGC	---	✓
p53 For	GCCAAGGGAGGGAAAAGG	---	✓
p53 Rev	CTCTAACTAGGCTCAGGCTACC	---	✓
Jag1 For 1	CAACCGTGCCGTGACTATTTCTGC	---	✓
Jag1 Rev 1	TGTTCCCGTGAAGCCTTTGTTACAG	---	✓
p73 L	TGCGACATCTTTTGGTTCTG	---	✓
p73 R	GTCCCAAGTCCAGCAGAGAG	---	✓
Foxj1 L2	AAGCCTCCCTACTCGTATGC	---	✓
Foxj1 R2	GCAGCCGTTGTCCGTGATCC	---	✓
Traf3ip1 L2	TGGTTGTAATGGTGTCGGGA	---	✓
Traf3ip1 R2	ACCGCATCGTCACTAGAGAG	---	✓
Stk33 L	CGGTATTTGGGGTGGTCTC	---	✓
Stk33 R	AGGTCCCCACAGTAAGTTCG	---	✓
Myb L3	GACTTTGAGATGTGTGACCATGA	---	✓
Myb R3	CTTTCCAGTCATCTGTTCCATTC	---	✓
Cct4 L	TGCTTTGCAGATGCTATGG	---	✓
Cct4 R	GGACAACCAGTTCCTCCAAA	---	✓
Spag16 L	ACGACGGGGAGATTCTCTT	---	✓
Spag 16 R	ACCTGCTGGCACATTTAACC	---	✓
Dvl3 L	GAGGCTGAGGCACAAGAATC	---	✓
Dvl3 R	GCAGGCAAGATTGAGTCACA	---	✓
Mink1 L	AAGAAGCGGGGTGAGAAAGA	---	✓
Mink1 R	CAGGCACGTTCATGATGGAG	---	✓
Cp110 L2	TGACTGTGGGAAGATGGAGG	---	✓
Cp110 R2	GCCACTCCATGAAAGCGAA	---	✓
Rbl2 L3	AGATCTCTCTTGGCCTGCTG	---	✓
Rbl2 R3	ACACCTCTCTACAAAGGCC	---	✓
E2f4 L	TCCTCATGAGTGACGTAGGC	---	✓
E2F4 R	CGGGCGCAAGAACTAGACGA	---	✓
Lztfk L2	TCTGCAGAGTTGGGCCTAAA	---	✓
Lztfk R2	AGCCTCTCTTTGAACGAGCA	---	✓
B-actin For	GTTTGAGACCTTCAACACCC	---	✓
B-actin Rev	CATTGCCAATGGTGATGACC	---	✓
Gapdh For	AGGTCGGTGTGAACGGATTT	✓	---
Gapdh Rev	GGGGTCGTTGATGGCAACA	✓	---
Gapdh For	CATGGCCTTCCGTGTTCCTA	✓	---
Gapdh Rev	CCTGCTTCACCACCTTCTTGAT	✓	---

Table 2. Primers Used for the Study of p73 and its Biological Roles. The primer target is listed along with the sequence of the primer itself. Checkmarks annotate the species (human and/or mouse) to which the primers were designed target.

efficiency, purity, and quality of the final products. The cycling conditions used were: 95°C for 3 minutes, 40 cycles of 95°C for 10 seconds with annealing temperatures between 55-62°C (proper primer specific annealing temperatures were determined before experimental usage).

MURINE MODEL

Generation of *p73* Knockout Mice

The generation of a mouse model with a conditional *p73* allele is illustrated in Figure 3. A vector targeting *p73* exons 7, 8, and 9 was made using BAC recombineering vectors and methods[352]. The targeting vector was electroporated in 129S6 mouse ES cells and neomycin resistant clones were screened by southern blot hybridization (Figure 3). Male chimeric mice made by the microinjection of clone 2A7 into blastocysts isolated from C57Bl6 mice were bred to C57/Bl6 females mice for detection of germline transmission of the *p73* allele referred to as $p73^{floxE7\text{-}9N}$. The FRT-flanked neomycin resistance gene was removed by crossing to a global *FlpE* 'deleter' mouse[353] line to derive mice with $p73^{floxE7\text{-}9}$ allele. For the experiments described herein, we globally deleted exons 7-9 by crossing $p73^{floxE7\text{-}9}$ to a BALB/c-Tg (CMV-Cre)1Cgn/J then interbreeding to obtain *p73+/+, p73+/-* and *p73-/-* animals. All procedures were conducted in compliance with NIH guidelines and following IACUC approved protocols. The experiments presented occurred in mixed strain mice, however we have confirmed the lack of ciliated cells in BALB/c congenic *p73*-/- mice.

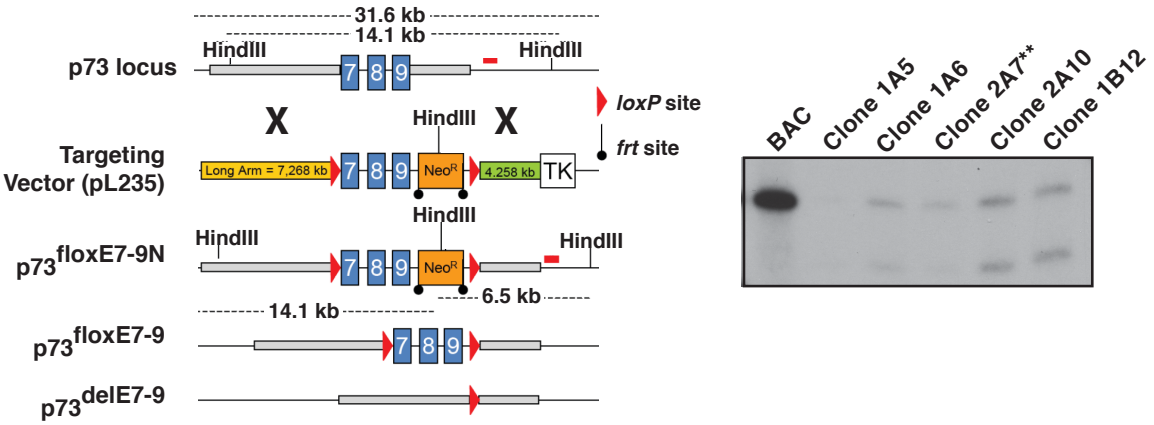

Figure 3. Generation of the *p73*$^{floxE7-9}$ Mice. Schematic representation of the targeting strategy used to conditionally delete exons 7, 8, and 9 of p73. Red triangles denote the introduced loxP sites. Black circles represent Frt sites utilized to remove the neomycin resistance cassette (NeoR) (orange box) by crossing with a FlpE deleter mouse. The red rectangle marks the location of an exon 14 Southern probe for identification of recombinant clones in combination with Cla1 and HindII restriction enzymes. A second probe located outside the long DNA homology arm that was used to screen the mESCs. Clone 2A7 (**) had germline transmission leading to the mice utilized for this study. Mouse targeting strategy was designed by Mark Magnuson, Jennifer Rosenbluth, and Lucy Tang. Southern blot was generated by Deborah Mays.

Murine Tissue Harvest

Animals were sacrificed following all Institutional Animal Care and Use Committee (IACUC) approved methods. Mice were overdosed using isoflurane and the tissues of interest were removed for analysis following cervical dislocation. Tissues that were utilized for further analysis by H&E or immunofluorescence were fixed in cassettes submerged in 10% neutral buffered formalin (NBF) (EMB Chemicals, Gibbstown, NJ) overnight. After overnight fixation the samples were delivered to Vanderbilt University Translational Pathology Shared Resource (TPSR) for further processing and paraffin embedding. Tissue utilized for protein or RNA were immediately flash frozen in liquid N_2 upon removal from the animal.

Histological Staining of Murine Tissue

Alcian Blue: Unstained paraffin embedded tissues were de-paraffinized and re-hydrated through xylene and successive alcohol washes. The mucins were stained with 1% alcian blue solution at pH 2.5 for 30 minutes at room temperature as previously described[354]. The nuclei of these sections were then counterstained with nuclear fast red for five minutes. The slides were then dehydrated and coversliped using xylene-based Cytoseal (Thermo Scientific, Waltham, MA).

Hemotoxylin and Eosin (H&E): Unstained paraffin sections of tissue were rehydrated and stained for 5 minutes using modified Mayer's hematoxylin (Richard-Allen Scientific, Thermo Scientific, Waltham, MA). Tissue sections were

washed thoroughly to remove any remaining stain and then stained using Eosin Y (Richard-Allen Scientific, Thermo Scientific, Waltham, MA) for 1 minute. Cells were then dehydrated and coverslipped using xylene-based Cytoseal.

Immunofluorescence

De-paraffinization and rehydration of tissue sections was followed by antigen retrieval using citra buffer and heating. Tissue was permeablized using 0.1% Tween 20 in PBS. The tissue sections were blocked with 5% goat serum and 0.3% Triton X in PBS for one hour at room temperature. Some of the antibodies listed in Table 1 required amplification of signal in order to observe positive immunofluorescence (**). For those tissues that were stained with an amplification step, endogenous HRP background was quenched by processing the tissue through a three percent hydrogen peroxide solution for at least five minutes. Tissues were all blocked using Image-it Enhancer (Life Technologies, Carlsbad, CA) for 30 minutes at room temperature, and if the sections were to be stained with antibodies generated in mice the section was incubated in M.O.M block (Vector, Golden, CO) at room temperature for one hour. Primary antibodies were incubated on respective tissues overnight at 4˚C. We used either fluorescently labeled secondary AlexaFlour (Life Technologies, Carlsbad, CA) or CY3/FITC TSA amplification kit (Perkin Elmer, Waltham, MA) for visualization of immunoflourescence. For TSA amplification we utilized HRP-conjugated secondary antibodies commonly used in Western blotting to bind to the respective primaries that require amplification. After one hour of incubation in

secondary the tissue was incubated for eight minutes using CY3/FITC diluted 1:50 in dilution buffer for eight minutes. After this incubation tissue was washed and cover slipped using SlowFade Gold with DAPI (4'6-diamidino-2-phenylindole) (Life Technologies, Carlsbad, CA).

MTECs were processed in a similar manner as the tissue sections stained by immunofluorescence except that the cells were fixed using four percent paraformaldehyde (PFA) for 10 minutes.

Image Capture and quantification: All images were captured using Leica DM IL LED microscope (Leica, Solms, Germany) and qCapturePro 6.0 software paired with a QiCam Fast1394 (QImiging, Burnaby, BC, Canada). Immunofluorescence images were quantified using ImageJ software.

Tissue Protein Harvest

Tissue was placed in RIPA buffer containing the phosphatase and protease inhibitors listed in the protein harvest section above. The tissue was homogenized on ice for one minute with care to ensure that the sample did not go through a period of foaming which results in loss of protein yield. After homogenization the tissue was incubated on ice for 30 minutes, and were vortexed for 10 seconds every ten minutes for a total of 3 vortex cycles. The samples were pelleted at 4˚C by centrifugation at 13,500 rpm for 15 minutes. Immunoblot analysis of protein was performed as described above.

Tissue mRNA Isolation and Quantification:

Flash frozen tissue was weighed and appropriate amount of trizol was added to the tissue (1 ml TRIzol per 50-200 mg tissue). The tissue was homogenized for 1 minute using a hand-held homogenizer, and chloroform was used to separate the RNA from the rest of the lysate. The RNA was then column purified using the Aurum Total RNA mini-kit in the mRNA isolation and expression analysis by qRT-PCR section above. cDNA preparation and qRT-PCR was completed as described above.

Murine Tracheal Epithelial Cell (MTEC) Isolation

Mice were euthanized following IACUC guidelines and the entire mouse was rinsed with ethanol in order to best sterilize the animal and reduce the amount of hair that will carry over into the cell culturing system. Tracheas were removed from above the larynx to the bifurcation of the trachea and placed in Ham's F12 (Gibco, Life Technologies, Carlsbad, CA) media. They were then cleaned of any excess tissue in a laminar flow hood, and the tracheas were cut lengthwise to expose the inner tracheal epithelium. The tracheas washed three times with Ham's F12 [supplemented with 0.002% Gentamicin (Life Technologies, Carlsbad, CA), 0.001% Fungizone (Life Technologies, Carlsbad, CA), and 1% Penicillin-Streptomycin], and placed in a 0.15% protease from Streptomyces grisseus (Sigma-Aldrich, St. Louis, MO) solution (1 ml protease per trachea) for an overnight incubation at 4˚C.

Tracheas were inverted 20-25 times after the overnight incubation and then further incubated for one hour at 4°C. After the overnight protease incubation epithelial cells were isolated from the tracheas by washing them three times with Ham's F12 supplemented with twenty percent FBS in order to inactivate any protease before culturing the subsequent epithelium. After the three washes the remaining tracheal tissue was discarded and the supernatant containing the epithelial cells was pelleted at 1400 RPM for 10 minutes at 4˚C. Cells were then suspended in DNase solution (100 μL per mouse trachea) and incubated at room temperature for ten minutes. Fibroblasts were selected against in MTEC cultures by culturing the cells for four hours in PRIMARIA coated tissue culture dishes (Falcon, Thermo Fisher Scientific, Waltham, MA) (up to 15 tracheas per dish). After the separation of loosely adherent fibroblasts from the non-adherent epithelial cells the MTECs can be grown on collagen coated plates and transwells for differentiation.

Air Liquid Interface (ALI) Differentiation

MTECs have been utilized to recapitulate the developing mouse airway epithelium in a transwell organotypic culturing system. Cell isolation and methods for differentiation[355,356] of these cultures in an organotypic submerged culture or at an air liquid interface (ALI) were utilized have been previously reported[253,254]. Transwells were coated with collagen using 4.1 mg/ml rat-tail collagen (Gibco, Life Technologies, Carlsbad, CA) mixed with 0.02 N acetic acid. Plates or transwells were collagen coated overnight at 37˚C by adding 1 ml

collagen to each 12-well transwell or a 24-well plate. After overnight incubation the remaining liquid was removed from the well and allowed to dry. PBS was used to wash the collagen-coated wells three times and then the plates were allowed to dry before plating of the cells.

MTEC were seeded at a density to reach 100% confluent within two to three days of growth on the collagen-coated well and maintained in MTEC Plus Growth Media (Gibco, Life Technologies, Carlsbad, CA) for approximately five days. After the cells reached 100% confluency, the cells were stimulated to differentiate by removing the media above the transwells (generating an air interface) and adding MTEC differentiation media [MTEC Plus Growth Media supplemented with 2% NuSerum (Sigma-Aldrich, St. Louis, MO) and Retinoic Acid (Sigma-Aldrich, St. Louis, MO)] to the lower chamber of the transwell. Cells were fed every 48 hours during the period of differentiation (generally a fully differentiated epithelium is evident by day 14-16).

Immediate *ex vivo* Murine Tracheal Crosslinking and ChIP-seq

Immediate ex vivo epithelial cell harvest and crosslinking: For each of the individual chromatin immunopreciptation (ChIP) experiments utilizing mouse tracheal epithelial cells in this dissertation work 50 animals (~50 million tracheal epithelial cells) were combined per ChIP condition. The crosslinking and cellular processing took place immediately following sacrifice without freezing in between. Following IACUC approved guidelines mice were sacrificed and the tracheas of the animals were removed within 60 seconds of death. Tracheas

were removed as cleanly as possible while retaining the larynx. After the trachea was removed from the organism it was opened lengthwise using small scissors and proteins were cross-linked with 1 ml of 1% formaldehyde for eight minutes. Of note the tissue turns more opaque and white throughout the crosslinking protocol. After the eight minute incubation in formaldehyde the crosslinking was quenched by adding glycine (Thermo Fisher Scientific, Waltham, MA) to a final concentration of 0.125 M. The trachea was incubated in the formaldehyde/glycine mixture for two to five minutes.

After quenching of the crosslinking reaction the tracheas were stored on ice in PBS + complete protease inhibitor (CPI) (Roche, Basel Switzerland) to protect from degradation. All 50 tracheas were scraped one at a time into 1ml of RIPA + CPI. After scraping the tracheas they were placed back in PBS + CPI on ice. At the end of tracheal scraping, trachea PBS/CPI mixture was slightly vortexed and the leftover tracheas were removed. The mixture was centrifuged at 2000 RPM for ten minutes in order to collect any residual epithelial cells that were missed during scraping, and the pelleted cells were added to the RIPA buffer used for scraping. Once all of the tracheal epithelial cells were combined into the RIPA + CPI, the solution was vortexed every 15 minutes for a total 45 minutes of lysis.

Human cell line crosslinking: Human cell line ChIP-seq was also conducted with 50 million cells alongside the scraped tracheal cells as a control for experimental methods. HCC1806 and HMEC lines were grown to 70%

confluency and prior to crosslinking they were washed once with PBS. Cells were cross-linked with 30 ml of 1% formaldehyde (Thermo Fisher Scientific, Waltham, MA) was added to each 15 cm dish (Sarstedt Nümbrecht, Germany) and the cells were incubated at room temperature for 10 minutes. The crosslinking process was quenched by adding glycine as discussed above. The cells were then scraped from the plate into ice-cold PBS/CPI, pelleted at 2000 RPM for 5 minutes at 4˚C, and then re-suspended for sonication.

Sonication: All sonication procedures were conducted on ice and at 4˚C. A Biorupter (Diagnode, Denville, NJ) sonicator was used to shear genomic DNA to fragments averaging 300bp in size. To prevent warming of the samples, the Biorupter probes and water tank was refilled with ice-cold water after each session of sonication. All samples were processed as pairs and sonicated for 20 minutes on the high setting with 30 second on 30 second off cycles. The Biorupter water bath was cooled after the first 10 minute sonication. After completing sonication of each sample, nuclear and cellular debris were pelleted by centrifugation at 14,000 RPM at 4°C. The supernatant of each sample was collected. 50 μL of each sample was checked by agarose gel electrophoresis to verify proper sonication.

ChIP: The p73, p63, and Pol II antibodies that were optimized for ChIP using Protein G Dynabeads (Invitrogen, Life Technologies, Carlsbad, CA). For each ChIP, 90 μL of bead slurry was washed using blocking buffer [1xPBS, 0.5% Tween20, 0.5% BSA] + CPI for 30 minutes. The respective antibodies that were

to be used in the ChIP were then coupled to the magnetic beads for three hours by adding 30 μg of the antibody to the beads in 500 μL of cold blocking buffer/CPI. Each sonicated sample of 50 million cells was added to the antibody/bead mixture and rotated end-over-end for 2-4 hours at 4˚C.

After the four hour incubation the samples were washed four times with RIPA and four times with IP wash buffer [100mM Tris pH 8.5, 500 mM LiCl, 1% NP40, 1% deoxycholic acid] + CPI. The ChIP beads were then resuspended in ChIP elution buffer [25mM Tris pH 7.5, 2mM EDTA, 200mM NaCl, and 0.5% SDS] and incubated at 65˚C for fifteen minutes with intermittent vortexing. For optimal elution the first eluate was saved and a second elution was conducted following the same steps as above, and both elusions were combined before purification of enriched DNA.

DNA purification and Library generation: Proteinase K was used to digest the proteins that were attached to the sonicated DNA overnight at 56˚C. We then used phenol-chloroform extraction followed by ethanol precipitation to purify the DNA. To each of the DNA sheared samples we added 200 μl of phenol chloroform (pH 8.0) and vortexed to adequately mix the sample. They were then centrifuged on full speed for 5 minutes. The aqueous top layer was removed to a clean tube avoiding touching any of the lower separated phases of liquid. We then added 150 μl of 10 mM Tris (pH 8.3) and again the samples were vortexed to mix then centrifuged for 5 minutes at top speed. The uppermost aqueous phase was combined with the earlier separated fraction. Ethanol was added (2.5

volumes) as well as 0.1 volume of 3 M NaAc and 3 μl of glycogen to the phenol chloroform separated samples. These samples were centrifuged at top speed at room temperature for 45 minutes. The aqueous solution was then removed from the precipitated DNA pellet and the samples were dried. The DNA was re-suspended in 30 μl of water.

The protocol used to generate libraries was a modification of standard Illumina protocols. After DNA was purified we initially polished the ends of the sonicated fragments to make sure that the ends were filled and optimal for later steps of library generation (polishing). Sonication of chromatin generally produces 5' phosphates; however, in order to aid in the efficiency of the library generation we utilized a kinase step that ensures that all of the chromatin possesses 5' phosphates (kinase). The next step in library generation was to add a single adenosine nucleotide to the 3' end of DNA (A-tailing), which aids in the ligation of indexes. In our modified protocol, the index sequence used to identify each sample after next generation sequencing (NGS) was included in the adapters used for library preparation thereby allowing a single ligation step (ligation).

Many library generation protocols utilize purification steps between the polishing, kinase, and A-tailing steps. However, since the amount of DNA isolated from our protocol was very low, we conducted a single purification step after ligation. We used AMPure beads (Agilent Technologies, Santa Clara, CA)

that bind to ChIP DNA of select size but not to any residual larger oligos remaining in the sample to purify the DNA fragments of interest.

After our ChIP DNA was purified the samples were PCR amplified (18 cycles [98˚C 20 sec., 52˚C 1 min., 72˚C 1 min.] to generate sufficient DNA for NGS. The PCR reaction was gel purified (Qiagen Gel Extraction kit) from an agarose gel that was run long enough to separate 100-500 bp fragments the PCR libraries from any primer dimers or primers that remained in the samples as well as fragments that were much longer. All three ChIP-seq experiments were conducted in duplicate. Input DNA was harvested from the pooled trachea samples that cross-linked and sonicated, but did not undergo immunoprecipitation to serve as a comparison control for systematic bias.

ChIP-seq Data Analysis

Twenty to fifty million single-end 50 bp reads were generated for each ChIP-seq library using the Illumina HiSeq platform. Reads were trimmed to remove adapters sequences with Flexbar v2.4[357], aligned to GRCm38 using BWA-backtrack v0.6.1[358] with default parameters, and filtered to remove reads with mapping qualities less than 30. MACS2 v2.0.10.20131216[359] was used to identify sites of genomic binding with default parameters and a q-value threshold of 0.05 using an input control. MACS2 binding sites were filtered to remove mouse ENCODE blacklisted regions[360] and mitochondrial DNA sites. Annotation of binding sites with the nearest GENCODE M7 comprehensive TSS and overlap with genomic features was performed using Homer[361] v4.7. Motif analysis was

conducted using the GLAM2[362] command line tool. Correlation of read counts between ChIP-seq samples at sites of p63, p73, or Pol II genomic binding was performed with the deepTools bamCorrelate command line tool[363]. The read alignments of ChIP-seq samples were 1X depth of coverage normalized for display in IGV using deepTools[363] bamCoverage command line tool. To analyze the overlap between our p73 ChIP-seq and the cilia-associated gene list[364], we restricted our analysis to those genes shared between the different annotation methods used between the two studies.

Scraped Murine Tracheal RNA Harvest, qRT-PCR, and Sanger Sequencing

RNA was harvested from tissue by scraping the epithelium of the trachea in TRIzol and purified using the Aurum Total RNA Mini kit (Bio-Rad). qRT-PCR experiments were conducted using oligo(dT)-mediated first-strand synthesis and SYBR Green (Bio-Rad) quantification. mRNA levels were quantified using primers targeting exon 5, the exon 6/7 junction, and exon 10 of p73 (Table 2). Sanger sequencing was conducted using identical primers.

MTEC Exogenous Expression and RNA Harvest

MTECs were isolated, cultured, and differentiated as previously described. MTECs harvested from p73+/+ and p73-/- mice were infected twice (at time of plating and 12 h later) with TAp73β and FG12-CMV control expression vectors as described previously[31,60]. For Fig. 17, MTECs were grown as submerged cultures on collagen-coated plates for 3 d in MTEC growth media (DMEM/F12 supplemented with HEPES, L-glutamine, $NaHCO_3$, penicillin-streptomycin,

fungizone, insulin, apo-transferrin, cholera toxin, EGF, bovine pituitary extract and FBS). For Fig. 16 and Fig. 17, MTECs were grown as submerged cultures on collagen-coated plates for 3 d in DMEM and then switched to differentiation media containing 2% NuSerum for 3 d [355,356]. For Fig. 15, MTECs were grown in transwells containing MTEC growth media for 5 days and then lifted to air-liquid interface for 24 h in differentiation media, followed by RNA harvest using the Aurum Total RNA Mini kit (Bio-Rad).

shRNA-Mediated Gene Knockdown in MTECs

shRNAs directed to the 3' untranslated region (shRNA 1-GAACTGCCCTTAGCTACATAT) and exon 6 (shRNA 2-AGTGTGGTTGTGCCGTATG) of p73 were purchased from Sigma Aldrich. MISSION TRC2 Non-Mammalian shRNA (Sigma Aldrich) was used as a negative control. Viral production and transduction was performed as described above in the cell culture section. For knockdown within the harvested MTEC cultures we determined that optimal gene knockdown was obtained by plating the MTEC cells in viral media that was concentrated using the Lenti-X Concentrator (Takara, Clontech, Mountain View, CA). The cells were treated 16 h with lentivirus and a second infection was conducted by refreshing the cells with viral media for 8 h.

RNA-seq and analysis

For Figure 15, RNA from five scraped tracheas was pooled in duplicate experiments and submitted to the Vanderbilt Technologies for Advanced Genomics core for library preparation and RNA-seq. For Fig. 15 and Fig. 16,

duplicate samples for each of the four genotype/expression conditions (total n=8) were submitted to the HudsonAlpha Genomic Services Lab for library preparation and RNA-seq. For both experiments, reads were trimmed to remove adapter sequences with Flexbar v2.4 [357] and aligned to mm10 using STAR [365] v2.4.2a with GENCODE [366] M7 comprehensive gene annotations. Cufflinks v2.1.1 [367] was used to assemble transcripts and quantify their abundance. Cufflinks FPKM estimates were converted to TPM estimates[368]. For differential gene expression analysis, reads were assigned to GENCODE M7 comprehensive genes using feature Counts [369] (v1.4.6-p5) and tested for differential expression using DESeq2 [370] v1.8.1 with default parameters. Genes with an adjusted p-value <0.1 in the DESeq2 output were considered significantly differentially expressed. Raw sequencing data have been deposited at the NCBI Sequence Read Archive under bioproject number PRJNA310161.

CHAPTER III

p73 IS REQUIRED FOR MULTICILIOGENESIS AND REGULATES THE FOXJ1-ASSOCIATED GENE NETWORK

Introduction

The p53 family of proteins, including p53, p63 and p73, are sequence-specific transcription factors required for cell cycle control, DNA repair, apoptosis and cell differentiation[15,18,21,371,372]. There are functional and physical interactions amongst the family, including coordinate binding and regulation of target genes. *p63* and *p73* have two promoters; isoforms transcribed from P1 contain a transactivation domain (TAp63 and TAp73), whereas isoforms transcribed from P2 lack the TA domain (ΔNp63 and ΔNp73) and have been shown to act in a dominant-negative manner to TA isoforms[15,21].

p73 and p63 share 63% and 60% sequence identity, respectively, with the p53 DNA binding domain, and the residues that contact DNA are identical. In contrast to the tumor-suppressive role of p53, p63 is essential for maintaining the progenitor cell populations required to sustain epithelial development and morphogenesis[23]. p63-null mice die shortly after birth and exhibit profound developmental defects in ectodermal-derived tissues[22,23,85].

Compared to p53 and p63, the physiological role of p73 is poorly understood. Mice lacking p73 exhibit runting, sterility, hippocampal dysgenesis, hydrocephalus and chronic infection and inflammation in the lungs, sinus and ears[16]. To date, no unifying mechanism has been identified to explain these

diverse phenotypes. Through analysis of a p73-deficient mouse model developed in our laboratory, we discovered that the affected tissues share in common a loss of multiciliated cells (MCCs).

Motile cilia are located on the apical surface of epithelial cells lining tissues that require fluid movement. Coordinated beating of cilia is essential for mucus/infiltrate clearance in the airway, sinus and ears and the prevention of infections and inflammation in these tissues[373]. In the reproductive tract, dysfunction of motile cilia lining the efferent duct and oviduct has been implicated in the sterility of both males and females[297,298]. In the brain, lack of ependymal flow due to defective motile cilia can cause closure of the cerebral aqueduct and result in hydrocephalus and hippocampal dysgenesis[220,299,302]. In all of these tissues, transcription factor Forkhead box J1 (Foxj1) is required for the transactivation of genes encoding proteins involved in ciliogenesis. In Foxj1-deficient mice, multiple basal bodies are produced, however the basal bodies do not dock properly on the apical surface of the cell to initiate the formation of cilia, leading to dysfunctional MCCs[339].

We provide evidence that p73 is a direct regulator of *Foxj1* and is required for proper MCC differentiation[1]. In addition, we found that p73 is expressed in terminally-differentiated MCCs as well as a subset of basal cells in the tracheal epithelium. p73-/- mice exhibit hyperplasia of epithelial cells followed by loss of the airway epithelium in older animals, implying that p73 may also be required for airway homeostasis. Using *in situ* protein-DNA crosslinking in the tracheal

epithelium and chromatin immunoprecipitation with massively parallel DNA sequencing (ChIP-seq), we found that p73 binds in close proximity to 105 cilia-associated genes, some of which have been previously described as regulators of MCC development. We identified three p73 binding sites within 10,000 base pairs of the *Foxj1* transcriptional start site (TSS) and discovered that p73 regulates and is required for Foxj1 expression in primary cultures of tracheal epithelial cells[1].

Results

p73-/- Mice Lack MCCs, Have Areas of Focal Epithelial Hyperplasia but Overall Loss of Airway Epithelium

Our *p73* knockout mouse model exhibits phenotypes previously reported in p73-deficient animals[16], including runting (Figure 4A); hippocampal dysgenesis; hydrocephalus (Figure 4B); chronic infections and inflammation of the lungs, middle ear and sinus (Figure 4B) as well as increased mortality (Figure 5A) and sterility (Figure 5B). Through histological analysis, we noted defects in the developing follicles of the *p73-/-* females (Figure 5C) as well as severe degeneration as well as compaction of seminiferous tubules of the *p73-/-* males (Figure 5D). After histological analysis, we noted an apparent absence of MCCs in *p73-/-* mice and hypothesized that the loss of this cell type could provide a unifying mechanism for the well documented, multi-organ defects occurring in these animals.

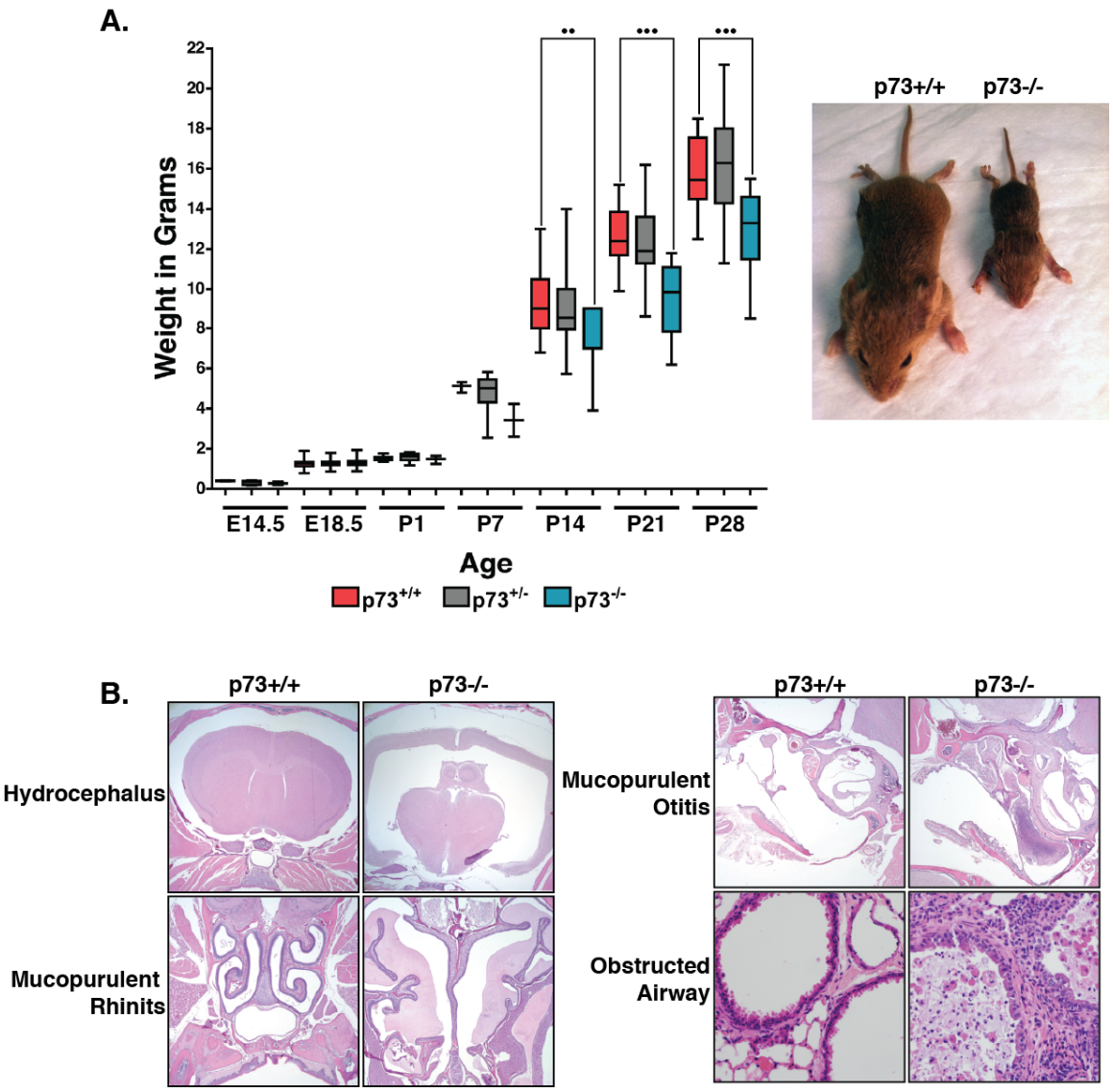

Figure 4. Novel *p73* Knockout Mouse Recapitulates Earlier Published Phenotypes (A) Box and whisker plot representing the weight of mice from E14.5 through P28. More than eight mice were weighed from p73+/+ (red), p73+/- (gray), and p73-/- (blue) at the given timepoints. . p-values are annotated as <0.0001 (•••) and <0.001 (••). Littermate male *p73+/+* and *p73-/-* mice photographed at P28. (B) Micrographs of H&E stained tissues representing reported phenotypes of Hydrocephalus, Mucopurulent rhinitis, Mucopurulent otitis, as well as obstruction to airways observed in the *p73-/-* animals. Mouse targeting strategy was designed by Mark Magnuson, Jennifer Rosenbluth, and Lucy Tang. All data represented was collected by Clayton Marshall with technical assistance from Deborah Mays.

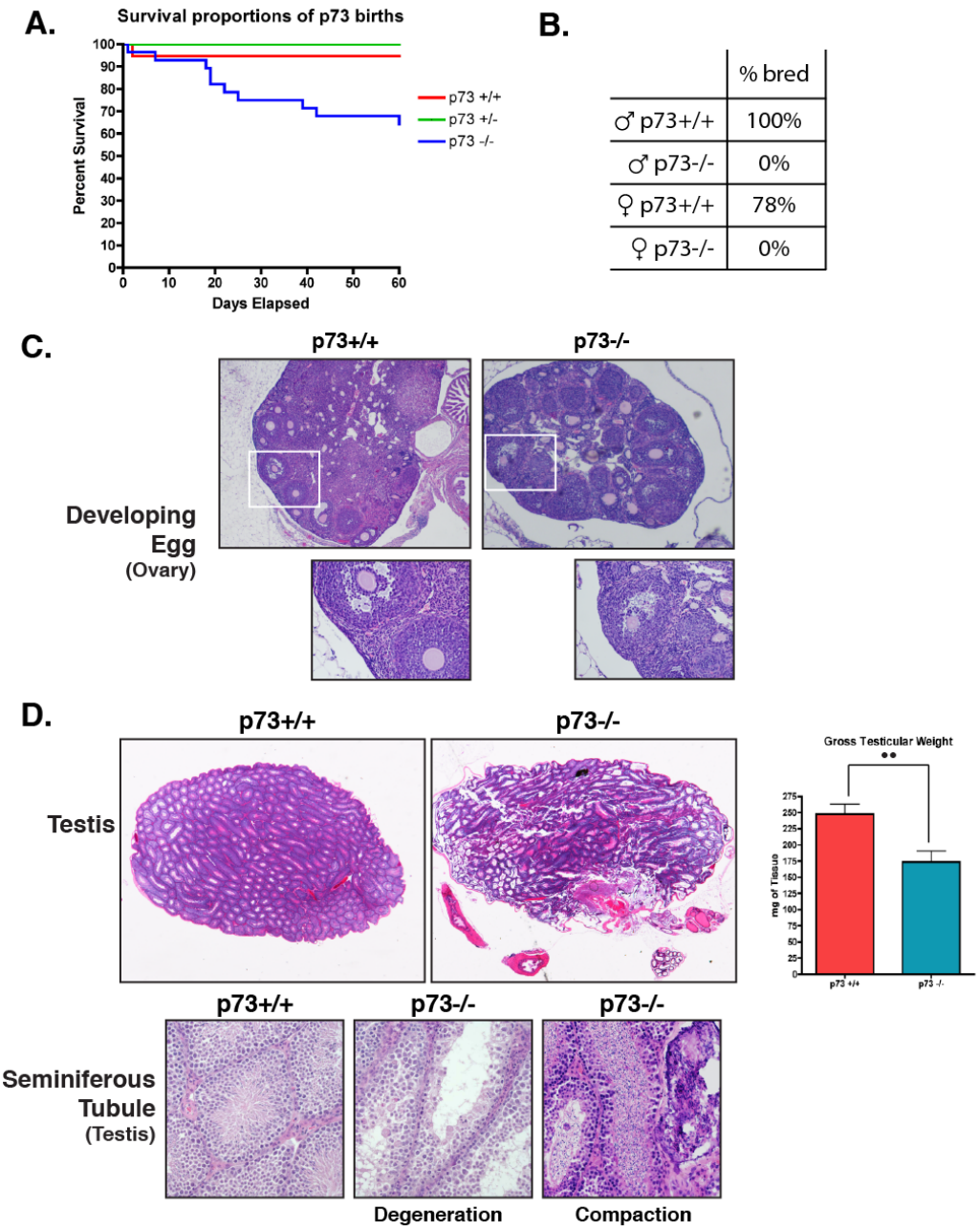

Figure 5. p73-/- Mice Have Increased Mortality and are Sterile (A) The viability of 12 litters of pups was tracked graphically represented here. (B) Eight pairs of each genotype were placed with the opposite gender for 14 days to observe if the animals were fertile. (C) representative micrographs of H&E stained ovaries from p73+/+ and p73-/- post-puberty animals. (D) Representative micrographs of H&E stained p73+/+ and p73-/- testis of six month old males. The testis of males ranging from two to six months old were weighed and are represented in the column graph. . p-value of <0.001 is represented as (••). Representative micrographs of seminiferous tubule degeneration and compaction observed in p73-/- animals. All data represented was collected by Clayton Marshall.

To confirm the absence of MCCs, we performed hematoxylin and eosin (H&E) staining and immunofluorescence (IF) detection of p73 and acetylated alpha-tubulin (*α-tubulin), a well-established marker of cilia[374]. In contrast to *p73+/+* control animals, we observed a lack of cilia in the oviduct, middle ear and sinus mucosa, flagella of sperm in the testis, and respiratory tract of *p73-/-* mice (Figure 6A). We also noted a lack of MCCs in the ependymal cells (data not shown). It was recently reported that p73 is strongly expressed in murine ciliated ependymal cells and is required for their survival[107]. p73 protein expression appeared nuclear by IF and was detected in the epithelium of *α-tubulin-positive tissues in *p73+/+* animals (Figure 6A). To determine if ciliated epithelium failed to develop *in utero* or was lost over time after birth, as well as to determine if other members of the p53 family have roles in MCC development, we performed IF for *α-tubulin on the respiratory tracts of E18.5 wild type mice and animals deficient in p53[32], p63[33], or p73. We found p73 knockout animals lacked cilia in bronchioles *in utero*, *p63-/-* animals had increased cilia as previously reported[250] and p53-/- animals were similar to wild type (Figure 6B).

The p73 mouse model characterized herein was generated by flanking exons 7 through 9 of *p73* with tandemly-oriented loxP sites by gene targeting in mouse ES cells (Figure 7A and Experimental Procedures). Mice containing the $p73^{floxE7\text{-}9}$ allele were bred with CMV-Cre mice to globally impair p73 in all tissues (*p73-/-*). Sanger sequencing of p73 cDNA verified that *p73-/-* animals express an mRNA variant that encodes the amino-terminal portion of the protein up to Q243

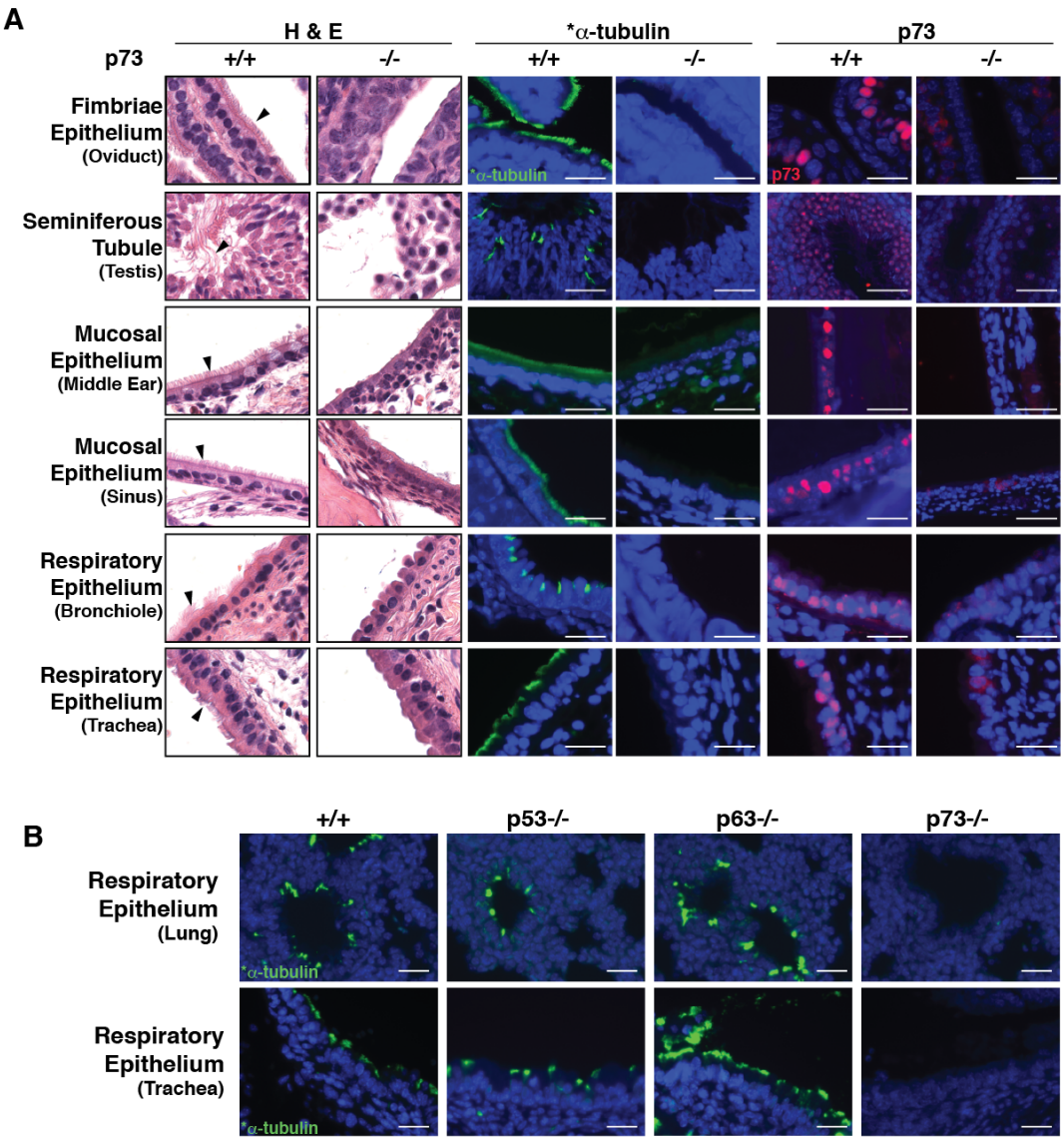

Figure 6. Global Ablation of p73 Eliminates MCCs (A) Representative H&E and immunofluorescence (IF) micrographs of the indicated tissues from *p73+/+* and *-/-* mice. Arrowheads mark cilia and flagella (testis). IF was performed using antibodies recognizing the cilia marker *α-tubulin (green) and p73 (red). (B) Representative micrographs of IF staining of *α-tubulin in embryonic day 18.5 tracheas and lungs from *p53-/-, p63-/-* and *p73-/-* animals. (scale bars = 25 μm). All data represented was collected by Clayton Marshall.

(in exon 6), which is then spliced to the codon for the first amino acid in exon 10, V358 (Figure 7B). This truncated version of p73, which lacks part of the DNA binding domain, nuclear localization signal, and oligomerization domain[6], is functionally inactive as a transcription factor. qRT-PCR from *p73-/-* animals confirmed loss of full-length p73 mRNA (Figure 7C). Western blot analysis of lung tissue also showed loss of the full-length p73 protein and appearance of a faster-migrating immunoreactive band in *p73+/-* and *p73-/-* animals, with a molecular weight consistent with expression of a truncated p73 protein (Figure 7D). By IF staining, the truncated p73 protein is occasionally visible in the cytoplasm of *p73-/-* cells (Figure 6A).

To further validate the role of p73 in proper MCC differentiation, murine tracheal epithelial cells (MTECs) were isolated from *p73+/+* and *p73-/-* mice as previously described and grown as air liquid interface (ALI) or 2-D submerged cultures[355,356]. Under either culture condition, MCCs were not evident until differentiation was induced by transfer of confluent cultures to differentiation media[355,375]. After transfer to differentiation media in ALI or 2-D culture, *α-tubulin-positive MCCs were observed in *p73+/+* MTECs but not in *p73-/-* cells, recapitulating the phenotype we observed *in vivo* (Figure 6 and 7E). To evaluate potential confounding effects of the truncated, cytoplasmic protein generated in our p73 knockout model, we expressed two shRNAs targeting exon 6 and the 3'-UTR of p73 in the *p73+/+* and *p73-/-* MTECs. In *p73+/+* cells, we observed an acute loss of p73 expression and a concomitant loss of *α-tubulin-

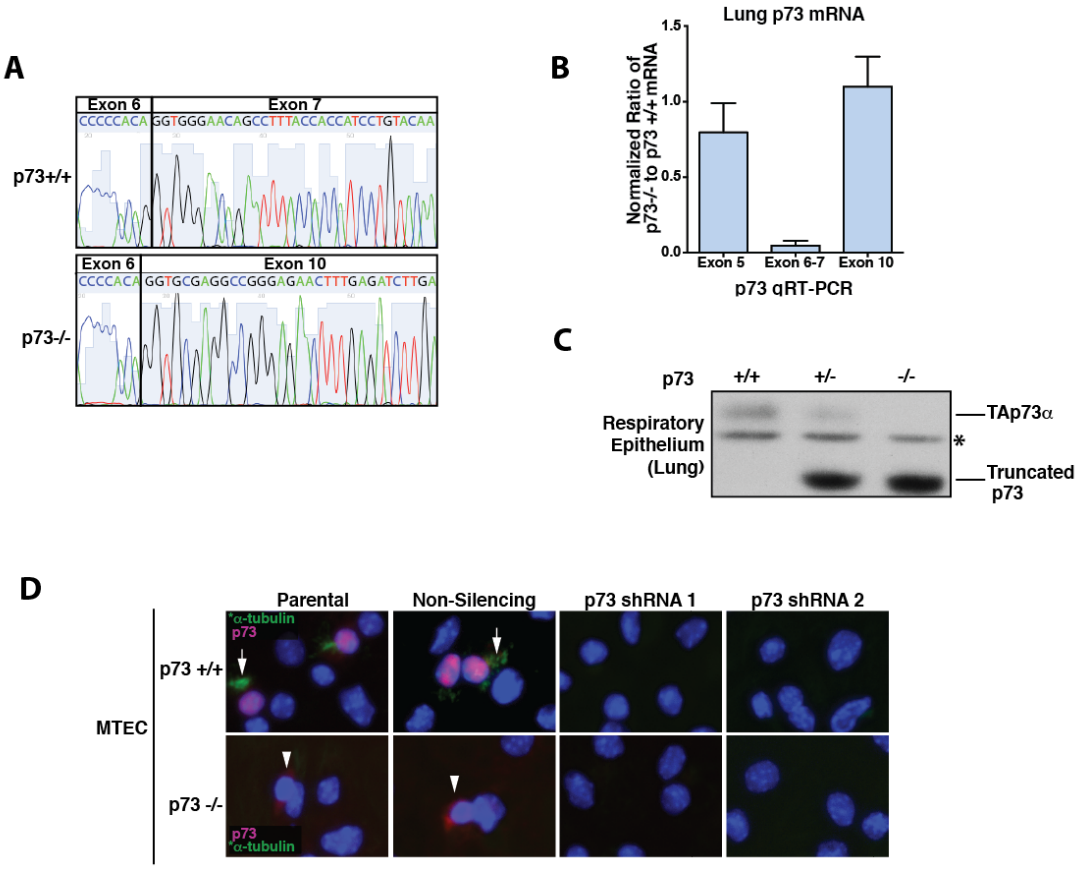

Figure 7. Generation of the *p73*$^{floxE7\text{-}9}$ Mice (A) Sanger sequencing of a PCR product from lung cDNA indicates in-frame splicing of exons 6 and 7 (p73+/+) and exons 6 and 10 (p73-/-). (B) qRT-PCR of lung cDNA was performed using primers within exon 5, across the exon 6/7 boundary, and within exon 10 of p73. Data are represented as normalized ratios of *p73-/-* to *p73+/+* mRNA expression. (C) Western analysis of protein harvested from lung tissue of the indicated genotyped animals shows absence of full-length p73 protein in the *p73-/-* animals and a faster migrating immuno-reactive band in the *p73+/-* and *-/-* samples, with a molecular weight consistent with expression of a p73 protein lacking exons 7-9 (* = non-specific band). (D) Micrographs of MTECs isolated from tracheas of *p73+/+* or *p73-/-* animals, infected with non-silencing (NS) or two different p73 short hairpin RNA silencing constructs (shRNA 1 & 2), and grown in differentiation media. Representative IF staining of p73 (red) and *α-tubulin (green) is shown for each condition. Arrows indicate cilia and flagella within *p73+/+* animals. All data represented was collected by Clayton Marshall with technical assistance from Deborah Mays.

positive MCCs (Figure 7E). In *p73-/-* MTECs, shRNA expression resulted in loss of the cytoplasmic, truncated p73 visible in control cells (Figure 7E, arrowheads); after knockdown, these cells were still unable to differentiate into MCCs (Figure 7E). These data confirm that both p73 mRNA knockdown and *p73-/-* exon 7-9 deletion led to an absence of MCCs, ruling out confounding or dominant-negative effects of the truncated protein observed in *p73-/-* cells.

To evaluate the long-term consequences of MCC loss in *p73-/-* mice, we necropsied 10 mice of each genotype at 18 months of age. In contrast to *p73+/+* controls, all *p73-/-* mice evaluated had significant loss of epithelium in a majority of bronchioles with areas of focal hyperplasia (Figure 8A) that were positive for expression of cytokeratins (Figure 8B). In the areas of epithelial loss, there was hypertrophy and hyperplasia of underlying alpha smooth-muscle actin (α-SMA)-positive cells (Figure 8B). The lack of MCCs led to retained debris, mucus and inflammatory cells in the bronchioles, which resulted in crystalline pneumonia in many animals (Figure 9A). This loss of bronchiole epithelium was exhibited as early as six months of age (data not shown) and its severity increased in the older animals. We also observed chronic mucopurulent otitis and rhinitis in our *p73-/-* animals of all ages (Figure 9B), consistent with previous reports[16].

We did not observe tumor formation in *p73-/-* animals. Both our model and the mice previously generated by the McKeon group[16] harbor functional inactivation of both TA and ΔN isoforms of p73, and neither model exhibits an increased susceptibility to lung tumors. TAp73 has been

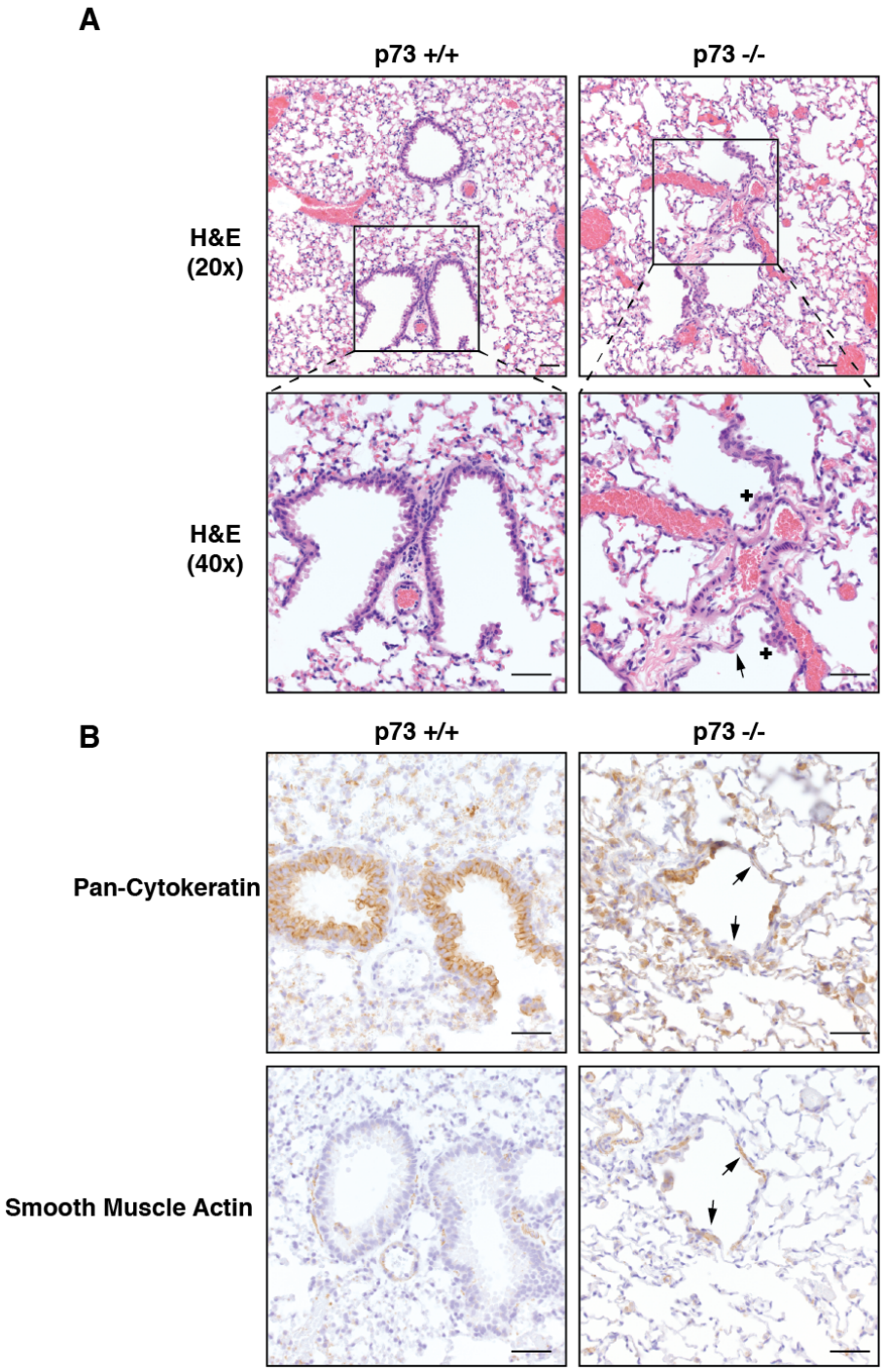

Figure 8. *p73-/-* Mice Exhibit Severe Airway Phenotypes Including Hyperplasia and Epithelial Loss (A) Representative H&E images of the terminal airways in 18 month old *p73+/+* and *p73-/-* mice. The *p73-/-* mice exhibit areas of epithelial loss (arrow) and small nodules of hyperplastic epithelium (+). (B) Immunohistochemistry (IHC) staining of pan-cytokeratin and α-SMA of above mice. Arrows in panel B indicate areas of epithelial loss as well as hypertrophy and hyperplasia of the smooth muscle (scale bar= 50 μm). All data represented was collected by Kelli Boyd.

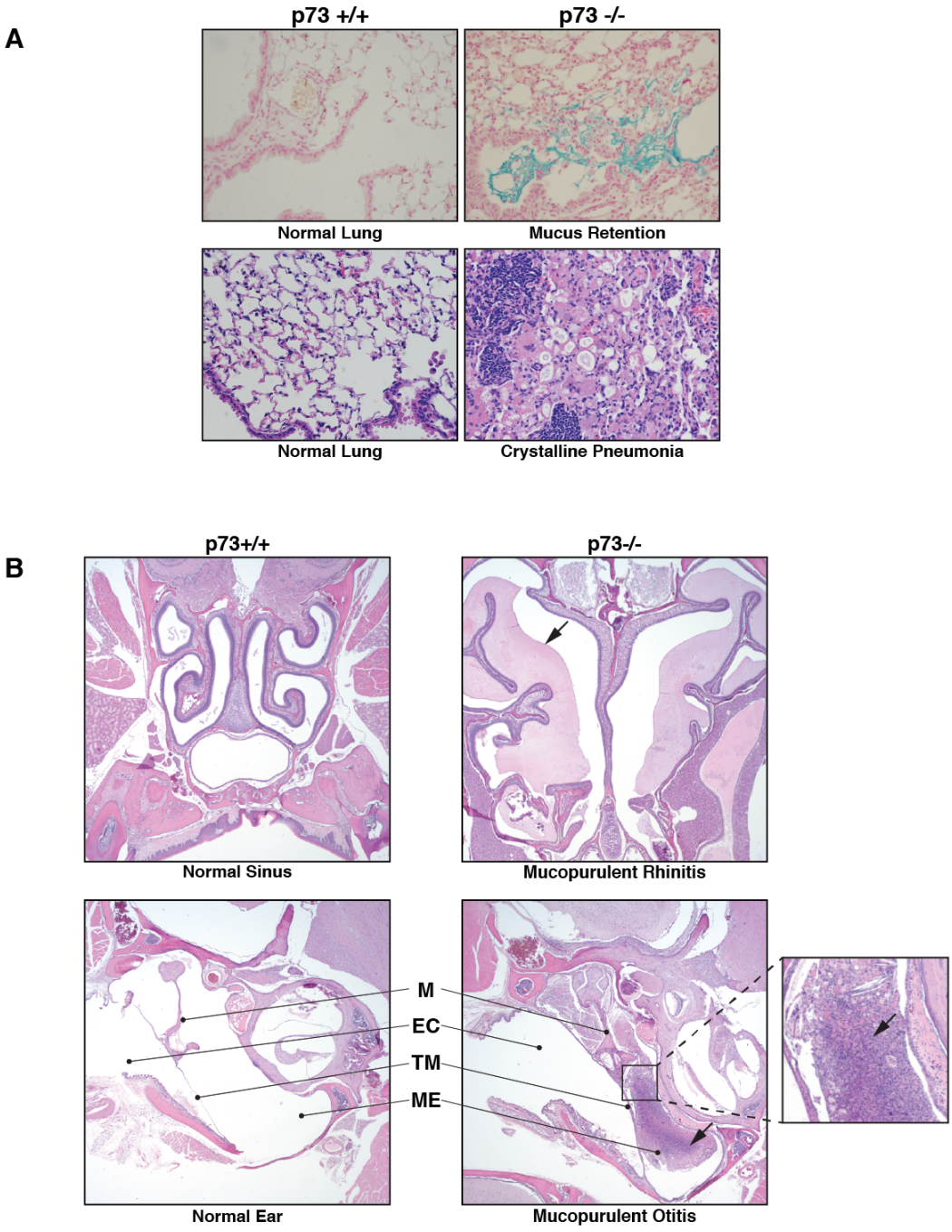

Figure 9. *p73-/-* Mice Show Evidence of Infection and Inflammation in the Lung, Sinus and Ears (A) Representative images of alcian blue (top panel) and H&E (bottom panel)-stained lungs from *p73+/+* and *p73-/-* mice. Mucin-producing cells and retained mucus are stained blue. (B) Representative H&E images of sinus and ears of *p73+/+* and *p73-/-* mice. The external ear canal (EC), middle ear (ME), tympanic membrane (TM) and malleus (M) are labeled. Arrows indicate areas of mucus and inflammation in the upper and lower panel, respectively. All data represented was collected by Kelli Boyd and Clayton Marshall.

demonstrated to possess tumor suppressive activity *in vivo*, as knockout of this isoform without removal of ΔNp73 in mice led to spontaneous lung adenocarcinoma[17]. We hypothesize that the loss of all isoforms of p73 results in a reduction or an absence of lung tumor progenitor cells.

The Airways of p73-/- Mice Have Reduced Numbers of Basal cells in Addition to MCC-Deficient Phenotype

To determine the impact of MCC loss on the distribution of other cell types in the murine airway, we performed IF with antibodies to well-established cell-type specific markers including: Scgb1a1 (club), Foxj1 (MCC), Pgp9.5 (neuroendocrine), Alcian blue (mucin) and p63 (basal) (Figure 10; data are presented as percentage of total epithelial cells with representative micrographs in Figure 11). In *p73-/-* mice, we observed a 90% loss of Foxj1-positive MCCs in the trachea and bronchiole ($p<0.0001$), a 35% reduction of basal cells in the trachea ($p<0.0001$), and a significant increase in mucin-producing, club, and neuroendocrine cells throughout the airway (Figure 10). In *p73+/-* mice, MCCs were reduced by 23% and 44% in the trachea and bronchiole, respectively.

The Airways of p63-/- Mice Have Reduced Numbers of Club and Basal Cells

p63 is commonly used as an airway basal cell marker[34,241,251] and is implicated in regulation of the murine tracheal epithelium[250] and human bronchial cell differentiation[253]. In *p63-/-* mice, we observed an increase in MCCs,

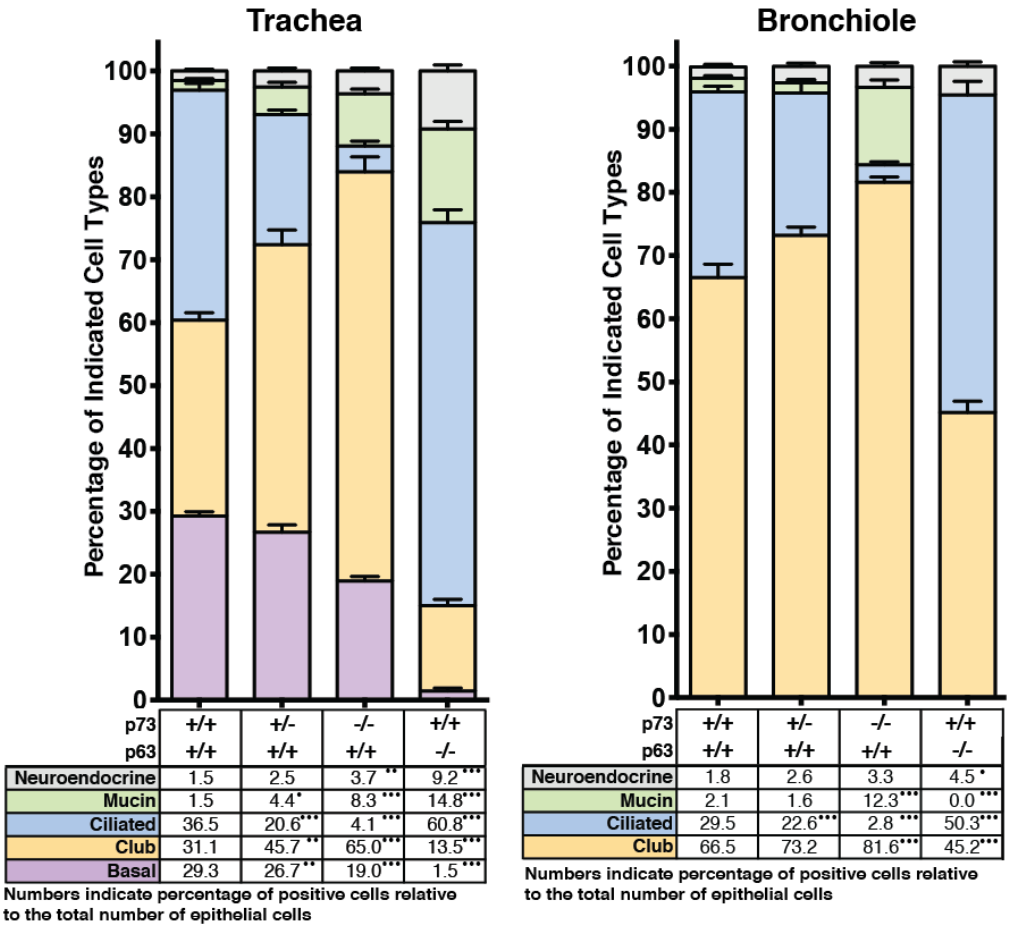

Figure 10. Loss of p73 and p63 in the Respiratory Epithelium Leads to Significant Changes in Cellular Composition. Respiratory epithelium from murine tracheas and bronchioles with the indicated genotypes were analyzed for cell type as percent of total DAPI nuclear marker. Due to the perinatal lethality of *p63-/-* mice, E18.5 mice were assessed for this genotype. Both E18.5 and post-pubertal mice were assessed for p73 genotypes. Manual quantification was performed on micrographs from at least eight animals with four fields of view per animal. Representative images can be found in Figure S3. p-values are annotated in the table under the bar graphs in panels A and B as <0.0001 (•••), <0.001 (••), and <0.01 (•).All data represented was collected by Clayton Marshall.

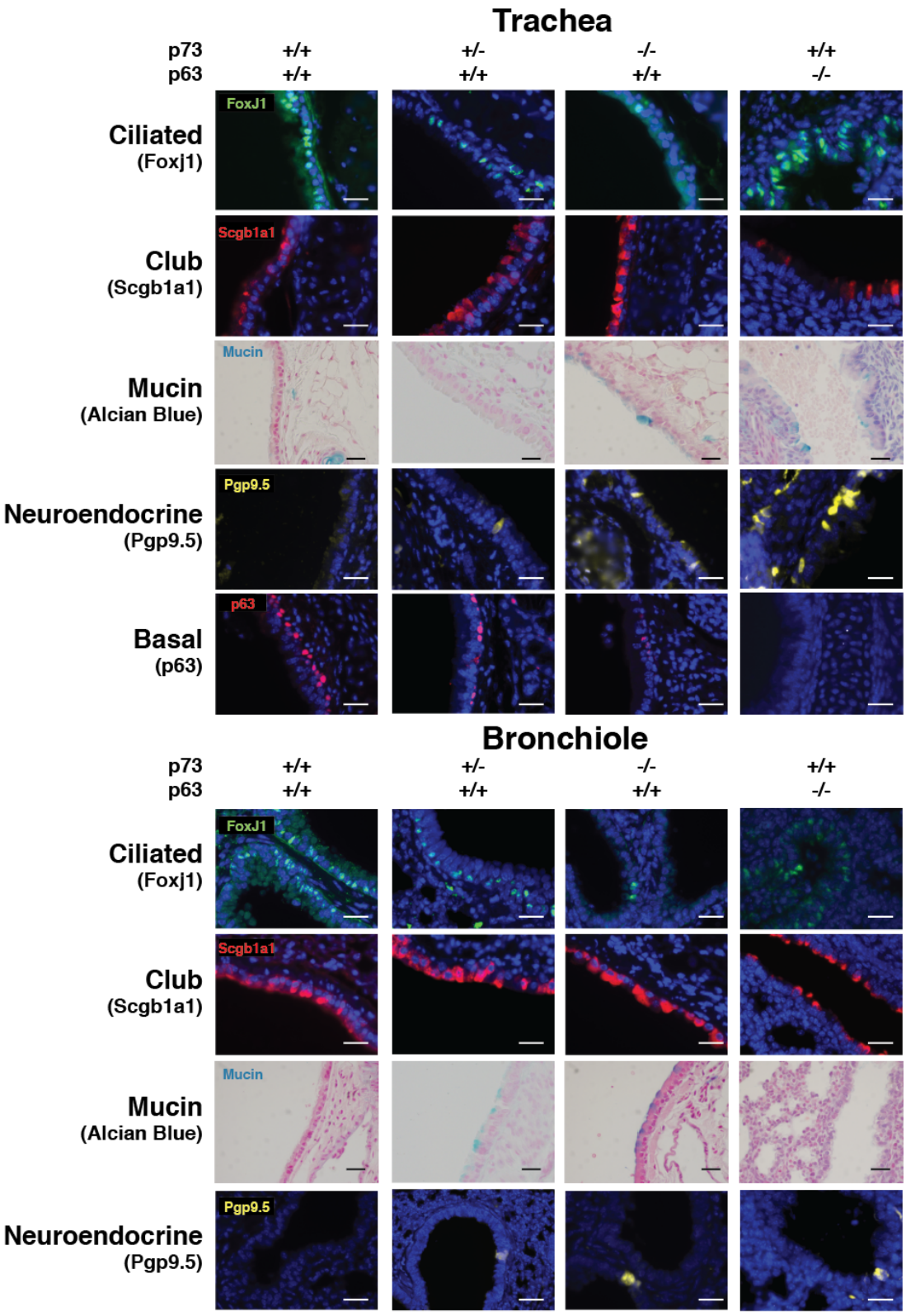
Trachea
p73 +/+ +/- -/- +/+
p63 +/+ +/+ +/+ -/-
Ciliated (Foxj1)
FoxJ1
Club (Scgb1a1)
Scgb1a1
Mucin (Alcian Blue)
Mucin
Neuroendocrine (Pgp9.5)
Pgp9.5
Basal (p63)
p63
Bronchiole
p73 +/+ +/- -/- +/+
p63 +/+ +/+ +/+ -/-
Ciliated (Foxj1)
FoxJ1
Club (Scgb1a1)
Scgb1a1
Mucin (Alcian Blue)
Mucin
Neuroendocrine (Pgp9.5)
Pgp9.5

Figure 11. Representative Images from the Trachea and Bronchioles Used for the Quantification of Respiratory Epithelium Cell Types Shown in Figure 10. IF detection of the indicated proteins in murine tracheal and bronchiolar tissue from mice of the indicated genotype. Foxj1 (green) was used as a marker of the ciliated cells. Scgb1a1 (red) was used as a marker of club cells. Alcian blue staining was used to detect mucin-producing goblet cells. Pgp9.5 (yellow) was used as a marker of neuroendocrine cells. p63 (red) was used as a marker of the basal cells within the murine trachea (scale bars = 25 μm). All data represented was collected by Clayton Marshall.

neuroendocrine and mucin cells and a reduction in basal and club cells (Figure 10). These data suggest that the lack of p63-positive basal cells results in a shift in cell fate specification away from the club cell lineage.

p73 is Expressed in Basal Cells of the Airway Epithelium and Co-Expressed with Foxj1 in MCCs

To further assess cell types in which p73 is expressed, we performed dual IF for p73 and Foxj1, a protein marker of MCCs that is required for motile ciliogenesis. In both bronchioles and trachea, all Foxj1-positive cells express p73 (Figure 12A, table). In the trachea, however, not all p73-positive cells express Foxj1. We observed p73 single positivity in ~13% of total p73-positive cells, and these cells appeared basally located (Figure 12B, table). Thus, p73 is not solely expressed in terminally differentiated MCCs in the trachea.

Co-staining of p73 and p63 identified three populations of cells: p73 single-positive, p63 single-positive and p73/p63 dual-positive cells (Figure 12B). We found that p73 is expressed in almost 50% of the tracheal epithelial cells and is co-expressed with p63 in a fraction of basal cells (Figure 12B). Of the p63-positive basal cells, 50% were p63 single-positive and 50% were dual-positive for

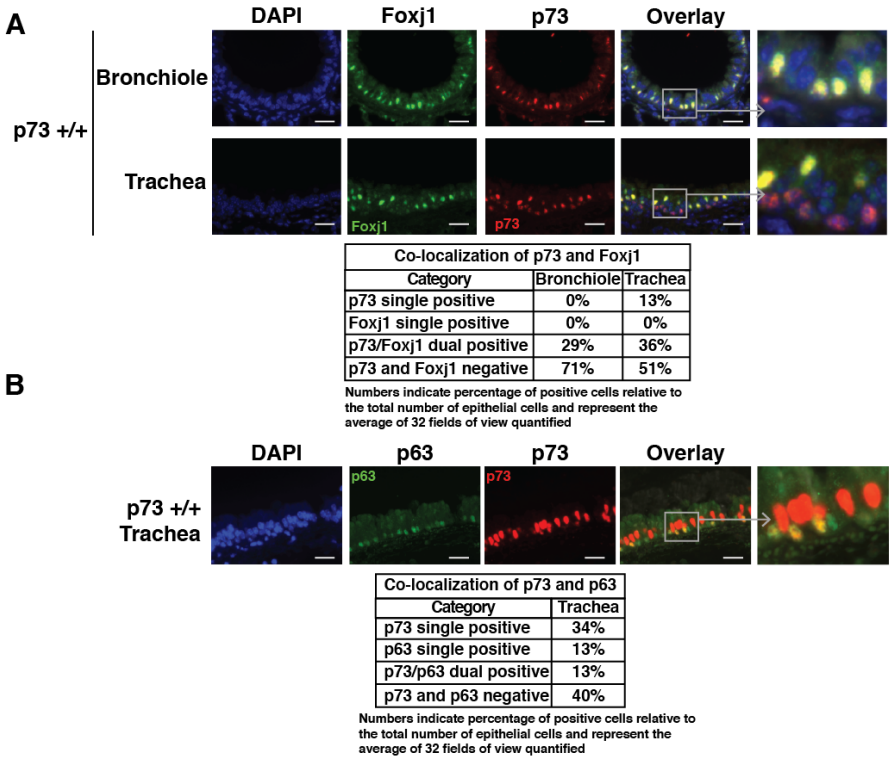

Co-localization of p73 and Foxj1		
Category	Bronchiole	Trachea
p73 single positive	0%	13%
Foxj1 single positive	0%	0%
p73/Foxj1 dual positive	29%	36%
p73 and Foxj1 negative	71%	51%

Numbers indicate percentage of positive cells relative to the total number of epithelial cells and represent the average of 32 fields of view quantified

Co-localization of p73 and p63	
Category	Trachea
p73 single positive	34%
p63 single positive	13%
p73/p63 dual positive	13%
p73 and p63 negative	40%

Numbers indicate percentage of positive cells relative to the total number of epithelial cells and represent the average of 32 fields of view quantified

Figure 12. p73 is Expressed in a Subset of Basal Cells in the Murine Trachea as well as in MCCs Representative IF staining of murine tracheas and bronchioles. (A) p73 (red) is 100% co-localized with Foxj (green) in MCCs in the bronchioles (upper panel). p73 (red) co-localizes with Foxj1 (green) in a subset of cells in the trachea (lower panel). (B) IF staining of p73 (red) and p63 (green) shows co-localization of p63 and p73 in a subset of basal tracheal epithelial cells (scale bars = 25 μm). Tables provide the percentage of cells that have single or dual expression of p73, p63 or Foxj1. Values represent the average of 32 fields of view that were quantified (four views from eight animals). All data represented was collected by Clayton Marshall.

p63 and p73 (Figure 12B). Similar percentages were identified using the alternative basal cell markers Krt5 and Krt14 (Figure 13).

To assess the expression pattern of p73 in human airways, we conducted IF staining of normal lung tissue from 10 individuals. The human lung epithelium is highly ciliated, with a greater number of cells expressing p73 compared to mice (Figure 12 and 14). As in mice, expression of p73 is localized proximally to *α-tubulin (Figure 14A), and Foxj1 co-localizes with p73 in the nucleus of all ciliated cells (Figure 14B). Consistent with the murine lung, we found dual expression of p73 and p63 in a subset of basal cells (Figure 14C), supporting a model whereby p73 is an early marker for the MCC lineage and regulates the MCC differentiation process through its activity as a sequence-specific transcriptional regulator[15,18,21,35,68].

***In situ* p73 and p63 ChIP-seq in Murine Tracheal Epithelial Cells**

To identify genomic loci to which p73 and p63 are bound in airway epithelium *in vivo*, we performed *in situ* protein-DNA crosslinking in the murine tracheal epithelium at the time of euthanasia. The tracheal epithelial cells from 50 p73+/+ mice were cross-linked *in situ*, harvested, and processed in duplicate for p73, p63, and RNA polymerase II (Pol II) ChIP-seq as described in Experimental Procedures.

Twenty to fifty million single-end 50 bp reads were generated for each ChIP-seq library. The resulting sequencing reads were aligned to the mouse genome and genomic binding sites enriched in each condition were identified

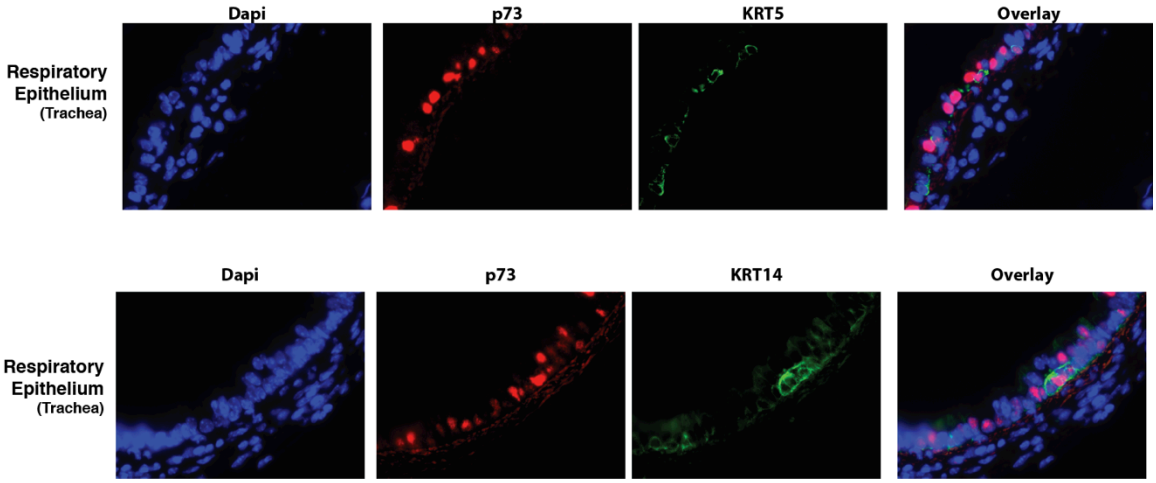

Figure 13. p73 is Expressed in a Subset of Basal Cells Within the Murine Airway Representative IF micrographs for the indicated proteins on sections of lung tissue from murine trachea . (A) KRT5 and KRT14 (green) and p73 (red) staining is consistent with a subset of murine tracheal basal cells express p73. All data represented was collected by Clayton Marshall.

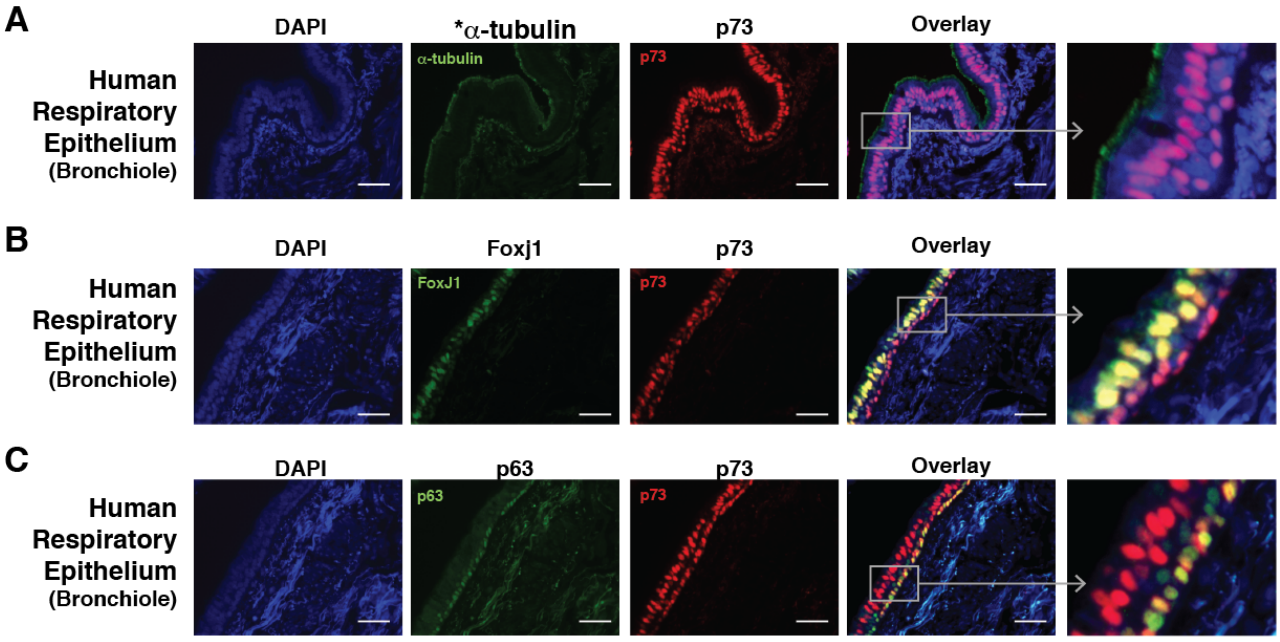

Figure 14. p73 is Expressed in Ciliated and Basal Cells Within the Human Airway Representative IF micrographs for the indicated proteins on sections of lung tissue from ten individual human patients . (A) *α-tubulin (green) and p73 (red) staining is consistent with a much higher percentage of MCC in human bronchiolar epithelium as compared to murine. (B) Foxj1 (green) and p73 (red) staining showing basal cells with single p73 positivity as well as luminal MCCs with co-expression of p73 and Foxj1. (C) p63 (green) and p73 (red) IF shows basal localization of p63 while p73 protein expression patterns are similar to that observed in the murine tracheal epithelium - both basal and ciliated (scale bar= 50 μm). All data represented was collected by Clayton Marshall.

using input DNA as a control. When comparing read coverage at identified binding sites, we found the replicates to be similar (Pearson correlation of 0.85, 0.92 and 0.95 for p73, p63 and Pol II, respectively) (Figure 15A); thus, each condition was pooled for further analyses.

In total, we identified 1,767 (p73), 3,861 (p63) and 53,684 (Pol II) genomic binding sites (Figure 15C). The median distance from p73 and p63 binding sites to the nearest transcriptional start site (TSS) was 9,531 and 12,810 bp, respectively (Figure 15C). We observed a significant enrichment of p73, p63 and Pol II binding in transcriptionally active areas of the genome such as promoters, 5' UTRs, and exons, with a lack of enrichment in intragenic regions (Figure 15B).

Based on our finding that p73 was bound to transcriptionally active areas of the genome, we tested the hypothesis that genes bound proximally by p73 exhibit higher RNA expression. At the time of tracheal ChIP-seq, we performed parallel RNA-seq from tracheal epithelium to determine expression levels of genes within the tissue. ChIP-seq and RNA-seq data were combined to generate a cumulative distribution function (CDF) of RNA expression for genes with observed p73 binding within 25,000 bp of a TSS versus those without. Analysis of the CDF indicates that genes with p73 binding within 25,000 bp of their TSS are more likely to be expressed and have higher RNA expression than genes without (Figure 15D).

Motif analysis showed enrichment of the p53 family binding motif[30,31,376-380] within p73 and p63 genomic binding sites (1764 of 1767 and 3846 of 3861,

respectively) (Figure 15E). Our ChIP-seq analysis identified well-validated p73 and p63 target genes such as *Mdm2*, *Cdkn1a*, *Bbc3*, and *Jag1*; and, example genomic binding profiles of *Mdm2* and *Cdkn1a* [381-383] are presented in Figure S5F[384,385].

p73 Binds and Regulates Genes Required for the Development and Function of MCCs

In order to identify a mechanism for the loss of MCCs in *p73-/-* mice, we analyzed the nearest protein-coding genes whose TSS fell within 25,000 bp of p73 genomic binding sites. We identified 1,011 such genes nearby 1,096 binding sites. Many of these putative target genes have documented roles in MCC formation and maintenance. To formally test for overrepresentation of genes involved in multiociliogenesis, we obtained a list of cilia-associated genes identified through previously published, single-cell RNA-seq[364]. Overall, we observed highly significant overrepresentation of the cilia-associated gene set within our p73-proximal protein-coding genes (p=4.53E-06). The 105 overlapping genes are listed in Figure S6.

To determine if the putative target genes could be transcriptionally regulated in a p73-dependent manner, we infected *p73+/+* and *p73-/-* MTEC cultures with a lentivirus containing a TAp73β expression construct or an empty vector control. We grew the cells as ALI cultures, performed RNA-seq, and conducted differential gene expression analyses comparing p73 overexpression to vector control for each genotype (Table 16). Of the 21,867 protein-coding

A

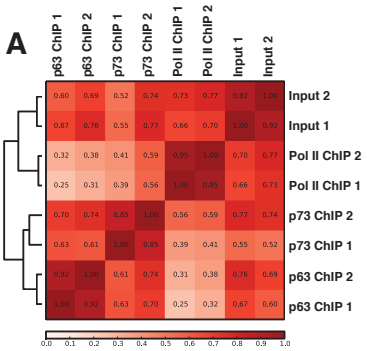

B

	Analysis of the Genomic Binding Sites								
	p73			p63			Pol II		
	# of Peaks	Log Ratio Enrichment	P-value	# of Peaks	Log Ratio Enrichment	P-value	# of Peaks	Log Ratio Enrichment	P-value
Promoters	259	2.11	1.0E-114	127	0.75	4.1E-13	16943	3.14	0.0E+00
CpG Island	175	2.52	3.5E-83	59	1.19	6.3E-16	14635	3.93	0.0E+00
UTR 5'	151	2.58	3.9E-38	33	0.7	1.1E-02	11795	3.95	0.0E+00
Exons	217	0.53	8.3E-07	204	0.22	3.3E-03	18323	1.95	0.0E+00
TTS	37	0.19	2.2E-01	63	-0.01	4.9E-01	4889	1.85	0.0E+00
Coding	85	-0.05	3.9E-01	123	0.14	1.3E-01	10425	1.5	0.0E+00
UTR 3'	18	-0.12	3.5E-01	62	0.23	5.4E-02	2735	1.19	0.0E+00
Introns	791	-0.07	2.4E-03	1928	0.04	7.1E-03	25776	-0.26	0.0E+00
Intergenic	730	-0.66	0.0E+00	1740	-0.62	0.00E+00	13864	-1.37	0.0E+00

C

Sample	Number of Binding Sites	Median Distance to Nearest TSS (bp)
Pol II ChIP	53,684	1,484
p73 ChIP	1,767	9,531
p63 ChIP	3,861	12,810

D

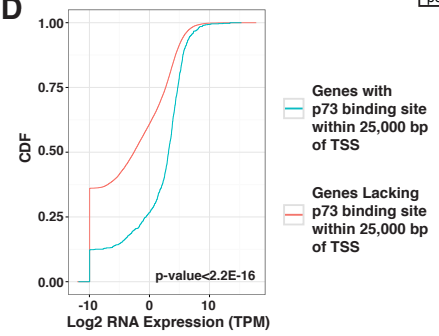

E

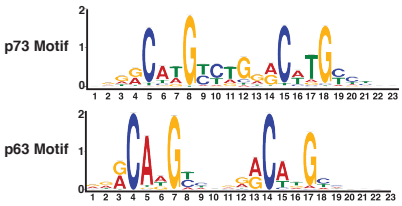

F

Representative Genes Previously Reported as p73 Target Genes			
Gene Symbol	q-value	Distance (bp) from TSS	Overlapping p63 Binding
Mdm2	7.9E-46	-7,029	
	1.3E-16	-15	✓
Cdkn1a	1.6E-27	-11,938	✓
	1E-12	740	
	1E-09	-9	

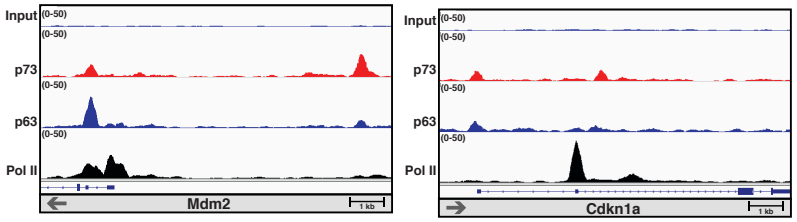

Figure 15. Analysis of DNA-Binding Profiles after *in situ* Protein-DNA Crosslinking and ChIP-seq (p73, p63 and Pol II) of Murine Tracheal Cells (A) Heatmap of hierarchically clustered Pearson correlations between ChIP-seq samples. (B) Analysis of the genomic features of the p73, p63 and Pol II binding sites. The first column under each protein section indicates the number of peaks observed within each respective genomic feature. The second column indicates the log ratio of binding enrichment for the peaks identified over the expected overlap based on the size of the given genomic feature. The final column lists the p-values for the observed enrichment of each feature type. (C) Summary of the number of binding sites and median distance to transcriptional start sites (TSS) for the Pol II, p73, and p63 ChIP-seq datasets. (D) CDF plot comparing the RNA expression levels of genes bound by p73 within 25,000 kb of their TSS versus genes not bound. Significance testing was performed using the Kolmogorov-Smirnov test. (E) Binding motifs identified in p73 and p63 ChIP-seq peaks. (F) Table of binding profiles of known target genes Mdm2 and Cdkn1a, including the q-value significance of the binding sites observed at each of the genes, and the bp distance from the middle of each binding site to the TSS, along with notation for whether a corresponding p63 binding site was found at the same location. Below the table are Integrative Genomics Viewer screenshots of Mdm2 and Cdkn1a in which the four tracks show ChIP-seq data normalized to 1x depth of coverage and presented with identical scales. The bottom three tracks represent DNA reads that were obtained following ChIP with the antibodies listed to the left, and the top track is the input sample for comparison. At the bottom of each panel is an annotated exon/intron gene structure displayed on the same scale as the ChIP-seq tracks with a gray arrow at the bottom annotating the gene orientation. Data was generated by Clayton Marshall through collaboration with Bryan Venters. Clayton Marshall was assisted in bioinformatic analysis by Scott Beeler and Timothy Shaver.

---

genes queried, more than 3,300 were significantly differentially expressed after ectopic expression of p73 in both *p73+/+* and *-/-* MTECs. (Figure 16A). Importantly, genes with p73 binding sites within 25 kb of their TSS were specifically enriched among differentially expressed genes (Figure 16A). Among the 105 genes overlapping with the cilia-associated gene set, 49 had significant, p73-dependent changes in gene expression in *p73+/+* or *p73-/-* MTECs (Figure

17, highlighted in gray). Of immediate interest were 14 genes that have been reported to have roles in MCC differentiation and homeostasis[386-388] (Figure 16B), including *Foxj1*, *Traf3ip1*, and *Spata18* (Figure 16C). We found that greater than 25% of genes in the cilia-associated gene set (397/1398) were differentially expressed after ectopic p73 expression, not just those with p73 binding sites nearby (Figure 16A). These data support a model in which p73 acts as a regulator of multiciliogenesis through both direct and indirect regulation of key genes.

The protein-coding gene with the most significant differential expression after rescue of *p73-/-* MTECs by ectopic p73 expression was a key regulator of ciliary biogenesis, Foxj1. We identified three dual p73/p63 genomic binding sites within 10,000 bp of the *Foxj1* TSS (Figure 16B and C). *Traf3ip1* (Figure 16B and C) had the most significant q-value from the p73 ChIP-seq and has been previously shown to bind basal bodies and regulate the acetylation of microtubules[389]. Also present in our p73 and p63 ChIPseq datasets are *Jag1*, a known p73 and p63 target gene[390] and a regulator of the Notch pathway implicated in ciliogenesis[238]. The Rfx family member, *Rfx3* was also in the p73 dataset. The Rfx family of transcription factors is implicated in regulation of ciliary biogenesis[308]. We additionally provide evidence that *Spata18*, a target gene of both p53 and p63[391], is regulated by p73 (Figure 16B and C).

A

	Differentially Expressed Genes in Indicated MTECs (Ectopic p73 Relative to Control)										
	All Genes		p73 Proximal Genes			Cilia-Associated Gene Set			p73 Proximal Cilia-Associated		
	Total Queried	Differential Expression	Total Queried	Differential Expression	Enrichment vs. All Genes	Total Queried	Differential Expression	Enrichment vs. All Genes	Total Queried	Differential Expression	Enrichment vs. All Genes
p73-/- MTEC	21867	3768 (17.2%)	1011	348 (34.4%)	< 2.2e-16	1398	397 (28.4%)	< 2.2e-16	105	38 (36.2%)	8.6E-07
p73+/+ MTEC	21867	3380 (15.5%)	1011	268 (26.5%)	< 2.2e-16	1398	309 (22.1%)	4.5E-12	105	23 (21.9%)	0.029

B

	p73 Binding and Regulation of Cilia-Associated Genes					
	Tracheal ChIP-seq			RNA-seq p73-/- MTECs + Ectopic p73 Relative to Control		
Gene Symbol	q-value	Distance (bp) From TSS	Overlapping p63 Binding	Log2Fold Change	Adjusted p-value	
Traf3ip1	7.9E-123	-4,151	✔	0.51	3.1E-10	
Foxj1	1.6E-103	8,146	✔	1.75	3.7E-246	
	5.0E-37	5,006	✔			
	1.3E-09	5,828	✔			
Spata18	3.2E-84	-1,498		0.40	0.07	
Lztfl1	1.9E-75	5,409		0.32	0.0009	
Trp73**	1.6E-64	-8,719	✔	3.70	1.5E-112	
	1.3E-39	-161				
Ccdc113	1.6E-47	13,738		0.55	0.006	
Stk33	3.9E-45	3,531		2.06	2.1E-24	
Fam161a	6.3E-40	-16	✔	0.51	0.002	
Tubb4b	3.9E-37	-767	✔	0.11	0.06	
Sec24b	1E-16	6,221	✔	0.17	0.01	
Dnaic1	6.3E-12	-3,120		0.63	0.0006	
Rfx3	2.5E-09	-13,813		0.31	0.03	
Jag1	6.3E-09	8,416	✔	1.11	4.3E-81	
Dpcd	1.6E-06	5,594		0.25	0.03	

C

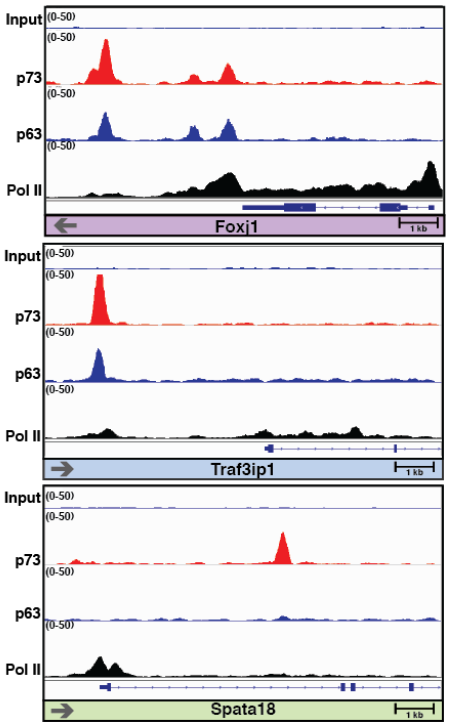

Figure 16. p73 Binds and Regulates Target Genes Found in Cilia-Associated Gene Set (A) Table showing differentially expressed genes in indicated MTECs after ectopic p73 expression (results shown are relative to control). Cells were infected with a lentivirus containing a TAp73β overexpression construct or an empty vector control. Cultures were maintained for five days in basal growth media and one day in differentiation media, followed by RNA harvest and sequencing. Differential gene expression analysis between duplicate p73 overexpression and control samples was performed for each genotype. The number of differentially expressed genes (adjusted p-value <0.1) was quantified for four different categories: all protein-coding genes (All Genes), genes with p73 binding sites within 25 kb of their transcriptional start sites (TSS) (p73 Proximal Genes), a Cilia-Associated Gene Set, and the overlap of the previous two categories (p73 Proximal Cilia-Associated) For the three latter categories, the p-value for category-specific enrichment versus all protein-coding genes was calculated using the hypergeometric test. (B) Table indicating cilia-associated genes bound and regulated by p73. For each binding site, the q-value significance and distance to the respective TSS are indicated along with notation for whether a corresponding p63 binding site was found at the same location. For each gene, the log2 fold change and adjusted p-value from the differential gene expression analysis performed in A are presented. p73 (**) is included as a reference for expression change and genes are ordered based upon increasing q-value. (C) Integrative Genomics Viewer screenshots for select genes from panel B in which the four tracks show ChIP-seq data normalized to 1x depth of coverage and presented with identical scales. The bottom three tracks represent DNA reads that were obtained after ChIP with the antibodies listed to the left, and the top track is the input sample for comparison. At the bottom of each panel is an annotated exon/intron gene structure displayed on the same scale as the ChIP-seq tracks, and the arrow in the bottom left annotates the gene orientation. Data was generated by Clayton Marshall through collaboration with Bryan Venters. Clayton Marshall was assisted in bioinformatic analysis by Scott Beeler and Timothy Shaver.

To determine whether the p73-dependent increase in Foxj1 mRNA required differentiation cues from the culture medium or if p73 expression alone was sufficient to modulate Foxj1, we analyzed expression of p73 and Foxj1 in parallel cultures of submerged *p73+/+* and *p73-/-* MTECs under non-differentiating culture conditions, with and without ectopic expression of p73. Infection of *p73+/+* MTEC cultures with a control lentiviral vector resulted in very few p73-positive cells and no Foxj1-positive cells. Under the same conditions, no p73- or Foxj1-postitive cells were observed in p73-/- MTECs cultures. However,

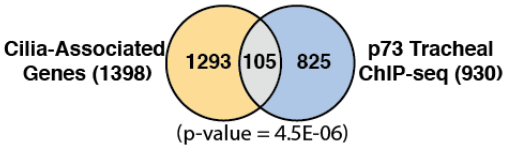

Overlap of Cilia-Associated Gene Set and p73 ChIP-seq			
Gene Symbol	q-value	Distance (bp) from TSS	Overlapping p63 Binding
Traf3ip1	7.9E-123	-4,151	✔
4833427G06Rik	5.0E-114	-3,895	✔
Hs6st2	1.9E-110	8,582	✔
Rbl2	1.3E-107	12,036	✔
Foxj1	1.6E-103	8,146	✔
Cct4	6.3E-96	-1,122	✔
Ercc3	1E-92	20,031	
Spata18	3.2E-84	-1,498	
Lztfl1	1.9E-75	5,409	
Glipr1	3.9E-75	-209	
Usp2	2.5E-72	-180	✔
Slc38a6	1.3E-70	8,104	✔
6430531B16Rik	5.0E-69	8,233	✔
Rgs3	6.3E-69	2,338	✔
Slc25a17	3.2E-68	3,624	✔
Myb	5.0E-67	4,187	✔
Trp73	1.6E-64	-8,719	✔
Gm684	5.0E-57	9,498	✔
Zfp51	3.9E-50	-11,405	
Ccdc113	1.6E-47	13,738	
Trit1	2.5E-46	-2,229	✔
Gnpnat1	1.3E-45	-17,281	
Stk33	3.9E-45	3,531	
Glis3	5.0E-42	22,548	✔
Fam161a	6.3E-40	-16	✔
Tp73	1.3E-39	-161	
Exo1	7.9E-38	-4,782	
Cyp2s1	7.9E-38	-2,1047	✔
Tubb4b	3.9E-37	-767	✔
Foxj1	5.0E-37	5,006	✔
Dcdc2a	1.6E-36	-24,669	
Aox1	6.3E-35	22,462	
Ppil6	1.3E-32	814	✔
Wdr38	1.6E-32	-9,073	✔
Sirt3	3.2E-32	558	
Cyp2s1	2.5E-31	-15,181	✔
Pex3	5.0E-31	-39	
Banp	6.3E-28	303	
Fxn	3.2E-26	10,028	✔
Mtg1	3.2E-26	-17	
Cmbl	1.3E-25	1,029	✔
Ankrd10	3.2E-22	-8,753	
Arc	6.3E-21	6,716	
Tmem57	2.5E-20	-2,702	
Zfp667	5.0E-20	-1,941	
Spag16	1E-19	2,678	
Stx16	6.3E-19	-46	✔
Tiam1	3.9E-18	-15,934	✔
Hipk1	5.0E-18	-19,180	
2310007B03Rik	5.0E-18	7	✔
Atp6v1h	1E-17	20,715	✔
Krr1	1.9E-17	29	
Sec24b	1E-16	6,221	✔
Megf6	3.9E-16	10,490	✔
Rbm34	1E-15	-27	
Mphosph10	1.9E-15	-20	

Overlap of Cilia-Associated Gene Set and p73 ChIP-seq			
Gene Symbol	q-value	Distance (bp) from TSS	Overlapping p63 Binding
Rrp15	1.9E-15	-26	
Tmem101	1.9E-15	-22	
Pih1d2	3.9E-15	-7	
Hdac8	1.3E-14	23,315	✔
Lgals12	1.6E-14	23,839	✔
Eps8	1.9E-13	-537	✔
Med12l	1.9E-13	-15,360	
Pla2g16	3.2E-13	-4,289	
Edc4	5.0E-13	-23	
Cep135	1.6E-12	411	
Ugt1a6a	1.6E-12	-192	✔
Mrpl39	5.0E-12	-61	
Dnaic1	6.3E-12	-3,120	
Rel	1.3E-11	189	
Pepd	1.9E-11	4,566	
Tmem69	3.2E-11	-45	
Man2c1	5.0E-11	55	
Sord	1.3E-10	-3,167	✔
Psmf1	1.6E-10	-53	
Alkbh3	1.9E-10	-42	
Gapvd1	6.3E-10	987	
Riiad1	7.9E-10	3,844	✔
Ap3m2	1E-09	-5,110	✔
Ccdc17	1E-09	-45	✔
Foxj1	1.3E-09	5,828	✔
Dnaic2	1.9E-09	-24,855	✔
Rfx3	2.5E-09	-13,813	
Jag1	6.3E-09	8,416	✔
1110004E09Rik	7.9E-09	-26	
B230118H07Rik	1.3E-08	-961	
Anxa8	3.2E-08	-148	
2610028H24Rik	3.9E-08	-1,709	
Golga3	5.0E-08	-54	
Nhsl1	7.9E-08	-19,948	
1700001C02Rik	7.9E-08	1596	
Ect2	1.6E-07	11,005	✔
Cryaa	2.5E-07	8,583	✔
Faf2	2.5E-07	7,552	✔
2700049A03Rik	2.5E-07	208	
Bms1	5.0E-07	3	
Entpd5	7.9E-07	482	✔
Slc25a17	1E-06	3,919	✔
Dgcr6	1.3E-06	4,841	
Dpcd	1.6E-06	5,594	
Lrpprc	1.6E-06	2,588	
Slc47a2	1.6E-06	22,724	
Slc35b1	1.9E-06	3,663	✔
Dpagt1	1.9E-06	-31	
Mettl15	7.9E-06	-32	
Mllt10	1E-05	-7,089	✔
Nek2	3.2E-05	-1,283	
Glipr1	6.3E-05	549	
Ces1b	6.3E-05	-222	✔
B230118H07Rik	6.3E-05	-82	
Tnpo3	6.3E-05	77	
Rcbtb2	1E-04	-12,004	✔

***Gray highlighting indicates genes that were differentially expressed after ectopic overexpression of p73 in either p73+/+ and/or p73-/- MTEC cultures**

Figure 17. Additional p73 Binding to Novel Target Genes in Cilia-Associated Gene Set At top, a Venn diagram illustrates the overlap of genes featuring a p73 binding site within 25 kb of their transcriptional start site (930 total) with the cilia-associated gene set (1398 total). The 105 overlapping genes are detailed at bottom. For each gene, the q-value significance and distance to the respective TSS for the associated binding sites are indicated along with notation for whether a corresponding p63 binding site was found at the same location. Genes are ranked by decreasing q-value and are highlighted in gray if they were significantly differentially expressed after exogenous overexpression of p73 in either *p73+/+* or *p73-/-* MTEC cultures. Data was generated by Clayton Marshall through collaboration with Bryan Venters. Clayton Marshall was assisted in bioinformatic analysis by Scott Beeler and Timothy Shaver.

after ectopic TAp73β expression, we observed increased expression of Foxj1 in both *p73+/+* and *p73-/-* MTEC cells (Figure 18A). These data indicate that p73 is sufficient to modulate Foxj1 expression in the absence of differentiation media and demonstrate the ability of ectopic p73 expression to rescue Foxj1 expression in *p73-/-* MTECs.

In parallel experiments, MTEC cultures were transferred to differentiation media after lentiviral infection. We observed an increase in p73 and Foxj1 expression in *p73+/+* MTECs under both expression conditions, consistent with a differentiation-induced elevation of p73 and Foxj1 expression. However, Foxj1 expression was not detectable in the control *p73-/-* MTEC cultures and only became apparent after ectopic expression of p73 (Figure 18B). Twenty-four fields of view of IF staining from quadruplicate experiments of cells cultured in differentiation media were quantified and showed tight concordance between p73 and Foxj1 expression ($p < 0.001$) (Figure 18B).

In summary, p73 binds to three sites within 10,000 bp of the *Foxj1* TSS. Further, ectopic p73 expression is sufficient to upregulate Foxj1 expression in

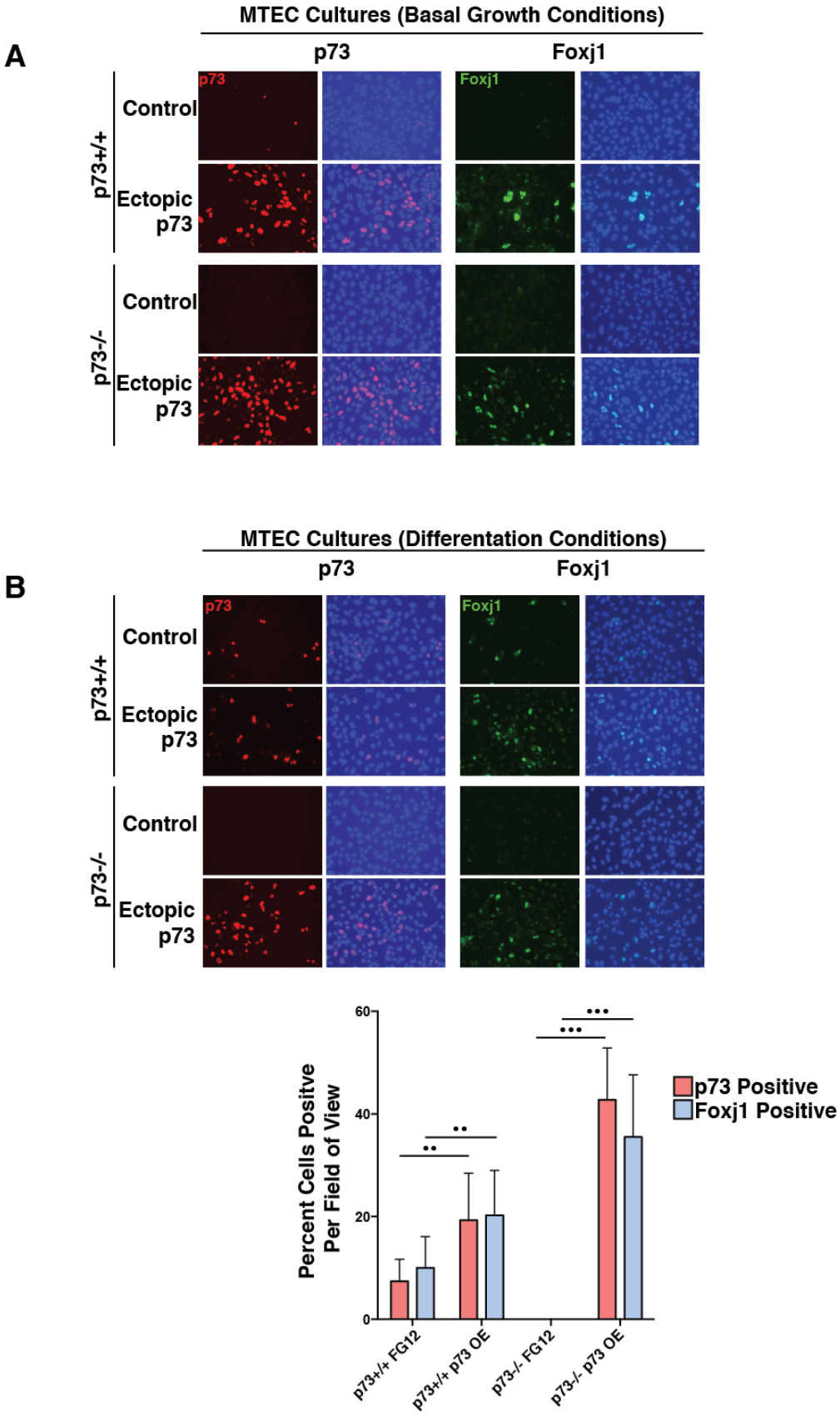
A
MTEC Cultures (Basal Growth Conditions)
p73
Foxj1
p73+/+
Control
Ectopic p73
p73-/-
Control
Ectopic p73
p73
Foxj1
B
MTEC Cultures (Differentation Conditions)
p73
Foxj1
p73+/+
Control
Ectopic p73
p73-/-
Control
Ectopic p73
p73
Foxj1
Percent Cells Positve Per Field of View
60
40
20
0
••
••
•••
•••
p73 Positive
Foxj1 Positive
p73+/+ FG12
p73+/+ p73 OE
p73-/- FG12
p73-/- p73 OE

Figure 18. p73 Regulates the Expression of Foxj1 (A) MTECs were infected with a lentivirus containing a TAp73β overexpression construct (Ectopic p73) or an empty vector control (Control) and grown in basal growth media for three days, after which immunofluorescence (IF) was performed for the indicated proteins. (B) Parallel cultures were transferred to differentiation media for three days after three days of growth in basal media and stained identically. For both panels A and B, DAPI counterstaining (blue) was performed to determine the percentage of cells expressing the indicated proteins. The bottom graph presents quantification of p73- and Foxj1-positive cells averaged from quadruplicate experiments with six fields of view per condition (•• represents p-value <0.001, ••• represents p-value <0.0001) with error bars representing standard deviation. All data represented was collected by Clayton Marshall with technical assistance from Deborah Mays.

MTEC cultures in the absence of differentiation signaling and rescues Foxj1 expression in a *p73-/-* background. Collectively, the data provide evidence that p73-dependent regulation of a cilia-associated gene network plays a causative Role in licensing cells to the MCC fate.

Discussion

Herein we report that p73 is required for the formation of MCCs in mice through binding and regulation of a broad array of gene targets. Of importance is our finding that p73 directly modulates *Foxj1* and a network of cilia-associated genes required for the development of MCCs in the airway, choroid plexus, ependyma, oviducts and testis of mice[334,336,339,340,392-395]. We propose that like its family member p63, p73 is required for tissue-specific cell differentiation through its role as a sequence-specific transcription factor. Given our finding that p73 regulates a cilia-associated gene signaling network required for proper MCC differentiation, it will be of interest to determine the interplay of p73 target genes with other pathways involved in MCC lineage formation, including those controlled by E2f4[396], Myb[346,347], Mcidas[345], Ccno[397], the Rfx family[308] and the

Notch family[238].

The observed co-expression of p73 with p63 in a subset of basal cells lining the tracheal epithelium raises the possibility that similar to p63, p73 is involved in progenitor cell fate determination and is required for MCC specification and differentiation. In the respiratory epithelium, p63 expression is restricted to basal and progenitor cells[235,253,398]. Unlike in skin, where p63 is necessary for the development and maintenance of a stratified epithelium[22,23], a subset of airway luminal cells forms in the absence of p63[250,253]. Because p63-null animals die at birth, the long-term functionality of their airway epithelium cannot be determined; future studies are needed to determine how targeted ablation of p63 and p73 in adult mouse tracheas affects homeostasis and repair of the airway after damage. Greater understanding of the functional interaction between p53 family members in the airway epithelium has implications for both regenerative medicine and prevalent diseases such as COPD and asthma.

p73 and p63 heteroligomerize when co-expressed; as such, it is difficult to study the transcriptional activity of p73 in basal cells of the airway without considering the contribution of p63[399]. ΔNp63 has the ability to bind TAp73 and act as a transcriptional repressor of p73[91,400]. To parse the individual functions of these proteins, future transcriptional profiling experiments are needed in which cells are separated into p73 and p63 single- and dual-positive populations. The engineering of mouse models to enable p73- and p63-specific lineage tracing during development and in response to damage would also be of significant

value in defining the unique and overlapping roles of these developmental regulators.

From analysis of our ChIP-seq data, we observed that p73 and p63 co-occupy 804 genomic loci. We hypothesize that p63 represses the expression of many of these genes within dual-positive, MCC-specified basal cells until a signal promotes differentiation. This might occur by several mechanisms: p73 protein levels may increase, p73 binding and distribution on the chromatin may shift, changes in the stoichiometry of TAp73 versus ΔN expression may occur relative to p63 levels, or p63 levels or chromatin binding may be reduced. Future studies investigating the mechanism by which the balance of p63 and p73 signaling is regulated in the airway epithelium in response to developmental cues and cellular stress will be of interest in both development and disease.

After ectopic expression of p73 in MTEC cultures, we observed a significant increase in the expression of many cytokeratins, including Krt5 and Krt14; however, our ChIP-seq data did not indicate a TSS-proximal p73 binding profile for these genes in adult mouse trachea. Further studies are needed to determine the direct or indirect mechanisms by which p73 and p63 regulate the expression of genes required for basal cell maintenance.

There is a significant reduction in the proportion of basal cells in the tracheal epithelium of *p73-/-* mice. This reduction implies that p73 is required for the maintenance of a subset of basal cells, or that increased differentiation of basal cells is required to compensate for a lack of the MCCs due to inflammatory

stress in the *p73-/-* mice. We did observe an eventual loss of epithelial cells in older *p73-/-* mice, and we hypothesize that the progenitor cell population is eventually depleted through constant damage, inflammation and infections from impaired clearance of foreign particles and toxins. Immunohistochemistry (IHC) staining of Ki67, a marker of proliferation, we did observe increased positive nuclei in murine trachea and bronchioles (Figure 19A). Further quantification of 30 fields of view from 1 week old pups to 4 month old animals indicated significant increases in the percentage of Ki67 positive cells within the *p73-/-* trachea and bronchioles (Figure 19B). In the timepoints investigated (1 week-4 months) to date there was no significant difference in the frequency of epithelial cells that exhibit apoptosis through IHC of cleaved Caspase 3 (Figure 19C). Further timepoints investigating apoptosis within the *p73-/-* animals are needed to better determine at what point the epithelium is being lost, and if that loss is due to apoptosis.

As early as seven days postnatally, we observed an increased proportion of mucin-producing cells in *p73-/-* mice, perhaps indicating that their airways were already challenged due to a lack of MCCs. The McKeon group reported the presence of p63-positive cells in the bronchiolar epithelium of mice that had been challenged with H1N1 infection [256], and demonstrated that these distal stem cells are required for alveolar regeneration within damaged lungs[255,257]. In support of this model, we found p63-expressing cells in the bronchiolar epithelium of our *p73-/-* with increased concentration in areas of increased inflammation and

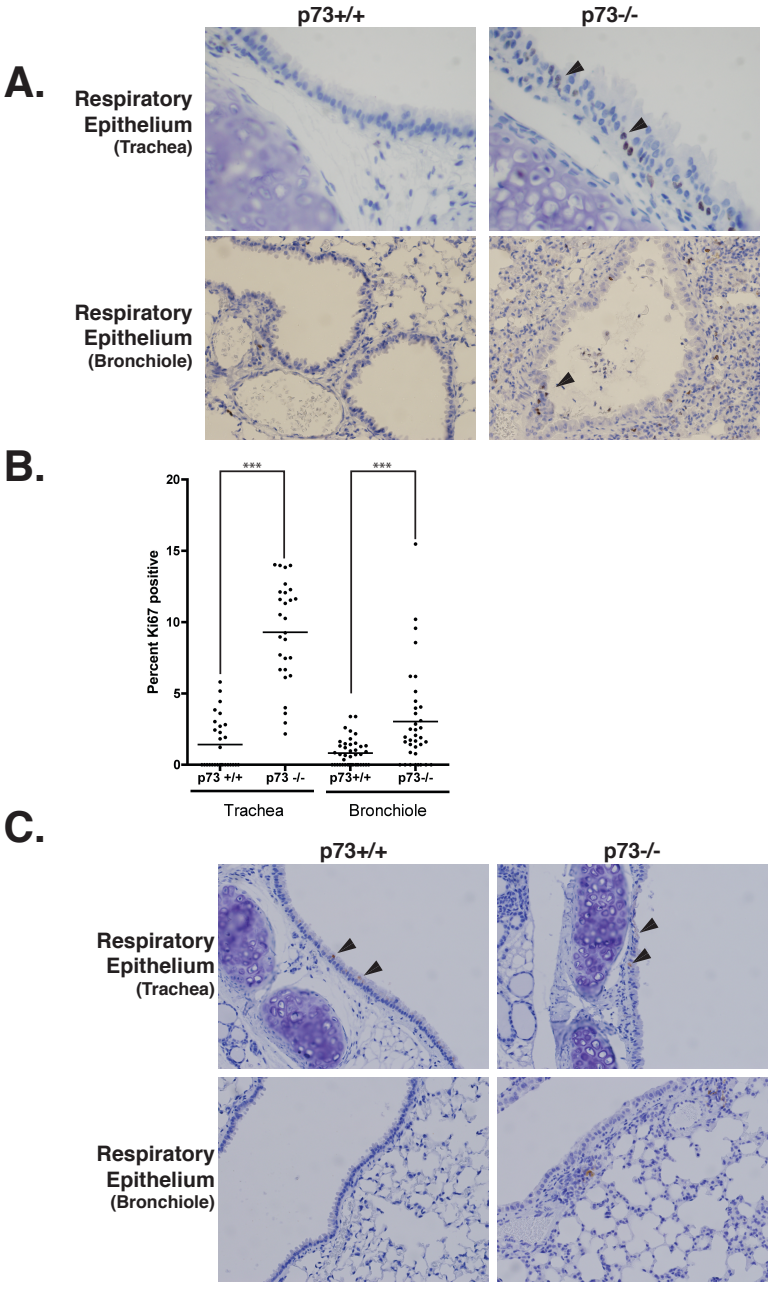

Figure 19. *p73-/-* Mice Exhibit Increased Proliferation of the Bronchiole Epithelium. (A) Representative micrographs of IHC staining of Ki67, a marker of proliferation, within the trachea and bronchioles of *p73+/+* and *p73-/-* bronchioles. (B) Quantification of 4 fields of view from 8 animals ranging in age from 7 days postnatal to 4 months old. Data for the tracheal and bronchiole quantification are represented as percentage epithelial cells positive to the total number of contiguous epithelial cells within the field of view. (C) Micrographs of IHC staining of cleaved Caspase 3, a marker of apoptosis. Arrowheads mark nuclei counted as positive for each IHC stain. All data represented was collected by Clayton Marshall.

mucus retention of adult murine bronchioles (Figure 20A). Analysis of the developing lungs additionally supported p63 presence in the airways as a reaction to stress. We did not observe p63 positive cells in the bronchioles of embryonic *p73-/-* animals (Figure 20B). The first p63 positive cells observed were seen as early as 7 days postnatal life (Figure 20B). We did not observe p63 positive cells within the lungs of *p73+/+* animals investigated. Additionally, Foxj1 has been previously reported to regulate T cell activation through modulation of the NF-κB pathway, with Foxj1 deficiency leading to systemic inflammation and autoimmunity defects[401]. Given our finding that p73 is a direct regulator of Foxj1, future studies are needed to evaluate the mechanistic importance of Foxj1 deficiency in the inflammatory defects observed in the *p73-/-* setting.

Numerous human diseases and conditions have been linked to dysfunctional ciliogenesis, including hydrocephalus; hippocampal dysgenesis; primary ciliary dyskinesia; Bardet-Biedl syndrome; asthma; anosmia; COPD and sterility[387,402]. Pointing to a potential link between p53 family members and inflammatory stress response in the airway, Li and colleagues observed increased levels of p73 and p63 in the hyperplastic regions of patients with nasal polyps[403], as well as increased cilia density and length[404]. Given the findings of our study, it would be of interest to investigate the activity of p73 within patient samples or mouse models of cilia-related diseases. With the increased availability and depth of GWAS and SNP data, it may also be possible to

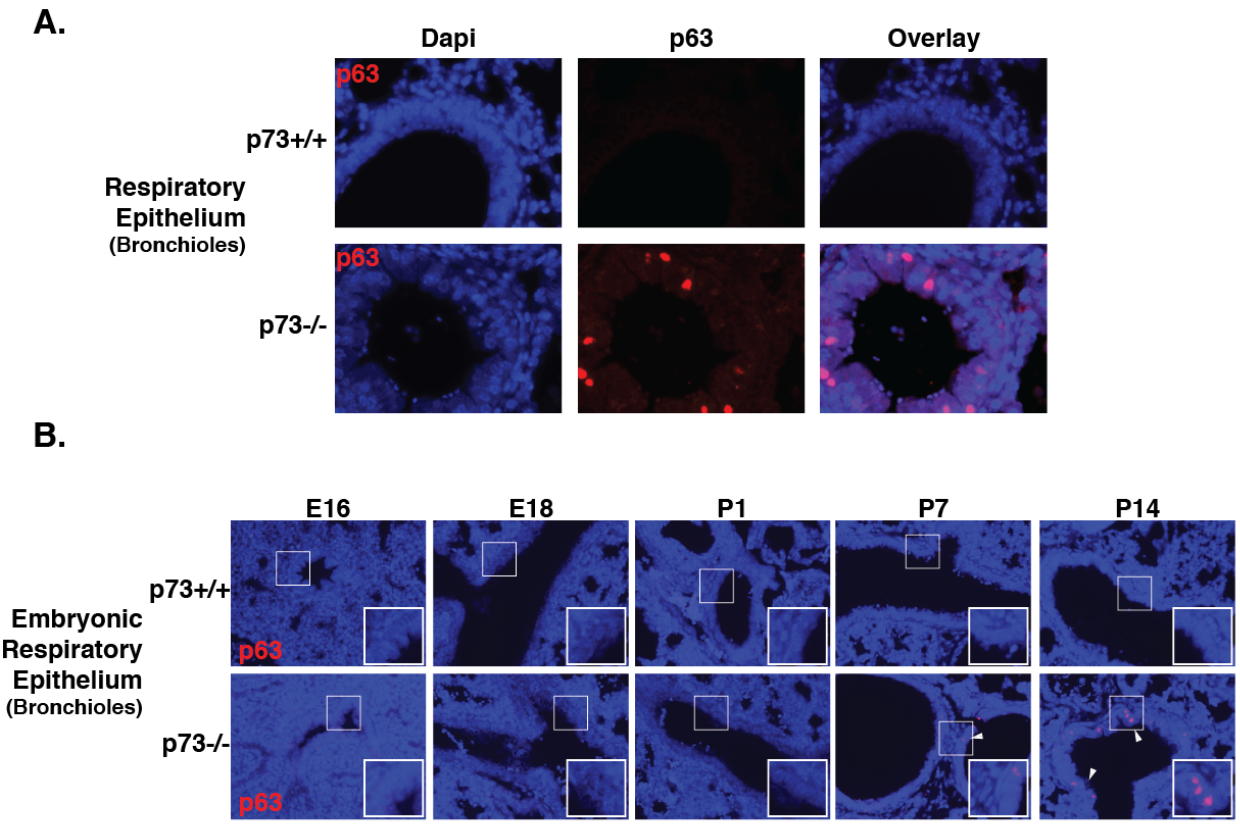

Figure 20. p63 Positive Cells Observed Within the Bronchioles of *p73-/-* Animals. (A) Micrographs of p63 (red) IF within 6 month old bronchioles of *p73+/+* and *p73-/-* animals. (B) IF staining of p63 (red) within developing bronchioles of mice ranging from Embryonic day 16 through postnatal day 14. All data represented was collected by Clayton Marshall.

associate polymorphic variants in the p73 gene with altered expression or activity and disease susceptibility.

Conclusions

In summary, we discovered that p73 deficiency leads to an organism-wide absence of multiciliated cells, providing a unifying mechanism to explain the multiple-organ defects observed in *p73-/-* mice[1]. Through *in situ* ChIP-seq of the murine trachea, we identified p73 genomic binding sites in proximity to genes that regulate the spectrum of events required for MCC differentiation, from cell cycle arrest (*Cdkn1a*[405]) and amplification of centrioles (*Myb*[346]) to apical docking of centrioles with components that make up the axoneme [*Foxj1*[339], *Traf3ip1*[389]]. By combining our ChIP-seq data with RNA-seq of primary murine tracheal epithelial cultures, we obtained evidence for p73-dependent, direct and indirect transcriptional regulation of a broad network of cilia-associated genes. We propose a model found in (Figure 21) in which p73 is implicated not only in the differentiation of MCCs, but also in MCC homeostasis and thus airway-protective function. We propose that p73 acts as a critical regulator of multiciliogenesis in its capacity as a sequence-specific transcription factor, through genomic binding and regulation of genes that are required along the continuum of MCC development and maintenance.

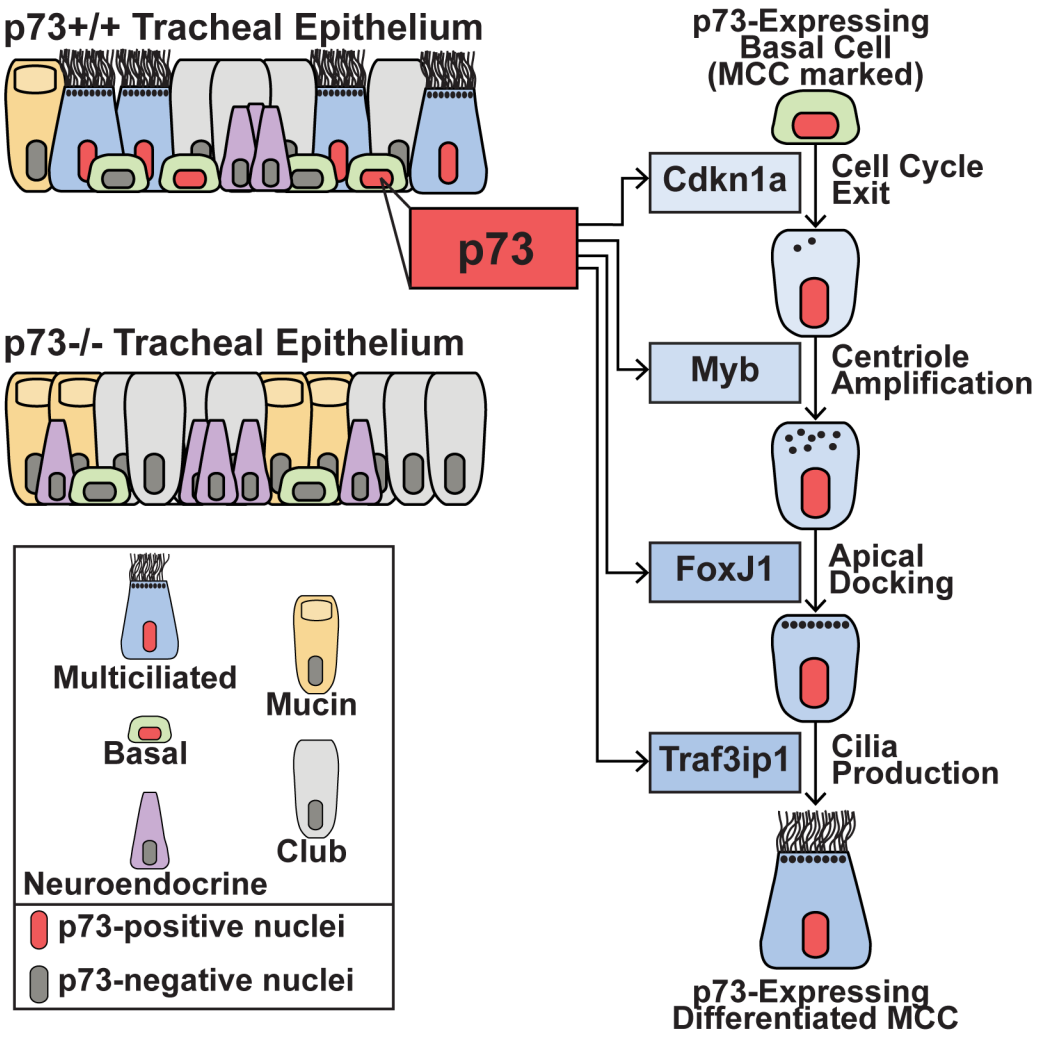

Figure 21. Graphical Representation of the Role of p73 Within the Pulmonary Epithelium On the Left, *p73+/+* and *p73-/-* tracheal epithelium is represented with Multiciliated (blue), Basal (green), Mucin (yellow), Club (gray), and Neuroendocrine (purple) cells. Those cells that express nuclear p73 are annotated with nuclei colored red. The p73 transcription factor genomically binds to components with roles throughout MCC development (Cdkn1a, Myb, FoxJ1, and Traf3ip1).

CHAPTER IV

MECHANISMS OF p73 REGULATION

Introduction

Several cellular responses to stress and developmental cues are dependent on the transcription factors: p53, p63 and p73[12]. This family of transcription factors regulate cellular functions including metabolism, apoptosis, cell cycle, angiogenesis, differentiation, migration, and motility[406]. mRNA variants of p73 are generated by alternate splicing and the use of separate, alternate promoters. The different protein isoforms are capable of independent and distinct functions depending on the presence or absence of specific domains[21,26]. p73 can be transcribed from two separate promoters. The first promoter for p73 is located upstream of the first exon, and the other promoter is located in the third intron. Transcription from the promoter in the third intron creates a truncated form of p73 known as ΔNp73 that lacks the TA domain[15,38]. ΔNp73 can inhibit the activities of full-length p53, p63, and p73 by competition for the same DNA binding sites on downstream promoters[47]. TAp73 can activate apoptosis through transcriptional regulation of p21, BAX, PUMA, NOXA, PIG3, and PARP, all of which are common targets shared with p53[27].

From whole genome chromatin precipitation analyses, p53, p63, and p73 have a significant overlap in transcriptional targets[349,378,407,408]. However, differential regulation of non-overlapping targets by p53, p63, and p73 is likely dependent upon differing DNA binding affinities for select sites, posttranslational

modifications, and variation in p53 family interacting proteins. Thus, we sought to identify and characterize p73-interacting proteins as a means to provide important insight into the regulatory mechanisms of p73. Better understanding of interacting and regulatory partners of p73 could provide insight into possible mechanisms to therapeutically target p73 in cancers in which p53 is mutated.

Many therapeutic agents are capable of inducing cell death through p73-mediated apoptosis[27]. p73 activity, in cells lacking functional p53, can initiate apoptosis in reaction to treatment with captothecin, etoposide, cisplatin, doxorubicin, and taxol[64]. Thus, if p73 can be successfully activated in tumors with mutant p53, it could be considered an attractive target for therapeutic development[409]. In fact, p73 is often more highly expressed in different tumor types relative to normal tissue, and this upregulation correlates with poor patient prognosis[77]. Current theories suggest that TAp73 is 'tolerated' in tumor cells and is negatively regulated by the concomitant expression of ΔNp63, ΔNp73, or mutant p53[91,400,410]. However, we have identified many tumor cell lines and tumors that have elevated levels of p73 in the absence of p63 and mutant p53 expression; thus, other mechanisms of p73 inactivation are in play. Thus, p73 is an attractive therapeutic target that we do not fully understand. This chapter discusses the known interaction of p73 and MDM2 as well as discusses putative interacting proteins identified through a yeast two-hybrid screen, with the goal to better understand the regulation of p73.

Results

Known Regulator of p73, MDM2, Inhibition by Nutlin 3

The levels of p53 are highly dependent upon the rate at which it is degraded by the proteosome[12]. MDM2 is the E3 ligase that is responsible for p53 ubiquitination that leads to its degradation. Interestingly, p73 is not targeted for degradation by MDM2; but the latter has been shown to bind, and reduce the function of p73[411]. A small molecule inhibitor of the MDM2-p53 interaction, Nutlin-3a, has been identified and further shown to induce apoptosis in cell types that retain functional p53[412]; however, Nutlin-3 can also suppress cellular growth independent of wild-type p53. A potential mechanism for the latter is provided by the discovery that Nutlin-3a can dissociate p73-MDM2 interactions, resulting in elevated levels of p73 activity[413] and presumably growth arrest or apoptosis. It is with this knowledge that we sought to understand possible mechanisms for p73 regulation as well as determine if exploiting the MDM2-p73 interaction could provide a method for activating apoptosis in cells lacking functional p53.

p73 expression is retained within some tumors (typically in those with deficient p53 activity), but is not thought to be deregulated in these conditions[6,414]. A further understanding of how p73 is regulated is important as it will lead to a better understanding of p73 function in normal and transformed cells, and it may provide therapeutic targets for tumors with mutated p53.

As proof-of-concept that manipulation of the interaction of p73 and a modulatory protein could lead to activation of p73 pro-apoptotic activity, we used

Nutlin-3a to disrupt MDM2 and p73 binding. The Johnston laboratory in the Department of Chemistry at Vanderbilt University has developed a novel method for synthesis of the Nutlin-3 inhibitors that enables large-scale, relatively inexpensive synthesis[415]. Thus, through an ongoing collaboration we have been able to perform some relatively large-scale experiments in culture with various genetically-defined cell lines, to determine if the MDM2-p73 interaction is a potential protein-protein interaction to target in tumors with mutated p53.

Nutlin 3a exists as two enantiomers within the same compound. One of which is significantly more potent than the other, the Johnston group can selectively synthesize the two enantiomers of Nutlin that are both present in the commercially available Nutlin 3a. As part of the collaborative studies, we determined if the synthesized active enantiomer of the Nutlin inhibitor (henceforth defined as (-)- Nutlin 3)[415] was comparable to the previously reported Nutlin 3a[412]. We utilized the p53 wild-type HCT116, RKO, and primary human mammary epithelial cells (HMEC) cell lines and observed increases in the expression of p53 as well as the downstream target of p53, MDM2 (Figure 22A). Isogenic lines of HCT116 *p53+/+* and HCT116 *p53-/-* have been used commonly as cell line models to characterize p53-dependent activities and biologies[416]. We utilized these isogenic cell lines to show p53-dependent elevation of known

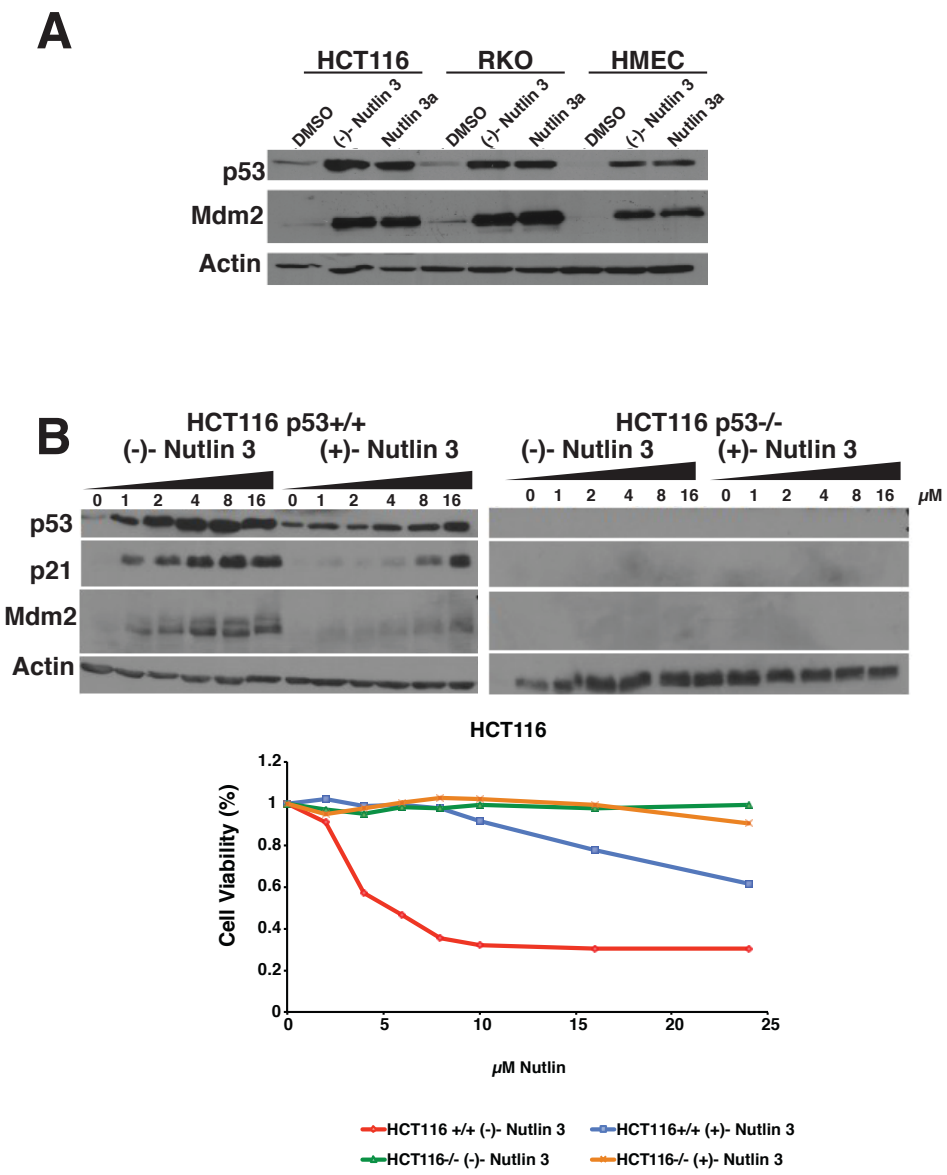

Figure 22. Newly Synthesized (-)- Nutlin 3 Exhibits Comparable Activity to Nutlin 3. (A) HCT116, RKO, and HMEC cells lines were treated with DMSO, (-)- Nutlin 3 and commercially available Nutlin 3a. The levels of p53, Mdm2, and Actin were analyzed by Western blot. (B) The active ((-)- Nutlin 3) and inactive ((+)- Nutlin 3) enantiomer were utilized to treat HCT116 p53 wild-type and isogenic null cell line. Downstream targets p21 and MDM2 were analyzed for p53 activity. The metabolic activities of cells were measured using Alamar Blue assays with treatment of HCT116 cells with either (-)- Nutlin 3 and (+)- Nutlin 3. All data represented was collected by Clayton Marshall.

targets, p21 and MDM2, after treatment with (-)- Nutlin 3 (Figure 22B).

We determined that 1000 nM (-)- Nutlin 3 for eight hours significantly activated p53-dependent transcription of downstream targets p21 and MDM2 (Figure 22B). The same cell lines required 8000 nM of the inactive enantomer (+)- Nutlin 3 for eight hours to give comparable elevations in p53 targets (Figure 22B). The viability of these isogenic lines was also measured, and we observed that the growth of HCT116 *p53+/+* line is most inhibited by the active (-)- Nutlin 3 and much less so by (+)- Nutlin 3, while the HCT116 *p53-/-* cell line was not growth inhibited either enantiomer of Nutlin 3 (Figure 22B).

We treated a panel of 28 triple negative breast cancer (TNBC) cell lines as well as HMECs with (-)- Nutlin 3 and graphically represented the μM value of their IC_{50} value observed after 72 h of treatment (Figure 23). Cell lines with functional p53, including HMECs, which express all three p53 family members, were determined to be most growth inhibited by Nutlin treatment; however, there was also a group of p53 mutant/null cell lines that displayed intermediate sensitivity, while others were insensitive to (-)- Nutlin 3 (Figure 23). Western blot analysis of 19 of the TNBC cell lines treated with (-)- Nutlin 3 and the p53 activating chemotherapeutic doxorubicin (Dox)[417] indicate that those lines that are most sensitive to either drug have retained wild-type p53 that elevates after treatment with the genotoxic agent Dox (Figure 24A). The 15 less sensitive TNBC cell lines expressed either mutant p53 or were null for p53 expression (Figure 24B).

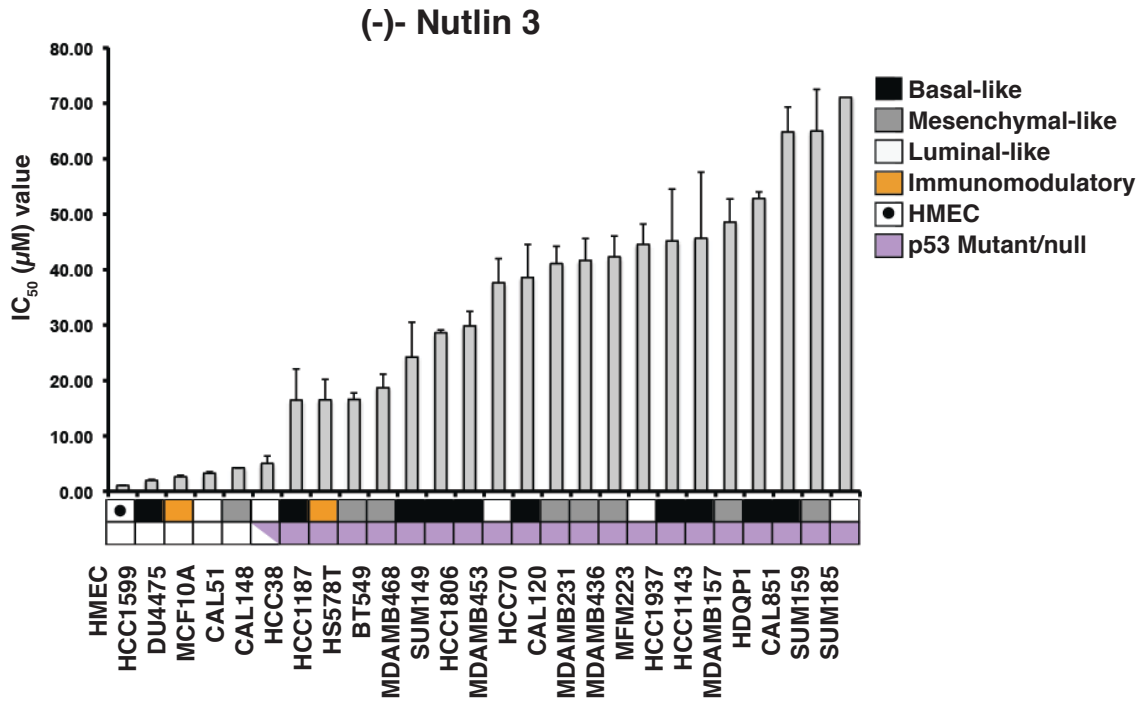

Figure 23: IC_{50} Values for TNBC Cell Lines Treated with (-)- Nutlin 3 The IC_{50} values for all TNBC cell lines are graphically represented. Sub-classification of tumor type within TNBC of each of the cell lines are annotated by black (basal-like), gray (mesenchymal-like), white (luminal-like), and orange (immunomodulatory) boxes beneath the respective columns. HMEC primary cells are annotated by a black dot in a white square for comparison to the TNBC cells. In the lowest row of boxes those cells with either mutant or p53 loss are noted by purple shaded boxes at the bottom of the graph, and those annotated in white have wild-type p53. All data represented was collected by Clayton Marshall, Brian Lehmann, and Josh Bauer.

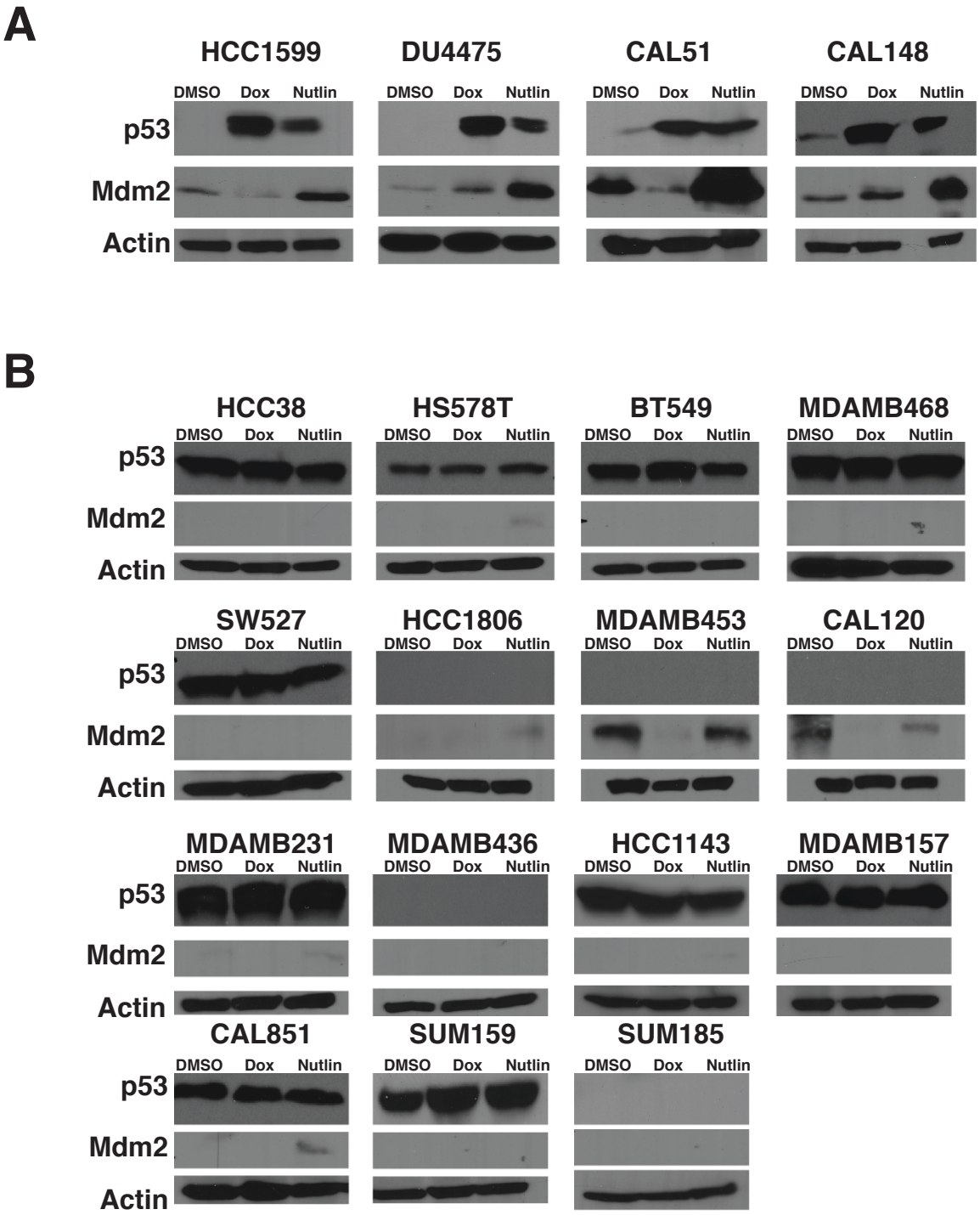

Figure 24. Immunoblot Analysis of TNBC Cell Lines after Treatment with Doxorubicin and (-)- Nutlin 3 (A) Cells with at least one wild-type copy of p53 or (B) cells with either mutant p53 or which are null for p53 expression were treated for 8 hours with 10 μM doxorubicin as well as the IC_{50} concentration of (-)- Nutlin 3 and were analyzed by Western blot for p53, Mdm2, and Actin. All data represented was collected by Clayton Marshall.

The cells expressing wild-type p53 had elevated MDM2 expression, and those that did not express functional p53 had variable and low levels of expression. We hypothesize that those TNBC cell lines with functional wild-type p53 have the greatest sensitivity to Nutlin. However, we also wanted to know the molecular feature of those lines that had intermediate sensitivity. Others have reported treatment of some TNBC cell lines with Nutlin 3 and their treatment regimen exhibited differential expression of MDM2 within some of the same cell lines we tested (e.g. BT549, MDAMB468,MDAMB453 and MDAMB231). This differential expression could be due to treatment with both enantiomers of Nutlin, whereas we were utilizing only the active enantiomer (-)- Nutlin 3.

MDM2 binds p73 but is not capable of ubiquitination or signaling for degradation of p73. The interaction of MDM2 and p73 lead to the sequestration of p73 from the nucleus; thus, affecting its transactivation capabilities[411]. Thus, we hypothesized that cells with intermediate sensitivity may express p73 that is functionally reactivated after treatment with (-)- Nutlin. We focused on lines that express some isoform of p73 and retain wild-type p53 (DU4475 and CAL148), express mutant p53 (HS578T and BT549) as well as lines that are null for expression of p53 (MDAMB436, MDAMB453, and HCC1806) (Figure 23). We observed that CAL148, and MDAMB453 had increased protein levels of the more transcriptionally active TAp73β[47,418,419] protein after treatment with (-)- Nutlin 3 (Figure 25A). p73 has been shown to transcriptionally regulate itself, so it is

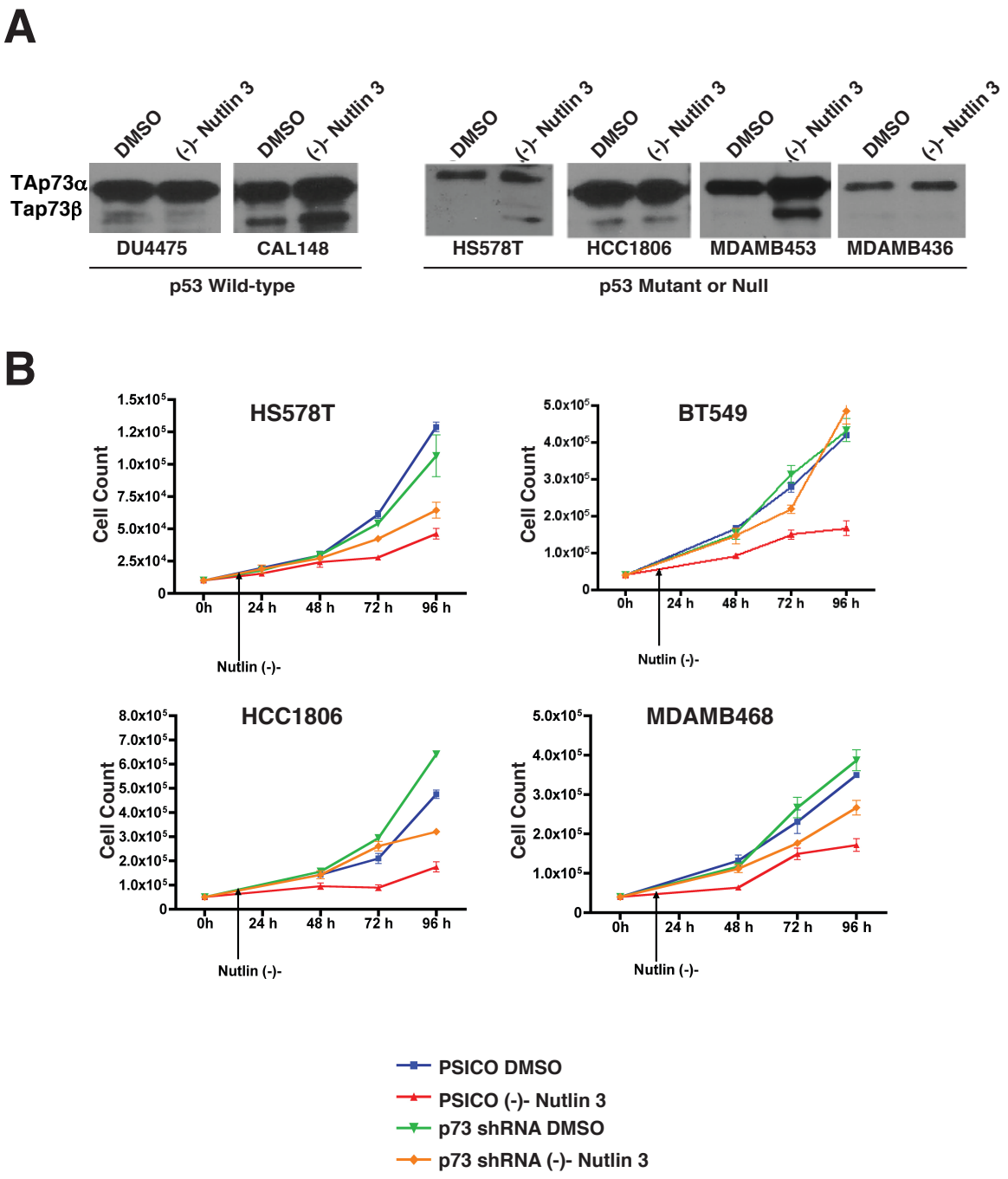

Figure 25. (-)- Nutlin 3 Activity Affects p73 Protein Levels and p73 Dependent Activity (A) Representative western blots of TNBC cell lines with WT p53 (DU4475 and CAL148), mutant p53 (HS578T), and null for expression of p53 (MDAMB436, MDAMB453, and HCC1806) treated with either DMSO or (-)- Nutlin 3. (B) Proliferation counts of cell lines from above Western blots with either control (PSICO shRNA) or p73 shRNA in which the respective IC_{50} value of (-)- Nutlin 3 was added after the cells seated (16h). Quadruplicate experiments of triplicate counts of cells were averaged and the error bars shown are the standard deviation of those 12 cell counts. All data represented was collected by Clayton Marshall.

likely that Nutlin inhibition of p73-MDM2 binding activates self regulation of p73 transcription.

To determine if p73 is responsible for the effect of (-)- Nutlin 3 in the somewhat sensitive TNBC cell lines, it was stably knocked down in HS578T, BT549, HCC1806, and MDAMB468 by utilizing lentiviral shRNA. Each of these lines were treated with (-)- Nutlin 3 over the period of 96 h. The cells containing non-targeting shRNA (PSICO) exhibited significantly reduced proliferation. The proliferation rate of cells in which p73 was ablated were less sensitive to the administration of Nutlin, indicating p73 dependent regulation of proliferation (Figure 25B).

Using RNAi knockdown of p73, our preliminary data suggest that the sensitivity to Nutlin in cell lines with mutant and null p53 is p73-dependent. Induction of p73-mediated growth arrest or apoptotic function in tumor cells with non-functional p53 signaling is an attractive method for treatment of the many cancers in which p53 is lost or mutated.

Further studies investigating of the shift in expression of isoforms that observed in CAL148, HS578T and MDAMB453 (Figure 25) will be of interest. Since p73 is not targeted for degradation by MDM2[411] it is likely that Nutlin induced release of p73 from MDM2 allows for p73 transcriptional activity regulating itself[75]. It is also possible that the interruption of the p73-MDM2 allows for enhanced transcriptional activation and splicing of alternate isoforms of p73 Understanding the regulatory loop surrounding the p73-MDM2 signaling axis will

provide further evidence as to whether the targeting of p73, in p53-deficient tumors, by exploiting the MDM2 interaction is a viable therapeutic option.

Yeast Two-Hybrid Screen to Identify p73 Co-Associated Proteins

A yeast two-hybrid screen was performed with ΔNp73β serving as the 'bait' against a library of 'preys' generated from a mixture of T47D, MDA-MB-468, BT10, and MCF-7 mRNA (Hybridgenics). The resulting dataset of positive 'hits' contained 28 possible interactions, from 18 candidate interacting proteins, that were above the false discovery threshold (Figure 26). Evidence that the screen was relatively robust came in the form of the following known p73-interacting proteins as positive hits: WWOX[420,421], WWP1[422], WWP2[422], YAP[423,424], ITCH[425], and mutant TP53[410,426]. Further the cDNAs encoding the known p73-interacting proteins contained domains of the interacting proteins previously mapped and reported to be required for p73 binding. Of note, MDM2 is a known binding partner of p73 that we did not identify in our two-hybrid given that it interacts with the TA domain, which was not present in our bait protein.

Many of the novel interacting proteins share similar domain structures, namely Ubiquitin Interacting Motifs (UIMs) and Coiled Domains (CDs). Of the 28 proteins from our two-hybrid screen, 10 contain at least two UIMs, while 11 contain CDs that reside within the probable binding site, based on overlap of multiple positive clones. Some of the candidate interacting proteins contain both CDs and UIMs. Many known p73-interacting proteins use CDs for protein-protein

Protein Name	Number of Fragments Bound	Domain In Bound Fragment
UBQLN1	7	UIM
EPN1	5	UIM
EPN2	5	UIM
UBC	3	UIM
ANKRD13D	1	UIM
UBA52	1	UIM
ANKRD13	5	CD/UIM
RAP80	1	CD/UIM
HUWE1	4	CD
GRIPAP1	3	CD
CTR9	1	CD
SESTD1	1	CD
TAB2	8	Unkown
INF2	7	Unkonwn
NDUFV1	7	Unkown
FREM2	3	Unkonwn
RSL1D1	1	Unkown
CUEDC1	1	Unknown
WWOX	1	WW
WWP1	2	WW
WWP2	18	CD/WW
YAP	5	CD/WW
ITCH	4	CD/WW
Tp53	2	**

Figure 26. Yeast Two-Hybrid Identified Putative Binding Partners of ΔNp73β. Proteins identified in the yeast two-hybrid using ΔNp73β as bait are listed on this table. The number of fragments bound to the p73 bait are listed in the middle column. The domains within the fragments of interaction are listed in the right-most column. The table is colored depending upon the domains observed within the area of bound fragments including Ubiquitin interacting motifs (UIM) (blue), Coiled domain (CD) (yellow), both UIM and CD (green) as well as unknown domain structures (gray). Those proteins in red font have previously been reported to be found in protein-protein interacting complexes with p73.

interactions. However, UIMs containing proteins have not been published to exhibit protein-protein interactions with p73.

EPN1

Both Epsin 1 (EPN1) and Epsin 2 (EPN2) were observed to bind to ΔNp73B in the yeast two-hybrid screen. The Epsins are accessory proteins involved in Catherin mediated endocytosis. The Epsins induce bending stress to the bilayer of lipids at the membrane creating curvature and directly inducing vesicle formation[427]. Epsins directly bind to endocytic machinery such as AP2 adaptors and Catherin itself[428,429]. Most cell types express the Epsins with some enrichment in the Brain, and keratinocytes[430,431]. Subcellular localization studies have shown that the Epsin family of proteins have cytoplasmic localization as well as punctate staining at the plasma membrane[432]. EPN1 and 2 localize in the nucleus indicating they may play a role in a signaling pathway linking endocytosis to regulation of nuclear factors[433]. EPN1 binds to the promyelocytic leukemia zinc finger protein, a transcription factor, and regulate its function within the nucleus[429,433]. Transportation into the nucleus has been shown to be increased after treatment with the antibiotic leptomycin B indicating nuclear Epsin transport is responsive to external signals[433,434]. Approximately five percent of clathrin heavy chain has been shown to be present in the nuclei[435] and has been found to bind to the p53-responsive promoter and enhances the transactivation of targets in a p53-dependent manner[436]. EPN1 has been found to directly bind clathrin[434]. We hypothesized that in a similar way Epsin and p73 may be forming a complex

that regulates the downstream transactivation of target genes through a common binding partner, possibly clathrin.

To further investigate the putative interaction of EPN1 with p73, we generated a FLAG-tagged EPN1 expression vector and ectopically expressed the protein in H1299 cells with TAp73β or ΔNp73β. The cells were grown for 24 h, proteins harvested and immunoprecipiations performed p73-specific antibodies. We detected binding of ΔNp73β and FLAG tagged EPN1 (Figure 27A). When the cells were immunoprecipitated in the reverse direction, using FLAG antibodies, we recapitulated an interaction between ΔNp73 and EPN1 from ectopically expressed proteins within H1299s (Figure 27A).

The significant increase in p21 reporter activation after ΔNp73β and EPN1 co-expression is of interest (Figure 27B). The immunoprecipitated complexes observed suggest that EPN1 binding to p73 may be ΔNp73-specific. These data lead to two interesting hypothesis i) EPN1 binds ΔNp73 and acts as an enhancer of its activity ii) or EPN1 binds to ΔNp73 and down regulates its binding to the canonical p53 binding site allowing for endogenous p53 family members to activate the transcription of downstream target genes. These hypotheses will require further experiments to validate and understand the role of the EPN1-p73 interaction.

The TNBC cell line HCC1806 expresses multiple isoforms of p73 at high levels and thus is an ideal cell line to initially investigate interactions with candidate interacting proteins. Immunoprecipitation using antibodies directed to

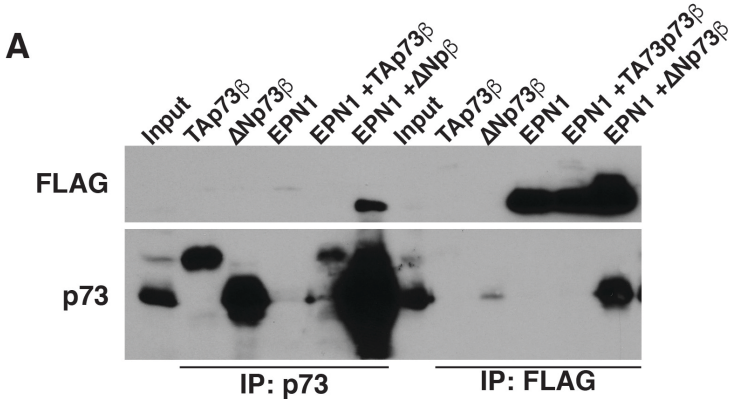

Figure 27. p73-EPN1 Interaction and EPN1-Mediated Regulation of p73 Activity. (A) H1299 cells were transfected with exogenous expression vectors of TAp73β, ΔNp73β, EPN1 (FLAG tagged). After 48 hours cells were lysed and immunoprecipitation (IP) conducted using antibodies for p73 and FLAG as annotated at the bottom of the image. Immunoblot analysis was conducted using antibodies generated to recognize FLAG and p73 as annotated on the left. All data represented was collected by Clayton Marshall.

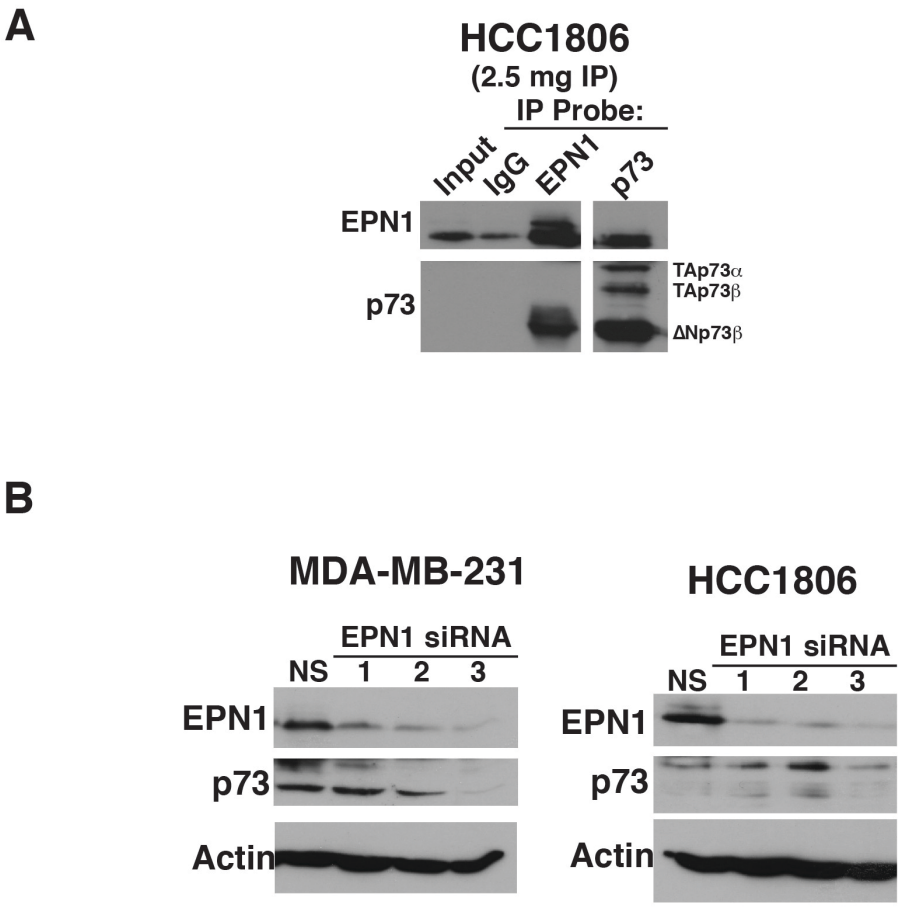

Figure 28. Endogenous Validation of p73-EPN1 Interaction (A) Rapidly growing HCC1806 were lysed and immunoprecipitated using antibodies directed against EPN1 and p73 (Right two lanes). Immunoblot analysis using antibodies generated to recognize p73 and EPN1 as indicated on the left of the image. Isoforms (TAp73α, TAp73β, and ΔNp73β) are annotated on the right of the image. (B) Three independent siRNA were utilized to ablate the expression of EPN1. Immunoblot of lysates generated from MDA-MB-231 and HCC1806 were analyzed using antibodies generated to recognize EPN1, p73, and Actin as annotated on the left of the images. All data represented was collected by Clayton Marshall.

EPN1 as well as p73 indicate that in this cell line EPN1 and p73 can be found in complex (Figure 28A). This cell line provides further evidence that the interaction is isoform specific; immunoprecipitation of EPN1 resulted in a band migrating at the same weight as ΔNp73β.

To further characterize the EPN1 and p73 interaction we knocked down EPN1 in MDA-MB-231 and HCC1806 with transfection of three EPN1 siRNAs. In MDA-MB-231 cells, reduction of EPN1 also resulted in decreased protein levels of all p73 isoforms in similar levels to the knockdown achieved by use of each of the independent siRNAs (Figure 28B). HCC1806 EPN1 knockdown also resulted in differential expression levels of p73, but not to the same degree as what was observed in the MDA-MB-231s (Figure 28B).

Determining the biological significance of the p73 and EPN1 interaction will provide insight to a novel p73-interacting protein. EPN1 has been reported to induce bending stress to the bilayer of lipids at the membrane creating curvature[427]. This function of EPN1 has not been studied in the context of MCCs and the curvature of membranes at and around individual cilia. Future experiments in MTEC cultures as well as within the context of ciliary biogenesis may provide a biological context for the interaction between p73 and EPN1.

RAP80

Receptor associated protein 80 (RAP80) is ubiquitously expressed but most highly in testis and ovaries[437]. RAP80 is associated with the BRCA1-BARD1 complex and is key to translocation of this complex to sites of DNA

damage[438]. The translocation of RAP80 to foci of damage is not dependent upon BRCA1 but it does require MDC1 and γ-H2AX[439,440]. Interestingly, through the use of the ΔNp73 knockout mouse, Wilhelm and colleagues observed ΔNp73 to co-localize to sites of DNA damage[99]. In this study they determined ΔNp73 co-localized with γ-H2AX through an interaction with 53BP1. The interaction with 53BP1 also inhibited the activation of ATM and subsequent phosphorylation of p53. Further study of other co-factors and mechanisms of these interactions have not been reported to date.

Other studies have implicated RAP80 interaction within the p53/MDM2 complex. The p53-RAP80 interaction led to an increased level of p53 ubuqiutination dependent upon MDM2 expression. This interaction led to the degradation of p53[441]. Yan and colleagues discovered a noncanonical p53 response element within the promoter of *RAP80* that is responsive to p53 expression, implicating that the p53-MDM2 autoregulatory feedback loop also includes feedback from p53 regulation of RAP80. This study also showed that depletion of RAP80 leads to stabilization of p53 increasing the level of transcription of p53 targets as well as downstream apoptosis[441]. We hypothesize that, RAP80 is a part of a complex that links p73 to the DNA damage response pathway providing a link to the earlier work implicating ΔNp73 translocating to sites of DNA damage. Also we hypothesize that, like p53, p73 will be capable of transcriptionally activating the expression of RAP80 through a noncanonical binding site.

Initial experiments investigating the RAP80 and p73 interaction focused on exogenous overexpression and immunoprecpitation-based experiments in the H1299 cell line. Cells were transfected with TAp73β, ΔNp73β, and 3xFLAG-RAP80 alone and in combination. Protein lysates were immunoprecipitated using p73 antibodies, and immunoblot analysis was conducted using antibodies that recognize p73 as well as FLAG peptide. Our data indicate that both isoforms of p73 are in complex with RAP80 in the setting of overexpression (Figure 29). Furthermore, IF analysis of H1299 cultures showed TAp73β co-localization with RAP80 in the nucleus of the cells in which both factors were co-expressed (Figure 29).

To further delineate the role of a p73-Rap80 complex more work needs to be completed to verify an interaction of the endogenously expressed protein as well as determine the effect of knockdown on the p73 transcriptional activity and biological endpoints. We hypothesize that, like p53, p73 regulates the expression of Rap80. Our data provide rationale to further pursue the interaction of p73-Rap80.

Further investigation of the interaction between TAp73 and RAP80 will focus on the DNA damage response pathway as well as the MDM2-p73 interaction. We hypothesize that both of these pathways may be connected through the regulation of 53BP1 regulation of ATM, which would then regulate the interaction of MDM2 and p73. As stated in the beginning of this Chapter, describing our results with the Nutlin-3 inhibitor data, developing a more in depth

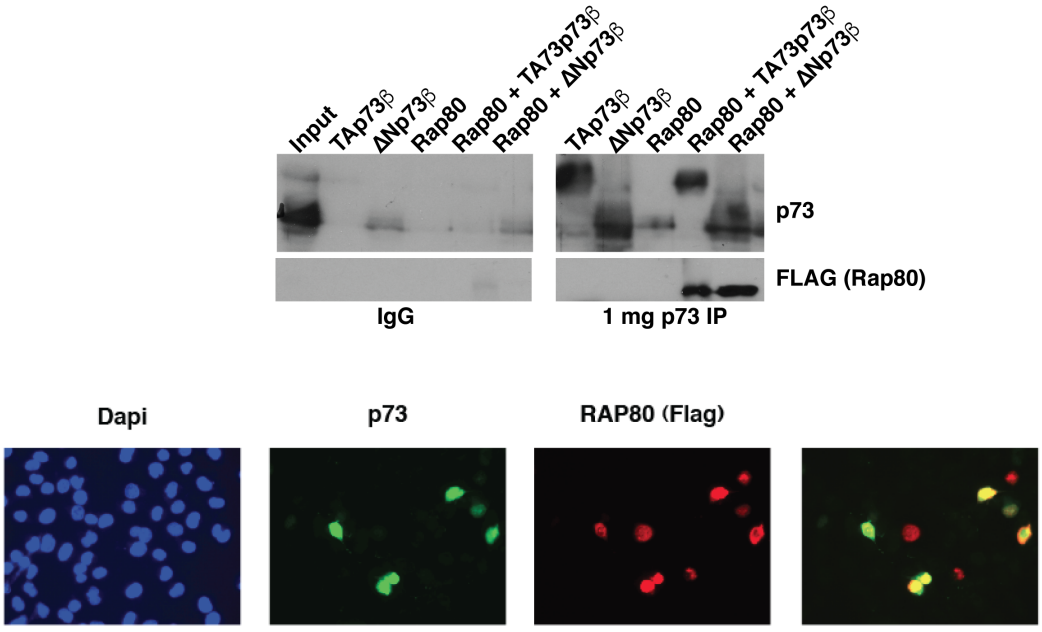

Figure 29. Exogenous p73-Rap80 Interaction and Co-localization H1299 cells were transfected with vectors that overexpress TAp73β, ΔNp73β, as well as Rap80 (3xFLAG). (A) Input, IgG and 1 mg p73 IP were Immunoblotted using antibodies directed to recognize FLAG and p73. Representative micrographs of IF experiments in which H1299s were co-transfected with TAp73β (green) and Rap80 (3xFLAG) (red). DAPI is shown in blue and the overlay of p73 and FLAG immunofluorescence channels are shown as the rightmost image. All data represented was collected by Clayton Marshall.

understanding of the complex signaling pathway that regulates the MDM2-p73 provides a window that may be exploited therapeutically in patients with mutated p53.

TAB2

TAB1 and TAB2 were discovered in 1996 in a yeast two-hybrid system using TGF-β activated kinase (TAK1) as bait[442]. Upon overexpression of TAB1/2/3, the kinase activity of TAK1 increases[442,443]. TAB2 has been shown not only to mediate activation of TAK1, but also be essential to its deactivation[444]. TAB proteins, through binding with TAK1, are implicated in several distinct pathways in response to extracellular signaling, including but not limited to TGF-β[442], NF-κB[445,446], and JNK[447]. Previous research into the protein-protein interactions of TAB proteins has been focused on the binding of monoubiquitinated partners through their respective CUE domains[448] as well as binding to polyubiquitin chains through their respective zinc finger domains[449].

Ectopic expression of TAB2-FLAG and p73 isoforms in H1299 cells followed by immunoprecipitation using antibodies for p73 or TAB2, we showed that both TAp73β as well as ΔNp73β bind to TAB2 (Figure 30A & B). As a negative control, we overexpressed BAX and did not observe binding of BAX with either p73 or TAB2 (Figure 30A and 30B). We also investigated the localization of p73 and TAB2 after ectopic, concurrent overexpression of both proteins in H1299s. We noted nuclear and perinucliar expression of p73 and predominately

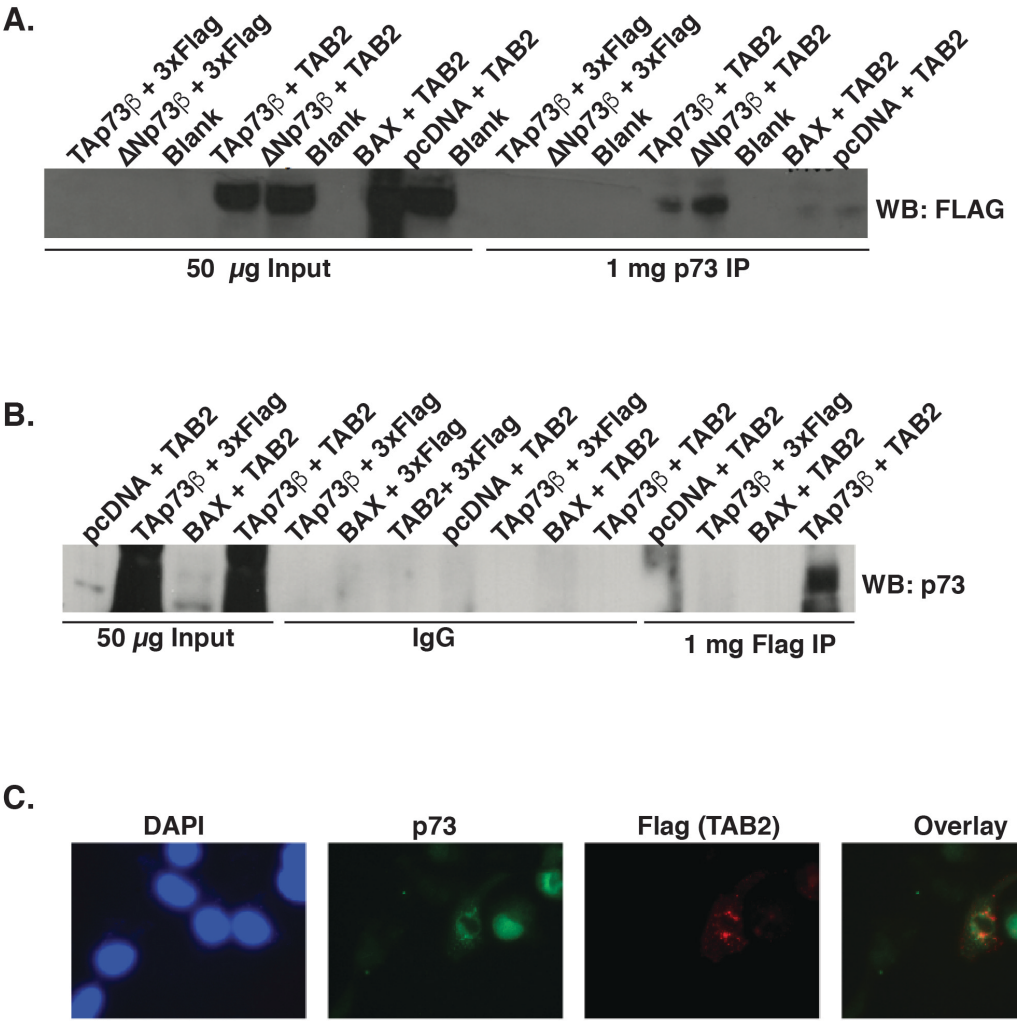

Figure 30. Exogenous Validation of p73-TAB2 Interaction and Localization (A and B). H1299 cells were transfected with vectors that overexpress TAp73β, ΔNp73β, BAX, 3xFLAG, as well as TAB2 (3xFLAG). (A) Input and 1 mg p73 IP were Immunoblotted using antibodies directed to recognize FLAG. (B) Input, 1 mg IgG IP, and 1 mg FLAG IP were Immunoblotted using antibodies directed to recognize p73. (C) Representative micrographs of IF experiments in which H1299s were co-transfected with TAp73β (green) and TAB2 (3xFLAG) (red). DAPI is shown in blue and the overlay of p73 and FLAG immunofluorescence channels are shown as the rightmost image. All data represented was collected by Clayton Marshall.

perinuclear expression of TAB2. The cells in which we noted perinuclear p73 were the same cells in which we observed TAB2 overexpression (Figure 30C).

We did not observe robust p73-TAB2 complexes in many cell lines initially tested. TAB2 has been shown to be implicated in biological signaling after cells have undergone DNA damage[450]. Cisplatin (CDDP) has been shown to activate p73 activity in a c-Abl-dependent manner[112]. We tested the hypothesis that the p73-TAB2 interaction was DNA-damage regulated, and treated cells with CDDP and analyzed the proteins. Initially we noticed a shift in molecular weight of the TAB2 protein in some cell lines tested. Immunoprecipititation of p73 in TNBC cells (HCC1806 and MDA-MB231) as well as a rhabdomyosarcoma line (RH30) indicated that the interaction of p73 and TAB2 was significantly increased after CDDP treatment (Figure 31). As a negative control, stable lines in which p73 has been removed using shRNA were also immunoprecipitated for p73 to test whether the interaction observed was p73 dependent. Our data indicate there are two TAB2 species on a Western blot in certain cell lines, both of which are capable of knockdown with TAB2 specific shRNAs. ΔNp73 appears to preferentially bind to the slower migrating band only (Figure 31). This expression pattern implies that TAB2 may be alternatively spliced and not all variants bind p73. Further experiments are needed to determine the binding domains for the interaction ofthese two proteins. Future experiments to validate the preliminary findings and extend them will be necessary to determine the role of the TAB2 and p73 interaction under conditions of normal cell growth and DNA damage.

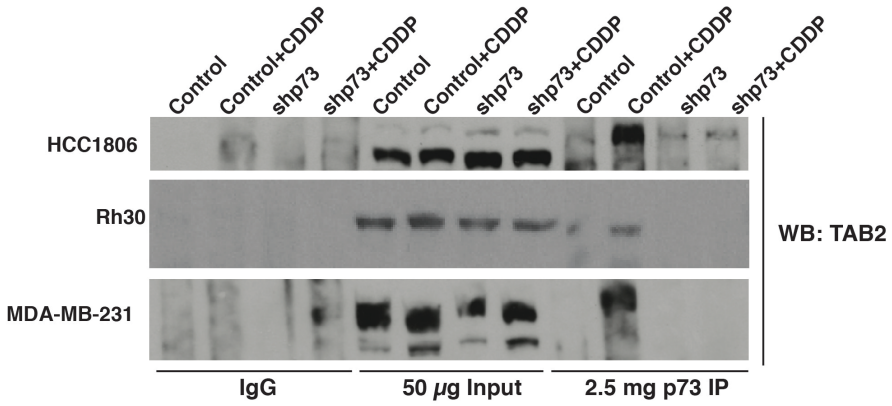

Figure 31. Endogenous Validation of p73-TAB2 Interaction. Isogenic cell lines (HCC1806, Rh30, and MDA-MB-231) expressing p73 (control) and those in which p73 has been stably removed (shp73), were either untreated or treated with cisplatin (CDDP). IgG IP, 50 μg input, and 2.5 mg p73 IP samples are annotated on the bottom of the immunoblot images. Immunoblot analysis was conducted using antibody directed to TAB2. All data represented was collected by Clayton Marshall.

Our experiments do not indicate that the levels of TAB2 are altered after CDDP treatment, however we do observe a shift in the migration of TAB2 in some of the cell lines tested by Western blot. In previous studies of the signaling effect of TAK1, the co-associated TAB proteins have been observed to be cytoplasmic as well as nuclear in localization after treatment with TNF-α as well as lipopolysaccharide (LPS)[451]. Since the levels do not appear to change after treatment, but p73-TAB2 complexes are increased. We hypothesize that the localization of TAB2 changes after treatment with CDDP. Exogenously overexpressed TAB2 in H1299s did not appear to localize within the nucleus but was predominately observed to be present in punctate foci in close proximity to the nucleus. Exogenous overexpression of TAB2 also did not increase p73-mediated expression of p21, Noxa, or PUMA. There must be other factors that are necessary to induce TAB2 translocation into the nucleus within specific biological contexts, so to further determine the functional relevance of TAB2-p73 interaction we will continue to focus on those treatments that have been shown to activate a p73 signaling.

Conclusions

Identification of p73-interacting partners provides insight to p73 regulation and function and also biological contexts in which p73 may be therapeutically targeted. Also, it will be important to consider the candidate p73-interacting proteins in the context of MCC differentiation. For example, EPN1 has been reported to induce bending stress to the bilayer of lipids at the membrane[427].

This function of EPN1 has not been studied in the context of MCCs and the curvature of membranes at and around individual cilia. RNAseq experiments from our investigation of the murine pulmonary epithelium showed that EPN1 was highly expressed in the tracheal epithelium. Our data indicate that the interaction between EPN1 and p73 may be specific between EPN1 and ΔNp73 isoforms. However, further experiments in MTEC cultures as well as within the context of ciliary biogenesis may also be of great interest to better define the role of ΔNp73 within a specific developmental process. The discovery of p73 regulation of MCC differentiation has presented a relevant context for future study of p73 activity. We now have model systems of MTEC growth and differentiation in culture from p73 wild-type and deficient tracheal cells. This system will provide a much-needed system to the investigation of p73, as we can now directly measure the activity of p73 within a developmental process. The knowledge of this role for p73 did not exist at the time of discovery for these candidate interacting proteins. Now that we better understand a biological context of p73, it will allow for a broadening of the investigation of these interacting proteins into a newly discovered biological relevant process dependent upon the transcriptional activity of p73.

CHAPTER V

FUTURE DIRECTIONS AND CONCLUSIONS

Introduction

Our findings have provided insight to signaling pathways that govern epithelial cell differentiation and transformation and offer an exciting starting point for subsequent discovery. MCCs that line the airways provide essential innate defense against agents that can drive transformation. Dysfunction of motile cilia has been linked to several human diseases[387,402] and, despite its clinical significance, little is known about the molecules and signaling pathways that govern motile cilogenesis and MCC differentiation. In the future it will be important to determine the cooperative and antagonistic roles of p73 and p63 in MCC fate determination. We further identified multiple putative binding partners of p73 that we hypothesize regulate its function in both a tumor setting as well as during epithelial cell development. Placing p73 in a new developmental context has provided many new directions to experimentally investigate the complex nature of transcription factor regulation; this chapter will outline a few hypotheses that should be pursued to better understand the roles and regulation of p73.

p73 and MCC Differentiation

Our p73 and Pol II ChIP-seq identified many novel p73 targets linked to MCC fate. We will initially focus on Foxj1, Myb, Mcidas, Traf3ip1 mRNA targets, and miR-449, as they have known links to multiciliogenesis programs[334,335,346]. We determined p73 bound to regulatory regions and Pol II to coding regions of

these genes in murine tracheal cells. During the dissertation work, we focused specifically on the role of p73 transcriptional regulation of Foxj1. Future studies determining how p73 regulates these mRNA as well as other miRNAs that regulate MCC fate will further determine at what stage of MCC differentiation p73 is critical.

In the *Foxj1* knockout mouse model, basal bodies are amplified but do not adequately dock to the cell membrane and cilia are not formed[339]. Preliminary IF experiments utilizing antibodies directed against the basal body markers γ–tubulin as well as Traf3ip1 indicate that our *p73-/-* mice are deficient of amplified basal bodies. This absence of basal bodies indicates that the role of p73 is upstream of that of Foxj1. It will be of interest to determine the role that p73 plays in licensing progenitor cells to become MCCs, both at the level of transactivation of FoxJ1 and subsequent basal body amplification as well as the necessity for p73 in later steps of MCC differentiation. Our finding that p73 directly regulates Foxj1 provides a starting point. Future experiments with the other 105 genes we discovered to be bound by p73 and also observed to be cilia-associated genes (Figures 16 and 17) will provide insight into all of the pathways in ciliogenesis that are regulated by p73. In MTEC cultures we can determine the effect of the presence or absence (through gene knockdown) of the newly identified target genes of p73 (e.g., Myb, Mcidas, Traf3ip1 and mIR-449) on MCC differentiation. These experiments will be necessary to decipher which p73-dependent gene expression is required for MCC differentiation.

Our discovery of p73 expression within a subset of basal cells, as well as p73 binding in close proximity to a significant proportion of cilia-associated genes within the airway epithelium (Figures 16, 17, and 18), leads us to hypothesize that p73 is an apex regulator of ciliogenesis that is regulated through its interaction with p63, and without p73, progenitor cells are not licensed to the differentiate along MCC lineage. The predominate isoform of p63 expressed in pulmonary epithelium is the suppressive ΔNp63α isoform. There must be a biological switch mechanism by which p73 transcriptional activity is released from ΔNp63 negative regulation to allow for MCC differentiation.

Interplay of p73 and p63 Within a Subset of Basal Cells

Given the known interplay of p73 with p63 and p53[6], it is important to determine the role, if any, of the other two p53 family members in regulating MCC differentiation. Using murine models as well as gene knockout and overexpression strategies in well-established cell culture models, we will further investigate p53 and p63 roles in MCCs. Based on our mouse model results, we predict that targeting p53 will not have any effect on FoxJ1, Mcidas, miR-449 and MYB-mediated MCCs. To our knowledge, there is not a defect in multiciliogenesis in *p21* knockout mice nor any observed phenotypes consistent with lack of MCCs[452,453]. Since we observed a decreased number of basal cells and an increased number of ciliated cells in E18.5 mice with p63 knockdown, we predict that loss of the predominant isoform of p63 expressed, the repressive ΔN, will result in an increase in the activity of TAp73 on target genes and 'drive' more

stems to early licensing to MCCs. p63-deficient human bronchial epithelial cells are unable to form cultures due to a proliferation defect[253]. With this in mind, we can attempt to acutely knock out p63 after the cultures are established. Given the results from the *p63* knockdown E18.5 mice, we anticipate an increase in MCCs and a reduction/loss of secretory, club cells in our cultures. Since the airway epithelium still develops in both p63- and p73-deficient animals, albeit skewed in cell type, this suggests: i) a cell that does not depend upon the expression of p63 gives rise to the progenitors that get licensed for MCCs differentiation in the p63- mice; and/or ii) there is an airway stem cell that does not require p63 or p73 activity. Examination of the airway in *p63-/p73-* E18.5 mice would provide insight. It will be interesting to determine if p73/p63 dual knockout mice are even capable of producing an epithelium or if there is a projenitor cell that promotes a fully neuroendocrine cell lined epithelium.

Using the *p73-/-* mouse model we can begin to separate the independent functions of these transcription factors by investigating the profile of p63 binding to genomic sites when p73 is absent. Performing an *in situ* ChIP-seq of p63 in p73-deficient animals and comparing the data to our p63 ChIP from *p73+/+* animals will begin to indicate the p63 genomic binding that is dependent and independent on p73. Also it will provide insight into the signaling in the basal cell population that is retained in the *p73-/-* animals.

p63-/- mice are not viable and not suited to *in situ* tracheal ChIP-seq (due to small size of airway in E18.5 mice). To determine the binding profile of p73 in

the absence of p63 from the tracheal epithelium, we could achieve p63 recombination using inhalable Cre delivery which would targeting directly the tracheal epithelium of *p63*$^{floxE5\text{-}7/floxE5\text{-}7}$ mice, and follow with ChIPseq of p73. Alternatively, we could also use wild-type MTEC cultures in which we target p63 using shRNAs to determine the p73 genomic binding sites in the presence and absence of p63. These experiments could be paired with ectopic expression of p63 and p73 in MTEC cultures to further determine the regulatory changes in mRNA expression under the various experimental conditions.

During the initial characterization of the *p73-/-* mice and control wild-type animals, we noted that in a majority of the p63-expressing basal epithelial cell containing tissues (e.g. mammary and skin), p73 was co-expressed in a significant fraction of basal cells. We hypothesize that the balance of p63 and p73 activity is necessary for the proper basal cell homeostatis in the many tissues in which they are co-expressed.

p73 and p63 Regulation of Pulmonary Epithelial Repair After Damage and Stress

Little is known about the interplay of the p53 family members in controlling airway epithelium and repair after damage. We can exploit the tracheobronchial epithelium in mouse models and MTEC cultures derived from these mice as genetically tractable human airway models. We can determine if the p53 family is expressed and necessary in injury-induced suprabasal expansion in the tracheobronchial epithelium.

We can use p53 family mouse strains and perform crosses to study MCCs in the context of homeostasis and stress-induced repair. This can allow us to answer the following questions: i) can we gain insight to the signal that dictates p73 expression and activity in the basal cells by analyzing p73 before, during, and after injury/repair? Is expression stochastic or due to spatiotemporal growth factor gradients that are known upstream activators of p73 (e.g. E2F1)?; ii) how do downstream signaling (e.g. Foxj1, Notch, Myb, Mcidas) become attenuated at the time of commitment of the undifferentiated basal cells that co-express p73 and p63?; and iii) what is the signal that attenuates the p63 signaling at the time of commitment to MCC differentiation of the basal cells that co-express p73 and p63? Is the loss of the repressive activities of p63 releasing the activity of p73 licensing MCCs? Or is it elevation of p73 that outcompetes the antagonistic activity of p63? Does TAp73 activity elevate a downstream target gene product that in turn downregulates p63? There are ample data indicating that persistence of Notch signaling blocks MCC development, and that loss of Notch results in overpopulation of MCCs in the airway (discussed further in following section). It will be important to determine the interplay of p73, p63 and Notch and the 'signaling switches' in the undifferentiated basal cells co-expressing p63 and p73 that stimulate commitment to MCC cell fate.

The McKeon group reported the presence of p63-positive cells in the bronchiolar epithelium of mice that had been challenged with H1N1 infection[256,454], and demonstrated that these distal stem cells are required for

alveolar regeneration within damaged lungs[255,257]. Others have shown that ΔNp63 is necessary for maintenance and regeneration of the airway epithelium after damage[252,253]. We determined p63-expressing cells in the bronchiolar epithelium of our *p73-/-* with increased concentration in areas of increased inflammation and mucus retention observed in adjacent tissue. These data indicate that the lungs of *p73-/-* mice exist in a state of continual stress or damage.

There are many damaging toxins (e.g. bleomycin, naphtaliene, H1N1, O_2, and SO_2) utilized in murine models to mimic damaging events to pulmonary epithelium[455]. These damaging events ablate specific cells (naphthalene- Club cells; O_2-alveolar cells) or all cells (bleomycin, H1N1 and SO_2) and require the pulmonary progenitor cells to proliferate to re-populate and repair the epithelium[455]. We can utilize these treatments within the context of *p73+/+* and *p73-/-* to determine the ability of the remaining basal cells in the *p73-/-* mice to repopulate the pulmonary epithelium. Challenging adult mouse airways with these damaging agents would give us a timeline to monitor the capacity of cells to react in real time. It will also be of interest to determine the mechanism of death that the epithelial cells undergo after treatments with the toxins. We hypothesize that the p53 family will be integral to the process of epithelial turnover. The *p73-/-* epithelium may exhibit decreased or differential reaction to the toxins as compared to *p73+/+* animals. It is also possible that other p53 family members are responsible for epithelial death or that they are capable of

compensating in the p73-deficient animals. These experiments will further clarify the role of the p53 family within the pulmonary epithelial basal cells after a damaging event, as well as provide insight to the timeline of p73 activity in MCC development.

The Role of p73 in Inflammatory Response

p73 knockout mouse models display increased levels of inflammation[1,16] with very little mechanistic follow-up since the original discovery to further understand the ramifications of this phenotype. In one study, Tomasini and colleagues used a model of lethal dosage of lipopolysaccharide (LPS) intravenously to determine the contribution of p73 to innate immunity. The *TAp73-/-* mice exhibited higher levels of proinflamatory cytokines in circulation and significantly greater mortality as compared to wild-type littermates[456]. The investigators further determined that the *TAp73-/-* mice have an impaired resolution of inflammatory response due to a role in macrophage polarization[456].

We noted the lungs of our *p73-/-* mouse are in a constant state of inflammation and mucous retention. At this time we have not determined that the inflammatory response is due to the increased level of foreign bodies due to the loss of MCCs or if there is a defect in cell lineages that contribute to inflammatory responses. Tracheal administration of LPS is much more mild than intravenous administration used in the previous sepsis model work[456], tracheal administration does not result in a sepsis rather pulmonary-based immune activation[457,458]. Intratracheal LPS migrates through the epithelial barrier[459-463]

and activates the CD14/TLR-4 complex trigging an inflammatory response[464-466]. This model would be ideal for treatment of the *p73-/-* mice to determine if there is a differential inflammatory response that is p73-dependent. Comparing the inflammatory cells of untreated- and LPS-treated *p73+/+* and *p73-/-* lungs can provide a system in which we can start to determine if the inflammation we observe is dependent on p73 or if it is secondary to the dysregulation of the cell composition of the pulmonary epithelium.

Additionally, Foxj1 has been previously reported to regulate T cell activation through modulation of the NF-κB pathway, with Foxj1 deficiency leading to systemic inflammation and autoimmunity defects[401]. Foxj1 transcriptioanlly regulates IκBβ, the negative regulator of NF-κB, and in the absence of Foxj1 the NF-κB pathway is hyperactive leading to immune dysregulation[401]. Given our finding that p73 is a direct regulator of Foxj1, future studies are needed to evaluate the mechanistic importance of Foxj1 deficiency in T cells and the inflammatory defects observed in the *p73-/-* setting.

Notch Pathway

TAp63 and TAp73 can transactivate the Notch ligands Jag1 and Jag2 and regulate Notch signaling in neighboring cells[52,390]. Another means for interaction between the Notch pathway and the p53 family is binding of the Notch Intracellular Domain (NICD) by p53 or TAp73 with a resultant inhibition of downstream Notch signaling[467,468]. A further regulation of Notch and the p53 family involves activation/repression of the Notch co-activator MAML, which is

potentially engaged by p53, p63 and p73[469]. A well-studied example of the interplay between the p53 family and Notch is the skin, where basal cell self-renewal and the terminal differentiation gradient are determined in part by antagonistic p63/Notch signaling. Notch is an essential factor in skin differentiation, and TAp63 and p53 have been shown to transactivate Notch1[470,471]. In basal cells of the skin, ΔNp63 can inhibit TAp63 and attenuate Notch signaling through binding to Notch target genes[472]. We propose that in the airway epithelium, ΔNp63 is a major antagonist of differentiation and TAp73 is the major driver of MCC differentiation. An understanding of the interplay of the p53 family and Notch signaling in lung epithelium will provide molecular insight to signaling dysfunction during tumorigenesis and other lung diseases.

The Notch pathway plays a key role in development and maintenance of the lung epithelium[238]. There are four Notch receptors (Notch 1-4) and five ligands (JAG1, JAG2, DLL1, DLL3, DLL4). The interaction of ligand and receptor causes cleavage of the Notch receptor at the membrane and release of the Notch intracellular domain (NICD). Notch and its ligands are differentially expressed in the various cell lineages and tightly regulated through lateral crosstalk[238,267]. There is evidence for a link between Notch signaling and the observed lung phenotype in the *p73-/-* mice. When NICD was overexpressed within the developing lung, there was a reduction in the numbers of ciliated cells with increased club and mucin cells[237]. In mice with lung-specific knockout of Pofut1 and RBPJK, two activators of Notch, there was an increase in MCCs and

neuroendocrine cells and a reduction of club and secretory cells[238,473].

As is the case for all biological systems, the integration of numerous signaling networks results in the proper cell function under a given condition. The role of p73 in formation and maintenance of airway epithelium was unknown prior to our findings and now it is important to determine how p73 is integrated with other relevant pathways to control multiciliogenesis *in vivo*. Further, it is critical to determine the *in vivo* role of p73 in the injury/repair response in the airway epithelium given that disruption of p73-mediated multiciliogensis likely contributes to susceptibility conditions (e.g. COPD) that cause predisposition to lung cancer. Combining data from our studies and others[171,235,236,251,398], we hypothesize that the p63 and p73 signaling axes are critical for differentiated airway epithelium; however, they most likely integrate with other signaling modules in the lung, with Notch being a primary candidate. Notch signaling and its spatiotemporal regulation have been previously linked to differentiation of the adult airway[267].

Our laboratory and others have identified interplay between p63, p73 and Notch family signaling. Notch signaling plays an essential role in cell fate and communication. The p53 family members receive signals from Notch and assist in arbitrating stem cell maintenance, differentiation and regulation of tissue homeostasis. The coordinated transactivation of genes by the Notch pathway and p53 family is associated with the initiation of cellular programs that lead to inhibition of proliferation and/or differentiation in the skin and central nervous

system[474]. In contrast, Notch-mediated transcription in the absence of p53 family signaling is observed in cells in which the proliferative capacity is to be maintained and differentiation is biologically unfavorable, as is the case in cancer cells. In the latter scenario, the activity of p53 family members is absent or selected against through several mechanisms[474].

The disruption of Notch signaling in airway epithelial progenitor cells results in overpopulation with ciliated cells. We hypothesize that the proper coordination of p63, p73 and Notch signaling is required for normal development and homeostasis of complex multiciliated epithelium and loss of this coordination leads to lack of proper epithelial function. We can begin to investigate this utilizing MTEC culture systems as well as genetic engineered murine models.

Lung Branching Phenotype

Apart from p73 regulation of MCC development, we noted phenotypic differences in the branching of the *p73-/-* adult animals (Figure 32). Micrographs spanning the entire lung of 14 animals were quantified for the number of bronchioles observed. *p73+/+* mice averaged 103 bronchiole openings throughout the entire section of the lung while *p73-/-* mice averaged 65 (Figure 32). We can generate several hypotheses to explain the differences observed in the bronchiole tree. First, the reduction in branching is due a result of mucus retention and inflammation within the lungs of the *p73-/-* animals, which causes inadequate air exchange. It has been shown that the physical cue of air pressure/exchange is a regulator of signaling required for proper pulmonary

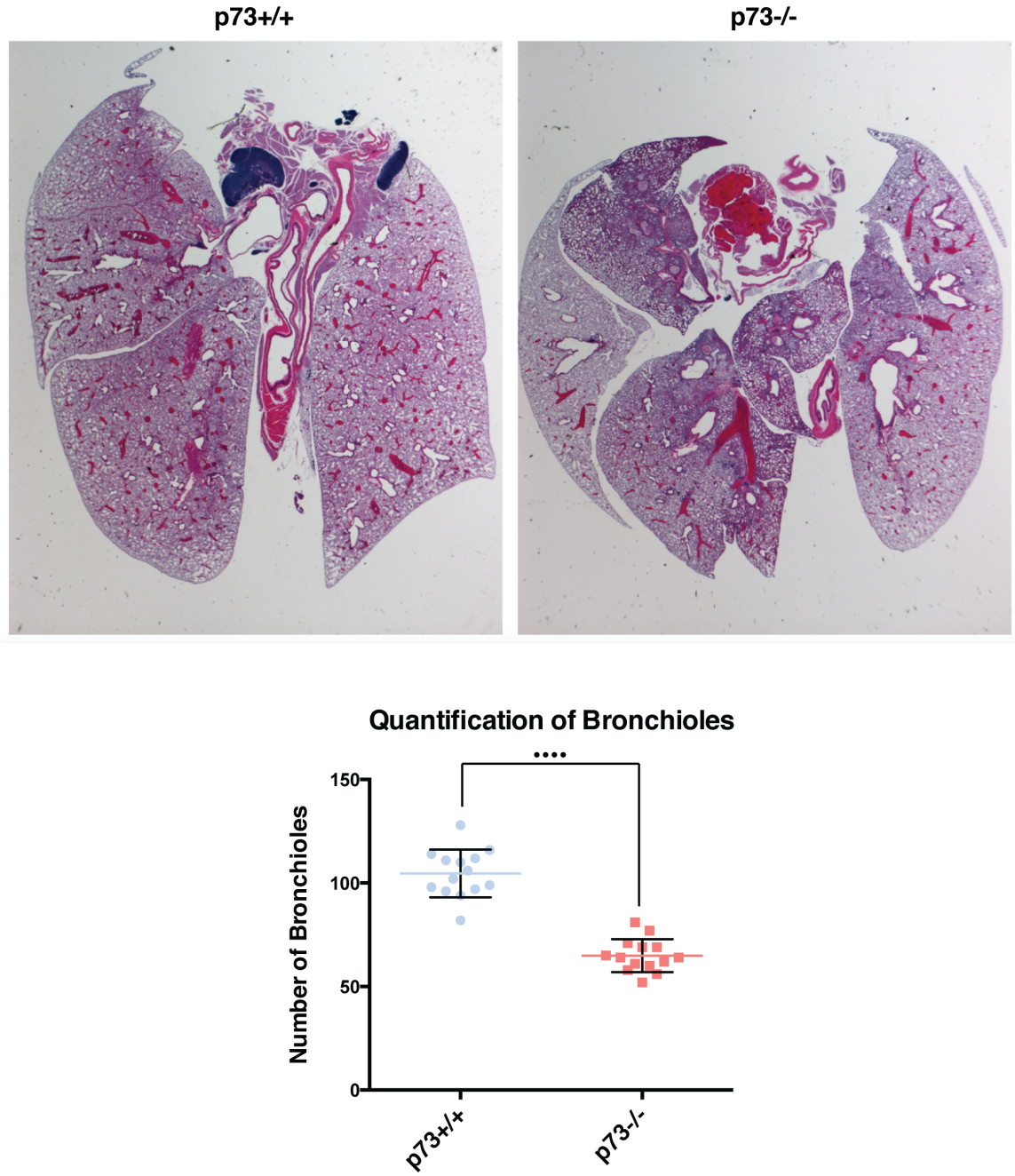

Figure 32. Quantification of Bronchioles. Images included are representative micrographs of whole lungs from *p73+/+* and *p73-/-* animals. Whole lung sections including trachea as well as main bronchioles to ensure similar depth of sectioning of 14 mice were photographed and the bronchioles were quantified. The raw counts are represented in the scatter plot with the lines in black demarcating the 25th 50th (median) and 75th percentile values. (•••• p-value<0.0001). All data represented was collected by Clayton Marshall.

branching[475]. Second, p73 signaling is directly involved in the process of pulmonary branching. To begin to determine if there is relevance to testing this hypothesis, it will be important to examine embryonic *p73-/-* and *p63-/-* animals to determine if there are significant changes *in utero* to the bronchiole branching tree. If defects in branching are present *in utero*, it will provide insight as to whether p73 signaling is regulating more than MCC fate and basal cell regulation within the pulmonary epithelium.

Regulation of p73 Through Protein-Protein Interactions

Fox proteins act as part of an enhanceosome to drive the transcriptional programs of other TFs (e.g. ERα, FOXA1, and GATA3 in breast cancer)[476]. Our finding that both p63 and p73 directly bind and regulate Myb expression prompted us to further explore the potential role of Myb in epithelial cell differentiation. A recent ChIP of Myb and p63 in adenoid cystic carcinomas revealed that 81% of p63 binding sites were co-bound by Myb[477]. We hypothesize that Myb functions within an enhanceosome that contains p63 and p73 (and perhaps Mcidas and/or Foxj1) to modulate regions of the chromatin surrounding genes required for basal body formation, amplification and core cilia gene expression. Thus, p73 “marks” a transcriptome that includes key regulators such as Foxj1 and Myb. We determined that p73 binds to more than 1700 promoter sites in basal progenitor cells as well as MCCs[1], and that even if Pol II is bound at those sites in progenitor cells, it may be ‘paused’ and not elongating transcripts until other co-activators are present and/or repressor activity is

reduced to activate the transcriptome for MCC differentiation. We hypothesize that co-binding of p63, which is co-expressed with p73 in the basal cells, represses transcription of key regulators such as p21 and miR-449 and prevents exit from an S-phase state and attenuation of Notch signaling. Cells must exit the cell cycle to allow for basal body amplification and further development of individual cilia. Repression of p73 transcription of cell cycle arrest factors would be another mechanism by which downstream factors of ciliogenesis are regulated by p73 activity. For example, Mcidas activity is cell cycle dependent and without its activity downstream targets such as FoxJ1 are not expressed{Pan, 2014 #1123}. Of note, ChIP-seq data from whole trachea epithelium demonstrate p63 co-binding at 46% of the p73 identified binding sites[1]. We postulate that there is a signaling event that function as a switch (perhaps during injury) to attenuate p63 repressive activity and thus, elevate TAp73 activity, driving MCC fate. This can be formally tested, in part, by determining if p73 requires Mcidas as a co-activator to elevate Foxj1 levels and Myb levels. The p73-mediated expression and coordination of Myb and p21 activity likely enable cell cycle exit and basal body amplification. Further analysis of target genes of Myb and Foxj1 and their proximity of binding to newly discovered p73 binding sites will assist in determining if p73 is implicated in a complex of protein-protein interactions to act as an enhancesome of transcription.

The putative binding partners of p73 within our yeast two-hybrid should be

further investigated to determine if there are pulmonary-specific roles for their biological functions. For example, Epsins coordinate endocytosis by causing in membrane bending to cause invaginations in the cellular membrane[431]. They mediate signaling from the endocytotic pathway to the nucleus. MCCs require dynamic membrane potential to properly develop membranes that cover the chains of actin that make up the individual cilia. It would be of interest to determine if the binding between p73 and Epsin1 and/or Epsin 2 has a further role during development of MCC cells and regulation of the membrane of MCCs.

Results from our tracheal ChIP-seq of p63 and p73 indicated that two of the putative binding partners, Cuedc1 and Ubc, of p73 might also be transcriptionally regulated by p73. CUE domain containing 1 (Cuedc1) was first described as one of five genes that was differentially expressed in patients with metastatic cervical cancer as compared to those without metastatic lesions[478]. Cuedc1 has been observed to be expressed at a significantly lower rate in patients with preeclampsia[479]. Little else is known about the mechanistic function of Cuedc1. We observed two binding sites for p63 and a single site for p73 within 25,000 bp or the Cuedc1 TSS (Figure 33). Polyubiquitin-C (Ubc) is a ubiquitin coding gene that is a polyubiquitn precursor. Ubiquitin is coded by four genes. UBA52 and RPS27A code for single copies of ubiquitin fused to ribosomal proteins L40 and S27A respectively[480]. UBB and UBC code for polyubquitin with head to tail repeats of ubiquitin[480]. Polyubquitin is linked through different lysine residues within the ubiquitin itself, and the pattern of

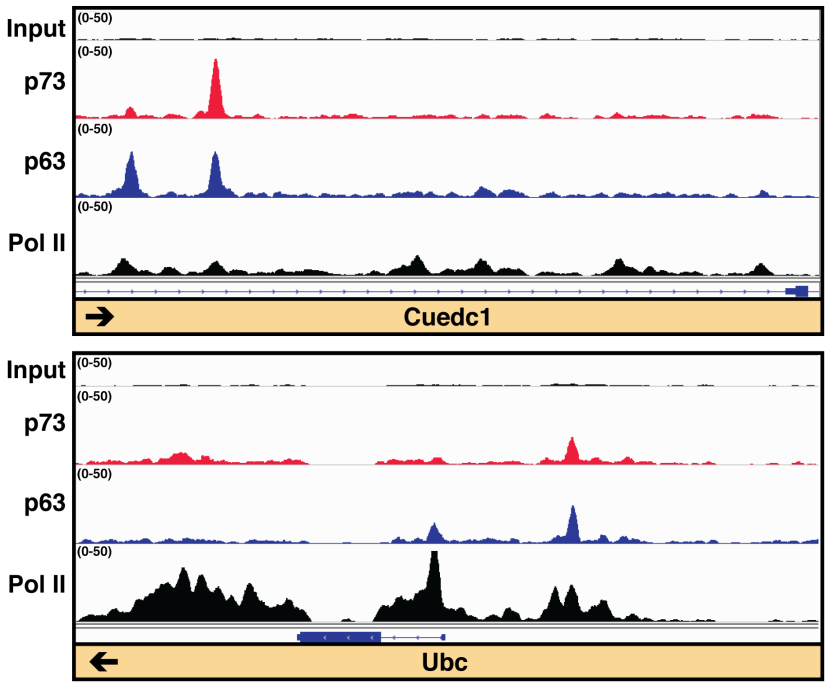

Figure 33. Tracheal ChIP-seq binding of p73/p63 in Proximity to *Cuedc1* and *Ubc*. Integrative Genomics Viewer screenshots for genes identified in the p73 yeast two-hybrid screen to which p73 and p63 are bound. The four tracks show ChIP-seq data normalized to 1x depth of coverage and presented with identical scales. The bottom three tracks represent DNA reads that were obtained after ChIP with the antibodies listed to the left, and the top track is the input sample for comparison. At the bottom of each panel is an annotated exon/intron gene structure displayed on the same scale as the ChIP-seq tracks, and the arrow in the bottom left annotates the gene orientation. Data was generated by Clayton Marshall through collaboration with Bryan Venters. Clayton Marshall was assisted in bioinformatic analysis by Scott Beeler and Timothy Shaver.

Lysine linkage regulate the downstream function of the ubiquitination of target proteins. For example, Lys-6 linked polyubuiquitin has been implicated in the process of DNA repair[439,481], Lys-11 linked ubiquitin is involved in cell cycle regulation[481], Lys-48 linked ubiquitin leads to proteosomal protein degradation[482], and Lys-63 linked ubiquitin is involved in endocytosis and DNA damage response[483].

These data lead us to hypothesize that p73 may be in an auto-regulatory loop with the co-associated proteins Cuedc1 and Ubc by directly regulating their transcription. Function of Cuedc1 is relatively understudied so any insights into the function of Cuedc1 would be beneficial for the field. UBC as a precursor for polyubiquitin chains could regulate protein activity both modulation of through turn over and activation of function. Future investigations into these interactions and the role in regulating p73 transcriptional activity will be of interest to better understand p73 regulation within a defined biological role of MCC differentiation.

p73 Status in Diseases and Cancer

To decipher a role of p73 within disease, we must investigate the expression of each of the isoforms within diagnosed disease states. The discoveries made as part of this dissertation research led to the conceptually innovative hypothesis that p73 functions as a tumor suppressor through regulation of novel target gene transcription required for determination of MCC fate in complex epithelium. In this, it is likely that p73 signaling within this cell type effects the tissue as a whole, and we must broaden our investigation of p73

from cancer-only to include the adjacent “normal” tissue in disease states.

Numerous motile cilia are located on the apical surface of epithelial cells lining select tissues that require fluid movement for proper function. The coordinated beating of multiple motile cilia is essential for mucus/infiltrate clearance in the airway, sinus and ears and the prevention of infections and inflammation in these tissues[373]. In the reproductive tract, dysfunction of motile cilia lining the efferent duct and oviduct has been implicated in the sterility of both males and females, respectively[297,298]. In the brain, lack of ependymal flow due to defective motile cilia can cause closure of the cerebral aqueduct and result in hydrocephalus and hippocampal dysgenesis[220,299,302]. Disruption of ciliated epithelium has been linked to several other human diseases, including: primary ciliary dyskinesia (PCD)[296]; Bardet-Biedl syndrome (BBS)[484]; asthma[485-489]; anosmia[402] and chronic obstructive pulmonary disease (COPD)[490-492].

As more and more datasets in which mRNA expression and gene mutation have been investigated within diseases and cancer become available, we must use our findings implicating p73 in MCCs to focus on tissues and diseases of relevance to this biological function of p73. It is important to investigate differential isoform expression within disease and cancer, for example, the alternatively spliced N-terminal inactive isoforms Δex2p73 and Δex2/3p73. As a reminder these isoforms are generated when exon 2 or exons 2 and 3 are alternatively spliced from the full-length p73[89,90]. These are of particular interest because in NSCLC they are higher expressed while other

isoforms are down modulated[145]. The study of these isoforms has been predominately limited to their role in tumorigenesis, and they have been shown to be biologically similar to ΔNp73 and to be preferentially expressed in tumors[89-93]. Studies have indicated that the ΔTAp73 isoforms are upregulated in many cancer types and further correlates with poor survival[90,97,98]. The focus on these, as well as all of the other isoforms must be broadened now that we have discovered biological function in MCCs to include tumorigenesis, but not be limited therein. Attention must be paid to all diseases in which the functionality of MCCs has been compromised to determine if differential p73 expression levels play a causative role in disease progression.

Conclusions

The adult lung airway epithelium is composed of a balance of MCCs and secretory cells together with undifferentiated basal cells. The architecture of this epithelium is disrupted in many respiratory diseases, several of which predispose patients to lung cancer. The research results presented in this dissertation lay the foundation through identification of key signaling pathways that may influence individual susceptibility to pulmonary diseases such as COPD and lung cancer.

Collectively our data provide a unifying mechanism to explain the diverse range of phenotypes observed in the p73-deficient mice and place p73 as an upstream transcriptional modulator of the many previously identified transcription factors required for multiciliogenesis. Further investigation into the novel p73 target genes we identified will provide the field mechanistic insights in to the

essential roles of p63 and p73 in the development and maintenance of the airway epithelium. A greater understanding of the protein-protein interactions that regulate the function of p73 and p63 will provide clues to control mechanisms or biochemical switches that govern the activity of these p53 family members. The most significant contribution of this dissertation to the field is that p73 is required for multiciliogenesis. The collective work provides an appropriate biological context in which to further study the biochemical activity and regulation of p73 as well as new signaling pathways that may be subverted during tumorigenesis to alter basal epithelial cells function and progenitor cell differentiation.

REFERENCES

1. Marshall, C.B., Mays, D., Beeler, J.S., Rosenbluth, J.M., Boyd, K.L., Santos Guasch, G.L., Shaver, T.M., Tang, L., Liu, Q., Shyr, Y., Venters, B.J., Magnusson, M.K. & Pietenpol, J. p73 is Required for Multiciliogenesis and Regulates the Foxj1-Associated Gene Network. *Cell Rep* (2016).

2. Linzer, D.I. & Levine, A.J. Characterization of a 54K dalton cellular SV40 tumor antigen present in SV40-transformed cells and uninfected embryonal carcinoma cells. *Cell* **17**, 43-52 (1979).

3. Lane, D.P. & Crawford, L.V. T antigen is bound to a host protein in SV40-transformed cells. *Nature* **278**, 261-3 (1979).

4. DeLeo, A.B., Jay, G., Appella, E., Dubois, G.C., Law, L.W. & Old, L.J. Detection of a transformation-related antigen in chemically induced sarcomas and other transformed cells of the mouse. *Proc Natl Acad Sci U S A* **76**, 2420-4 (1979).

5. Nigro, J.M., Baker, S.J., Preisinger, A.C., Jessup, J.M., Hostetter, R., Cleary, K., Bigner, S.H., Davidson, N., Baylin, S., Devilee, P. & et al. Mutations in the p53 gene occur in diverse human tumour types. *Nature* **342**, 705-8 (1989).

6. Moll, U.M. & Slade, N. p63 and p73: roles in development and tumor formation. *Mol Cancer Res* **2**, 371-86 (2004).

7. Donehower, L.A., Harvey, M., Slagle, B.L., McArthur, M.J., Montgomery, C.A., Jr., Butel, J.S. & Bradley, A. Mice deficient for p53 are developmentally normal but susceptible to spontaneous tumours. *Nature* **356**, 215-21 (1992).

8. el-Deiry, W.S., Tokino, T., Velculescu, V.E., Levy, D.B., Parsons, R., Trent, J.M., Lin, D., Mercer, W.E., Kinzler, K.W. & Vogelstein, B. WAF1, a potential mediator of p53 tumor suppression. *Cell* **75**, 817-25 (1993).

9. Nakano, K. & Vousden, K.H. PUMA, a novel proapoptotic gene, is induced by p53. *Mol Cell* **7**, 683-94 (2001).

10. Pietenpol, J.A., Tokino, T., Thiagalingam, S., el-Deiry, W.S., Kinzler, K.W. & Vogelstein, B. Sequence-specific transcriptional activation is essential for growth suppression by p53. *Proc Natl Acad Sci U S A* **91**, 1998-2002 (1994).

11. Stewart, Z.A. & Pietenpol, J.A. p53 Signaling and cell cycle checkpoints. *Chem Res Toxicol* **14**, 243-63 (2001).

12. Vogelstein, B., Lane, D. & Levine, A.J. Surfing the p53 network. *Nature* **408**, 307-10 (2000).

13. Kuribayashi, K. & El-Deiry, W.S. Regulation of programmed cell death by the p53 pathway. *Adv Exp Med Biol* **615**, 201-21 (2008).

14. Lane, D.P. Cancer. p53, guardian of the genome. *Nature* **358**, 15-6 (1992).

15. Kaghad, M., Bonnet, H., Yang, A., Creancier, L., Biscan, J.C., Valent, A., Minty, A., Chalon, P., Lelias, J.M., Dumont, X., Ferrara, P., McKeon, F. & Caput, D. Monoallelically expressed gene related to p53 at 1p36, a region frequently deleted in neuroblastoma and other human cancers. *Cell* **90**, 809-19 (1997).

16. Yang, A., Walker, N., Bronson, R., Kaghad, M., Oosterwegel, M., Bonnin, J., Vagner, C., Bonnet, H., Dikkes, P., Sharpe, A., McKeon, F. & Caput, D. p73-deficient mice have neurological, pheromonal and inflammatory defects but lack spontaneous tumours. *Nature* **404**, 99-103 (2000).

17. Tomasini, R., Tsuchihara, K., Wilhelm, M., Fujitani, M., Rufini, A., Cheung, C.C., Khan, F., Itie-Youten, A., Wakeham, A., Tsao, M.S., Iovanna, J.L., Squire, J., Jurisica, I., Kaplan, D., Melino, G., Jurisicova, A. & Mak, T.W. TAp73 knockout shows genomic instability with infertility and tumor suppressor functions. *Genes Dev* **22**, 2677-91 (2008).

18. Osada, M., Ohba, M., Kawahara, C., Ishioka, C., Kanamaru, R., Katoh, I., Ikawa, Y., Nimura, Y., Nakagawara, A., Obinata, M. & Ikawa, S. Cloning and functional analysis of human p51, which structurally and functionally resembles p53. *Nat Med* **4**, 839-43 (1998).

19. Zeng, X., Levine, A.J. & Lu, H. Non-p53 p53RE binding protein, a human transcription factor functionally analogous to P53. *Proc Natl Acad Sci U S A* **95**, 6681-6 (1998).

20. Bian, J. & Sun, Y. p53CP, a putative p53 competing protein that specifically binds to the consensus p53 DNA binding sites: a third member of the p53 family? *Proc Natl Acad Sci U S A* **94**, 14753-8 (1997).

21. Yang, A., Kaghad, M., Wang, Y., Gillett, E., Fleming, M.D., Dotsch, V., Andrews, N.C., Caput, D. & McKeon, F. p63, a p53 homolog at 3q27-29, encodes multiple products with transactivating, death-inducing, and dominant-negative activities. *Mol Cell* **2**, 305-16 (1998).

22. Mills, A.A., Zheng, B., Wang, X.J., Vogel, H., Roop, D.R. & Bradley, A. p63 is a p53 homologue required for limb and epidermal morphogenesis. *Nature* **398**, 708-13 (1999).

23. Yang, A., Schweitzer, R., Sun, D., Kaghad, M., Walker, N., Bronson, R.T., Tabin, C., Sharpe, A., Caput, D., Crum, C. & McKeon, F. p63 is essential for regenerative proliferation in limb, craniofacial and epithelial development. *Nature* **398**, 714-8 (1999).

24. Blandino, G. & Dobbelstein, M. p73 and p63: why do we still need them? *Cell Cycle* **3**, 886-94 (2004).

25. Yang, A., Kaghad, M., Caput, D. & McKeon, F. On the shoulders of giants: p63, p73 and the rise of p53. *Trends Genet* **18**, 90-5 (2002).

26. Yang, A. & McKeon, F. P63 and P73: P53 mimics, menaces and more. *Nat Rev Mol Cell Biol* **1**, 199-207 (2000).

27. Vilgelm, A., El-Rifai, W. & Zaika, A. Therapeutic prospects for p73 and p63: rising from the shadow of p53. *Drug Resist Updat* **11**, 152-63 (2008).

28. Harms, K., Nozell, S. & Chen, X. The common and distinct target genes of the p53 family transcription factors. *Cell Mol Life Sci* **61**, 822-42 (2004).

29. Levrero, M., De Laurenzi, V., Costanzo, A., Gong, J., Wang, J.Y. & Melino, G. The p53/p63/p73 family of transcription factors: overlapping and distinct functions. *J Cell Sci* **113 (Pt 10)**, 1661-70 (2000).

30. el-Deiry, W.S., Kern, S.E., Pietenpol, J.A., Kinzler, K.W. & Vogelstein, B. Definition of a consensus binding site for p53. *Nat Genet* **1**, 45-9 (1992).

31. Rosenbluth, J.M., Mays, D.J., Pino, M.F., Tang, L.J. & Pietenpol, J.A. A gene signature-based approach identifies mTOR as a regulator of p73. *Mol Cell Biol* **28**, 5951-64 (2008).

32. Jacks, T., Remington, L., Williams, B.O., Schmitt, E.M., Halachmi, S., Bronson, R.T. & Weinberg, R.A. Tumor spectrum analysis in p53-mutant mice. *Curr Biol* **4**, 1-7 (1994).

33. Mills, A.A., Qi, Y. & Bradley, A. Conditional inactivation of p63 by Cre-mediated excision. *Genesis* **32**, 138-41 (2002).

34. Crum, C.P. & McKeon, F.D. p63 in epithelial survival, germ cell surveillance, and neoplasia. *Annu Rev Pathol* **5**, 349-71 (2010).

35. Zhu, J., Jiang, J., Zhou, W. & Chen, X. The potential tumor suppressor p73 differentially regulates cellular p53 target genes. *Cancer Res* **58**, 5061-5 (1998).

36. Osada, M., Park, H.L., Nagakawa, Y., Yamashita, K., Fomenkov, A., Kim, M.S., Wu, G., Nomoto, S., Trink, B. & Sidransky, D. Differential recognition of response elements determines target gene specificity for p53 and p63. *Mol Cell Biol* **25**, 6077-89 (2005).

37. Sasaki, Y., Naishiro, Y., Oshima, Y., Imai, K., Nakamura, Y. & Tokino, T. Identification of pigment epithelium-derived factor as a direct target of the p53 family member genes. *Oncogene* **24**, 5131-6 (2005).

38. Liu, G., Nozell, S., Xiao, H. & Chen, X. DeltaNp73beta is active in transactivation and growth suppression. *Mol Cell Biol* **24**, 487-501 (2004).

39. King, N., Westbrook, M.J., Young, S.L., Kuo, A., Abedin, M., Chapman, J., Fairclough, S., Hellsten, U., Isogai, Y., Letunic, I., Marr, M., Pincus, D., Putnam, N., Rokas, A., Wright, K.J., Zuzow, R., Dirks, W., Good, M., Goodstein, D., Lemons, D., Li, W., Lyons, J.B., Morris, A., Nichols, S., Richter, D.J., Salamov, A., Sequencing, J.G., Bork, P., Lim, W.A., Manning, G., Miller, W.T., McGinnis, W., Shapiro, H., Tjian, R., Grigoriev, I.V. & Rokhsar, D. The genome of the choanoflagellate Monosiga brevicollis and the origin of metazoans. *Nature* **451**, 783-8 (2008).

40. Rutkowski, R., Hofmann, K. & Gartner, A. Phylogeny and function of the invertebrate p53 superfamily. *Cold Spring Harb Perspect Biol* **2**, a001131 (2010).

41. Dehal, P., Satou, Y., Campbell, R.K., Chapman, J., Degnan, B., De Tomaso, A., Davidson, B., Di Gregorio, A., Gelpke, M., Goodstein, D.M., Harafuji, N., Hastings, K.E., Ho, I., Hotta, K., Huang, W., Kawashima, T., Lemaire, P., Martinez, D., Meinertzhagen, I.A., Necula, S., Nonaka, M., Putnam, N., Rash, S., Saiga, H., Satake, M., Terry, A., Yamada, L., Wang, H.G., Awazu, S., Azumi, K., Boore, J., Branno, M., Chin-Bow, S., DeSantis, R., Doyle, S., Francino, P., Keys, D.N., Haga, S., Hayashi, H., Hino, K., Imai, K.S., Inaba, K., Kano, S., Kobayashi, K., Kobayashi, M., Lee, B.I., Makabe, K.W., Manohar, C., Matassi, G., Medina, M., Mochizuki, Y., Mount, S., Morishita, T., Miura, S., Nakayama, A., Nishizaka, S., Nomoto, H., Ohta, F., Oishi, K., Rigoutsos, I., Sano, M., Sasaki, A., Sasakura, Y., Shoguchi, E., Shin-i, T., Spagnuolo, A., Stainier, D., Suzuki, M.M., Tassy, O., Takatori, N., Tokuoka, M., Yagi, K., Yoshizaki, F., Wada, S., Zhang, C., Hyatt, P.D., Larimer, F., Detter, C., Doggett, N., Glavina, T., Hawkins, T., Richardson, P., Lucas, S., Kohara, Y., Levine, M., Satoh, N. & Rokhsar, D.S. The draft genome of Ciona intestinalis: insights into chordate and vertebrate origins. *Science* **298**, 2157-67 (2002).

42. Putnam, N.H., Srivastava, M., Hellsten, U., Dirks, B., Chapman, J., Salamov, A., Terry, A., Shapiro, H., Lindquist, E., Kapitonov, V.V., Jurka, J., Genikhovich, G., Grigoriev, I.V., Lucas, S.M., Steele, R.E., Finnerty, J.R., Technau, U., Martindale, M.Q. & Rokhsar, D.S. Sea anemone genome reveals ancestral eumetazoan gene repertoire and genomic organization. *Science* **317**, 86-94 (2007).

43. Pankow, S. & Bamberger, C. The p53 tumor suppressor-like protein nvp63 mediates selective germ cell death in the sea anemone Nematostella vectensis. *PLoS One* **2**, e782 (2007).

44. Sogame, N., Kim, M. & Abrams, J.M. Drosophila p53 preserves genomic stability by regulating cell death. *Proc Natl Acad Sci U S A* **100**, 4696-701 (2003).

45. Brodsky, M.H., Nordstrom, W., Tsang, G., Kwan, E., Rubin, G.M. & Abrams, J.M. Drosophila p53 binds a damage response element at the reaper locus. *Cell* **101**, 103-13 (2000).

46. Hu, W. The role of p53 gene family in reproduction. *Cold Spring Harb Perspect Biol* **1**, a001073 (2009).

47. Murray-Zmijewski, F., Lane, D.P. & Bourdon, J.C. p53/p63/p73 isoforms: an orchestra of isoforms to harmonise cell differentiation and response to stress. *Cell Death Differ* **13**, 962-72 (2006).

48. Bourdon, J.C., Fernandes, K., Murray-Zmijewski, F., Liu, G., Diot, A., Xirodimas, D.P., Saville, M.K. & Lane, D.P. p53 isoforms can regulate p53 transcriptional activity. *Genes Dev* **19**, 2122-37 (2005).

49. Prives, C. & Manfredi, J.J. The continuing saga of p53--more sleepless nights ahead. *Mol Cell* **19**, 719-21 (2005).

50. Harms, K.L. & Chen, X. The functional domains in p53 family proteins exhibit both common and distinct properties. *Cell Death Differ* **13**, 890-7 (2006).

51. Dohn, M., Zhang, S. & Chen, X. p63alpha and DeltaNp63alpha can induce cell cycle arrest and apoptosis and differentially regulate p53 target genes. *Oncogene* **20**, 3193-205 (2001).

52. Wu, G., Nomoto, S., Hoque, M.O., Dracheva, T., Osada, M., Lee, C.C., Dong, S.M., Guo, Z., Benoit, N., Cohen, Y., Rechthand, P., Califano, J., Moon, C.S., Ratovitski, E., Jen, J., Sidransky, D. & Trink, B. DeltaNp63alpha and TAp63alpha regulate transcription of genes with distinct biological functions in cancer and development. *Cancer Res* **63**, 2351-7 (2003).

53. Stiewe, T. & Putzer, B.M. Role of the p53-homologue p73 in E2F1-induced apoptosis. *Nat Genet* **26**, 464-9 (2000).

54. Serber, Z., Lai, H.C., Yang, A., Ou, H.D., Sigal, M.S., Kelly, A.E., Darimont, B.D., Duijf, P.H., Van Bokhoven, H., McKeon, F. & Dotsch, V. A C-terminal inhibitory domain controls the activity of p63 by an intramolecular mechanism. *Mol Cell Biol* **22**, 8601-11 (2002).

55. Schavolt, K.L. & Pietenpol, J.A. p53 and Delta Np63 alpha differentially bind and regulate target genes involved in cell cycle arrest, DNA repair and apoptosis. *Oncogene* **26**, 6125-32 (2007).

56. Deyoung, M.P., Johannessen, C.M., Leong, C.O., Faquin, W., Rocco, J.W. & Ellisen, L.W. Tumor-Specific p73 Up-regulation Mediates p63 Dependence in Squamous Cell Carcinoma. *Cancer Res* **66**, 9362-8 (2006).

57. Chan, W.M., Siu, W.Y., Lau, A. & Poon, R.Y. How many mutant p53 molecules are needed to inactivate a tetramer? *Mol Cell Biol* **24**, 3536-51 (2004).

58. Rocco, J.W., Leong, C.O., Kuperwasser, N., DeYoung, M.P. & Ellisen, L.W. p63 mediates survival in squamous cell carcinoma by suppression of p73-dependent apoptosis. *Cancer Cell* **9**, 45-56 (2006).

59. Leong, C.O., Vidnovic, N., DeYoung, M.P., Sgroi, D. & Ellisen, L.W. The p63/p73 network mediates chemosensitivity to cisplatin in a biologically defined subset of primary breast cancers. *J Clin Invest* **117**, 1370-80 (2007).

60. Rosenbluth, J.M., Mays, D.J., Jiang, A., Shyr, Y. & Pietenpol, J.A. Differential regulation of the p73 cistrome by mammalian target of rapamycin reveals transcriptional programs of mesenchymal differentiation and tumorigenesis. *Proc Natl Acad Sci U S A* **108**, 2076-81 (2011).

61. Rosenbluth, J.M., Johnson, K., Tang, L., Triplett, T. & Pietenpol, J.A. Evaluation of p63 and p73 antibodies for cross-reactivity. *Cell Cycle* **8**, 3702-6 (2009).

62. Gaiddon, C., Lokshin, M., Ahn, J., Zhang, T. & Prives, C. A subset of tumor-derived mutant forms of p53 down-regulate p63 and p73 through a direct interaction with the p53 core domain. *Mol Cell Biol* **21**, 1874-87 (2001).

63. Bergamaschi, D., Gasco, M., Hiller, L., Sullivan, A., Syed, N., Trigiante, G., Yulug, I., Merlano, M., Numico, G., Comino, A., Attard, M., Reelfs, O., Gusterson, B., Bell, A.K., Heath, V., Tavassoli, M., Farrell, P.J., Smith, P., Lu, X. & Crook, T. p53 polymorphism influences response in cancer chemotherapy via modulation of p73-dependent apoptosis. *Cancer Cell* **3**, 387-402 (2003).

64. Irwin, M.S., Kondo, K., Marin, M.C., Cheng, L.S., Hahn, W.C. & Kaelin, W.G., Jr. Chemosensitivity linked to p73 function. *Cancer Cell* **3**, 403-10 (2003).

65. Hagiwara, K., McMenamin, M.G., Miura, K. & Harris, C.C. Mutational analysis of the p63/p73L/p51/p40/CUSP/KET gene in human cancer cell lines using intronic primers. *Cancer Res* **59**, 4165-9 (1999).

66. Sunahara, M., Shishikura, T., Takahashi, M., Todo, S., Yamamoto, N., Kimura, H., Kato, S., Ishioka, C., Ikawa, S., Ikawa, Y. & Nakagawara, A. Mutational analysis of p51A/TAp63gamma, a p53 homolog, in non-small cell lung cancer and breast cancer. *Oncogene* **18**, 3761-5 (1999).

67. Melino, G., Lu, X., Gasco, M., Crook, T. & Knight, R.A. Functional regulation of p73 and p63: development and cancer. *Trends Biochem Sci* **28**, 663-70 (2003).

68. Jost, C.A., Marin, M.C. & Kaelin, W.G., Jr. p73 is a simian [correction of human] p53-related protein that can induce apoptosis. *Nature* **389**, 191-4 (1997).

69. Bjorkqvist, A.M., Husgafvel-Pursiainen, K., Anttila, S., Karjalainen, A., Tammilehto, L., Mattson, K., Vainio, H. & Knuutila, S. DNA gains in 3q occur frequently in squamous cell carcinoma of the lung, but not in adenocarcinoma. *Genes Chromosomes Cancer* **22**, 79-82 (1998).

70. Strano, S., Munarriz, E., Rossi, M., Cristofanelli, B., Shaul, Y., Castagnoli, L., Levine, A.J., Sacchi, A., Cesareni, G., Oren, M. & Blandino, G. Physical and functional interaction between p53 mutants and different isoforms of p73. *J Biol Chem* **275**, 29503-12 (2000).

71. Olive, K.P., Tuveson, D.A., Ruhe, Z.C., Yin, B., Willis, N.A., Bronson, R.T., Crowley, D. & Jacks, T. Mutant p53 gain of function in two mouse models of Li-Fraumeni syndrome. *Cell* **119**, 847-60 (2004).

72. Lang, G.A., Iwakuma, T., Suh, Y.A., Liu, G., Rao, V.A., Parant, J.M., Valentin-Vega, Y.A., Terzian, T., Caldwell, L.C., Strong, L.C., El-Naggar, A.K. & Lozano, G. Gain of function of a p53 hot spot mutation in a mouse model of Li-Fraumeni syndrome. *Cell* **119**, 861-72 (2004).

73. Chene, P. The role of tetramerization in p53 function. *Oncogene* **20**, 2611-7 (2001).

74. Grob, T.J., Novak, U., Maisse, C., Barcaroli, D., Luthi, A.U., Pirnia, F., Hugli, B., Graber, H.U., De Laurenzi, V., Fey, M.F., Melino, G. & Tobler, A. Human delta Np73 regulates a dominant negative feedback loop for TAp73 and p53. *Cell Death Differ* **8**, 1213-23 (2001).

75. Nakagawa, T., Takahashi, M., Ozaki, T., Watanabe Ki, K., Todo, S., Mizuguchi, H., Hayakawa, T. & Nakagawara, A. Autoinhibitory regulation of p73 by Delta Np73 to modulate cell survival and death through a p73-specific target element within the Delta Np73 promoter. *Mol Cell Biol* **22**, 2575-85 (2002).

76. Kartasheva, N.N., Contente, A., Lenz-Stoppler, C., Roth, J. & Dobbelstein, M. p53 induces the expression of its antagonist p73 Delta N, establishing an autoregulatory feedback loop. *Oncogene* **21**, 4715-27 (2002).

77. Oswald, C. & Stiewe, T. In good times and bad: p73 in cancer. *Cell Cycle* **7**, 1726-31 (2008).

78. Pozniak, C.D., Radinovic, S., Yang, A., McKeon, F., Kaplan, D.R. & Miller, F.D. An anti-apoptotic role for the p53 family member, p73, during developmental neuron death. *Science* **289**, 304-6 (2000).

79. De Laurenzi, V., Costanzo, A., Barcaroli, D., Terrinoni, A., Falco, M., Annicchiarico-Petruzzelli, M., Levrero, M. & Melino, G. Two new p73 splice variants, gamma and delta, with different transcriptional activity. *J Exp Med* **188**, 1763-8 (1998).

80. Grespi, F., Amelio, I., Tucci, P., Annicchiarico-Petruzzelli, M. & Melino, G. Tissue-specific expression of p73 C-terminal isoforms in mice. *Cell Cycle* **11**, 4474-83 (2012).

81. De Laurenzi, V.D., Catani, M.V., Terrinoni, A., Corazzari, M., Melino, G., Costanzo, A., Levrero, M. & Knight, R.A. Additional complexity in p73: induction by mitogens in lymphoid cells and identification of two new splicing variants epsilon and zeta. *Cell Death Differ* **6**, 389-90 (1999).

82. Tschan, M.P., Grob, T.J., Peters, U.R., Laurenzi, V.D., Huegli, B., Kreuzer, K.A., Schmidt, C.A., Melino, G., Fey, M.F., Tobler, A. & Cajot, J.F. Enhanced p73 expression during differentiation and complex p73 isoforms in myeloid leukemia. *Biochem Biophys Res Commun* **277**, 62-5 (2000).

83. De Laurenzi, V., Rossi, A., Terrinoni, A., Barcaroli, D., Levrero, M., Costanzo, A., Knight, R.A., Guerrieri, P. & Melino, G. p63 and p73 transactivate differentiation gene promoters in human keratinocytes. *Biochem Biophys Res Commun* **273**, 342-6 (2000).

84. Qiao, F. & Bowie, J.U. The many faces of SAM. *Sci STKE* **2005**, re7 (2005).

85. Brunner, H.G., Hamel, B.C. & Van Bokhoven, H. The p63 gene in EEC and other syndromes. *J Med Genet* **39**, 377-81 (2002).

86. Barrera, F.N., Poveda, J.A., Gonzalez-Ros, J.M. & Neira, J.L. Binding of the C-terminal sterile alpha motif (SAM) domain of human p73 to lipid membranes. *J Biol Chem* **278**, 46878-85 (2003).

87. Ueda, Y., Hijikata, M., Takagi, S., Chiba, T. & Shimotohno, K. New p73 variants with altered C-terminal structures have varied transcriptional activities. *Oncogene* **18**, 4993-8 (1999).

88. Lee, C.W. & La Thangue, N.B. Promoter specificity and stability control of the p53-related protein p73. *Oncogene* **18**, 4171-81 (1999).

89. Concin, N., Hofstetter, G., Berger, A., Gehmacher, A., Reimer, D., Watrowski, R., Tong, D., Schuster, E., Hefler, L., Heim, K., Mueller-Holzner, E., Marth, C., Moll, U.M., Zeimet, A.G. & Zeillinger, R. Clinical relevance of dominant-negative p73 isoforms for responsiveness to chemotherapy and survival in ovarian cancer: evidence for a crucial p53-p73 cross-talk in vivo. *Clin Cancer Res* **11**, 8372-83 (2005).

90. Concin, N., Becker, K., Slade, N., Erster, S., Mueller-Holzner, E., Ulmer, H., Daxenbichler, G., Zeimet, A., Zeillinger, R., Marth, C. & Moll, U.M. Transdominant DeltaTAp73 isoforms are frequently up-regulated in ovarian cancer. Evidence for their role as epigenetic p53 inhibitors in vivo. *Cancer Res* **64**, 2449-60 (2004).

91. Zaika, A.I., Slade, N., Erster, S.H., Sansome, C., Joseph, T.W., Pearl, M., Chalas, E. & Moll, U.M. DeltaNp73, a dominant-negative inhibitor of wild-type p53 and TAp73, is up-regulated in human tumors. *J Exp Med* **196**, 765-80 (2002).

92. Fillippovich, I., Sorokina, N., Gatei, M., Haupt, Y., Hobson, K., Moallem, E., Spring, K., Mould, M., McGuckin, M.A., Lavin, M.F. & Khanna, K.K. Transactivation-deficient p73alpha (p73Deltaexon2) inhibits apoptosis and competes with p53. *Oncogene* **20**, 514-22 (2001).

93. Stiewe, T., Theseling, C.C. & Putzer, B.M. Transactivation-deficient Delta TA-p73 inhibits p53 by direct competition for DNA binding: implications for tumorigenesis. *J Biol Chem* **277**, 14177-85 (2002).

94. Ishimoto, O., Kawahara, C., Enjo, K., Obinata, M., Nukiwa, T. & Ikawa, S. Possible oncogenic potential of DeltaNp73: a newly identified isoform of human p73. *Cancer Res* **62**, 636-41 (2002).

95. Petrenko, O., Zaika, A. & Moll, U.M. deltaNp73 facilitates cell immortalization and cooperates with oncogenic Ras in cellular transformation in vivo. *Mol Cell Biol* **23**, 5540-55 (2003).

96. Stiewe, T., Stanelle, J., Theseling, C.C., Pollmeier, B., Beitzinger, M. & Putzer, B.M. Inactivation of retinoblastoma (RB) tumor suppressor by oncogenic isoforms of the p53 family member p73. *J Biol Chem* **278**, 14230-6 (2003).

97. Dominguez, G., Garcia, J.M., Pena, C., Silva, J., Garcia, V., Martinez, L., Maximiano, C., Gomez, M.E., Rivera, J.A., Garcia-Andrade, C. & Bonilla, F. DeltaTAp73 upregulation correlates with poor prognosis in human tumors: putative in vivo network involving p73 isoforms, p53, and E2F-1. *J Clin Oncol* **24**, 805-15 (2006).

98. Casciano, I., Mazzocco, K., Boni, L., Pagnan, G., Banelli, B., Allemanni, G., Ponzoni, M., Tonini, G.P. & Romani, M. Expression of DeltaNp73 is a molecular marker for adverse outcome in neuroblastoma patients. *Cell Death Differ* **9**, 246-51 (2002).

99. Wilhelm, M.T., Rufini, A., Wetzel, M.K., Tsuchihara, K., Inoue, S., Tomasini, R., Itie-Youten, A., Wakeham, A., Arsenian-Henriksson, M., Melino, G., Kaplan, D.R., Miller, F.D. & Mak, T.W. Isoform-specific p73 knockout mice reveal a novel role for delta Np73 in the DNA damage response pathway. *Genes Dev* **24**, 549-60 (2010).

100. Rufini, A., Niklison-Chirou, M.V., Inoue, S., Tomasini, R., Harris, I.S., Marino, A., Federici, M., Dinsdale, D., Knight, R.A., Melino, G. & Mak, T.W. TAp73 depletion accelerates aging through metabolic dysregulation. *Genes Dev* **26**, 2009-14 (2012).

101. Inoue, S., Tomasini, R., Rufini, A., Elia, A.J., Agostini, M., Amelio, I., Cescon, D., Dinsdale, D., Zhou, L., Harris, I.S., Lac, S., Silvester, J., Li, W.Y., Sasaki, M., Haight, J., Brustle, A., Wakeham, A., McKerlie, C., Jurisicova, A., Melino, G. & Mak, T.W. TAp73 is required for spermatogenesis and the maintenance of male fertility. *Proc Natl Acad Sci U S A* **111**, 1843-8 (2014).

102. Talos, F., Abraham, A., Vaseva, A.V., Holembowski, L., Tsirka, S.E., Scheel, A., Bode, D., Dobbelstein, M., Bruck, W. & Moll, U.M. p73 is an essential regulator of neural stem cell maintenance in embryonal and adult CNS neurogenesis. *Cell Death Differ* **17**, 1816-29 (2010).

103. Holembowski, L., Kramer, D., Riedel, D., Sordella, R., Nemajerova, A., Dobbelstein, M. & Moll, U.M. TAp73 is essential for germ cell adhesion and maturation in testis. *J Cell Biol* **204**, 1173-90 (2014).

104. Tomasini, R., Tsuchihara, K., Tsuda, C., Lau, S.K., Wilhelm, M., Ruffini, A., Tsao, M.S., Iovanna, J.L., Jurisicova, A., Melino, G. & Mak, T.W. TAp73 regulates the spindle assembly checkpoint by modulating BubR1 activity. *Proc Natl Acad Sci U S A* **106**, 797-802 (2009).

105. Niklison-Chirou, M.V., Steinert, J.R., Agostini, M., Knight, R.A., Dinsdale, D., Cattaneo, A., Mak, T.W. & Melino, G. TAp73 knockout mice show morphological and functional nervous system defects associated with loss of p75 neurotrophin receptor. *Proc Natl Acad Sci U S A* **110**, 18952-7 (2013).

106. Alexandrova, E.M., Talos, F. & Moll, U.M. p73 is dispensable for commitment to neural stem cell fate, but is essential for neural stem cell maintenance and for blocking premature differentiation. *Cell Death Differ* **20**, 368 (2013).

107. Medina-Bolivar, C., Gonzalez-Arnay, E., Talos, F., Gonzalez-Gomez, M., Moll, U.M. & Meyer, G. Cortical hypoplasia and ventriculomegaly of p73-deficient mice: Developmental and adult analysis. *J Comp Neurol* **522**, 2663-79 (2014).

108. Gonzalez-Cano, L., Fuertes-Alvarez, S., Robledinos-Anton, N., Bizy, A., Villena-Cortes, A., Farinas, I., Marques, M.M. & Marin, M.C. p73 is required for ependymal cell maturation and neurogenic SVZ cytoarchitecture. *Dev Neurobiol* (2015).

109. Hibi, K., Trink, B., Patturajan, M., Westra, W.H., Caballero, O.L., Hill, D.E., Ratovitski, E.A., Jen, J. & Sidransky, D. AIS is an oncogene amplified in squamous cell carcinoma. *Proc Natl Acad Sci U S A* **97**, 5462-7 (2000).

110. Massion, P.P., Taflan, P.M., Jamshedur Rahman, S.M., Yildiz, P., Shyr, Y., Edgerton, M.E., Westfall, M.D., Roberts, J.R., Pietenpol, J.A., Carbone, D.P. & Gonzalez, A.L. Significance of p63 amplification and overexpression in lung cancer development and prognosis. *Cancer Res* **63**, 7113-21 (2003).

111. Redon, R., Muller, D., Caulee, K., Wanherdrick, K., Abecassis, J. & du Manoir, S. A simple specific pattern of chromosomal aberrations at early stages of head and neck squamous cell carcinomas: PIK3CA but not p63 gene as a likely target of 3q26-qter gains. *Cancer Res* **61**, 4122-9 (2001).

112. Gong, J.G., Costanzo, A., Yang, H.Q., Melino, G., Kaelin, W.G., Jr., Levrero, M. & Wang, J.Y. The tyrosine kinase c-Abl regulates p73 in apoptotic response to cisplatin-induced DNA damage. *Nature* **399**, 806-9 (1999).

113. Agami, R., Blandino, G., Oren, M. & Shaul, Y. Interaction of c-Abl and p73alpha and their collaboration to induce apoptosis. *Nature* **399**, 809-13 (1999).

114. Yuan, Z.M., Shioya, H., Ishiko, T., Sun, X., Gu, J., Huang, Y.Y., Lu, H., Kharbanda, S., Weichselbaum, R. & Kufe, D. p73 is regulated by tyrosine kinase c-Abl in the apoptotic response to DNA damage. *Nature* **399**, 814-7 (1999).

115. Hu, H., Xia, S.H., Li, A.D., Xu, X., Cai, Y., Han, Y.L., Wei, F., Chen, B.S., Huang, X.P., Han, Y.S., Zhang, J.W., Zhang, X., Wu, M. & Wang, M.R. Elevated expression of p63 protein in human esophageal squamous cell carcinomas. *Int J Cancer* **102**, 580-3 (2002).

116. Weber, A., Bellmann, U., Bootz, F., Wittekind, C. & Tannapfel, A. Expression of p53 and its homologues in primary and recurrent squamous cell carcinomas of the head and neck. *Int J Cancer* **99**, 22-8 (2002).

117. Sniezek, J.C., Matheny, K.E., Westfall, M.D. & Pietenpol, J.A. Dominant negative p63 isoform expression in head and neck squamous cell carcinoma. *Laryngoscope* **114**, 2063-72 (2004).

118. Park, B.J., Lee, S.J., Kim, J.I., Lee, S.J., Lee, C.H., Chang, S.G., Park, J.H. & Chi, S.G. Frequent alteration of p63 expression in human primary bladder carcinomas. *Cancer Res* **60**, 3370-4 (2000).

119. Wang, X., Mori, I., Tang, W., Nakamura, M., Nakamura, Y., Sato, M., Sakurai, T. & Kakudo, K. p63 expression in normal, hyperplastic and malignant breast tissues. *Breast Cancer* **9**, 216-9 (2002).

120. Reis-Filho, J.S., Milanezi, F., Amendoeira, I., Albergaria, A. & Schmitt, F.C. Distribution of p63, a novel myoepithelial marker, in fine-needle aspiration biopsies of the breast: an analysis of 82 samples. *Cancer* **99**, 172-9 (2003).

121. Reis-Filho, J.S., Simpson, P.T., Martins, A., Preto, A., Gartner, F. & Schmitt, F.C. Distribution of p63, cytokeratins 5/6 and cytokeratin 14 in 51 normal and 400 neoplastic human tissue samples using TARP-4 multi-tumor tissue microarray. *Virchows Arch* **443**, 122-32 (2003).

122. Koker, M.M. & Kleer, C.G. p63 expression in breast cancer: a highly sensitive and specific marker of metaplastic carcinoma. *Am J Surg Pathol* **28**, 1506-12 (2004).

123. Koga, F., Kawakami, S., Fujii, Y., Saito, K., Ohtsuka, Y., Iwai, A., Ando, N., Takizawa, T., Kageyama, Y. & Kihara, K. Impaired p63 expression associates with poor prognosis and uroplakin III expression in invasive urothelial carcinoma of the bladder. *Clin Cancer Res* **9**, 5501-7 (2003).

124. Koga, F., Kawakami, S., Kumagai, J., Takizawa, T., Ando, N., Arai, G., Kageyama, Y. & Kihara, K. Impaired Delta Np63 expression associates with reduced beta-catenin and aggressive phenotypes of urothelial neoplasms. *Br J Cancer* **88**, 740-7 (2003).

125. Urist, M.J., Di Como, C.J., Lu, M.L., Charytonowicz, E., Verbel, D., Crum, C.P., Ince, T.A., McKeon, F.D. & Cordon-Cardo, C. Loss of p63 expression is associated with tumor progression in bladder cancer. *Am J Pathol* **161**, 1199-206 (2002).

126. Zangen, R., Ratovitski, E. & Sidransky, D. DeltaNp63alpha levels correlate with clinical tumor response to cisplatin. *Cell Cycle* **4**, 1313-5 (2005).

127. Perou, C.M., Sorlie, T., Eisen, M.B., van de Rijn, M., Jeffrey, S.S., Rees, C.A., Pollack, J.R., Ross, D.T., Johnsen, H., Akslen, L.A., Fluge, O., Pergamenschikov, A., Williams, C., Zhu, S.X., Lonning, P.E., Borresen-Dale, A.L., Brown, P.O. & Botstein, D. Molecular portraits of human breast tumours. *Nature* **406**, 747-52 (2000).

128. Ribeiro-Silva, A., Ramalho, L.N., Garcia, S.B., Brandao, D.F., Chahud, F. & Zucoloto, S. p63 correlates with both BRCA1 and cytokeratin 5 in invasive breast carcinomas: further evidence for the pathogenesis of the basal phenotype of breast cancer. *Histopathology* **47**, 458-66 (2005).

129. Koster, M.I., Lu, S.L., White, L.D., Wang, X.J. & Roop, D.R. Reactivation of developmentally expressed p63 isoforms predisposes to tumor development and progression. *Cancer Res* **66**, 3981-6 (2006).

130. Barbieri, C.E., Tang, L.J., Brown, K.A. & Pietenpol, J.A. Loss of p63 leads to increased cell migration and up-regulation of genes involved in invasion and metastasis. *Cancer Res* **66**, 7589-97 (2006).

131. Barton, C.E., Tahinci, E., Barbieri, C.E., Johnson, K.N., Hanson, A.J., Jernigan, K.K., Chen, T.W., Lee, E. & Pietenpol, J.A. DeltaNp63 antagonizes p53 to regulate mesoderm induction in Xenopus laevis. *Dev Biol* **329**, 130-9 (2009).

132. Cam, H., Griesmann, H., Beitzinger, M., Hofmann, L., Beinoraviciute-Kellner, R., Sauer, M., Huttinger-Kirchhof, N., Oswald, C., Friedl, P., Gattenlohner, S., Burek, C., Rosenwald, A. & Stiewe, T. p53 family members in myogenic differentiation and rhabdomyosarcoma development. *Cancer Cell* **10**, 281-93 (2006).

133. Dominguez, G., Silva, J.M., Silva, J., Garcia, J.M., Sanchez, A., Navarro, A., Gallego, I., Provencio, M., Espana, P. & Bonilla, F. Wild type p73 overexpression and high-grade malignancy in breast cancer. *Breast Cancer Res Treat* **66**, 183-90 (2001).

134. Wager, M., Guilhot, J., Blanc, J.L., Ferrand, S., Milin, S., Bataille, B., Lapierre, F., Denis, S., Chantereau, T., Larsen, C.J. & Karayan-Tapon, L. Prognostic value of increase in transcript levels of Tp73 DeltaEx2-3 isoforms in low-grade glioma patients. *Br J Cancer* **95**, 1062-9 (2006).

135. Senoo, M., Matsumura, Y. & Habu, S. TAp63gamma (p51A) and dNp63alpha (p73L), two major isoforms of the p63 gene, exert opposite effects on the vascular endothelial growth factor (VEGF) gene expression. *Oncogene* **21**, 2455-65 (2002).

136. Barbieri, C.E. & Pietenpol, J.A. p53 family members: similar biochemistry, different biology. *Cancer Biol Ther* **4**, 419-20 (2005).

137. Zhang, X., Cao, P., Zhai, Y., Zhang, H., Cui, Y., Wu, Z., Yuan, X., Wang, Z., Li, P., Yu, L., Xia, X., He, F. & Zhou, G. Association between the p73 G4C14-to-A4T14 polymorphism and risk of nasopharyngeal carcinoma: a case-control and family-based study. *Carcinogenesis* (2014).

138. Wang, L., Gao, R. & Yu, L. Combined analysis of the association between p73 G4C14-to-A4T14 polymorphisms and cancer risk. *Mol Biol Rep* **39**, 1731-8 (2012).

139. Deng, B., Liu, F., Wei, Y., Luo, L., Chen, X., Yan, L. & Li, B. Association of a p73 exon 2 G4C14-to-A4T14 polymorphism with risk of hepatocellular carcinoma in a Chinese population. *Tumour Biol* **34**, 293-9 (2013).

140. Shibukawa, K., Miyokawa, N., Tokusashi, Y., Sasaki, T., Osanai, S. & Ohsaki, Y. High incidence of chromosomal abnormalities at 1p36 and 9p21 in early-stage central type

squamous cell carcinoma and squamous dysplasia of bronchus detected by autofluorescence bronchoscopy. *Oncol Rep* **22**, 81-7 (2009).

141. Zhang, X., Li, X., Wu, Z., Lin, F. & Zhou, H. The p73 G4C14-to-A4T14 polymorphism is associated with risk of lung cancer in the Han nationality of North China. *Mol Carcinog* **52**, 387-91 (2013).

142. Tokuchi, Y., Hashimoto, T., Kobayashi, Y., Hayashi, M., Nishida, K., Hayashi, S., Imai, K., Nakachi, K., Ishikawa, Y., Nakagawa, K., Kawakami, Y. & Tsuchiya, E. The expression of p73 is increased in lung cancer, independent of p53 gene alteration. *Br J Cancer* **80**, 1623-9 (1999).

143. Uramoto, H., Sugio, K., Oyama, T., Nakata, S., Ono, K., Morita, M., Funa, K. & Yasumoto, K. Expression of deltaNp73 predicts poor prognosis in lung cancer. *Clin Cancer Res* **10**, 6905-11 (2004).

144. Uramoto, H., Sugio, K., Oyama, T., Nakata, S., Ono, K., Nozoe, T. & Yasumoto, K. Expression of the p53 family in lung cancer. *Anticancer Res* **26**, 1785-90 (2006).

145. Lo Iacono, M., Monica, V., Saviozzi, S., Ceppi, P., Bracco, E., Papotti, M. & Scagliotti, G.V. p63 and p73 isoform expression in non-small cell lung cancer and corresponding morphological normal lung tissue. *J Thorac Oncol* **6**, 473-81 (2011).

146. Di Vinci, A., Sessa, F., Casciano, I., Banelli, B., Franzi, F., Brigati, C., Allemanni, G., Russo, P., Dominioni, L. & Romani, M. Different intracellular compartmentalization of TA and DeltaNp73 in non-small cell lung cancer. *Int J Oncol* **34**, 449-56 (2009).

147. Nicholson, S.A., Okby, N.T., Khan, M.A., Welsh, J.A., McMenamin, M.G., Travis, W.D., Jett, J.R., Tazelaar, H.D., Trastek, V., Pairolero, P.C., Corn, P.G., Herman, J.G., Liotta, L.A., Caporaso, N.E. & Harris, C.C. Alterations of p14ARF, p53, and p73 genes involved in the E2F-1-mediated apoptotic pathways in non-small cell lung carcinoma. *Cancer Res* **61**, 5636-43 (2001).

148. Teodoridis, J.M., Hall, J., Marsh, S., Kannall, H.D., Smyth, C., Curto, J., Siddiqui, N., Gabra, H., McLeod, H.L., Strathdee, G. & Brown, R. CpG island methylation of DNA damage response genes in advanced ovarian cancer. *Cancer Res* **65**, 8961-7 (2005).

149. Kawano, S., Miller, C.W., Gombart, A.F., Bartram, C.R., Matsuo, Y., Asou, H., Sakashita, A., Said, J., Tatsumi, E. & Koeffler, H.P. Loss of p73 gene expression in leukemias/lymphomas due to hypermethylation. *Blood* **94**, 1113-20 (1999).

150. Corn, P.G., Kuerbitz, S.J., van Noesel, M.M., Esteller, M., Compitello, N., Baylin, S.B. & Herman, J.G. Transcriptional silencing of the p73 gene in acute lymphoblastic leukemia and Burkitt's lymphoma is associated with 5' CpG island methylation. *Cancer Res* **59**, 3352-6 (1999).

151. Casciano, I., Banelli, B., Croce, M., Allemanni, G., Ferrini, S., Tonini, G.P., Ponzoni, M. & Romani, M. Role of methylation in the control of DeltaNp73 expression in neuroblastoma. *Cell Death Differ* **9**, 343-5 (2002).

152. Banelli, B., Gelvi, I., Di Vinci, A., Scaruffi, P., Casciano, I., Allemanni, G., Bonassi, S., Tonini, G.P. & Romani, M. Distinct CpG methylation profiles characterize different clinical groups of neuroblastic tumors. *Oncogene* **24**, 5619-28 (2005).

153. Banelli, B., Casciano, I. & Romani, M. Methylation-independent silencing of the p73 gene in neuroblastoma. *Oncogene* **19**, 4553-6 (2000).

154. Liu, K., Zhuang, X. & Mai, Z. p73 expression is associated with cellular chemosensitivity in human non-small cell lung cancer cell lines. *Oncol Lett* **5**, 583-587 (2013).

155. Daskalos, A., Logotheti, S., Markopoulou, S., Xinarianos, G., Gosney, J.R., Kastania, A.N., Zoumpourlis, V., Field, J.K. & Liloglou, T. Global DNA hypomethylation-induced DeltaNp73 transcriptional activation in non-small cell lung cancer. *Cancer Lett* **300**, 79-86 (2011).

156. Liu, K., Zhan, M. & Zheng, P. Loss of p73 expression in six non-small cell lung cancer cell lines is associated with 5'CpG island methylation. *Exp Mol Pathol* **84**, 59-63 (2008).

157. Schabath, M.B., Wu, X., Wei, Q., Li, G., Gu, J. & Spitz, M.R. Combined effects of the p53 and p73 polymorphisms on lung cancer risk. *Cancer Epidemiol Biomarkers Prev* **15**, 158-61 (2006).

158. Mai, M., Yokomizo, A., Qian, C., Yang, P., Tindall, D.J., Smith, D.I. & Liu, W. Activation of p73 silent allele in lung cancer. *Cancer Res* **58**, 2347-9 (1998).

159. Li, G., Wang, L.E., Chamberlain, R.M., Amos, C.I., Spitz, M.R. & Wei, Q. p73 G4C14-to-A4T14 polymorphism and risk of lung cancer. *Cancer Res* **64**, 6863-6 (2004).

160. Hu, Y., Jiang, L., Zheng, J., You, Y., Zhou, Y. & Jiao, S. Association between the p73 exon 2 G4C14-to-A4T14 polymorphism and cancer risk: a meta-analysis. *DNA Cell Biol* **31**, 230-7 (2012).

161. Wang, S.S., Guo, H.Y., Dong, L.L., Zhu, X.Q., Ma, L., Li, W. & Tang, J.X. Association between a p73 gene polymorphism and genetic susceptibility to non-small cell lung cancer in the South of China. *Asian Pac J Cancer Prev* **15**, 10387-91 (2014).

162. Liu, H., Liang, Y., Liao, H., Li, L. & Wang, H. Association of p73 G4C14-to-A4T14 polymorphism with lung cancer risk. *Tumour Biol* **35**, 9311-6 (2014).

163. Jun, H.J., Park, S.H., Lee, W.K., Choi, J.E., Jang, J.S., Kim, E.J., Cha, S.I., Kim, D.S., Kam, S., Kim, C.H., Kang, Y.M., Jung, T.H. & Park, J.Y. Combined effects of p73 and MDM2 polymorphisms on the risk of lung cancer. *Mol Carcinog* **46**, 100-5 (2007).

164. Liu, L., Wu, C., Wang, Y., Zhong, R., Duan, S., Wei, S., Lin, S., Zhang, X., Tan, W., Yu, D., Nie, S., Miao, X. & Lin, D. Combined effect of genetic polymorphisms in P53, P73, and MDM2 on non-small cell lung cancer survival. *J Thorac Oncol* **6**, 1793-800 (2011).

165. Rackley, C.R. & Stripp, B.R. Building and maintaining the epithelium of the lung. *J Clin Invest* **122**, 2724-30 (2012).

166. Bishop, A.E. Pulmonary epithelial stem cells. *Cell Prolif* **37**, 89-96 (2004).

167. Lazzaro, D., Price, M., de Felice, M. & Di Lauro, R. The transcription factor TTF-1 is expressed at the onset of thyroid and lung morphogenesis and in restricted regions of the foetal brain. *Development* **113**, 1093-104 (1991).

168. Di Palma, T., Nitsch, R., Mascia, A., Nitsch, L., Di Lauro, R. & Zannini, M. The paired domain-containing factor Pax8 and the homeodomain-containing factor TTF-1 directly interact and synergistically activate transcription. *J Biol Chem* **278**, 3395-402 (2003).

169. Bohinski, R.J., Di Lauro, R. & Whitsett, J.A. The lung-specific surfactant protein B gene promoter is a target for thyroid transcription factor 1 and hepatocyte nuclear factor 3, indicating common factors for organ-specific gene expression along the foregut axis. *Mol Cell Biol* **14**, 5671-81 (1994).

170. Minoo, P. & King, R.J. Epithelial-mesenchymal interactions in lung development. *Annu Rev Physiol* **56**, 13-45 (1994).

171. Hogan, B.L. Morphogenesis. *Cell* **96**, 225-33 (1999).

172. Warburton, D., Schwarz, M., Tefft, D., Flores-Delgado, G., Anderson, K.D. & Cardoso, W.V. The molecular basis of lung morphogenesis. *Mech Dev* **92**, 55-81 (2000).

173. deMello, D.E., Sawyer, D., Galvin, N. & Reid, L.M. Early fetal development of lung vasculature. *Am J Respir Cell Mol Biol* **16**, 568-81 (1997).

174. Mailleux, A.A., Kelly, R., Veltmaat, J.M., De Langhe, S.P., Zaffran, S., Thiery, J.P. & Bellusci, S. Fgf10 expression identifies parabronchial smooth muscle cell progenitors and is required for their entry into the smooth muscle cell lineage. *Development* **132**, 2157-66 (2005).

175. Davis, S., Bove, K.E., Wells, T.R., Hartsell, B., Weinberg, A. & Gilbert, E. Tracheal cartilaginous sleeve. *Pediatr Pathol* **12**, 349-64 (1992).

176. Thurlbeck, W.M. Lung growth and alveolar multiplication. *Pathobiol Annu* **5**, 1-34 (1975).

177. Kauffman, S.L. Cell proliferation in the mammalian lung. *Int Rev Exp Pathol* **22**, 131-91 (1980).

178. Blenkinsopp, W.K. Proliferation of respiratory tract epithelium in the rat. *Exp Cell Res* **46**, 144-54 (1967).

179. Rawlins, E.L. & Hogan, B.L. Ciliated epithelial cell lifespan in the mouse trachea and lung. *Am J Physiol Lung Cell Mol Physiol* **295**, L231-4 (2008).

180. Rawlins, E.L., Ostrowski, L.E., Randell, S.H. & Hogan, B.L. Lung development and repair: contribution of the ciliated lineage. *Proc Natl Acad Sci U S A* **104**, 410-7 (2007).

181. Sorokin, S.P., Hoyt, R.F., Jr. & Shaffer, M.J. Ontogeny of neuroepithelial bodies: correlations with mitogenesis and innervation. *Microsc Res Tech* **37**, 43-61 (1997).

182. Sunday, M.E. Pulmonary Neuroendocrine Cells and Lung Development. *Endocr Pathol* **7**, 173-201 (1996).

183. Cutz, E. Neuroendocrine cells of the lung. An overview of morphologic characteristics and development. *Exp Lung Res* **3**, 185-208 (1982).

184. Khoor, A., Gray, M.E., Singh, G. & Stahlman, M.T. Ontogeny of Clara cell-specific protein and its mRNA: their association with neuroepithelial bodies in human fetal lung and in bronchopulmonary dysplasia. *J Histochem Cytochem* **44**, 1429-38 (1996).

185. Hoyt, R.F., Jr., Sorokin, S.P., McDowell, E.M. & McNelly, N.A. Neuroepithelial bodies and growth of the airway epithelium in developing hamster lung. *Anat Rec* **236**, 15-22; discussion 22-4 (1993).

186. Hoyt, R.F., Jr., McNelly, N.A., McDowell, E.M. & Sorokin, S.P. Neuroepithelial bodies stimulate proliferation of airway epithelium in fetal hamster lung. *Am J Physiol* **260**, L234-40 (1991).

187. Keith, I.M. & Will, J.A. Dynamics of the neuroendocrine cell--regulatory peptide system in the lung. Specific overview and new results. *Exp Lung Res* **3**, 387-402 (1982).

188. Peake, J.L., Reynolds, S.D., Stripp, B.R., Stephens, K.E. & Pinkerton, K.E. Alteration of pulmonary neuroendocrine cells during epithelial repair of naphthalene-induced airway injury. *Am J Pathol* **156**, 279-86 (2000).

189. Cutz, E., Yeger, H. & Pan, J. Pulmonary neuroendocrine cell system in pediatric lung disease-recent advances. *Pediatr Dev Pathol* **10**, 419-35 (2007).

190. Van Lommel, A., Bolle, T., Fannes, W. & Lauweryns, J.M. The pulmonary neuroendocrine system: the past decade. *Arch Histol Cytol* **62**, 1-16 (1999).

191. Scheuermann, D.W. Comparative histology of pulmonary neuroendocrine cell system in mammalian lungs. *Microsc Res Tech* **37**, 31-42 (1997).

192. Chua, B.A. & Perks, A.M. The effect of dopamine on lung liquid production by in vitro lungs from fetal guinea-pigs. *J Physiol* **513 (Pt 1)**, 283-94 (1998).

193. Barnard, M.L., Olivera, W.G., Rutschman, D.M., Bertorello, A.M., Katz, A.I. & Sznajder, J.I. Dopamine stimulates sodium transport and liquid clearance in rat lung epithelium. *Am J Respir Crit Care Med* **156**, 709-14 (1997).

194. Chua, B.A. & Perks, A.M. The pulmonary neuroendocrine system and drainage of the fetal lung: effects of serotonin. *Gen Comp Endocrinol* **113**, 374-87 (1999).

195. Gandhi, S.G., Law, C., Duan, W., Otulakowski, G. & O'Brodovich, H. Pulmonary neuroendocrine cell-secreted factors may alter fetal lung liquid clearance. *Pediatr Res* **65**, 274-8 (2009).

196. Pezzulo, A.A., Gutierrez, J., Duschner, K.S., McConnell, K.S., Taft, P.J., Ernst, S.E., Yahr, T.L., Rahmouni, K., Klesney-Tait, J., Stoltz, D.A. & Zabner, J. Glucose depletion in the airway surface liquid is essential for sterility of the airways. *PLoS One* **6**, e16166 (2011).

197. Bartlett, J.A., Fischer, A.J. & McCray, P.B., Jr. Innate immune functions of the airway epithelium. *Contrib Microbiol* **15**, 147-63 (2008).

198. Rhodin, J. & Dalhamn, T. Electron microscopy of the tracheal ciliated mucosa in rat. *Z Zellforsch Mikrosk Anat* **44**, 345-412 (1956).

199. Tizzano, M., Cristofoletti, M., Sbarbati, A. & Finger, T.E. Expression of taste receptors in solitary chemosensory cells of rodent airways. *BMC Pulm Med* **11**, 3 (2011).

200. Pack, R.J., Al-Ugaily, L.H., Morris, G. & Widdicombe, J.G. The distribution and structure of cells in the tracheal epithelium of the mouse. *Cell Tissue Res* **208**, 65-84 (1980).

201. Krasteva, G., Canning, B.J., Hartmann, P., Veres, T.Z., Papadakis, T., Muhlfeld, C., Schliecker, K., Tallini, Y.N., Braun, A., Hackstein, H., Baal, N., Weihe, E., Schutz, B., Kotlikoff, M., Ibanez-Tallon, I. & Kummer, W. Cholinergic chemosensory cells in the trachea regulate breathing. *Proc Natl Acad Sci U S A* **108**, 9478-83 (2011).

202. Chang, L.Y., Mercer, R.R. & Crapo, J.D. Differential distribution of brush cells in the rat lung. *Anat Rec* **216**, 49-54 (1986).

203. Meyrick, B. & Reid, L. The alveolar brush cell in rat lung--a third pneumonocyte. *J Ultrastruct Res* **23**, 71-80 (1968).

204. Luciano, L., Reale, E. & Ruska, H. [On a glycogen containing brusc cell in the rectum of the rat]. *Z Zellforsch Mikrosk Anat* **91**, 153-8 (1968).

205. Luciano, L., Reale, E. & Ruska, H. [On a "chemoreceptive" sensory cell in the tachea of the rat]. *Z Zellforsch Mikrosk Anat* **85**, 350-75 (1968).

206. Sbarbati, A. & Osculati, F. A new fate for old cells: brush cells and related elements. *J Anat* **206**, 349-58 (2005).

207. Hofer, D. & Drenckhahn, D. Identification of the taste cell G-protein, alpha-gustducin, in brush cells of the rat pancreatic duct system. *Histochem Cell Biol* **110**, 303-9 (1998).

208. Hofer, D. & Drenckhahn, D. Identification of brush cells in the alimentary and respiratory system by antibodies to villin and fimbrin. *Histochemistry* **98**, 237-42 (1992).

209. Tizzano, M., Gulbransen, B.D., Vandenbeuch, A., Clapp, T.R., Herman, J.P., Sibhatu, H.M., Churchill, M.E., Silver, W.L., Kinnamon, S.C. & Finger, T.E. Nasal chemosensory cells use bitter taste signaling to detect irritants and bacterial signals. *Proc Natl Acad Sci U S A* **107**, 3210-5 (2010).

210. Krasteva, G., Canning, B.J., Papadakis, T. & Kummer, W. Cholinergic brush cells in the trachea mediate respiratory responses to quorum sensing molecules. *Life Sci* **91**, 992-6 (2012).

211. Krasteva, G. & Kummer, W. "Tasting" the airway lining fluid. *Histochem Cell Biol* **138**, 365-83 (2012).

212. Finger, T.E. & Kinnamon, S.C. Taste isn't just for taste buds anymore. *F1000 Biol Rep* **3**, 20 (2011).

213. Chou, Y.L., Scarupa, M.D., Mori, N. & Canning, B.J. Differential effects of airway afferent nerve subtypes on cough and respiration in anesthetized guinea pigs. *Am J Physiol Regul Integr Comp Physiol* **295**, R1572-84 (2008).

214. Canning, B.J. & Mori, N. Encoding of the cough reflex in anesthetized guinea pigs. *Am J Physiol Regul Integr Comp Physiol* **300**, R369-77 (2011).

215. Fliegauf, M., Benzing, T. & Omran, H. When cilia go bad: cilia defects and ciliopathies. *Nat Rev Mol Cell Biol* **8**, 880-93 (2007).

216. Sloboda, R.D. Intraflagellar transport and the flagellar tip complex. *J Cell Biochem* **94**, 266-72 (2005).

217. Salathe, M. Regulation of mammalian ciliary beating. *Annu Rev Physiol* **69**, 401-22 (2007).

218. Satir, P. & Sleigh, M.A. The physiology of cilia and mucociliary interactions. *Annu Rev Physiol* **52**, 137-55 (1990).

219. Del Bigio, M.R. Ependymal cells: biology and pathology. *Acta Neuropathol* **119**, 55-73 (2010).

220. Ibanez-Tallon, I., Pagenstecher, A., Fliegauf, M., Olbrich, H., Kispert, A., Ketelsen, U.P., North, A., Heintz, N. & Omran, H. Dysfunction of axonemal dynein heavy chain Mdnah5 inhibits ependymal flow and reveals a novel mechanism for hydrocephalus formation. *Hum Mol Genet* **13**, 2133-41 (2004).

221. O'Callaghan, C., Sikand, K. & Rutman, A. Respiratory and brain ependymal ciliary function. *Pediatr Res* **46**, 704-7 (1999).

222. Dempsey, L.C. & Nielsen, S.L. Surface ultrastructure of human ependyma. *J Neurosurg* **45**, 52-5 (1976).

223. Fahy, J.V. & Dickey, B.F. Airway mucus function and dysfunction. *N Engl J Med* **363**, 2233-47 (2010).

224. Sleigh, M.A., Blake, J.R. & Liron, N. The propulsion of mucus by cilia. *Am Rev Respir Dis* **137**, 726-41 (1988).

225. Matsui, H., Grubb, B.R., Tarran, R., Randell, S.H., Gatzy, J.T., Davis, C.W. & Boucher, R.C. Evidence for periciliary liquid layer depletion, not abnormal ion composition, in the pathogenesis of cystic fibrosis airways disease. *Cell* **95**, 1005-15 (1998).

226. Plopper, C.G., Mariassy, A.T. & Hill, L.H. Ultrastructure of the nonciliated bronchiolar epithelial (Clara) cell of mammalian lung: II. A comparison of horse, steer, sheep, dog, and cat. *Exp Lung Res* **1**, 155-69 (1980).

227. Plopper, C.G., Mariassy, A.T. & Hill, L.H. Ultrastructure of the nonciliated bronchiolar epithelial (Clara) cell of mammalian lung: I. A comparison of rabbit, guinea pig, rat, hamster, and mouse. *Exp Lung Res* **1**, 139-54 (1980).

228. Plopper, C.G., Hill, L.H. & Mariassy, A.T. Ultrastructure of the nonciliated bronchiolar epithelial (Clara) cell of mammalian lung. III. A study of man with comparison of 15 mammalian species. *Exp Lung Res* **1**, 171-80 (1980).

229. Yoneda, K. Pilocarpine stimulation of the bronchiolar Clara cell secretion. *Lab Invest* **37**, 447-52 (1977).

230. Massaro, G.D., Fischman, C.M., Chiang, M.J., Amado, C. & Massaro, D. Regulation of secretion in Clara cells: studies using the isolated perfused rat lung. *J Clin Invest* **67**, 345-51 (1981).

231. Cutz, E. & Conen, P.E. Ultrastructure and cytochemistry of Clara cells. *Am J Pathol* **62**, 127-41 (1971).

232. Warburton, D., Perin, L., Defilippo, R., Bellusci, S., Shi, W. & Driscoll, B. Stem/progenitor cells in lung development, injury repair, and regeneration. *Proc Am Thorac Soc* **5**, 703-6 (2008).

233. Cardoso, W.V. Molecular regulation of lung development. *Annu Rev Physiol* **63**, 471-94 (2001).

234. Hong, K.U., Reynolds, S.D., Watkins, S., Fuchs, E. & Stripp, B.R. In vivo differentiation potential of tracheal basal cells: evidence for multipotent and unipotent subpopulations. *Am J Physiol Lung Cell Mol Physiol* **286**, L643-9 (2004).

235. Rock, J.R., Onaitis, M.W., Rawlins, E.L., Lu, Y., Clark, C.P., Xue, Y., Randell, S.H. & Hogan, B.L. Basal cells as stem cells of the mouse trachea and human airway epithelium. *Proc Natl Acad Sci U S A* **106**, 12771-5 (2009).

236. Morrisey, E.E. & Hogan, B.L. Preparing for the first breath: genetic and cellular mechanisms in lung development. *Dev Cell* **18**, 8-23 (2010).

237. Guseh, J.S., Bores, S.A., Stanger, B.Z., Zhou, Q., Anderson, W.J., Melton, D.A. & Rajagopal, J. Notch signaling promotes airway mucous metaplasia and inhibits alveolar development. *Development* **136**, 1751-9 (2009).

238. Tsao, P.N., Vasconcelos, M., Izvolsky, K.I., Qian, J., Lu, J. & Cardoso, W.V. Notch signaling controls the balance of ciliated and secretory cell fates in developing airways. *Development* **136**, 2297-307 (2009).

239. Morimoto, M., Nishinakamura, R., Saga, Y. & Kopan, R. Different assemblies of Notch receptors coordinate the distribution of the major bronchial Clara, ciliated and neuroendocrine cells. *Development* **139**, 4365-73 (2012).

240. Morimoto, M., Liu, Z., Cheng, H.T., Winters, N., Bader, D. & Kopan, R. Canonical Notch signaling in the developing lung is required for determination of arterial smooth muscle cells and selection of Clara versus ciliated cell fate. *J Cell Sci* **123**, 213-24 (2010).

241. Rawlins, E.L., Okubo, T., Xue, Y., Brass, D.M., Auten, R.L., Hasegawa, H., Wang, F. & Hogan, B.L. The role of Scgb1a1+ Clara cells in the long-term maintenance and repair of lung airway, but not alveolar, epithelium. *Cell Stem Cell* **4**, 525-34 (2009).

242. Evans, M.J., Johnson, L.V., Stephens, R.J. & Freeman, G. Renewal of the terminal bronchiolar epithelium in the rat following exposure to NO2 or O3. *Lab Invest* **35**, 246-57 (1976).

243. Evans, M.J., Cabral-Anderson, L.J. & Freeman, G. Role of the Clara cell in renewal of the bronchiolar epithelium. *Lab Invest* **38**, 648-53 (1978).

244. Boers, J.E., Ambergen, A.W. & Thunnissen, F.B. Number and proliferation of clara cells in normal human airway epithelium. *Am J Respir Crit Care Med* **159**, 1585-91 (1999).

245. Wang, X., Kruithof-de Julio, M., Economides, K.D., Walker, D., Yu, H., Halili, M.V., Hu, Y.P., Price, S.M., Abate-Shen, C. & Shen, M.M. A luminal epithelial stem cell that is a cell of origin for prostate cancer. *Nature* **461**, 495-500 (2009).

246. Nakagawa, T., Sharma, M., Nabeshima, Y., Braun, R.E. & Yoshida, S. Functional hierarchy and reversibility within the murine spermatogenic stem cell compartment. *Science* **328**, 62-7 (2010).

247. Schoch, K.G., Lori, A., Burns, K.A., Eldred, T., Olsen, J.C. & Randell, S.H. A subset of mouse tracheal epithelial basal cells generates large colonies in vitro. *Am J Physiol Lung Cell Mol Physiol* **286**, L631-42 (2004).

248. Hong, K.U., Reynolds, S.D., Watkins, S., Fuchs, E. & Stripp, B.R. Basal cells are a multipotent progenitor capable of renewing the bronchial epithelium. *Am J Pathol* **164**, 577-88 (2004).

249. Nakajima, M., Kawanami, O., Jin, E., Ghazizadeh, M., Honda, M., Asano, G., Horiba, K. & Ferrans, V.J. Immunohistochemical and ultrastructural studies of basal cells, Clara cells and bronchiolar cuboidal cells in normal human airways. *Pathol Int* **48**, 944-53 (1998).

250. Daniely, Y., Liao, G., Dixon, D., Linnoila, R.I., Lori, A., Randell, S.H., Oren, M. & Jetten, A.M. Critical role of p63 in the development of a normal esophageal and tracheobronchial epithelium. *Am J Physiol Cell Physiol* **287**, C171-81 (2004).

251. Rock, J.R., Randell, S.H. & Hogan, B.L. Airway basal stem cells: a perspective on their roles in epithelial homeostasis and remodeling. *Dis Model Mech* **3**, 545-56 (2010).

252. Halldorsson, S., Asgrimsson, V., Axelsson, I., Gudmundsson, G.H., Steinarsdottir, M., Baldursson, O. & Gudjonsson, T. Differentiation potential of a basal epithelial cell line established from human bronchial explant. *In Vitro Cell Dev Biol Anim* **43**, 283-9 (2007).

253. Arason, A.J., Jonsdottir, H.R., Halldorsson, S., Benediktsdottir, B.E., Bergthorsson, J.T., Ingthorsson, S., Baldursson, O., Sinha, S., Gudjonsson, T. & Magnusson, M.K. deltaNp63 has a role in maintaining epithelial integrity in airway epithelium. *PLoS One* **9**, e88683 (2014).

254. Koster, M.I., Kim, S., Mills, A.A., DeMayo, F.J. & Roop, D.R. p63 is the molecular switch for initiation of an epithelial stratification program. *Genes Dev* **18**, 126-31 (2004).

255. Vaughan, A.E., Brumwell, A.N., Xi, Y., Gotts, J.E., Brownfield, D.G., Treutlein, B., Tan, K., Tan, V., Liu, F.C., Looney, M.R., Matthay, M.A., Rock, J.R. & Chapman, H.A. Lineage-negative progenitors mobilize to regenerate lung epithelium after major injury. *Nature* (2014).

256. Kumar, P.A., Hu, Y., Yamamoto, Y., Hoe, N.B., Wei, T.S., Mu, D., Sun, Y., Joo, L.S., Dagher, R., Zielonka, E.M., Wang de, Y., Lim, B., Chow, V.T., Crum, C.P., Xian, W. & McKeon, F. Distal airway stem cells yield alveoli in vitro and during lung regeneration following H1N1 influenza infection. *Cell* **147**, 525-38 (2011).

257. Zuo, W., Zhang, T., Wu, D.Z., Guan, S.P., Liew, A.A., Yamamoto, Y., Wang, X., Lim, S.J., Vincent, M., Lessard, M., Crum, C.P., Xian, W. & McKeon, F. p63Krt5 distal airway stem cells are essential for lung regeneration. *Nature* (2014).

258. Rogers, D.F. The airway goblet cell. *Int J Biochem Cell Biol* **35**, 1-6 (2003).

259. Boucherat, O., Boczkowski, J., Jeannotte, L. & Delacourt, C. Cellular and molecular mechanisms of goblet cell metaplasia in the respiratory airways. *Exp Lung Res* **39**, 207-16 (2013).

260. Corfield, A.P. Mucins: a biologically relevant glycan barrier in mucosal protection. *Biochim Biophys Acta* **1850**, 236-52 (2015).

261. Holmen, J.M., Karlsson, N.G., Abdullah, L.H., Randell, S.H., Sheehan, J.K., Hansson, G.C. & Davis, C.W. Mucins and their O-Glycans from human bronchial epithelial cell cultures. *Am J Physiol Lung Cell Mol Physiol* **287**, L824-34 (2004).

262. Thai, P., Loukoianov, A., Wachi, S. & Wu, R. Regulation of airway mucin gene expression. *Annu Rev Physiol* **70**, 405-29 (2008).

263. Rose, M.C. & Voynow, J.A. Respiratory tract mucin genes and mucin glycoproteins in health and disease. *Physiol Rev* **86**, 245-78 (2006).

264. Voynow, J.A. & Rubin, B.K. Mucins, mucus, and sputum. *Chest* **135**, 505-12 (2009).

265. Whitsett, J.A., Haitchi, H.M. & Maeda, Y. Intersections between pulmonary development and disease. *Am J Respir Crit Care Med* **184**, 401-6 (2011).

266. Danahay, H., Pessotti, A.D., Coote, J., Montgomery, B.E., Xia, D., Wilson, A., Yang, H., Wang, Z., Bevan, L., Thomas, C., Petit, S., London, A., LeMotte, P., Doelemeyer, A., Velez-Reyes, G.L., Bernasconi, P., Fryer, C.J., Edwards, M., Capodieci, P., Chen, A., Hild, M. & Jaffe, A.B. Notch2 is required for inflammatory cytokine-driven goblet cell metaplasia in the lung. *Cell Rep* **10**, 239-52 (2015).

267. Rock, J.R., Gao, X., Xue, Y., Randell, S.H., Kong, Y.Y. & Hogan, B.L. Notch-dependent differentiation of adult airway basal stem cells. *Cell Stem Cell* **8**, 639-48 (2011).

268. Whitsett, J.A. & Alenghat, T. Respiratory epithelial cells orchestrate pulmonary innate immunity. *Nat Immunol* **16**, 27-35 (2015).

269. Wan, H., Kaestner, K.H., Ang, S.L., Ikegami, M., Finkelman, F.D., Stahlman, M.T., Fulkerson, P.C., Rothenberg, M.E. & Whitsett, J.A. Foxa2 regulates alveolarization and goblet cell hyperplasia. *Development* **131**, 953-64 (2004).

270. Park, K.S., Korfhagen, T.R., Bruno, M.D., Kitzmiller, J.A., Wan, H., Wert, S.E., Khurana Hershey, G.K., Chen, G. & Whitsett, J.A. SPDEF regulates goblet cell hyperplasia in the airway epithelium. *J Clin Invest* **117**, 978-88 (2007).

271. Chen, G., Korfhagen, T.R., Xu, Y., Kitzmiller, J., Wert, S.E., Maeda, Y., Gregorieff, A., Clevers, H. & Whitsett, J.A. SPDEF is required for mouse pulmonary goblet cell differentiation and regulates a network of genes associated with mucus production. *J Clin Invest* **119**, 2914-24 (2009).

272. Satir, P. Landmarks in cilia research from Leeuwenhoek to us. *Cell Motil Cytoskeleton* **32**, 90-4 (1995).

273. Dobell, C. & Leeuwenhoek, A.v. *Antony van Leeuwenhoek and his "Little animals"; being some account of the father of protozoology & bacteriology and his multifarious discoveries in these disciplines*, v, 435 p. (Russell & Russell, New York,, 1958).

274. Porter, M.E. & Sale, W.S. The 9 + 2 axoneme anchors multiple inner arm dyneins and a network of kinases and phosphatases that control motility. *J Cell Biol* **151**, F37-42 (2000).

275. Quarmby, L.M. & Parker, J.D. Cilia and the cell cycle? *J Cell Biol* **169**, 707-10 (2005).

276. Haimo, L.T. & Rosenbaum, J.L. Cilia, flagella, and microtubules. *J Cell Biol* **91**, 125s-130s (1981).

277. Praetorius, H.A. & Spring, K.R. The renal cell primary cilium functions as a flow sensor. *Curr Opin Nephrol Hypertens* **12**, 517-20 (2003).

278. Christensen, S.T., Pedersen, L.B., Schneider, L. & Satir, P. Sensory cilia and integration of signal transduction in human health and disease. *Traffic* **8**, 97-109 (2007).

279. Singla, V. & Reiter, J.F. The primary cilium as the cell's antenna: signaling at a sensory organelle. *Science* **313**, 629-33 (2006).

280. Berbari, N.F., O'Connor, A.K., Haycraft, C.J. & Yoder, B.K. The primary cilium as a complex signaling center. *Curr Biol* **19**, R526-35 (2009).

281. Sorokin, S.P. Reconstructions of centriole formation and ciliogenesis in mammalian lungs. *J Cell Sci* **3**, 207-30 (1968).

282. Ishikawa, H. & Marshall, W.F. Ciliogenesis: building the cell's antenna. *Nat Rev Mol Cell Biol* **12**, 222-34 (2011).

283. Molla-Herman, A., Ghossoub, R., Blisnick, T., Meunier, A., Serres, C., Silbermann, F., Emmerson, C., Romeo, K., Bourdoncle, P., Schmitt, A., Saunier, S., Spassky, N., Bastin, P. & Benmerah, A. The ciliary pocket: an endocytic membrane domain at the base of primary and motile cilia. *J Cell Sci* **123**, 1785-95 (2010).

284. Rosenbaum, J.L. & Child, F.M. Flagellar regeneration in protozoan flagellates. *J Cell Biol* **34**, 345-64 (1967).

285. Garcia-Gonzalo, F.R. & Reiter, J.F. Scoring a backstage pass: mechanisms of ciliogenesis and ciliary access. *J Cell Biol* **197**, 697-709 (2012).

286. Kartagener, M. Zur Pathogenese der Bronchiektasien: Bronchiektasien bei Situs viscerum inversus. *Beiträge zur Klinik der Tuberkulose und spezifischen Tuberkulose-Forschung* **84**, 73-85 (1933).

287. Essner, J.J., Vogan, K.J., Wagner, M.K., Tabin, C.J., Yost, H.J. & Brueckner, M. Conserved function for embryonic nodal cilia. *Nature* **418**, 37-8 (2002).

288. Supp, D.M., Witte, D.P., Potter, S.S. & Brueckner, M. Mutation of an axonemal dynein affects left-right asymmetry in inversus viscerum mice. *Nature* **389**, 963-6 (1997).

289. Supp, D.M., Brueckner, M., Kuehn, M.R., Witte, D.P., Lowe, L.A., McGrath, J., Corrales, J. & Potter, S.S. Targeted deletion of the ATP binding domain of left-right dynein confirms its role in specifying development of left-right asymmetries. *Development* **126**, 5495-504 (1999).

290. Okada, Y., Nonaka, S., Tanaka, Y., Saijoh, Y., Hamada, H. & Hirokawa, N. Abnormal nodal flow precedes situs inversus in iv and inv mice. *Mol Cell* **4**, 459-68 (1999).

291. Nonaka, S., Tanaka, Y., Okada, Y., Takeda, S., Harada, A., Kanai, Y., Kido, M. & Hirokawa, N. Randomization of left-right asymmetry due to loss of nodal cilia generating leftward flow of extraembryonic fluid in mice lacking KIF3B motor protein. *Cell* **95**, 829-37 (1998).

292. Pedersen, H. & Rebbe, H. Absence of arms in the axoneme of immobile human spermatozoa. *Biol Reprod* **12**, 541-4 (1975).

293. Afzelius, B.A., Eliasson, R., Johnsen, O. & Lindholmer, C. Lack of dynein arms in immotile human spermatozoa. *J Cell Biol* **66**, 225-32 (1975).

294. Camner, P., Mossberg, B. & Afzelius, B.A. Evidence of congenitally nonfunctioning cilia in the tracheobronchial tract in two subjects. *Am Rev Respir Dis* **112**, 807-9 (1975).

295. Afzelius, B.A. A human syndrome caused by immotile cilia. *Science* **193**, 317-9 (1976).

296. Narayan, D., Krishnan, S.N., Upender, M., Ravikumar, T.S., Mahoney, M.J., Dolan, T.F., Jr., Teebi, A.S. & Haddad, G.G. Unusual inheritance of primary ciliary dyskinesia (Kartagener's syndrome). *J Med Genet* **31**, 493-6 (1994).

297. Munro, N.C., Currie, D.C., Lindsay, K.S., Ryder, T.A., Rutman, A., Dewar, A., Greenstone, M.A., Hendry, W.F. & Cole, P.J. Fertility in men with primary ciliary dyskinesia presenting with respiratory infection. *Thorax* **49**, 684-7 (1994).

298. Afzelius, B.A. & Eliasson, R. Male and female infertility problems in the immotile-cilia syndrome. *Eur J Respir Dis Suppl* **127**, 144-7 (1983).

299. Banizs, B., Pike, M.M., Millican, C.L., Ferguson, W.B., Komlosi, P., Sheetz, J., Bell, P.D., Schwiebert, E.M. & Yoder, B.K. Dysfunctional cilia lead to altered ependyma and choroid plexus function, and result in the formation of hydrocephalus. *Development* **132**, 5329-39 (2005).

300. Garton, H.J. & Piatt, J.H., Jr. Hydrocephalus. *Pediatr Clin North Am* **51**, 305-25 (2004).

301. Bruni, J.E., Del Bigio, M.R. & Clattenburg, R.E. Ependyma: normal and pathological. A review of the literature. *Brain Res* **356**, 1-19 (1985).

302. Eley, L., Yates, L.M. & Goodship, J.A. Cilia and disease. *Curr Opin Genet Dev* **15**, 308-14 (2005).

303. Gajiwala, K.S., Chen, H., Cornille, F., Roques, B.P., Reith, W., Mach, B. & Burley, S.K. Structure of the winged-helix protein hRFX1 reveals a new mode of DNA binding. *Nature* **403**, 916-21 (2000).

304. Reith, W., Herrero-Sanchez, C., Kobr, M., Silacci, P., Berte, C., Barras, E., Fey, S. & Mach, B. MHC class II regulatory factor RFX has a novel DNA-binding domain and a functionally independent dimerization domain. *Genes Dev* **4**, 1528-40 (1990).

305. Emery, P., Strubin, M., Hofmann, K., Bucher, P., Mach, B. & Reith, W. A consensus motif in the RFX DNA binding domain and binding domain mutants with altered specificity. *Mol Cell Biol* **16**, 4486-94 (1996).

306. Emery, P., Durand, B., Mach, B. & Reith, W. RFX proteins, a novel family of DNA binding proteins conserved in the eukaryotic kingdom. *Nucleic Acids Res* **24**, 803-7 (1996).

307. Aftab, S., Semenec, L., Chu, J.S. & Chen, N. Identification and characterization of novel human tissue-specific RFX transcription factors. *BMC Evol Biol* **8**, 226 (2008).

308. Chu, J.S., Baillie, D.L. & Chen, N. Convergent evolution of RFX transcription factors and ciliary genes predated the origin of metazoans. *BMC Evol Biol* **10**, 130 (2010).

309. Reith, W., Siegrist, C.A., Durand, B., Barras, E. & Mach, B. Function of major histocompatibility complex class II promoters requires cooperative binding between factors RFX and NF-Y. *Proc Natl Acad Sci U S A* **91**, 554-8 (1994).

310. Reith, W., Kobr, M., Emery, P., Durand, B., Siegrist, C.A. & Mach, B. Cooperative binding between factors RFX and X2bp to the X and X2 boxes of MHC class II promoters. *J Biol Chem* **269**, 20020-5 (1994).

311. Morotomi-Yano, K., Yano, K., Saito, H., Sun, Z., Iwama, A. & Miki, Y. Human regulatory factor X 4 (RFX4) is a testis-specific dimeric DNA-binding protein that cooperates with other human RFX members. *J Biol Chem* **277**, 836-42 (2002).

312. Iwama, A., Pan, J., Zhang, P., Reith, W., Mach, B., Tenen, D.G. & Sun, Z. Dimeric RFX proteins contribute to the activity and lineage specificity of the interleukin-5 receptor alpha promoter through activation and repression domains. *Mol Cell Biol* **19**, 3940-50 (1999).

313. Zhang, D., Stumpo, D.J., Graves, J.P., DeGraff, L.M., Grissom, S.F., Collins, J.B., Li, L., Zeldin, D.C. & Blackshear, P.J. Identification of potential target genes for RFX4_v3, a transcription factor critical for brain development. *J Neurochem* **98**, 860-75 (2006).

314. Ou, G., Blacque, O.E., Snow, J.J., Leroux, M.R. & Scholey, J.M. Functional coordination of intraflagellar transport motors. *Nature* **436**, 583-7 (2005).

315. Efimenko, E., Bubb, K., Mak, H.Y., Holzman, T., Leroux, M.R., Ruvkun, G., Thomas, J.H. & Swoboda, P. Analysis of xbx genes in C. elegans. *Development* **132**, 1923-34 (2005).

316. Burghoorn, J., Piasecki, B.P., Crona, F., Phirke, P., Jeppsson, K.E. & Swoboda, P. The in vivo dissection of direct RFX-target gene promoters in C. elegans reveals a novel cis-regulatory element, the C-box. *Dev Biol* **368**, 415-26 (2012).

317. Weigel, D., Jurgens, G., Kuttner, F., Seifert, E. & Jackle, H. The homeotic gene fork head encodes a nuclear protein and is expressed in the terminal regions of the Drosophila embryo. *Cell* **57**, 645-58 (1989).

318. Lai, E., Prezioso, V.R., Smith, E., Litvin, O., Costa, R.H. & Darnell, J.E., Jr. HNF-3A, a hepatocyte-enriched transcription factor of novel structure is regulated transcriptionally. *Genes Dev* **4**, 1427-36 (1990).

319. Tsai, K.L., Huang, C.Y., Chang, C.H., Sun, Y.J., Chuang, W.J. & Hsiao, C.D. Crystal structure of the human FOXK1a-DNA complex and its implications on the diverse binding specificity of winged helix/forkhead proteins. *J Biol Chem* **281**, 17400-9 (2006).

320. Stroud, J.C., Wu, Y., Bates, D.L., Han, A., Nowick, K., Paabo, S., Tong, H. & Chen, L. Structure of the forkhead domain of FOXP2 bound to DNA. *Structure* **14**, 159-66 (2006).

321. Jin, C., Marsden, I., Chen, X. & Liao, X. Dynamic DNA contacts observed in the NMR structure of winged helix protein-DNA complex. *J Mol Biol* **289**, 683-90 (1999).

322. Clark, K.L., Halay, E.D., Lai, E. & Burley, S.K. Co-crystal structure of the HNF-3/fork head DNA-recognition motif resembles histone H5. *Nature* **364**, 412-20 (1993).

323. Cirillo, L.A. & Zaret, K.S. Specific interactions of the wing domains of FOXA1 transcription factor with DNA. *J Mol Biol* **366**, 720-4 (2007).

324. Romanelli, M.G., Tato, L., Lorenzi, P. & Morandi, C. Nuclear localization domains in human thyroid transcription factor 2. *Biochim Biophys Acta* **1643**, 55-64 (2003).

325. Hancock, W.W. & Ozkaynak, E. Three distinct domains contribute to nuclear transport of murine Foxp3. *PLoS One* **4**, e7890 (2009).

326. Carlsson, P. & Mahlapuu, M. Forkhead transcription factors: key players in development and metabolism. *Dev Biol* **250**, 1-23 (2002).

327. van der Vos, K.E. & Coffer, P.J. FOXO-binding partners: it takes two to tango. *Oncogene* **27**, 2289-99 (2008).

328. Blount, A.L., Schmidt, K., Justice, N.J., Vale, W.W., Fischer, W.H. & Bilezikjian, L.M. FoxL2 and Smad3 coordinately regulate follistatin gene transcription. *J Biol Chem* **284**, 7631-45 (2009).

329. Hannenhalli, S. & Kaestner, K.H. The evolution of Fox genes and their role in development and disease. *Nat Rev Genet* **10**, 233-40 (2009).

330. Benayoun, B.A., Caburet, S. & Veitia, R.A. Forkhead transcription factors: key players in health and disease. *Trends Genet* **27**, 224-32 (2011).

331. Clevidence, D.E., Overdier, D.G., Tao, W., Qian, X., Pani, L., Lai, E. & Costa, R.H. Identification of nine tissue-specific transcription factors of the hepatocyte nuclear factor 3/forkhead DNA-binding-domain family. *Proc Natl Acad Sci U S A* **90**, 3948-52 (1993).

332. Murphy, D.B., Seemann, S., Wiese, S., Kirschner, R., Grzeschik, K.H. & Thies, U. The human hepatocyte nuclear factor 3/fork head gene FKHL13: genomic structure and pattern of expression. *Genomics* **40**, 462-9 (1997).

333. Hackett, B.P., Brody, S.L., Liang, M., Zeitz, I.D., Bruns, L.A. & Gitlin, J.D. Primary structure of hepatocyte nuclear factor/forkhead homologue 4 and characterization of gene expression in the developing respiratory and reproductive epithelium. *Proc Natl Acad Sci U S A* **92**, 4249-53 (1995).

334. Tichelaar, J.W., Wert, S.E., Costa, R.H., Kimura, S. & Whitsett, J.A. HNF-3/forkhead homologue-4 (HFH-4) is expressed in ciliated epithelial cells in the developing mouse lung. *J Histochem Cytochem* **47**, 823-32 (1999).

335. Tichelaar, J.W., Lim, L., Costa, R.H. & Whitsett, J.A. HNF-3/forkhead homologue-4 influences lung morphogenesis and respiratory epithelial cell differentiation in vivo. *Dev Biol* **213**, 405-17 (1999).

336. Blatt, E.N., Yan, X.H., Wuerffel, M.K., Hamilos, D.L. & Brody, S.L. Forkhead transcription factor HFH-4 expression is temporally related to ciliogenesis. *Am J Respir Cell Mol Biol* **21**, 168-76 (1999).

337. Brody, S.L., Yan, X.H., Wuerffel, M.K., Song, S.K. & Shapiro, S.D. Ciliogenesis and left-right axis defects in forkhead factor HFH-4-null mice. *Am J Respir Cell Mol Biol* **23**, 45-51 (2000).

338. Chen, J., Knowles, H.J., Hebert, J.L. & Hackett, B.P. Mutation of the mouse hepatocyte nuclear factor/forkhead homologue 4 gene results in an absence of cilia and random left-right asymmetry. *J Clin Invest* **102**, 1077-82 (1998).

339. Gomperts, B.N., Gong-Cooper, X. & Hackett, B.P. Foxj1 regulates basal body anchoring to the cytoskeleton of ciliated pulmonary epithelial cells. *J Cell Sci* **117**, 1329-37 (2004).

340. You, Y., Huang, T., Richer, E.J., Schmidt, J.E., Zabner, J., Borok, Z. & Brody, S.L. Role of f-box factor foxj1 in differentiation of ciliated airway epithelial cells. *Am J Physiol Lung Cell Mol Physiol* **286**, L650-7 (2004).

341. Ramsay, R.G. & Gonda, T.J. MYB function in normal and cancer cells. *Nat Rev Cancer* **8**, 523-34 (2008).

342. Stubbs, J.L., Oishi, I., Izpisua Belmonte, J.C. & Kintner, C. The forkhead protein Foxj1 specifies node-like cilia in Xenopus and zebrafish embryos. *Nat Genet* **40**, 1454-60 (2008).

343. Yu, S.W., Baek, S.H., Brennan, R.T., Bradley, C.J., Park, S.K., Lee, Y.S., Jun, E.J., Lookingland, K.J., Kim, E.K., Lee, H., Goudreau, J.L. & Kim, S.W. Autophagic death of adult hippocampal neural stem cells following insulin withdrawal. *Stem Cells* **26**, 2602-10 (2008).

344. Larroux, C., Luke, G.N., Koopman, P., Rokhsar, D.S., Shimeld, S.M. & Degnan, B.M. Genesis and expansion of metazoan transcription factor gene classes. *Mol Biol Evol* **25**, 980-96 (2008).

345. Stubbs, J.L., Vladar, E.K., Axelrod, J.D. & Kintner, C. Multicilin promotes centriole assembly and ciliogenesis during multiciliate cell differentiation. *Nat Cell Biol* **14**, 140-7 (2012).

346. Tan, F.E., Vladar, E.K., Ma, L., Fuentealba, L.C., Hoh, R., Espinoza, F.H., Axelrod, J.D., Alvarez-Buylla, A., Stearns, T., Kintner, C. & Krasnow, M.A. Myb promotes centriole amplification and later steps of the multiciliogenesis program. *Development* **140**, 4277-86 (2013).

347. Choksi, S.P., Lauter, G., Swoboda, P. & Roy, S. Switching on cilia: transcriptional networks regulating ciliogenesis. *Development* **141**, 1427-41 (2014).

348. Ventura, A., Meissner, A., Dillon, C.P., McManus, M., Sharp, P.A., Van Parijs, L., Jaenisch, R. & Jacks, T. Cre-lox-regulated conditional RNA interference from transgenes. *Proc Natl Acad Sci U S A* **101**, 10380-5 (2004).

349. Rosenbluth, J.M. & Pietenpol, J.A. mTOR regulates autophagy-associated genes downstream of p73. *Autophagy* **5**(2009).

350. Niemantsverdriet, M., Vermeij, W.P. & Backendorf, C. RT-PCR analysis of p73 splice variants, ease or tease? *Leukemia* **19**, 1685-6 (2005).

351. S, R. & J., S.H. Primer 3. in *Code available at* http://www-genome.wi.mit.edu/genome_software/other/primer3.html (1998).

352. Liu, P., Jenkins, N.A. & Copeland, N.G. A highly efficient recombineering-based method for generating conditional knockout mutations. *Genome Res* **13**, 476-84 (2003).

353. Rodriguez, C.I., Buchholz, F., Galloway, J., Sequerra, R., Kasper, J., Ayala, R., Stewart, A.F. & Dymecki, S.M. High-efficiency deleter mice show that FLPe is an alternative to Cre-loxP. *Nat Genet* **25**, 139-40 (2000).

354. Hayat, M.A. *Stains and cytochemical methods*, xvii, 455 p. (Plenum Press, New York, 1993).

355. Vladar, E.K. & Brody, S.L. Analysis of ciliogenesis in primary culture mouse tracheal epithelial cells. *Methods Enzymol* **525**, 285-309 (2013).

356. Lam, H.C., Choi, A.M. & Ryter, S.W. Isolation of mouse respiratory epithelial cells and exposure to experimental cigarette smoke at air liquid interface. *J Vis Exp* (2011).

357. Dodt, M., Roehr, J.T., Ahmed, R. & Dieterich, C. FLEXBAR-Flexible Barcode and Adapter Processing for Next-Generation Sequencing Platforms. *Biology (Basel)* **1**, 895-905 (2012).

358. Li, H. & Durbin, R. Fast and accurate short read alignment with Burrows-Wheeler transform. *Bioinformatics* **25**, 1754-60 (2009).

359. Zhang, Y., Liu, T., Meyer, C.A., Eeckhoute, J., Johnson, D.S., Bernstein, B.E., Nusbaum, C., Myers, R.M., Brown, M., Li, W. & Liu, X.S. Model-based analysis of ChIP-Seq (MACS). *Genome Biol* **9**, R137 (2008).

360. Consortium, E.P. An integrated encyclopedia of DNA elements in the human genome. *Nature* **489**, 57-74 (2012).

361. Heinz, S., Benner, C., Spann, N., Bertolino, E., Lin, Y.C., Laslo, P., Cheng, J.X., Murre, C., Singh, H. & Glass, C.K. Simple combinations of lineage-determining transcription factors prime cis-regulatory elements required for macrophage and B cell identities. *Mol Cell* **38**, 576-89 (2010).

362. Frith, M.C., Saunders, N.F., Kobe, B. & Bailey, T.L. Discovering sequence motifs with arbitrary insertions and deletions. *PLoS Comput Biol* **4**, e1000071 (2008).

363. Ramirez, F., Dundar, F., Diehl, S., Gruning, B.A. & Manke, T. deepTools: a flexible platform for exploring deep-sequencing data. *Nucleic Acids Res* **42**, W187-91 (2014).

364. Treutlein, B., Brownfield, D.G., Wu, A.R., Neff, N.F., Mantalas, G.L., Espinoza, F.H., Desai, T.J., Krasnow, M.A. & Quake, S.R. Reconstructing lineage hierarchies of the distal lung epithelium using single-cell RNA-seq. *Nature* **509**, 371-5 (2014).

365. Dobin, A., Davis, C.A., Schlesinger, F., Drenkow, J., Zaleski, C., Jha, S., Batut, P., Chaisson, M. & Gingeras, T.R. STAR: ultrafast universal RNA-seq aligner. *Bioinformatics* **29**, 15-21 (2013).

366. Harrow, J., Frankish, A., Gonzalez, J.M., Tapanari, E., Diekhans, M., Kokocinski, F., Aken, B.L., Barrell, D., Zadissa, A., Searle, S., Barnes, I., Bignell, A., Boychenko, V., Hunt, T., Kay, M., Mukherjee, G., Rajan, J., Despacio-Reyes, G., Saunders, G., Steward, C., Harte, R., Lin, M., Howald, C., Tanzer, A., Derrien, T., Chrast, J., Walters, N., Balasubramanian, S., Pei, B., Tress, M., Rodriguez, J.M., Ezkurdia, I., van Baren, J., Brent, M., Haussler, D., Kellis, M., Valencia, A., Reymond, A., Gerstein, M., Guigo, R. & Hubbard, T.J. GENCODE: the reference human genome annotation for The ENCODE Project. *Genome Res* **22**, 1760-74 (2012).

367. Roberts, A., Pimentel, H., Trapnell, C. & Pachter, L. Identification of novel transcripts in annotated genomes using RNA-Seq. *Bioinformatics* **27**, 2325-9 (2011).

368. Li, B., Ruotti, V., Stewart, R.M., Thomson, J.A. & Dewey, C.N. RNA-Seq gene expression estimation with read mapping uncertainty. *Bioinformatics* **26**, 493-500 (2010).

369. Liao, Y., Smyth, G.K. & Shi, W. featureCounts: an efficient general purpose program for assigning sequence reads to genomic features. *Bioinformatics* **30**, 923-30 (2014).

370. Love, M.I., Huber, W. & Anders, S. Moderated estimation of fold change and dispersion for RNA-seq data with DESeq2. *Genome Biol* **15**, 550 (2014).

371. Trink, B., Okami, K., Wu, L., Sriuranpong, V., Jen, J. & Sidransky, D. A new human p53 homologue. *Nat Med* **4**, 747-8 (1998).

372. Schmale, H. & Bamberger, C. A novel protein with strong homology to the tumor suppressor p53. *Oncogene* **15**, 1363-7 (1997).

373. Wanner, A., Salathe, M. & O'Riordan, T.G. Mucociliary clearance in the airways. *Am J Respir Crit Care Med* **154**, 1868-902 (1996).

374. Chu, D.T. & Klymkowsky, M.W. The appearance of acetylated alpha-tubulin during early development and cellular differentiation in Xenopus. *Dev Biol* **136**, 104-17 (1989).

375. You, Y., Richer, E.J., Huang, T. & Brody, S.L. Growth and differentiation of mouse tracheal epithelial cells: selection of a proliferative population. *Am J Physiol Lung Cell Mol Physiol* **283**, L1315-21 (2002).

376. Yang, A., Zhu, Z., Kettenbach, A., Kapranov, P., McKeon, F., Gingeras, T.R. & Struhl, K. Genome-wide mapping indicates that p73 and p63 co-occupy target sites and have similar dna-binding profiles in vivo. *PLoS One* **5**, e11572 (2010).

377. Lokshin, M., Li, Y., Gaiddon, C. & Prives, C. p53 and p73 display common and distinct requirements for sequence specific binding to DNA. *Nucleic Acids Res* **35**, 340-52 (2007).

378. Smeenk, L., van Heeringen, S.J., Koeppel, M., van Driel, M.A., Bartels, S.J., Akkers, R.C., Denissov, S., Stunnenberg, H.G. & Lohrum, M. Characterization of genome-wide p53-binding sites upon stress response. *Nucleic Acids Res* **36**, 3639-54 (2008).

379. Yang, A., Zhu, Z., Kapranov, P., McKeon, F., Church, G.M., Gingeras, T.R. & Struhl, K. Relationships between p63 binding, DNA sequence, transcription activity, and biological function in human cells. *Mol Cell* **24**, 593-602 (2006).

380. Perez, C.A., Ott, J., Mays, D.J. & Pietenpol, J.A. p63 consensus DNA-binding site: identification, analysis and application into a p63MH algorithm. *Oncogene* (2007).

381. Juven, T., Barak, Y., Zauberman, A., George, D.L. & Oren, M. Wild type p53 can mediate sequence-specific transactivation of an internal promoter within the mdm2 gene. *Oncogene* **8**, 3411-6 (1993).

382. Barak, Y., Juven, T., Haffner, R. & Oren, M. mdm2 expression is induced by wild type p53 activity. *EMBO J* **12**, 461-8 (1993).

383. Espinosa, J.M. & Emerson, B.M. Transcriptional regulation by p53 through intrinsic DNA/chromatin binding and site-directed cofactor recruitment. *Mol Cell* **8**, 57-69 (2001).

384. Thorvaldsdottir, H., Robinson, J.T. & Mesirov, J.P. Integrative Genomics Viewer (IGV): high-performance genomics data visualization and exploration. *Brief Bioinform* **14**, 178-92 (2013).

385. Robinson, J.T., Thorvaldsdottir, H., Winckler, W., Guttman, M., Lander, E.S., Getz, G. & Mesirov, J.P. Integrative genomics viewer. *Nat Biotechnol* **29**, 24-6 (2011).

386. Thomas, J., Morle, L., Soulavie, F., Laurencon, A., Sagnol, S. & Durand, B. Transcriptional control of genes involved in ciliogenesis: a first step in making cilia. *Biol Cell* **102**, 499-513 (2010).

387. Tilley, A.E., Walters, M.S., Shaykhiev, R. & Crystal, R.G. Cilia Dysfunction in Lung Disease. *Annu Rev Physiol* (2014).

388. Maeda, Y., Dave, V. & Whitsett, J.A. Transcriptional control of lung morphogenesis. *Physiol Rev* **87**, 219-44 (2007).

389. Berbari, N.F., Kin, N.W., Sharma, N., Michaud, E.J., Kesterson, R.A. & Yoder, B.K. Mutations in Traf3ip1 reveal defects in ciliogenesis, embryonic development, and altered cell size regulation. *Dev Biol* **360**, 66-76 (2011).

390. Sasaki, Y., Ishida, S., Morimoto, I., Yamashita, T., Kojima, T., Kihara, C., Tanaka, T., Imai, K., Nakamura, Y. & Tokino, T. The p53 family member genes are involved in the Notch signal pathway. *J Biol Chem* **277**, 719-24 (2002).

391. Bornstein, C., Brosh, R., Molchadsky, A., Madar, S., Kogan-Sakin, I., Goldstein, I., Chakravarti, D., Flores, E.R., Goldfinger, N., Sarig, R. & Rotter, V. SPATA18, a spermatogenesis-associated gene, is a novel transcriptional target of p53 and p63. *Mol Cell Biol* **31**, 1679-89 (2011).

392. Whitsett, J.A. & Tichelaar, J.W. Forkhead transcription factor HFH-4 and respiratory epithelial cell differentiation. *Am J Respir Cell Mol Biol* **21**, 153-4 (1999).

393. Lim, L., Zhou, H. & Costa, R.H. The winged helix transcription factor HFH-4 is expressed during choroid plexus epithelial development in the mouse embryo. *Proc Natl Acad Sci U S A* **94**, 3094-9 (1997).

394. Jacquet, B.V., Salinas-Mondragon, R., Liang, H., Therit, B., Buie, J.D., Dykstra, M., Campbell, K., Ostrowski, L.E., Brody, S.L. & Ghashghaei, H.T. FoxJ1-dependent gene expression is required for differentiation of radial glia into ependymal cells and a subset of astrocytes in the postnatal brain. *Development* **136**, 4021-31 (2009).

395. Pan, J., You, Y., Huang, T. & Brody, S.L. RhoA-mediated apical actin enrichment is required for ciliogenesis and promoted by Foxj1. *J Cell Sci* **120**, 1868-76 (2007).

396. Danielian, P.S., Bender Kim, C.F., Caron, A.M., Vasile, E., Bronson, R.T. & Lees, J.A. E2f4 is required for normal development of the airway epithelium. *Dev Biol* **305**, 564-76 (2007).

397. Funk, M.C., Bera, A.N., Menchen, T., Kuales, G., Thriene, K., Lienkamp, S.S., Dengjel, J., Omran, H., Frank, M. & Arnold, S.J. Cyclin O (Ccno) functions during deuterosome-mediated centriole amplification of multiciliated cells. *EMBO J* **34**, 1078-89 (2015).

398. Rock, J.R. & Hogan, B.L. Epithelial progenitor cells in lung development, maintenance, repair, and disease. *Annu Rev Cell Dev Biol* **27**, 493-512 (2011).

399. Davison, T.S., Vagner, C., Kaghad, M., Ayed, A., Caput, D. & Arrowsmith, C.H. p73 and p63 are homotetramers capable of weak heterotypic interactions with each other but not with p53. *J Biol Chem* **274**, 18709-14 (1999).

400. Deyoung, M.P. & Ellisen, L.W. p63 and p73 in human cancer: defining the network. *Oncogene* **26**, 5169-83 (2007).

401. Lin, L., Spoor, M.S., Gerth, A.J., Brody, S.L. & Peng, S.L. Modulation of Th1 activation and inflammation by the NF-kappaB repressor Foxj1. *Science* **303**, 1017-20 (2004).

402. Kulaga, H.M., Leitch, C.C., Eichers, E.R., Badano, J.L., Lesemann, A., Hoskins, B.E., Lupski, J.R., Beales, P.L., Reed, R.R. & Katsanis, N. Loss of BBS proteins causes anosmia in humans and defects in olfactory cilia structure and function in the mouse. *Nat Genet* **36**, 994-8 (2004).

403. Li, C.W., Shi, L., Zhang, K.K., Li, T.Y., Lin, Z.B., Lim, M.K., McKeon, F., Xian, W. & Wang de, Y. Role of p63/p73 in epithelial remodeling and their response to steroid treatment in nasal polyposis. *J Allergy Clin Immunol* **127**, 765-72 e1-2 (2011).

404. Li, Y.Y., Li, C.W., Chao, S.S., Yu, F.G., Yu, X.M., Liu, J., Yan, Y., Shen, L., Gordon, W., Shi, L. & Wang, D.Y. Impairment of cilia architecture and ciliogenesis in hyperplastic nasal epithelium from nasal polyps. *J Allergy Clin Immunol* (2014).

405. Mikule, K., Delaval, B., Kaldis, P., Jurcyzk, A., Hergert, P. & Doxsey, S. Loss of centrosome integrity induces p38-p53-p21-dependent G1-S arrest. *Nat Cell Biol* **9**, 160-70 (2007).

406. Menendez, D., Inga, A. & Resnick, M.A. The expanding universe of p53 targets. *Nat Rev Cancer* **9**, 724-37 (2009).

407. Perez, C.A., Ott, J., Mays, D.J. & Pietenpol, J.A. p63 consensus DNA-binding site: identification, analysis and application into a p63MH algorithm. *Oncogene* **26**, 7363-70 (2007).

408. Flores, E.R., Tsai, K.Y., Crowley, D., Sengupta, S., Yang, A., McKeon, F. & Jacks, T. p63 and p73 are required for p53-dependent apoptosis in response to DNA damage. *Nature* **416**, 560-4 (2002).

409. Bell, H.S. & Ryan, K.M. iASPP inhibition: increased options in targeting the p53 family for cancer therapy. *Cancer Res* **68**, 4959-62 (2008).

410. Di Como, C.J., Gaiddon, C. & Prives, C. p73 function is inhibited by tumor-derived p53 mutants in mammalian cells. *Mol Cell Biol* **19**, 1438-49 (1999).

411. Zeng, X., Chen, L., Jost, C.A., Maya, R., Keller, D., Wang, X., Kaelin, W.G., Jr., Oren, M., Chen, J. & Lu, H. MDM2 suppresses p73 function without promoting p73 degradation. *Mol Cell Biol* **19**, 3257-66 (1999).

412. Vassilev, L.T., Vu, B.T., Graves, B., Carvajal, D., Podlaski, F., Filipovic, Z., Kong, N., Kammlott, U., Lukacs, C., Klein, C., Fotouhi, N. & Liu, E.A. In vivo activation of the p53 pathway by small-molecule antagonists of MDM2. *Science* **303**, 844-8 (2004).

413. Lau, L.M., Nugent, J.K., Zhao, X. & Irwin, M.S. HDM2 antagonist Nutlin-3 disrupts p73-HDM2 binding and enhances p73 function. *Oncogene* **27**, 997-1003 (2008).

414. Melino, G., De Laurenzi, V. & Vousden, K.H. p73: Friend or foe in tumorigenesis. *Nat Rev Cancer* **2**, 605-15 (2002).

415. Davis, T.A., Vilgelm, A.E., Richmond, A. & Johnston, J.N. Preparation of (-)-Nutlin-3 using enantioselective organocatalysis at decagram scale. *J Org Chem* **78**, 10605-16 (2013).

416. Bunz, F., Hwang, P.M., Torrance, C., Waldman, T., Zhang, Y., Dillehay, L., Williams, J., Lengauer, C., Kinzler, K.W. & Vogelstein, B. Disruption of p53 in human cancer cells alters the responses to therapeutic agents. *J Clin Invest* **104**, 263-9 (1999).

417. Wang, S., Konorev, E.A., Kotamraju, S., Joseph, J., Kalivendi, S. & Kalyanaraman, B. Doxorubicin induces apoptosis in normal and tumor cells via distinctly different mechanisms. intermediacy of H(2)O(2)- and p53-dependent pathways. *J Biol Chem* **279**, 25535-43 (2004).

418. Murray-Zmijewski, F., Slee, E.A. & Lu, X. A complex barcode underlies the heterogeneous response of p53 to stress. *Nat Rev Mol Cell Biol* **9**, 702-12 (2008).

419. Racek, T., Mise, N., Li, Z., Stoll, A. & Putzer, B.M. C-terminal p73 isoforms repress transcriptional activity of the human telomerase reverse transcriptase (hTERT) promoter. *J Biol Chem* **280**, 40402-5 (2005).

420. Aqeilan, R.I., Pekarsky, Y., Herrero, J.J., Palamarchuk, A., Letofsky, J., Druck, T., Trapasso, F., Han, S.Y., Melino, G., Huebner, K. & Croce, C.M. Functional association between Wwox tumor suppressor protein and p73, a p53 homolog. *Proc Natl Acad Sci U S A* **101**, 4401-6 (2004).

421. Aqeilan, R.I., Donati, V., Palamarchuk, A., Trapasso, F., Kaou, M., Pekarsky, Y., Sudol, M. & Croce, C.M. WW domain-containing proteins, WWOX and YAP, compete for interaction with ErbB-4 and modulate its transcriptional function. *Cancer Res* **65**, 6764-72 (2005).

422. Chaudhary, N. & Maddika, S. WWP2-WWP1 ubiquitin ligase complex coordinated by PPM1G maintains the balance between cellular p73 and DeltaNp73 levels. *Mol Cell Biol* **34**, 3754-64 (2014).

423. Levy, D., Adamovich, Y., Reuven, N. & Shaul, Y. The Yes-associated protein 1 stabilizes p73 by preventing Itch-mediated ubiquitination of p73. *Cell Death Differ* **14**, 743-51 (2007).

424. Danovi, S.A., Rossi, M., Gudmundsdottir, K., Yuan, M., Melino, G. & Basu, S. Yes-associated protein (YAP) is a critical mediator of c-Jun-dependent apoptosis. *Cell Death Differ* **15**, 217-9 (2008).

425. Rossi, M., De Laurenzi, V., Munarriz, E., Green, D.R., Liu, Y.C., Vousden, K.H., Cesareni, G. & Melino, G. The ubiquitin-protein ligase Itch regulates p73 stability. *EMBO J* **24**, 836-48 (2005).

426. Li, Y. & Prives, C. Are interactions with p63 and p73 involved in mutant p53 gain of oncogenic function? *Oncogene* **26**, 2220-5 (2007).

427. Hurley, J.H. & Wendland, B. Endocytosis: driving membranes around the bend. *Cell* **111**, 143-6 (2002).

428. Wendland, B. Epsins: adaptors in endocytosis? *Nat Rev Mol Cell Biol* **3**, 971-7 (2002).

429. Legendre-Guillemin, V., Wasiak, S., Hussain, N.K., Angers, A. & McPherson, P.S. ENTH/ANTH proteins and clathrin-mediated membrane budding. *J Cell Sci* **117**, 9-18 (2004).

430. Spradling, K.D., McDaniel, A.E., Lohi, J. & Pilcher, B.K. Epsin 3 is a novel extracellular matrix-induced transcript specific to wounded epithelia. *J Biol Chem* **276**, 29257-67 (2001).

431. Rosenthal, J.A., Chen, H., Slepnev, V.I., Pellegrini, L., Salcini, A.E., Di Fiore, P.P. & De Camilli, P. The epsins define a family of proteins that interact with components of the clathrin coat and contain a new protein module. *J Biol Chem* **274**, 33959-65 (1999).

432. Ford, M.G., Mills, I.G., Peter, B.J., Vallis, Y., Praefcke, G.J., Evans, P.R. & McMahon, H.T. Curvature of clathrin-coated pits driven by epsin. *Nature* **419**, 361-6 (2002).

433. Hyman, J., Chen, H., Di Fiore, P.P., De Camilli, P. & Brunger, A.T. Epsin 1 undergoes nucleocytosolic shuttling and its eps15 interactor NH(2)-terminal homology (ENTH) domain, structurally similar to Armadillo and HEAT repeats, interacts with the transcription factor promyelocytic leukemia Zn(2)+ finger protein (PLZF). *J Cell Biol* **149**, 537-46 (2000).

434. Vecchi, M., Polo, S., Poupon, V., van de Loo, J.W., Benmerah, A. & Di Fiore, P.P. Nucleocytoplasmic shuttling of endocytic proteins. *J Cell Biol* **153**, 1511-7 (2001).

435. Ohmori, K., Endo, Y., Yoshida, Y., Ohata, H., Taya, Y. & Enari, M. Monomeric but not trimeric clathrin heavy chain regulates p53-mediated transcription. *Oncogene* **27**, 2215-27 (2008).

436. Enari, M., Ohmori, K., Kitabayashi, I. & Taya, Y. Requirement of clathrin heavy chain for p53-mediated transcription. *Genes Dev* **20**, 1087-99 (2006).

437. Yan, Z., Kim, Y.S. & Jetten, A.M. RAP80, a novel nuclear protein that interacts with the retinoid-related testis-associated receptor. *J Biol Chem* **277**, 32379-88 (2002).

438. Yan, J. & Jetten, A.M. RAP80 and RNF8, key players in the recruitment of repair proteins to DNA damage sites. *Cancer Lett* **271**, 179-90 (2008).

439. Sobhian, B., Shao, G., Lilli, D.R., Culhane, A.C., Moreau, L.A., Xia, B., Livingston, D.M. & Greenberg, R.A. RAP80 targets BRCA1 to specific ubiquitin structures at DNA damage sites. *Science* **316**, 1198-202 (2007).

440. Kim, H., Chen, J. & Yu, X. Ubiquitin-binding protein RAP80 mediates BRCA1-dependent DNA damage response. *Science* **316**, 1202-5 (2007).

441. Yan, J., Menendez, D., Yang, X.P., Resnick, M.A. & Jetten, A.M. A regulatory loop composed of RAP80-HDM2-p53 provides RAP80-enhanced p53 degradation by HDM2 in response to DNA damage. *J Biol Chem* **284**, 19280-9 (2009).

442. Shibuya, H., Yamaguchi, K., Shirakabe, K., Tonegawa, A., Gotoh, Y., Ueno, N., Irie, K., Nishida, E. & Matsumoto, K. TAB1: an activator of the TAK1 MAPKKK in TGF-beta signal transduction. *Science* **272**, 1179-82 (1996).

443. Jin, G., Klika, A., Callahan, M., Faga, B., Danzig, J., Jiang, Z., Li, X., Stark, G.R., Harrington, J. & Sherf, B. Identification of a human NF-kappaB-activating protein, TAB3. *Proc Natl Acad Sci U S A* **101**, 2028-33 (2004).

444. Broglie, P., Matsumoto, K., Akira, S., Brautigan, D.L. & Ninomiya-Tsuji, J. Transforming growth factor beta-activated kinase 1 (TAK1) kinase adaptor, TAK1-binding protein 2, plays dual roles in TAK1 signaling by recruiting both an activator and an inhibitor of TAK1 kinase in tumor necrosis factor signaling pathway. *J Biol Chem* **285**, 2333-9 (2010).

445. Takaesu, G., Ninomiya-Tsuji, J., Kishida, S., Li, X., Stark, G.R. & Matsumoto, K. Interleukin-1 (IL-1) receptor-associated kinase leads to activation of TAK1 by inducing TAB2 translocation in the IL-1 signaling pathway. *Mol Cell Biol* **21**, 2475-84 (2001).

446. Kajino, T., Ren, H., Iemura, S., Natsume, T., Stefansson, B., Brautigan, D.L., Matsumoto, K. & Ninomiya-Tsuji, J. Protein phosphatase 6 down-regulates TAK1 kinase activation in the IL-1 signaling pathway. *J Biol Chem* **281**, 39891-6 (2006).

447. Takaesu, G., Kishida, S., Hiyama, A., Yamaguchi, K., Shibuya, H., Irie, K., Ninomiya-Tsuji, J. & Matsumoto, K. TAB2, a novel adaptor protein, mediates activation of TAK1 MAPKKK by linking TAK1 to TRAF6 in the IL-1 signal transduction pathway. *Mol Cell* **5**, 649-58 (2000).

448. Kishida, S., Sanjo, H., Akira, S., Matsumoto, K. & Ninomiya-Tsuji, J. TAK1-binding protein 2 facilitates ubiquitination of TRAF6 and assembly of TRAF6 with IKK in the IL-1 signaling pathway. *Genes Cells* **10**, 447-54 (2005).

449. Kanayama, A., Seth, R.B., Sun, L., Ea, C.K., Hong, M., Shaito, A., Chiu, Y.H., Deng, L. & Chen, Z.J. TAB2 and TAB3 activate the NF-kappaB pathway through binding to polyubiquitin chains. *Mol Cell* **15**, 535-48 (2004).

450. Hinz, M., Stilmann, M., Arslan, S.C., Khanna, K.K., Dittmar, G. & Scheidereit, C. A cytoplasmic ATM-TRAF6-cIAP1 module links nuclear DNA damage signaling to ubiquitin-mediated NF-kappaB activation. *Mol Cell* **40**, 63-74 (2010).

451. Ear, T., Fortin, C.F., Simard, F.A. & McDonald, P.P. Constitutive association of TGF-beta-activated kinase 1 with the IkappaB kinase complex in the nucleus and cytoplasm of human neutrophils and its impact on downstream processes. *J Immunol* **184**, 3897-906 (2010).

452. Missero, C., Di Cunto, F., Kiyokawa, H., Koff, A. & Dotto, G.P. The absence of p21Cip1/WAF1 alters keratinocyte growth and differentiation and promotes ras-tumor progression. *Genes Dev* **10**, 3065-75 (1996).

453. Deng, C., Zhang, P., Harper, J.W., Elledge, S.J. & Leder, P. Mice lacking p21CIP1/WAF1 undergo normal development, but are defective in G1 checkpoint control. *Cell* **82**, 675-84 (1995).

454. Zuo, W., Zhang, T., Wu, D.Z., Guan, S.P., Liew, A.A., Yamamoto, Y., Wang, X., Lim, S.J., Vincent, M., Lessard, M., Crum, C.P., Xian, W. & McKeon, F. p63(+)Krt5(+) distal airway stem cells are essential for lung regeneration. *Nature* **517**, 616-20 (2015).

455. Asselin-Labat, M.L. & Filby, C.E. Adult lung stem cells and their contribution to lung tumourigenesis. *Open Biol* **2**, 120094 (2012).

456. Tomasini, R., Secq, V., Pouyet, L., Thakur, A.K., Wilhelm, M., Nigri, J., Vasseur, S., Berthezene, P., Calvo, E., Melino, G., Mak, T.W. & Iovanna, J.L. TAp73 is required for macrophage-mediated innate immunity and the resolution of inflammatory responses. *Cell Death Differ* **20**, 293-301 (2013).

457. Matute-Bello, G., Frevert, C.W. & Martin, T.R. Animal models of acute lung injury. *Am J Physiol Lung Cell Mol Physiol* **295**, L379-99 (2008).

458. Looney, M.R. & Matthay, M.A. Animal models of transfusion-related acute lung injury. *Crit Care Med* **34**, S132-6 (2006).

459. Wiggs, B.R., English, D., Quinlan, W.M., Doyle, N.A., Hogg, J.C. & Doerschuk, C.M. Contributions of capillary pathway size and neutrophil deformability to neutrophil transit through rabbit lungs. *J Appl Physiol (1985)* **77**, 463-70 (1994).

460. Wiener-Kronish, J.P., Albertine, K.H. & Matthay, M.A. Differential responses of the endothelial and epithelial barriers of the lung in sheep to Escherichia coli endotoxin. *J Clin Invest* **88**, 864-75 (1991).

461. Conroy, D.M., Francischi, J.N. & Sirois, P. Effect of tumor necrosis factor receptor binding protein on cell infiltration induced by lipopolysaccharide and Sephadex beads in guinea pig lung. *Inflammation* **19**, 233-43 (1995).

462. Azghani, A.O., Miller, E.J. & Peterson, B.T. Virulence factors from Pseudomonas aeruginosa increase lung epithelial permeability. *Lung* **178**, 261-9 (2000).

463. Azghani, A.O. Pseudomonas aeruginosa and epithelial permeability: role of virulence factors elastase and exotoxin A. *Am J Respir Cell Mol Biol* **15**, 132-40 (1996).

464. Yang, R.B., Mark, M.R., Gray, A., Huang, A., Xie, M.H., Zhang, M., Goddard, A., Wood, W.I., Gurney, A.L. & Godowski, P.J. Toll-like receptor-2 mediates lipopolysaccharide-induced cellular signalling. *Nature* **395**, 284-8 (1998).

465. Wright, S.D., Ramos, R.A., Tobias, P.S., Ulevitch, R.J. & Mathison, J.C. CD14, a receptor for complexes of lipopolysaccharide (LPS) and LPS binding protein. *Science* **249**, 1431-3 (1990).

466. Tapping, R.I., Akashi, S., Miyake, K., Godowski, P.J. & Tobias, P.S. Toll-like receptor 4, but not toll-like receptor 2, is a signaling receptor for Escherichia and Salmonella lipopolysaccharides. *J Immunol* **165**, 5780-7 (2000).

467. Kim, S.B., Chae, G.W., Lee, J., Park, J., Tak, H., Chung, J.H., Park, T.G., Ahn, J.K. & Joe, C.O. Activated Notch1 interacts with p53 to inhibit its phosphorylation and transactivation. *Cell Death Differ* **14**, 982-91 (2007).

468. Hooper, C., Tavassoli, M., Chapple, J.P., Uwanogho, D., Goodyear, R., Melino, G., Lovestone, S. & Killick, R. TAp73 isoforms antagonize Notch signalling in SH-SY5Y neuroblastomas and in primary neurones. *J Neurochem* **99**, 989-99 (2006).

469. Zhao, Y., Katzman, R.B., Delmolino, L.M., Bhat, I., Zhang, Y., Gurumurthy, C.B., Germaniuk-Kurowska, A., Reddi, H.V., Solomon, A., Zeng, M.S., Kung, A., Ma, H., Gao, Q., Dimri, G., Stanculescu, A., Miele, L., Wu, L., Griffin, J.D., Wazer, D.E., Band, H. & Band, V. The notch regulator MAML1 interacts with p53 and functions as a coactivator. *J Biol Chem* **282**, 11969-81 (2007).

470. Blanpain, C., Lowry, W.E., Pasolli, H.A. & Fuchs, E. Canonical notch signaling functions as a commitment switch in the epidermal lineage. *Genes Dev* **20**, 3022-35 (2006).

471. Yugawa, T., Handa, K., Narisawa-Saito, M., Ohno, S., Fujita, M. & Kiyono, T. Regulation of Notch1 gene expression by p53 in epithelial cells. *Mol Cell Biol* **27**, 3732-42 (2007).

472. Dotto, G.P. Crosstalk of Notch with p53 and p63 in cancer growth control. *Nat Rev Cancer* **9**, 587-95 (2009).

473. Tsao, P.N., Chen, F., Izvolsky, K.I., Walker, J., Kukuruzinska, M.A., Lu, J. & Cardoso, W.V. Gamma-secretase activation of notch signaling regulates the balance of proximal and distal fates in progenitor cells of the developing lung. *J Biol Chem* **283**, 29532-44 (2008).

474. Roemer, K. Notch and the p53 clan of transcription factors. *Adv Exp Med Biol* **727**, 223-40 (2012).

475. Varner, V.D. & Nelson, C.M. Cellular and physical mechanisms of branching morphogenesis. *Development* **141**, 2750-9 (2014).

476. Kong, S.L., Li, G., Loh, S.L., Sung, W.K. & Liu, E.T. Cellular reprogramming by the conjoint action of ERalpha, FOXA1, and GATA3 to a ligand-inducible growth state. *Mol Syst Biol* **7**, 526 (2011).

477. Drier, Y., Cotton, M.J., Williamson, K.E., Gillespie, S.M., Ryan, R.J., Kluk, M.J., Carey, C.D., Rodig, S.J., Sholl, L.M., Afrogheh, A.H., Faquin, W.C., Queimado, L., Qi, J., Wick, M.J., El-Naggar, A.K., Bradner, J.E., Moskaluk, C.A., Aster, J.C., Knoechel, B. & Bernstein, B.E. An oncogenic MYB feedback loop drives alternate cell fates in adenoid cystic carcinoma. *Nat Genet* (2016).

478. Biewenga, P., Buist, M.R., Moerland, P.D., Ver Loren van Themaat, E., van Kampen, A.H., ten Kate, F.J. & Baas, F. Gene expression in early stage cervical cancer. *Gynecol Oncol* **108**, 520-6 (2008).

479. Yan, Y.H., Yi, P., Zheng, Y.R., Yu, L.L., Han, J., Han, X.M. & Li, L. Screening for preeclampsia pathogenesis related genes. *Eur Rev Med Pharmacol Sci* **17**, 3083-94 (2013).

480. Komander, D. The emerging complexity of protein ubiquitination. *Biochem Soc Trans* **37**, 937-53 (2009).

481. Jin, L., Williamson, A., Banerjee, S., Philipp, I. & Rape, M. Mechanism of ubiquitin-chain formation by the human anaphase-promoting complex. *Cell* **133**, 653-65 (2008).

482. Thrower, J.S., Hoffman, L., Rechsteiner, M. & Pickart, C.M. Recognition of the polyubiquitin proteolytic signal. *EMBO J* **19**, 94-102 (2000).

483. Chen, Z.J. & Sun, L.J. Nonproteolytic functions of ubiquitin in cell signaling. *Mol Cell* **33**, 275-86 (2009).

484. Badano, J.L., Mitsuma, N., Beales, P.L. & Katsanis, N. The ciliopathies: an emerging class of human genetic disorders. *Annu Rev Genomics Hum Genet* **7**, 125-48 (2006).

485. Thomas, B., Rutman, A., Hirst, R.A., Haldar, P., Wardlaw, A.J., Bankart, J., Brightling, C.E. & O'Callaghan, C. Ciliary dysfunction and ultrastructural abnormalities are features of severe asthma. *J Allergy Clin Immunol* **126**, 722-729 e2 (2010).

486. Laitinen, L.A., Heino, M., Laitinen, A., Kava, T. & Haahtela, T. Damage of the airway epithelium and bronchial reactivity in patients with asthma. *Am Rev Respir Dis* **131**, 599-606 (1985).

487. Dunnill, M.S. The pathology of asthma, with special reference to changes in the bronchial mucosa. *J Clin Pathol* **13**, 27-33 (1960).

488. Cokugras, H., Akcakaya, N., Seckin, Camcioglu, Y., Sarimurat, N. & Aksoy, F. Ultrastructural examination of bronchial biopsy specimens from children with moderate asthma. *Thorax* **56**, 25-9 (2001).

489. Beasley, R., Roche, W.R., Roberts, J.A. & Holgate, S.T. Cellular events in the bronchi in mild asthma and after bronchial provocation. *Am Rev Respir Dis* **139**, 806-17 (1989).

490. Yaghi, A., Zaman, A., Cox, G. & Dolovich, M.B. Ciliary beating is depressed in nasal cilia from chronic obstructive pulmonary disease subjects. *Respir Med* **106**, 1139-47 (2012).

491. Leopold, P.L., O'Mahony, M.J., Lian, X.J., Tilley, A.E., Harvey, B.G. & Crystal, R.G. Smoking is associated with shortened airway cilia. *PLoS One* **4**, e8157 (2009).

492. Hessel, J., Heldrich, J., Fuller, J., Staudt, M.R., Radisch, S., Hollmann, C., Harvey, B.G., Kaner, R.J., Salit, J., Yee-Levin, J., Sridhar, S., Pillai, S., Hilton, H., Wolff, G., Bitter, H., Visvanathan, S., Fine, J., Stevenson, C.S., Crystal, R.G. & Tilley, A.E. Intraflagellar transport gene expression associated with short cilia in smoking and COPD. *PLoS One* **9**, e85453 (2014).